

CATALYTIC OZONATION OF INDUSTRIAL TEXTILE  
WASTEWATERS IN A THREE PHASE FLUIDIZED BED  
REACTOR

A THESIS SUBMITTED TO  
THE GRADUATE SCHOOL OF NATURAL SCIENCES  
OF  
MIDDLE EAST TECHNICAL UNIVERSITY

BY

DİDEM POLAT

IN PARTIAL FULFILLMENT OF THE REQUIREMENTS  
FOR  
THE DEGREE OF MASTER OF SCIENCE  
IN  
CHEMICAL ENGINEERING

DECEMBER 2010

Approval of the thesis:

**CATALYTIC OZONATION OF INDUSTRIAL TEXTILE  
WASTEWATERS IN A THREE PHASE FLUIDIZED BED  
REACTOR**

submitted by **DİDEM POLAT** in partial fulfillment of the requirements for the degree of **Master of Science in Chemical Engineering Department, Middle East Technical University** by,

Prof. Dr. Canan Özgen

Dean, Graduate School of **Natural and Applied Sciences**

\_\_\_\_\_

Prof. Dr. Deniz Üner

Head of Department, **Chemical Engineering**

\_\_\_\_\_

Prof. Dr. A.Tülay Özbelge

Supervisor, **Chemical Engineering Dept., METU**

\_\_\_\_\_

**Examining Committee Members:**

Prof. Dr. Hayrettin Yücel

Chemical Engineering Dept., METU

\_\_\_\_\_

Prof. Dr. Tülay Özbelge

Chemical Engineering Dept., METU

\_\_\_\_\_

Prof. Dr. Ülkü Yilmazer

Chemical Engineering Dept., METU

\_\_\_\_\_

Asst. Prof. Dr Ayşegül Latifoğlu

\_\_\_\_\_

Assoc. Prof. Dr. Halil Kalıpçılar

Chemical Engineering Dept., METU

\_\_\_\_\_

Date: 23.12.2010

**I hereby declare that all information in this document has been obtained and presented in accordance with academic rules ethical conduct. I also declare that, as required by these rules and conduct, I have fully cited and referenced all material and results that are not original to this work.**

Name, Last name: Didem Polat

Signature:

## ABSTRACT

### CATALYTIC OZONATION OF INDUSTRIAL TEXTILE WASTEWATERS IN A THREE PHASE FLUIDIZED BED REACTOR

Polat, Didem

M.Sc. Department of Chemical Engineering

Supervisor: Prof. Dr. Tülay Özbelge

December 2010, 197 pages

Textile wastewaters are highly colored and non-biodegradable having variable compositions of colored dyes, surfactants and toxic chemicals. Recently, ozonation is considered as an effective method that can be used in the treatment of industrial wastewaters; catalytic ozonation being one of the advanced oxidation processes (AOPs), is applied in order to reduce the ozone consumption and to increase the chemical oxygen demand (COD) and total organic carbon (TOC) removals.

In this study, catalytic ozonation of industrial textile wastewater (ITWW) obtained from AKSA A.Ş. (Yalova, İstanbul) textile plant has been examined in a three phase fluidized bed reactor at different conditions. The effects of inlet chemical oxygen demand concentration ( $COD_{in}$ ), pH, different catalyst types [perfluorooctyl alumina (PFOA) and alumina] and catalyst dosage on ozonation process were determined. Moreover, the changes in the organic removal efficiencies with gas to liquid flow rate ratio were investigated. The dispersion coefficients ( $D_L$ ) and volumetric ozone-water mass transfer coefficients ( $k_{LA}$ ) were estimated at various gas and liquid flow rates in order to observe the effect of liquid mixing in the reactor on ozonation process. It was observed that increasing both gas and liquid flow rates by keeping

their ratio constant provided higher organic removal efficiencies due to the higher mixing in the liquid phase.

The dyes present in ITWW sample were known to be Basic Blue 41 (BB 41), Basic Red 18.1 (BR 18.1) and Basic Yellow 28 (BY 28). The “absorbance vs. concentration” calibration correlations were developed to estimate the amounts of these colored dyes in the ITWW sample. This provided the opportunity to examine the degradation of each dye in this wastewater separately.

While PFOA catalyst was found to increase the removal efficiency of BY 28 at an acidic pH of 4, alumina yielded highest color removals for BB 41 and BR 18.1 at a pH of 12. The highest TOC and COD reductions being 24.4% and 29.5%, respectively, were achieved in the catalytic ozonation of the ITWW using alumina as the catalyst at a pH of 12 and at a gas to liquid flow rate ratio of 1.36 ( $Q_G = 340$  L/h,  $Q_L = 250$  L/h). At the same conditions, also the highest overall color removal in terms of Pt-Co color unit, namely 86.49%, were obtained due to the lower BY 28 concentration in the WW sample than those of the BB 41 and BR 18.1.

In addition, the oxidation of BB 41, BR 18.1 and BY 28 dyes were investigated in a semi-batch reactor by sole and catalytic ozonations with alumina and PFOA catalyst particles. The sole and catalytic ozonation reactions followed a pseudo-first order kinetics with respect to dye concentration. The highest TOC and COD removals being 58.3% and 62.9%, respectively, were obtained at pH of 10 for BB 41 and 55.2% and 58.8%, respectively, for BR 18.1 with alumina catalyst. On the other hand, for BY 28 PFOA catalyst yielded highest TOC and COD reductions being 61.3% and 66.9%, respectively, at pH of 4.

**Keywords:** Catalytic ozonation, industrial textile wastewater, Perfluorooctyl alumina (PFOA), alumina

## ÖZ

### BOYA İÇEREN ENDÜSTRİYEL ATIK SULARIN AKIŞKAN YATAKLI BİR REAKTÖRDE KATALİTİK OZONLAMA İLE ARITILMASI

Polat, Didem

Yüksek Lisans, Kimya Mühendisliği Bölümü

Tez Yöneticisi: Prof. Dr. Tülay Özbelge

Aralık 2010, 197 sayfa

Çeşitli miktarlarda boyar madde, yüzey aktif madde ve zararlı kimyasallar içeren yoğun renkli tekstil atık sularının giderimi biyolojik yöntemlerle sağlanamamaktadır. Son dönemlerde, ozonlama tekstil atık sularının arıtımında etkileyici bir metot olarak görülürken, ileri oksidasyon tekniklerinden (İOP) birisi olan katalitik ozonlama, sudaki organik kirleticilerin, daha az ozon tüketimiyle daha yüksek verimlerde giderimlerini sağlamak amacıyla uygulanmaktadır.

Bu çalışmada, AKSA A.Ş. (Yalova, İstanbul)'den temin edilen endüstriyel tekstil atık suyunun (ITWW) katalitik ozonlanması üç fazlı akışkan yataklı bir reaktör kullanılarak farklı çalışma koşullarında araştırılmıştır. Reaktör girişindeki kimyasal oksijen ihtiyacı konsantrasyonunun ( $COD_{in}$ ), pH'nın, farklı katalizör tiplerinin [perflorooktil alümina (PFOA) ve alümina] ve katalizör miktarlarının ozonlama prosesi üzerindeki etkileri tayin edilmiştir. Bununla beraber, gaz ve sıvı akış hızlarının atık su bünyesindeki organiklerin giderim verimleri üzerindeki etkileri araştırılmıştır. Reaktördeki sıvı-faz kargaşasının (türbulans) ozonlama üzerindeki etkilerini inceleyebilmek amacıyla farklı gaz ve sıvı hızlarındaki dağılım katsayıları ( $D_L$ ) ve hacimsel ozon-su kütle transfer katsayıları ( $k_{La}$ ) hesaplanmıştır. Gaz akış hızının sıvı akış hızına oranı sabit tutularak, gaz ve sıvı akış hızlarının birlikte

arttırılmasıyla sıvı-faz kargaşasındaki seviyenin yükselmesi nedeniyle organik giderim verimlerinin yükseldiği gözlemlenmiştir.

Atık su örneğinin içerisinde Bazik Mavi 41 (BB 41), Bazik Kırmızı 18.1 (BR 18.1) ve Bazik Sarı 28 (BY 28) boyar maddelerinin olduğu bilinmektedir. Bu boyaların atık su içerisindeki miktarlarını tayin etmek amacıyla bazı “absorbans – konsantrasyon” kalibrasyon bağıntıları (korelasyonları) geliştirilmiş ve bu korelasyonlar atık su içerisinde boyaların ayrı ayrı giderimlerinin incelenmeleri fırsatını sunmuştur.

BY 28 için boya giderim verimleri asidik ortam olan pH 4’te PFOA katalizörü kullanıldığında artarken, BB 41 ve BR 18.1 için en yüksek renk giderimleri pH’nın 12 olduğu ortamda alümina kullanımı ile gerçekleşmiştir. Atık su için sırasıyla en yüksek TOK ve KOİ giderimleri olan % 24.4 ve % 29.5, ITWW’nin katalitik ozonlanması esnasında alümina katalizörü kullanılarak gaz akış hızının sıvı akış hızına oranının 1.36 ( $Q_G = 340$  L/h,  $Q_L = 250$  L/h) ve pH’nın 12 olduğu koşullarda elde edilmiştir. Pt-Co renk birimi cinsinden en yüksek genel renk giderimi olan % 86.5’in yine aynı koşullarda elde edilmesi atık su içerisindeki BY 28 miktarının BB 41 ve BR 18.1 miktarlarının toplamından daha az olmasından kaynaklanmıştır.

Bunlara ek olarak; BB 41, BR 18.1 ve BY 28 boyar maddelerinin arıtmaları yalnız ozonlama ve alümina veya PFOA eşliğinde katalitik ozonlama ile yarı-kesikli bir reaktörde incelenmiştir. Yalnız ve katalitik ozonlama prosesleri boya konsantrasyonuna göre yaklaşık (pseudo) birinci derece reaksiyon kinetiği izlemiştir. BB 41 için sırasıyla en yüksek TOK ve KOİ giderimleri olan % 58.3 ve % 62.9 bazik bir pH olan 10’da alümina katalizörü kullanılarak elde edilmiştir. Aynı şekilde BR 18.1 için yine alümina katalizörü pH’nın 10 olduğu durumda en yüksek TOK ve KOİ giderimlerinin (% 55.21 ve % 58.84) elde edilmesini sağlamıştır. BY 28 için ise sırasıyla en yüksek TOK ve KOİ giderimleri olan % 61.4 ve % 66.9, PFOA katalizörü kullanılarak ve pH’nın 4 olduğu durumda elde edilmiştir.

**Anahtar Kelimeler:** Katalitik ozonlama, endüstriyel tekstil atık suları, perflorooktil alümina (PFOA), alümina

*To my family...*

## ACKNOWLEDGEMENTS

I would like to extend my sincerest thanks to my supervisor Prof. Dr. Tlay A. zbelge for her continual advices, helpful discussions and corrections, major support as a supervisor and sincere behaviors as a person like a mother. I also want to thank to Prof. Dr. nder zbelge for his helpful suggestions.

I am very grateful to my lab mate A. İrem Balc for her sincere support, valuable contributions that she has made, all the decisions we made together in our lives, being with me and so many things I cannot count since the very start of my life.

I would like to thank to my lab mate, Saltuk Pirgaliglu for his support, continual patience, being there when something went wrong in the laboratory and the whole things that he showed or taught me throughout the study. And also I want to thank my newest lab mate Ayegl Sezdi for her greatest support and deepest friendship.

I wish to express my thanks to all my friends for being there whenever I ask; Ceren Aydın, Ő. Seda Yılmaz, Eda Oral, Gamzenur zsin, Nur Sena YzbaŐı, Merve BaŐdemir, Bijen Kadaifci, Efe and Aslı Boran, Hasan Zerze for the lunch, tea or coffee times we made together and all graduate students in the department I spent time throughout my study.

I also would like to thank Kerime Gney for her help and suggestions during my study and also to the staff in our department for their contributions during my work.

I also wish to express my sincere thanks to my team leader Songl Bayraktar for her support and understanding especially through the end of the study and my team mates Ceren Bayren and Hasret Grsoy for their support and friendship.

Finally, I also wish to send my special thanks to my family for their great support and encouragement and to my brother for his technical help in using my computer.

# TABLE OF CONTENTS

ABSTRACT .....	iv
ÖZ .....	vi
ACKNOWLEDGEMENTS .....	ix
TABLE OF CONTENTS .....	x
LIST OF TABLES .....	xiii
LIST OF FIGURES .....	xvi
LIST OF SYMBOLS .....	xxi
CHAPTER	
1 INTRODUCTION .....	1
2 LITERATURE SURVEY .....	4
2.1 Textile Wastewaters .....	4
2.1.1 Oxidation with Ozone in Textile Wastewater Treatment .....	6
2.2 Ozone... ..	7
2.2.1 Ozonation Process .....	8
2.2.2 Mass Transfer of Ozone into Liquid Phase .....	12
2.2.1.1 Mass Transfer in the Presence of Chemical Reactions .....	14
2.3 Advanced Oxidation Processes (AOPs) .....	16
2.3.1 Catalytic Ozonation .....	17
2.3.1.1 Homogeneous Catalytic Ozonation .....	17
2.3.1.2 Heterogeneous Catalytic Ozonation .....	19
2.3.1.2.1 Metal Oxides and Metals or Metal Oxides on Supports .....	19
2.3.1.2.2 Ozonation with Non-polar Alumina Bonded Phases .....	21
3 EXPERIMENTAL .....	24
3.1 Materials .....	24
3.1.1 Industrial Textile Wastewater .....	24

3.2	Experimental Set-up .....	27
3.2.1	Semi-batch reactor .....	27
3.2.2	Three Phase Fluidized bed reactor .....	28
3.3	Preparation and Characterization of the Catalysts .....	31
3.4	Semi-batch Experiments .....	32
3.5	Experiments Conducted in Fluidized Bed Reactor .....	33
3.5.1	Wastewater Ozonation Experiments .....	34
3.6	Analytical Methods .....	35
4	RESULTS AND DISCUSSION .....	39
4.1	Ozonation Reaction Kinetics .....	39
4.2	Effect of Operating Parameters on Ozonation of Wastewater in Fluidized Bed Reactor (FBR) .....	40
4.2.1	Effect of Inlet COD ( $COD_{in}$ ) .....	40
4.2.2	Effect of pH.....	48
4.3	Catalytic Ozonation Experiments in FBR with Alumina or PFOA .....	55
4.3.1	Catalyst Characterization .....	56
4.3.1.1	Surface Characterization Experiments .....	56
4.3.1.2	Density Analysis .....	57
4.3.1.3	FT-IR Spectroscopic Studies .....	57
4.3.1.4	ESCA (XPS) Analysis .....	62
4.3.2	Effect of pH on Catalytic Ozonation .....	63
4.3.3	Higher pH Effect on Catalytic Ozonation .....	70
4.3.4	Effect of Catalyst Dosage .....	75
4.3.5	Effect of $Q_G/Q_L$ on Catalytic Ozonation .....	82
4.4	Reactor Hydrodynamics .....	90
4.4.1	Minimum Fluidization Velocity in the Column .....	90
4.4.2	Determination of Hold-up Values for Gas, Liquid and Solid Phases .....	91
4.5	Experiments Conducted in Semi-Batch Reactor .....	94
4.5.1	Single Synthetic Dye Solution Experiments .....	94
4.5.1.1	Ozonation Experiments .....	94
4.5.1.2	Catalytic Ozonation Experiments .....	98
4.5.1.3	Kinetics of Non-Catalytic and Catalytic Ozonation .....	102
5	CONCLUSIONS .....	107

6 RECOMMENDATIONS .....	110
REFERENCES.....	112
APPENDICES	
A CALIBRATION CURVES OF BB 41, BR 18.1 AND BY 28 DYES .....	118
B ANALYTICAL METHODS .....	120
B.1 KI Method for Ozone .....	120
B.2 Indigo Method for Dissolved O <sub>3</sub> Concentration in the Liquid Phase .....	123
B.3 The Calculation of Concentrations of BB 41, BR 18.1 and BY 28 Dyes in WW Solution .....	125
B.4 Calculation of Dye, TOC removals, O <sub>3</sub> Consumption and O <sub>3</sub> Consumption Rate .....	127
C AKSA WASTEWATER OZONATION EXPERIMENTS DATA.....	130
D SEMI-BATCH EXPERIMENTS DATA .....	176
E ACCURACY OF TOC AND COD RESULTS .....	185
F REPEATIBILITY OF THE EXPERIMENTS .....	196

## LIST OF TABLES

### TABLES

Table 3.1: Properties of AKSA textile wastewater samples .....	24
Table 3.2: The characteristic properties of dyes found in AKSA wastewater .....	26
Table 3.3: The surface area and pore size of alumina and PFOA catalysts .....	31
Table 3.4: The bulk and true densities of alumina and PFOA catalysts .....	32
Table 3.5: The semi-batch experimental parameters .....	33
Table 3.6: The fluidized bed experimental parameters .....	35
Table 4.1: The dye removals for different $COD_{in}$ , pH = free (4), $C_{O_3,G,in} = 0.9 \pm 0.1$ mmol/L gas, catalyst: none .....	44
Table 4.2: The COD and TOC removals with ozone consumption for different $COD_{in}$ , pH = free (4), $C_{O_3,G,in} = 0.9 \pm 0.1$ mmol/L gas, catalyst: none .....	45
Table 4.3: The observed reaction rate constants in terms of dye concentrations, $Q_G = 340$ L/h, $Q_L = 250$ L/h, pH = free (4), $C_{O_3,G,in} = 0.9 \pm 0.1$ mmol/L gas, catalyst: none .....	48
Table 4.4: The dye removals for different pH and $COD_{in}$ , $C_{O_3,G,in} = 0.9 \pm 0.1$ mmol/L gas, $Q_G = 340$ L/h, $Q_L = 250$ L/h, catalyst: none .....	52
Table 4.5: The TOC and COD removals with ozone consumptions for different pH and $COD_{in}$ , $C_{O_3,G,in} = 0.9 \pm 0.1$ mmol/L gas, $Q_G = 340$ L/h, $Q_L = 250$ L/h, catalyst: none .....	53
Table 4.6: The observed reaction rate constants in terms of dye concentrations for different $COD_{in}$ and pH values, $Q_G = 340$ L/h, $Q_L = 250$ L/h, $C_{O_3,G,in} = 0.9 \pm 0.1$ mmol/L gas, catalyst: none .....	55
Table 4.7: The surface areas obtained by BET method and the pore diameters of the catalyst particles .....	56
Table 4.8: The bulk and true densities measured for alumina and PFOA particles .....	57

Table 4.9: Elemental percentages of the fresh PFOA catalyst particles before and after bombardment .....	63
Table 4.10: Elemental percentages of the PFOA catalyst particles used for one, three and five times before and after bombardment .....	63
Table 4.11: The dye removals for different pH, $COD_{in}$ and catalyst type $C_{O_3,G,in} = 0.9 \pm 0.1$ mmol/L gas, $Q_G = 340$ L/h, $Q_L = 250$ L/h, $m_{cat} = 300$ g, for $Al_2O_3$ $H_E = 17$ cm, for PFOA $H_E = 18.3$ cm, $H_S = 5$ cm .....	69
Table 4.12: The TOC, COD removals with ozone consumption for different pH, $COD_{in}$ and catalyst type $C_{O_3,G,in} = 0.9 \pm 0.1$ mmol/L gas, $Q_G = 340$ L/h, $Q_L = 250$ L/h, $m_{cat} = 300$ g, for $Al_2O_3$ $H_E = 17$ cm, for PFOA $H_E = 18.3$ cm, $H_S = 5$ cm .....	70
Table 4.13: The dye removals for different pH, and catalyst type, $COD_{in} = 300$ mg/L ( $C_{d,in,BB\ 41} = 150.9$ mg/L, $C_{d,in,BR\ 18.1} = 26.4$ mg/L, $C_{d,in,BY\ 28} = 26.2$ mg/L, $C_{d,in} = 1570$ Pt-Co), $C_{O_3,G,in} = 0.9 \pm 0.1$ mmol/L gas, $Q_G = 340$ L/h, $Q_L = 250$ L/h, $m_{cat} = 300$ g, for $Al_2O_3$ $H_E = 17$ cm, for PFOA $H_E = 18.3$ cm, $H_S = 5$ cm .....	72
Table 4.14: The TOC, COD and color removals with ozone consumptions for different pH, and catalyst type, $COD_{in} = 300$ mg/L ( $C_{d,in,BB\ 41} = 150.9$ mg/L, $C_{d,in,BR\ 18.1} = 26.4$ mg/L, $C_{d,in,BY\ 28} = 26.2$ mg/L, $C_{d,in} = 1570$ Pt-Co), $C_{O_3,G,in} = 0.9 \pm 0.1$ mmol/L gas, $Q_G = 340$ L/h, $Q_L = 250$ L/h, $m_{cat} = 300$ g, for $Al_2O_3$ $H_E = 17$ cm, for PFOA $H_E = 18.3$ cm, $H_S = 5$ cm.....	73
Table 4.15: The effect of catalyst dosage on dye removals (in terms dye concentrations for each dye in WW solution) for different pH and $COD_{in}$ , $Q_G = 340$ L/h, $Q_L = 250$ L/h, $C_{O_3,G,in} = 0.9 \pm 0.1$ mmol/L gas .....	80
Table 4.16: The effect of catalyst dosage on TOC, COD removals with ozone consumption for different pH and $COD_{in}$ , $Q_G = 340$ L/h, $Q_L = 250$ L/h, $C_{O_3,G,in} = 0.9 \pm 0.1$ mmol/L gas .....	81
Table 4.17: The dye, TOC and COD removals with dispersion coefficients and $k_{LA}$ values (dye removals are in terms of Pt-Co Color unit), $T = 22^\circ C$ , $COD_{in} = 300$ mg/L, $C_{O_3,G,in} = 0.9 \pm 0.1$ mmol/L gas, $m_{cat} = 100$ g, for alumina $H_E = 15$ cm, for PFOA $H_E = 16.4$ cm, $H_S = 3$ cm .....	85
Table 4.18: The Yate's algorithm analysis for the effect of $Q_G$ and $Q_L$ on $k_{LA}$ , $COD_{in} = 300$ mg/L, $C_{d,in,BB\ 41} = 150.9$ mg/L, $C_{d,in,BR\ 18.1} = 26.4$ mg/L, $C_{d,in,BY\ 28} = 26.2$ mg/L, pH = 4, $C_{O_3,G,in} = 0.9 \pm 0.1$ mmol/L gas, catalyst: none .....	87
Table 4.19: The Yate's algorithm analysis for the effect of $Q_G$ and $Q_L$ on percent dye removals (in terms of Pt-Co), $COD_{in} = 300$ mg/L, $C_{d,in,BB\ 41} = 150.9$ mg/L, $C_{d,in,BR\ 18.1} = 26.4$ mg/L, $C_{d,in,BY\ 28} = 26.2$ mg/L, pH = 4, $C_{O_3,G,in} = 0.9 \pm 0.1$ mmol/L gas, catalyst: none.....	87

Table 4.20: The TOC, COD removals with ozone consumption for different $Q_G$ and $Q_L$ $COD_{in} = 300$ mg/L, $C_{d,in, BB\ 41} = 150.9$ mg/L, $C_{d,in, BR\ 18.1} = 26.4$ mg/L, $C_{d,in, BY\ 28} = 26.2$ mg/L, pH = 4, $m_{cat} = 300$ g, for alumina $H_E = 17$ cm, for PFOA $H_E = 18.3$ cm, $H_S = 5$ cm $C_{O_3,G,in} = 0.9 \pm 0.1$ mmol/L gas .....	89
Table 4.21: The dye removals with $D_L$ and $k_{La}$ for different $Q_G$ and $Q_L$ (dye removals are in terms of Pt-Co Color unit), $COD_{in} = 300$ mg/L, $C_{d,in, BB\ 41} = 150.9$ mg/L, $C_{d,in, BR\ 18.1} = 26.4$ mg/L, $C_{d,in, BY\ 28} = 26.2$ mg/L, pH = 4, $m_{cat} = 300$ g, for alumina $H_E = 17$ cm, for PFOA $H_E = 18.3$ cm, $H_S = 5$ cm $C_{O_3,G,in} = 0.9 \pm 0.1$ mmol/L gas .....	90
Table 4.22: Minimum fluidization velocities at the studied gas velocities; catalyst: PFOA, $m_{cat} = 150$ g, $d_{cat} = 3.0$ mm .....	91
Table 4.23: Minimum fluidization velocities at the studied gas velocities; catalyst: alumina, $m_{cat} = 150$ g, $d_{cat} = 3.0$ mm .....	91
Table 4.24: The calculated gas, liquid and solid-phase hold-up values under different operating conditions, catalyst: alumina, $m_{cat} = 300$ g .....	93
Table 4.25: The calculated gas, liquid and solid-phase hold-up values under different operating conditions, catalyst: PFOA, $m_{cat} = 300$ g .....	93
Table 4.26: Moles of ozone required to oxidize one mole of dye for each dye, $C_{d,in} = 250$ mg/L (for each dye), $Q_G = 150$ L/h, pH = 4, $C_{O_3,G,in} = 0.9 \pm 0.1$ mmol/L gas, catalyst: none .....	97
Table 4.27: Dye removal percentages for BB 41, BY 28 and BR 18.1 for different pH values and catalyst types, $C_{d,in} = 300$ mg/L (for each dye), stirrer rate = 300 rpm, $Q_G = 150$ L/h, $C_{O_3,G,in} = 0.9 \pm 0.1$ mmol/L gas, reaction time = 30 min .....	99
Table 4.28: TOC and COD removal percentages for BB 41, BY 28 and BR 18.1 for different pH values and catalyst types, $C_{d,in} = 300$ mg/L (for each dye), stirrer rate = 300 rpm, $Q_G = 150$ L/h, $C_{O_3,G,in} = 0.9 \pm 0.1$ mmol/L gas, reaction time = 90 min .....	102
Table 4.29: The pseudo-first order kinetic rate constants for BB 41, BY 28 and BR 18.1 for sole and catalytic ozonation, $C_{d,in} = 300$ mg/L (for each dye), stirrer rate = 300 rpm, $Q_G = 150$ L/h, $C_{O_3,G,in} = 0.9 \pm 0.1$ mmol/L gas .....	106

## LIST OF FIGURES

### FIGURES

Figure 2.1: Four canonical forms of ozone molecule .....	7
Figure 2.2: Mass transfer between phases. $P_{O_3}$ is the partial pressure of ozone, $P_{O_3,i}$ ( $P_{O_3}^*$ ) is the partial pressure of ozone at gas-liquid interface, $C_{O_3}$ and $C_{O_3,i}$ ( $C_{O_3}^*$ ) are ozone concentrations in bulk liquid and at gas-liquid interface respectively .....	12
Figure 2.3 The proposed mechanism of ozonation in the presence of non-polar alumina bonded phase (Kasprzyk et al., 2003) .....	22
Figure 3.1: Semi-batch experimental set-up .....	27
Figure 3.2: The configuration of porous fritted discs .....	29
Figure 3.3: The schematic diagram of liquid distributor .....	30
Figure 3.4: The schematic of the overall fluidized bed reactor system .....	30
Figure 3.5: The wavelength spectra of BB 41, BR 18.1 and BY 28 .....	37
Figure 3.6: The calibration curves for three dyes in their own solutions and in their mixture solutions .....	37
Figure 4.1: The effect of inlet COD value on blue dye degradation in WW solution, $Q_G = 170$ L/h, $Q_L = 150$ L/h, pH = free (4), $C_{O_3,G,in} = 0.9 \pm 0.1$ mmol/L gas, catalyst: none, dye concentration is shown by line, and ozone concentration in liquid phase by dotted line (----) .....	41
Figure 4.2: The effect of inlet COD value on red dye degradation in WW solution, $Q_G = 170$ L/h, $Q_L = 150$ L/h, pH = free (4), $C_{O_3,G,in} = 0.9 \pm 0.1$ mmol/L gas, catalyst: none, dye concentration is shown by line, and ozone concentration in liquid phase by dotted line (----) .....	42
Figure 4.3: The effect of inlet COD value on yellow dye degradation in WW solution, $Q_G = 170$ L/h, $Q_L = 150$ L/h, pH = free (4), $C_{O_3,G,in} = 0.9 \pm 0.1$ mmol/L gas, catalyst: none, dye concentration is shown by line, and ozone concentration in liquid phase by dotted line (----) .....	42

Figure 4.4: The effect of inlet COD value on TOC, COD removals and ozone consumption, (a) $Q_G = 170$ L/h, $Q_L = 150$ L/h, (b) $Q_G = 340$ L/h, $Q_L = 250$ L/h, pH = free (4), $C_{O_3,G,in} = 0.9 \pm 0.1$ mmol/L gas, catalyst: none .....	43
Figure 4.5: The effect of inlet COD value on dye degradation including all dyes in the WW in terms of Pt-Co color unit, $Q_G = 340$ L/h, $Q_L = 250$ L/h, pH = free (4), $C_{O_3,G,in} = 0.9 \pm 0.1$ mmol/L gas, catalyst: none, dye concentration is shown by line, and ozone concentration in liquid phase by dotted line (----) .....	44
Figure 4.6: The kinetic analysis of the WW ozonation reaction for different $COD_{in}$ concentrations in terms of dye concentrations (mg/L) in WW solution, $Q_G = 340$ L/h, $Q_L = 250$ L/h, pH = free (4), $C_{O_3,G,in} = 0.9 \pm 0.1$ mmol/L gas, catalyst: none, (a) BB 41, (b) BR 18.1 and (c) BY 28 .....	47
Figure 4.7: The effect of pH on dye removals (in terms of Pt-Co Color unit) and ozone concentration, $Q_G = 340$ L/h, $Q_L = 250$ L/h, $C_{O_3,G,in} = 0.9 \pm 0.1$ mmol/L gas, catalyst: none, (a) $COD_{in} = 180$ mg/L; (b) $COD_{in} = 300$ mg/L. In figures dye concentration is shown by line and ozone concentration in liquid phase by dotted line (----) .....	49
Figure 4.8: The effect of pH on dye removals (in terms dye concentrations for each dye in WW solution) and ozone concentration, $Q_G = 340$ L/h, $Q_L = 250$ L/h, $C_{O_3,G,in} = 0.9 \pm 0.1$ mmol/L gas, catalyst: none, $COD_{in} = 300$ mg/L, $C_{d,in,BB\ 41} = 150.9$ mg/L, $C_{d,in,BR\ 18.1} = 26.4$ mg/L, $C_{d,in,BY\ 28} = 26.2$ mg/L (a) BB 41, (b) BR 18.1, (c) BY 28. In figures dye concentration is shown by line and ozone concentration in liquid phase by dotted line (----).....	51
Figure 4.9: The effect of pH on TOC, COD removals and ozone consumption, $Q_G = 340$ L/h, $Q_L = 250$ L/h, $C_{O_3,G,in} = 0.9 \pm 0.1$ mmol/L gas, catalyst: none, (a) $COD_{in} = 180$ mg/L, (b) $COD_{in} = 300$ mg/L .....	53
Figure 4.10: The kinetic analysis of the WW ozonation reaction in terms of dye concentrations (mg/L) in WW solution, $Q_G = 340$ L/h, $Q_L = 250$ L/h, $C_{O_3,G,in} = 0.9 \pm 0.1$ mmol/L gas, catalyst: none, $COD_{in} = 300$ mg/L, $C_{d,in,BB\ 41} = 150.9$ mg/L, $C_{d,in,BR\ 18.1} = 26.4$ mg/L, $C_{d,in,BY\ 28} = 26.2$ mg/L, (a) pH = free (4), (b) pH = 10 .....	54
Figure 4.11: FT-IR Spectrum of Alumina .....	59
Figure 4.12: FT-IR Spectrum of PFO Acid .....	59
Figure 4.13: FT-IR Spectrum of PFOA catalyst .....	60
Figure 4.14: FT-IR Spectrum of PFOA catalyst used for one time .....	60
Figure 4.15: FT-IR Spectrum of PFOA catalyst used for three times .....	61
Figure 4.16: FT-IR Spectrum of PFOA catalyst used for five times .....	61
Figure 4.17: The effect of catalyst addition on blue dye (BB 41) removal (in terms dye concentrations for each dye in WW solution) and ozone concentration, $Q_G = 340$	

L/h,  $Q_L=250$  L/h,  $C_{O_3,G,in}=0.9 \pm 0.1$  mmol/L gas,  $COD_{in} = 300$  mg/L,  $C_{d,in,BB\ 41} = 150.9$  mg/L,  $C_{d,in,BR\ 18.1} = 26.4$  mg/L,  $C_{d,in,BY\ 28} = 26.2$  mg/L,  $m_{cat} = 300$  g, (a) pH = 4, (b) pH = 10, In figures dye concentration is shown by line and ozone concentration in liquid phase by dotted line (----) ..... 64

Figure 4.18: The effect of catalyst addition on red dye (BR 18.1) removal (in terms dye concentrations for each dye in WW solution) and ozone concentration,  $Q_G = 340$  L/h,  $Q_L=250$  L/h,  $C_{O_3,G,in}=0.9 \pm 0.1$  mmol/L gas,  $COD_{in} = 300$  mg/L,  $C_{d,in,BB\ 41} = 150.9$  mg/L,  $C_{d,in,BR\ 18.1} = 26.4$  mg/L,  $C_{d,in,BY\ 28} = 26.2$  mg/L,  $m_{cat} = 300$  g, (a) pH = 4, (b) pH = 10, In figures dye concentration is shown by line and ozone concentration in liquid phase by dotted line (----) ..... 65

Figure 4.19: The effect of catalyst addition on yellow dye (BY 28) removal (in terms dye concentrations for each dye in WW solution) and ozone concentration,  $Q_G = 340$  L/h,  $Q_L=250$  L/h,  $C_{O_3,G,in}=0.9 \pm 0.1$  mmol/L gas,  $COD_{in} = 300$  mg/L,  $C_{d,in,BB\ 41} = 150.9$  mg/L,  $C_{d,in,BR\ 18.1} = 26.4$  mg/L,  $C_{d,in,BY\ 28} = 26.2$  mg/L,  $m_{cat} = 300$  g, (a) pH = 4, (b) pH = 10, In figures dye concentration is shown by line and ozone concentration in liquid phase by dotted line (----) ..... 66

Figure 4.20: The effect of Alumina and PFOA catalysts on TOC and COD removals with ozone consumption.  $Q_G=340$  L/h,  $Q_L=250$  L/h,  $C_{O_3,G,in}=0.9 \pm 0.1$  mmol/L gas, catalyst:  $Al_2O_3$  and PFOA,  $m_{cat}=300$  g,  $COD_{in}=300$  mg/L, (a) pH = 4; (b) pH = 10, for  $Al_2O_3\ H_E = 17$  cm, for PFOA  $H_E = 18.3$  cm,  $H_S = 5$  cm ..... 68

Figure 4.21: The effect of pH on overall color removals (in terms of Pt-Co unit) and ozone concentration,  $Q_G = 340$  L/h,  $Q_L=250$  L/h,  $C_{O_3,G,in}=0.9 \pm 0.1$  mmol/L gas, catalyst: (a) none, (b) Alumina, (c) PFOA,  $COD_{in} = 300$  mg/L ( $C_{d,in} = 1570$  Pt-Co),  $m_{cat} = 300$  g. In figures dye concentration is shown by line and ozone concentration in liquid phase by dotted line (----) ..... 72

Figure 4.22: The effect of pH on TOC, COD removals and ozone consumption,  $Q_G = 340$  L/h,  $Q_L=250$  L/h,  $C_{O_3,G,in}=0.9 \pm 0.1$  mmol/L gas, catalyst: (a) none, (b) Alumina, (c) PFOA,  $COD_{in} = 300$  mg/L ( $C_{d,in,BB\ 41} = 150.9$  mg/L,  $C_{d,in,BR\ 18.1} = 26.4$  mg/L,  $C_{d,in,BY\ 28} = 26.2$  mg/L,  $C_{d,in} = 1570$  Pt-Co),  $m_{cat} = 300$  g ..... 74

Figure 4.23: The effect of catalyst dosage on dye removals (in terms dye concentrations for each dye in WW solution) and ozone concentration,  $Q_G = 340$  L/h,  $Q_L=250$  L/h,  $C_{O_3,G,in}=0.9 \pm 0.1$  mmol/L gas, catalyst: Alumina, pH = 4,  $COD_{in} = 300$  mg/L ( $C_{d,in,BB\ 41} = 150.9$  mg/L,  $C_{d,in,BR\ 18.1} = 26.4$  mg/L,  $C_{d,in,BY\ 28} = 26.2$  mg/L), (a) BB 41, (b) BR 18.1, (c) BY 28. In figures dye concentration is shown by line and ozone concentration in liquid phase by dotted line (----) ..... 76

Figure 4.24: The effect of catalyst dosage on dye removals (in terms dye concentrations for each dye in WW solution) and ozone concentration,  $Q_G = 340$  L/h,  $Q_L=250$  L/h,  $C_{O_3,G,in}=0.9 \pm 0.1$  mmol/L gas, catalyst: PFOA, pH = 4,  $COD_{in} = 300$  mg/L ( $C_{d,in,BB\ 41} = 150.9$  mg/L,  $C_{d,in,BR\ 18.1} = 26.4$  mg/L,  $C_{d,in,BY\ 28} = 26.2$  mg/L), (a) BB 41, (b) BR 18.1, (c) BY 28. In figures dye concentration is shown by line and ozone concentration in liquid phase by dotted line (----) ..... 77

Figure 4.25: The effect of catalyst dosage on TOC, COD removals with ozone consumption, $Q_G = 340$ L/h, $Q_L=250$ L/h, $C_{O_3,G,in}=0.9 \pm 0.1$ mmol/L gas, catalyst: Alumina, pH = 4, $COD_{in} = 300$ mg/L .....	78
Figure 4.26: The effect of catalyst dosage on TOC, COD removals with ozone consumption, $Q_G = 340$ L/h, $Q_L=250$ L/h, $C_{O_3,G,in}=0.9 \pm 0.1$ mmol/L gas, catalyst: PFOA, pH = 4, $COD_{in} = 300$ mg/L .....	78
Figure 4.27: The effect of $Q_G/Q_L$ ratio on TOC and COD removals with ozone consumption (dye removals are in terms of Pt-Co Color unit), T = 22°C, $COD_{in} = 300$ mg/L, $C_{d,in,BB 41} = 150.9$ mg/L, $C_{d,in,BR 18.1} = 26.4$ mg/L, $C_{d,in,BY 28} = 26.2$ mg/L, $C_{O_3,G,in} = 0.9 \pm 0.1$ mmol/L gas, pH = 4, catalyst: none. In figures percent removals are shown by line and ozone consumption by dotted line (----) .....	83
Figure 4.28: The effect of $Q_G/Q_L$ ratio on dye removals (in terms dye concentrations for each dye in WW solution) with $D_L$ and $k_{La}$ values, T = 22°C, $COD_{in} = 300$ mg/L, $C_{d,in,BB 41} = 150.9$ mg/L, $C_{d,in,BR 18.1} = 26.4$ mg/L, $C_{d,in,BY 28} = 26.2$ mg/L, $C_{O_3,G,in} = 0.9 \pm 0.1$ mmol/L gas, pH = 4, catalyst: none. In figures percent removals are shown by line and $D_L$ and $k_{La}$ by dotted line (----) .....	83
Figure 4.29: The effect of $Q_G/Q_L$ ratio on TOC and COD removals with ozone consumption (dye removals are in terms of Pt-Co Color unit), T = 22°C, $COD_{in} = 300$ mg/L, $C_{d,in,BB 41} = 150.9$ mg/L, $C_{d,in,BR 18.1} = 26.4$ mg/L, $C_{d,in,BY 28} = 26.2$ mg/L, $C_{O_3,G,in} = 0.9 \pm 0.1$ mmol/L gas, pH = 4, catalyst: alumina. In figures percent removals are shown by line and ozone consumption by dotted line (----) .....	84
Figure 4.30: The effect of $Q_G/Q_L$ ratio on dye removals (in terms dye concentrations for each dye in WW solution) with $D_L$ and $k_{La}$ values, T = 22°C, $COD_{in} = 300$ mg/L, $C_{d,in,BB 41} = 150.9$ mg/L, $C_{d,in,BR 18.1} = 26.4$ mg/L, $C_{d,in,BY 28} = 26.2$ mg/L, $C_{O_3,G,in} = 0.9 \pm 0.1$ mmol/L gas, pH = 4, catalyst: alumina. In figures percent removals are shown by line and $D_L$ and $k_{La}$ by dotted line (----) .....	84
Figure 4.31: $C_d/C_{d,i}$ for different $Q_G$ and $Q_L$ on blue dye (BB 41) removals (in terms dye concentrations in WW solution) and ozone concentration in liquid phase, $Q_G/Q_L = 1$ $C_{O_3,G,in}=0.9 \pm 0.1$ mmol/L gas, catalyst: none, pH = 4, $COD_{in} = 300$ mg/L, $C_{d,in,BB41} = 150.9$ mg/L, $C_{d,in,BR 18.1} = 26.4$ mg/L, $C_{d,in,BY 28} = 26.2$ mg/L. In figures dye concentration is shown by line and ozone concentration in liquid phase by dotted line (----).....	88
Figure 4.32: $C_d/C_{d,i}$ for different $Q_G$ and $Q_L$ on red dye (BR 18.1) removals (in terms dye concentrations in WW solution) and ozone concentration in liquid phase, $Q_G/Q_L = 1$ $C_{O_3,G,in}=0.9 \pm 0.1$ mmol/L gas, catalyst: none, pH = 4, $COD_{in} = 300$ mg/L, $C_{d,in,BB41} = 150.9$ mg/L, $C_{d,in,BR 18.1} = 26.4$ mg/L, $C_{d,in,BY 28} = 26.2$ mg/L. In figures dye concentration is shown by line and ozone concentration in liquid phase by dotted line (----).....	88
Figure 4.33: $C_d/C_{d,i}$ for different $Q_G$ and $Q_L$ on yellow dye (BY 28) removals (in terms dye concentrations in WW solution) and ozone concentration in liquid phase, $Q_G/Q_L = 1$ $C_{O_3,G,in}=0.9 \pm 0.1$ mmol/L gas, catalyst: none, pH = 4, $COD_{in} = 300$ mg/L, $C_{d,in,BB 41} = 150.9$ mg/L, $C_{d,in,BR 18.1} = 26.4$ mg/L, $C_{d,in,BY 28} = 26.2$ mg/L. In figures dye	

concentration is shown by line and ozone concentration in liquid phase by dotted line (----) .....	89
Figure 4.34: Dye removals with ozonation for BB 41, BY 28 and BR 18.1, $C_{d,in} = 300$ mg/L (for each dye), stirrer rate = 300 rpm, $Q_G = 150$ L/h, $C_{O_3,G,in} = 0.9 \pm 0.1$ mmol/L gas, catalyst: none, (a) pH = 4, (b) pH = 10 .....	96
Figure 4.35: COD and TOC removals after 90 min. ozonation for BB 41, BY 28 and BR 18.1, $C_{d,in} = 300$ mg/L (for each dye), stirrer rate = 300 rpm, $Q_G = 150$ L/h, $C_{O_3,G,in} = 0.9 \pm 0.1$ mmol/L gas, catalyst: none, (a) pH = 4, (b) pH = 10 .....	98
Figure 4.36: COD and TOC removals after 90 min. ozonation for BB 41, $C_{d,in} = 300$ mg/L, stirrer rate = 300 rpm, $Q_G = 150$ L/h, $C_{O_3,G,in} = 0.9 \pm 0.1$ mmol/L gas, pH = 10 ..	100
Figure 4.37: COD and TOC removals after 90 min. ozonation for BY 28, $C_{d,in} = 300$ mg/L, stirrer rate = 300 rpm, $Q_G = 150$ L/h, $C_{O_3,G,in} = 0.9 \pm 0.1$ mmol/L gas, pH = 4 ....	101
Figure 4.38: COD and TOC removals after 90 min. ozonation for BR 18.1, $C_{d,in} = 300$ mg/L, stirrer rate = 300 rpm, $Q_G = 150$ L/h, $C_{O_3,G,in} = 0.9 \pm 0.1$ mmol/L gas, pH = 10 .....	101
Figure 4.39: The pseudo-first order kinetic analysis, $C_{d,in} = 300$ mg/L (for each dye), stirrer rate = 300 rpm, $Q_G = 150$ L/h, $C_{O_3,G,in} = 0.9 \pm 0.1$ mmol/L gas, catalyst: none; (a) pH = 4, (b) pH = 10 .....	103
Figure 4.40: The pseudo-first order kinetic analysis, $C_{d,in} = 300$ mg/L (for each dye), stirrer rate = 300 rpm, $Q_G = 150$ L/h, $C_{O_3,G,in} = 0.9 \pm 0.1$ mmol/L gas, catalyst: PFOA; (a) pH = 4, (b) pH = 10 .....	104
Figure 4.41: The pseudo-first order kinetic analysis, $C_{d,in} = 300$ mg/L (for each dye), stirrer rate = 300 rpm, $Q_G = 150$ L/h, $C_{O_3,G,in} = 0.9 \pm 0.1$ mmol/L gas, catalyst: alumina; (a) pH = 4, (b) pH = 10 .....	105

## LIST OF SYMBOLS

$a$	gas-liquid interfacial area for gas bubbles, $\text{m}^2/\text{m}^3$ reactor
$A$	crosssectional area of the fluidized bed reactor, $\text{m}^2$
$A_{BET}$	surface area of the catalyst as BET, $\text{m}^2/\text{g}$
$Appl_{O_3}$	applied $O_3$ dose, $\text{mmol/L}$ liq
$b$	stoichiometric coefficient
BB 41	Basic Blue 41
BR 18.1	Basic Red 18.1
BY 28	Basic Yellow 28
BOD	biological oxygen demand, $\text{mg/L}$
$C_B$	concentration of reactant B, $\text{mM}$
$C_d$	the concentration of dye in the liquid phase, $\text{mg/L}$
$C_{d,i}$	initial dye concentration, $\text{mg/L}$
$C_{d,i, BB41}$	initial BB 41 concentration, $\text{mg/L}$
$C_{d,i, BR18.1}$	inlet BR 18.1 concentration, $\text{mg/L}$
$C_{d,i, BY28}$	inlet BY 28 concentration, $\text{mg/L}$
$C_{d,in}$	inlet dye concentration, $\text{mg/L}$
$C_{d,in, BB41}$	inlet BB 41 concentration, $\text{mg/L}$
$C_{d,in, BR18.1}$	inlet BR 18.1 concentration, $\text{mg/L}$
$C_{d,in, BY28}$	inlet BY 28 concentration, $\text{mg/L}$
$C_{O_3,G}$	gas phase ozone concentration, $\text{mmol/L}$ gas
$C_{O_3,G,in}$	inlet gas phase ozone concentration, $\text{mmol/L}$ gas
$C_{O_3,G,out}$	outlet gas phase ozone concentration, $\text{mmol/L}$ gas
$C_{O_3}$	the concentration of $O_3$ in the liquid phase, $\text{mM}$
$C_{O_3}^*$	equilibrium concentration of dissolved ozone, $\text{mmol/L}$ liq
$C_{O_3,i}$	concentration of ozone at the gas-liquid interface, $\text{mmol/L}$ liq
COD	chemical oxygen demand, $\text{mg/L}$
$COD_{in}$	inlet COD, $\text{mg/L}$

$COD_{out}$	outlet COD, mg/L
$C_{OH^-}$	the concentration of hydroxyl ions, mmol/L
$Cons_{O_3}$	$O_3$ consumption in the fluidized bed reactor, mmol/L liq
$d_{cat}$	catalyst particle size, mm
$d_{pore}$	catalyst pore diameter, °A
$D_A$	diffusivity of reactant A, $m^2/s$
$D_B$	diffusivity of reactant B, $m^2/s$
$D_L$	axial dispersion coefficient for liquid phase, $m^2/s$
$D_{O_3}$	ozone dosage, mmol/h
$E$ :	enhancement factor
$E_i$	instantaneous enhancement factor
$h$	height of the aerated liquid in the column, m
$h_o$	original liquid height before the gas flow, m
$H$	Henry's Law constant for ozone, atm
$H_E$	expanded bed height, cm
$H_S$	static bed height, cm
$k_d$	decomposition rate constant of ozone in water, $s^{-1}$
$k_L$	mass transfer coefficient in the liquid film $m^3$ liquid/ $m^2$ surface.s
$k_{LA}$ :	volumetric mass transfer coefficient in liquid film, $s^{-1}$
$(k_{LA})_E$	enhanced volumetric mass transfer coefficient in liquid film, $s^{-1}$
$k_s$	film coefficient around the catalyst particle, $m^3$ reactor/ $(m^2$ catalyst.s)
$k$	rate constant between dye and ozone in the bulk liquid, $(mM)^{-1} (s)^{-1}$
$k'$	pseudo first order rate constant in the bulk liquid, $s^{-1}$
$m_{cat}$	catalyst dosage, g
$M_H$	<i>Hatta</i> number
$n$	the order of hydroxyl radical concentration in ozone decomp. reaction
$P_{O_3}$	pressure of reactant $O_3$ in the gas bulk, Pa or kPa
$P_{O_3,i}$	partial pressure of reactant $O_3$ at gas-liquid interface, Pa or kPa
$P_{O_3}^*$	equilibrium pressure of reactant $O_3$ at gas-liquid interface, Pa or kPa
PFOA	perfluorooctyl alumina
PZC	point of zero charge
$R_{cons,O_3}$	$O_3$ consumption rate, %
$Q_G$	volumetric flow rate of gas, L/h
$Q_L$	volumetric flow rate of liquid, L/h

$Re$	Reynolds number, $u_L \cdot d_{cat} \cdot \rho_{cat} / \mu_L$
$t$	time, s or min
$T$	temperature, °C or K
TOC	total organic carbon, mg/L
$TOC_{in}$	inlet TOC, mg/L
$TOC_{out}$	outlet TOC, mg/L
TSS	total suspended solids, mg/L
$u_G$	superficial gas velocity, m/s
$u_L$	superficial liquid velocity, m/s
$u_{L,min}$	minimum fluidization velocity, m/s
$z$	column or reactor height, m

***Greek Letters***

$\varepsilon_G$	gas hold-up
$\varepsilon_L$	liquid hold-up
$\varepsilon_S$	solid hold-up
$\lambda_{max}$	maximum wavelength, nm
$\rho_{cat}$	catalyst density, g catalyst/m <sup>3</sup> catalyst
$\rho_L$	liquid density, kg/m <sup>3</sup>
$\mu_L$	liquid viscosity, kg/(m.s)
$\rho_w$	water density, kg/m <sup>3</sup>
$\tau$	relative residence time of the liquid in the fluidized bed reactor, min
$\mu_w$	water viscosity, kg/(m.s)

## **CHAPTER 1**

### **INTRODUCTION**

The textile industry being one of the very important and developing industries in Turkey, is the source of large amounts of colored and toxic wastewaters; because of its need to large volumes of water is used in different production steps. After dyeing process, dyes which could not be fixed onto the cloth are released to wastewater streams and cause high color intensity. It is indicated in literature that about the half of reactive dyes, 8 to 20% of dispersed dyes and 1% of pigments remain unfixed in the solution and are sent to the treatment processes (Hassan et al., 2006; Pirgalioglu, 2008).

The treatment of wastewaters from the textile industry becomes an important problem, since they contain different dye types and harmful compounds reducing the rate of self-purification processes in the environment and causing carcinogenic effects on human health. One of the reasons for the treatment of textile wastewater being a problem is that the conventional treatment methods [chemical-physical methods (chemical precipitation and flocculation) and biological methods] are not sufficient because of the stability of textile wastes to light and biological degradation (Zhao et al., 2006). This is the reason why alternative methods are among recent studies such as chemical oxidation including ozonation, advanced oxidation processes, chlorination besides membrane and adsorption processes (Likou et al., 1997; Ciardelli, 2001).

The use of ozone as a chemical oxidant is one of the promising and recently used methods for the color removal of the industrial textile wastewaters. During ozonation of a wastewater, ozone firstly attacks unsaturated bonds of chromophores providing the rapid removal of color (Soares et al., 2006). Ozone can degrade the complex

organic molecules to smaller ones such as organic acids, aldehydes and ketones. This provides color removal; however, sole ozonation is not enough for the removal of by-products completely. The difficulty of removing recalcitrant by-products, low ozone solubility and stability in water and high cost of ozone production bring the need for advanced oxidation processes (AOPs). Thus, higher total organic carbon (TOC), biological oxygen demand (BOD) and chemical oxygen demand (COD) reductions are possible due to the mineralization of by-products to water and CO<sub>2</sub>. Some important AOPs can be listed as the use of ozone together with some chemicals or combination with UV radiation and some chemicals [O<sub>3</sub>/H<sub>2</sub>O<sub>2</sub>, H<sub>2</sub>O<sub>2</sub>/Fe<sup>+2</sup> (Fenton's reagent), O<sub>3</sub>/UV, H<sub>2</sub>O<sub>2</sub>/UV, O<sub>3</sub>/H<sub>2</sub>O<sub>2</sub>/UV] and catalytic ozonation (Acar and Özbelge, 2006). One of the main purposes of the AOPs is the generation of hydroxyl radicals (HO<sup>•</sup>) which are more powerful and active than ozone. In this case, ozone can decompose into these species which provide higher oxidation potential for organic pollutants and their by-products.

Although generation of powerful oxidants seems to be the solution to the removal of by-products from wastewater, the non-selective hydroxyl radicals can be scavenged by the other species that can be present in wastewaters and this may decrease the selectivity of the oxidation reaction against the target organic pollutants (Soares et al., 2006; Acar and Özbelge, 2006). This disadvantage necessitates new studies on ozonation systems to enhance the ozone solubility and stability in the reaction media. Catalytic ozonation using metals and metal oxides as catalysts is known as one of the AOP methods which is based on ozone decomposition and radical formation. On the other hand, solid-liquid ozonation systems carried out in the presence of non-polar heterogeneous catalysts, such as perfluorinated alumina bonded phases, involve the liquid-liquid extraction of organic substances from the aqueous phase into the organic phase and subsequent oxidation by molecular ozone dissolved also in this organic phase (non-polar perfluorinated hydrocarbon solvent saturated with ozone) (Kasprzyk-Hordern et al., 2005; Erol and Özbelge, 2007; Kasprzyk-Hordern et al., 2003). Ozone solubility is known to be ten times higher in fluorinated hydrocarbon solvents than that in water. Perfluorooctyl alumina (PFOA) prepared using perfluorooctanoic (PFO) acid was reported to increase the stability of ozone in perfluorinated solvent (Kasprzyk-Hordern et al., 2004). Accordingly, molecular

ozone and organics dissolve in non-polar perfluorinated alkyl chains on the alumina surface and react with each other.

The degree of color removal and the increase in biodegradability (BOD to COD ratio) are related to the applied ozone dosage and chemical composition of the wastewater. Sole ozonation and catalytic ozonation reactions are also pH dependent. At acidic pH, while ozone reacts directly with organic and/or inorganic pollutants, the radicals resulting from the decomposition of ozone at basic pH are the main oxidants. In other words, at basic pH indirect oxidation by radicals occurs (Chu et al., 1999). It is known that there are many variable compounds which act as an oxidation initiator (e.g., hydrogen peroxide or some metallic ions), a promoter (alcohol) or a scavenger ( $\text{CO}_3^{2-}$ ,  $\text{HCO}_3^-$ ) in these oxidation reactions (Erol and Özbelge, 2009). Therefore, their occurrences and amounts may be important on the removal rates of target organics.

In this study, an investigation for the oxidation of an industrial textile wastewater by catalytic ozonation was aimed by using alumina (a metal oxide) and PFOA catalysts. The ozonation experiments were conducted in a three phase fluidized bed reactor in order to see the efficiency of a continuous system thought to be more applicable to industry. In addition, the effect of different operating parameters (gas and liquid flowrates, solution pH and catalyst dosage) on dye decolorization and by-product mineralization in terms of dye, COD and TOC removals besides the kinetics of ozonation reaction were also examined.

## CHAPTER 2

### LITERATURE SURVEY

#### 2.1 Textile Wastewaters

Textile wastewaters are considered as one of the most important pollutants because of their large varieties of organic and inorganic contents and high color intensities. Textile industry basically includes the production of fabrics from fibers such as cotton, wool and synthetics (nylon, polyester, acrylics) with a number of processes (Cooper, 1978). The annual world production of textiles is about 30 million tons, requiring  $7 \times 10^5$  tons of different dyes per year (Zhao et al., 2006; Talarposhti et al., 2001). As a result, near large amounts of water, dyes and different chemicals are used in these processes causing polluted wastewaters to emerge (Yong et al., 2005). Wastewaters from textile industry are mainly discharged from two process steps being preparation and dyeing processes. Almost all of wastewater discharged from preparation processes has variable constituents depending on the type of products. The constituents of dyeing process wastewater consist of dyes, salts and surfactants (Srisukphun, 2006). The source of dye content of wastewater is obviously the residual dyes that are not fixed on the fibers during dyeing processes. It is known that about 30% of dyes applied remain in the solution unattached to the textiles (Vandevivere et al., 1998; Yong et al., 2005) depending on the fiber, depth of shade and dye type. Reactive dyes, for instance occur at high concentrations in waste streams due to their low fixation to cellulosic fibers.

Dyes used in textile dyeing processes have a great variety of different chemical structures, primarily based on aromatic and heterocyclic groups such as aromatic amine ( $C_6H_5-NH_2$ ) which is a suspected carcinogen, phenyl ( $C_6H_5-CH_2$ ) and naphthyle ( $NO_2-OH$ ) (Talarposhti et al., 2001). These dyes are mainly classified as

acid, basic, direct, disperse and reactive dyes due to their properties. Acid dyes are typically applied to acrylics, wool, nylon and nylon/cotton blends. These are usually used to dye nitrogenous fibers or fabrics in organic and inorganic acid solutions; a chemical reaction between the fiber and dye yields an insoluble color molecule on the fiber (Kulkarni et al., 1985). The two most commercially used acid dyes are azo and anthraquinone dyes. Direct dyes are mostly used in dyeing process of cotton and other cellulosic fibers. These dyes are applied to the fabrics in an aqueous solution of ionic salts or electrolytes; because in this case, dye attaches to the fiber by electrostatic forces. Disperse dyes, on the other hand, are more colloidal and have very low solubility. They are applied mostly to the polyester, nylon, acetate and triacetate fibers from a dye bath as dispersions by direct colloidal absorptions (Kulkarni et al., 1985). Reactive dyes have a chromophore type structure that provides a direct reaction with fiber substrates. Covalent bonds formed as a result of this reaction become responsible for the attaching of dye molecules to the fibers, mostly cotton or cellulosic based. Moreover, basic dyes also known as cationic dyes are used in acrylic, nylon and wool dyeing. They have positively charged colored part and can easily bond to the carboxyl or sulfonic groups on a fiber due to the formation of salt links with these anionic groups in the fiber.

The complex chemical structure of organic pigments in dyes prevents the breakdown of dye molecules and they can remain during the lifetime of fabrics. The structure also provides resistance to sunlight, water, soap etc. and thus, dye house effluent treatment becomes difficult. Near dye content, high 'chemical oxygen demand' (COD), 'total organic carbon' (TOC) and 'biological oxygen demand' (BOD) of textile wastewaters due to its contents make them problematic for the environment. In addition, very low BOD/COD ratio of dye house effluents makes the treatment of them a problem because conventional treatment methods are not efficient enough. Conventional treatment methods involves a primary treatment which separates the suspended solids, oils and fats followed by a biological treatment commonly activated sludge (Soares et al., 2006); but the non-biodegradability of textile wastewaters leads the researchers to technologies that are more efficient. In industry, membrane filtration processes, activated carbon adsorption, ion exchange resins, chemical coagulation, electrochemical methods and oxidation with Fenton's reagent or ozone have already been applied in the removal of colored effluents (Soares et al.,

2006; Erol, 2008). Even though by chemical coagulation and carbon adsorption a dye removal of about 90% of some types of dyes is possible, the production of large amounts of solid waste and the operational costs for sludge disposal make these processes not much useable (Zhao et al., 2006). Oxidation with ozone as Chu et. al. (1999) indicated might be an affordable and easy-operated control technology in the removal of colored dyestuffs and other pollutants from textile wastewaters.

### **2.1.1 Oxidation with Ozone in Textile Wastewater Treatment**

Ozonation for color degradation might be a promising process providing advantages such as leaving no chemical sludge after the process, having ability to degrade both color and organic pollutant in one step and having less danger because no stock of any chemical (like hydrogen peroxide) is essential and residual ozone can decompose easily to oxygen in water (Chu et al., 1999). As reported in literature, ozone can provide a color removal of above 90% depending on process conditions with a moderate TOC and COD reductions because of the resistance of by-products such as carboxylic acids or aldehydes to further oxidation by ozone (Slokar et al., 1998). There have been many studies done on ozonation of colored solutions in order to investigate if the process is viable or not.

Soares and her colleagues (2006) have done a study on ozonation of textile effluents and found out between 76 and 100% color removal efficiencies for different ozone doses. As a result, they indicated that ozonation is effective for decolorization of an acid dye; but slightly effective on TOC removal since they obtained not more than 20% removals for TOC. Hsu et. al. (2001) have studied the decolorisation of mixed dye solutions in a gas-induced reactor and obtained between 90.15% and 97.87% color removals depending on the dye concentrations; however, they could not achieve more than 33% COD removals. Moreover, a study made by Wu et. al. (2000) showed that a 100% of color removal can be achieved in 35 min with an applied ozone dose of 26.1 mg/L.min and an initial dye concentration of 0.5 g/L. Also they have found out that ozonation can increase the biodegradability of the wastewater 11 to 66 times by increasing BOD/COD ratio. Kos and Perkowski (2003) wanted to show the efficiency rates of different treatment processes on different types of dye

house effluents. They obtained between 92% and 100% of color removal by ozonation.

As it can be observed from the literature while oxidation processes with ozone only can yield higher decolorisation, it becomes inefficient for further organic removals. This disadvantage of ozonation leads researchers to investigate the ozonation process more deeply and design new methods combined with ozonation.

## 2.2 Ozone

Ozone ( $O_3$ ) whose structure is triatomic form of oxygen is an unstable gas having a very characteristic odor. Ozone is formed in the earth's stratosphere photochemically, but exists in ground levels only in low concentrations. Although ozone is a blue colored gas at normal temperatures and pressures; because of its low concentrations in its applications the observation of this blue color of ozone is impossible (Rice et al., 1982). Ozone gas is produced by electrical discharge method in ozone generators. Oxygen molecules ( $O_2$ ) with two oxygen atoms are disconnected to form oxygen atoms (O) and then these formed atoms combined with oxygen molecules to generate ozone molecules ( $O_3$ ). Ozone gas is sparingly soluble in water. It decomposes back to oxygen, from which it is formed, rapidly in aqueous solution containing impurities, but more slowly in pure water or in the gaseous phase (Rice et al., 1982).

Depending on many investigations as described in literature; ozone molecule has a structure of a resonance hybrid of the four canonical forms which are represented in Figure 2.1.

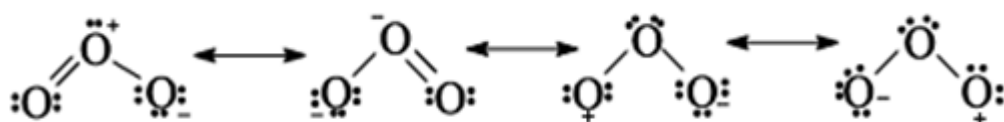


**Figure 2.1** Four canonical forms of ozone molecule

In the industry, ozonation has many different and wide application areas. Its oxidative properties and advantages provide ozone to be used in very different and interesting fields and give ozone the opportunity to leave the other methods behind in their application areas. It passes chlorination for instance in the field of disinfection due to its advantages such as killing bacteria and viruses more effectively. Some other applications of ozonation processes can be listed as drinking water purification, air purification, wastewater treatment, odor removal, sterilization, removal of pesticides, color removal, food industry and aquaculture (Hsing et al., 2006).

### 2.2.1 Ozonation Process

Ozone has an electrical potential of  $E^0 = 2.07$  Volts which gives ozone the ability of being a strong oxidizing agent (Soares et al., 2006). According to Eriksson (Eriksson, 2005), ozone reacts electrophilically due to its hybrid structure provided by the equally shared electrons between three oxygen atoms.

At ordinary temperatures and pressures ozone is in gas state, and thus, in order to give reactions in aqueous phase the mass transfer of ozone into liquid is needed. After ozone transferred into solution, it reacts with the organic pollutants by both directly as molecular ozone or indirectly taking role in the formation of oxidative radicals by its decomposition (Hoigné et al., 1976; Staehelin et al., 1985; Carriere et al., 1993). Direct or indirect ozonation reactions occur depending on pH. At acidic pH, decomposition rate of ozone is very slow and negligible; thus, molecular ozone reacts directly with organics or inorganics and oxidizes them according to the reactions given below (Yurteri et al., 1988):



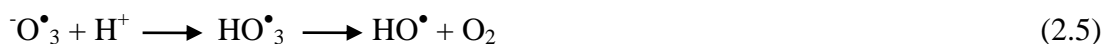
If ozone is used to oxidize the dye molecules in the solution, ozone firstly attacks the chromophore group of the dye and breaks the chromophore structure (Lopez-Lopez et al., 2007; Soares et al., 2007). According to the studies in literature, molecular ozone reacts with organics such as amines, phenols and aromatic compounds easily; but on the other hand, the reaction of carboxylic acids, aldehydes and alcohols with

ozone occur more slowly (Hoigné et al., 1983). Obviously, it can be concluded that the direct ozone reactions are selective and depends on the target compound.

Ozone decomposition starts to occur when pH exceeds 7 by the reaction of hydroxyl ions (OH<sup>-</sup>) with O<sub>3</sub>. The decomposition of ozone provides the formation of hydroxyl radicals and enhances the hydroxyl radical reactions with organics (Park et al., 2004). Oyama et al. (2000) and Chu et al. (1999) have mentioned that while at acidic pH, molecular ozone reacts with organics, at pH values above 7 the high rate of ozone decomposition causes the indirect reactions between hydroxyl radicals and organics to occur. The higher electrical potential (2.08 V) of hydroxyl radicals gave them a higher oxidation capability than that of ozone. This provides non-selective reactions to occur in the reaction media (Buxton et al., 1988). Hoigne et al. (Staehelin et al., 1985) proposed the possible decomposition reaction of ozone as follows:



Starting with the self-decomposition reaction of ozone, indirect oxidation reactions enhanced with HO<sup>•</sup> proceed to occur mostly in alkaline medium. After ozone decomposition, the following reactions in aqueous phase occur:



As a result, it can easily be seen that, in the ozonation process both direct and indirect oxidation by ozone and hydroxyl radicals are important for the dye, TOC and COD removals. The pH of the solution becomes an important parameter for the ozonation reactions, since it affects the mechanism and pathway of the reactions by causing direct or radical oxidation of the organics. Moreover, according to many studies, the structure of the target pollutant has an important effect on which reaction yields higher reaction rates (Beltran et al., 2002); in other words, while molecular ozone prefers to react with aromatic type structures, radicals are less selective and

attack both to dye molecules and by-products of dye oxidation reactions such as carboxylic acids or aldehydes achieving higher TOC and COD removals besides dye removals (Wang et al., 2003).

Obviously, since the effect of pH on the ozonation process should not be ignored, many studies investigating the pH effect have been made. Depending on these studies, it can be concluded that although COD and TOC removals increase with increasing pH (Alaton et al., 2002), dye decolorisation rates do not have a certain trend with pH. Moussavi and Mahmoudi (2009) obtained a dye removal of 91% at an acidic pH of 2 and 85% at pH 6 in the ozonation of an azo dye. At pH near 10, the removal reached to 97% due to the decomposition of ozone and formation of non-selective hydroxyl radicals. On the other hand, Arslan et al. (2001) obtained higher color removals by ozonation of a dispersed dye solution at acidic pH and concluded that the oxidation of the target compound by ozonation must depend on its structure and solubility at different pHs. Moreover, Konsowa (2003) have investigated the decolorisation time of a reactive dye and obtained a 32% decrease when increase the pH from 2 to 12. Similarly, Koyuncu et al. (1996) investigated the ozonation of several dyes at pH = 2 and pH = 9; and they observed an increase in the removals at basic pH of 9.

The uncertainty in the dye decolorization rates with pH leads the fact that the rate of decolorisation mainly depends on the type of dye to be ozonated. While for some dyes, molecular ozone attacks the dye molecule faster, others need more powerful oxidants namely hydroxyl radicals and this emerges dependency of effective ozonation on pH. According to Chu and Ma (1999) increasing pH enhances the removals of azo dyes; but on the other hand, acidic pH provides higher removals of anthraquinone dyes. Kornmüller et al. (2001) examined the ozonation process of a reactive dye and observed that below a certain pH (7.8) there appears no significant oxidation of dye; at this pH both molecular ozone and radicals take their roles in the oxidation mechanism, and pHs higher than 7.8 mostly radicals become responsible for the oxidation.

Besides dye removals, COD and TOC removals indicating generally the removals of ozonation by-product are also affected by solution pH. Carbajo et al. (2007) have

observed higher COD removals at pH = 11 than these at pH = 3 in the ozonation of phenolic wastewaters. Similarly, Soares et al (2006) stated that increasing pH from 5 to 9 enhanced TOC degradation rates and yielded a 5% increase in TOC removals. Sarayu et al. (2007) examined a commercial azo dye ozonation and found out that when pH of the solution was 5, ozonation provided a 20% COD removal; it increased to 80% when pH was increased to a basic pH of 10. Moreover, Balçioğlu et al. (2001) reported an increase in COD removal from 65% to 85% when the pH changed from an acidic pH of 2 to a basic pH of 10.

In addition to pH, the chemicals included to the wastewater during the steps of textile preparation processes form a significant effect on the ozonation process. Inorganics or organics found in wastewater act as initiators or scavengers in the formation of radicals or oxidation of the organics. While inorganics such as metal ions act as initiators for the radicals, carbonate or phosphate ions released from buffer solutions used in dyeing processes are scavenging agents for the radicals (Erol and Özbelge, 2009). Soares et al. (2006) observed the effect of phosphate buffer on decolorisation efficiency as a decrease with increasing pH from 5 to 9. Besides buffer ions, ions come from salts are also effective on ozonation chemistry. Sodium chloride (NaCl) and sodium sulphate ( $\text{Na}_2\text{SO}_4$ ) are very commonly used as exhausting and retarding agents in the textile industry (Muthukumar et al., 2004). Muthukumar and Selvakumar (2004) reported in their study that longer decolorisation time is necessary in the presence of NaCl and  $\text{Na}_2\text{SO}_4$ . They also indicated that NaCl salt solution enhanced the decomposition of ozone in both acidic and alkaline media. In contrast,  $\text{Na}_2\text{SO}_4$  consumes radicals at basic pH only and has no effect on the ozonation when the solution pH is low. Moreover, Erol and Özbelge (2009) investigated the effect of carbonate ( $\text{CO}_3^{2-}$ ) ions on the ozonation efficiency of Acid Red-151 and found out that at acidic pH adding  $\text{CO}_3^{2-}$  ions at high concentrations (500 mg/L) to solution increased the pH of the solution and enhanced the decomposition rate of ozone in the solution. Similarly, according to Arslan and Balçioğlu (2001) adding bicarbonate ( $\text{HCO}_3^-$ ) and  $\text{CO}_3^{2-}$  to the solution created high alkalinity and provided the cleaving of aromatic groups of dye molecules.

## 2.2.2 Mass Transfer of Ozone into Liquid Phase

It has been confirmed that the rate limiting step for the ozonation reactions is the mass transfer of ozone from the gas phase to the wastewater (Wu et al., 2000). Therefore, mass transfer of ozone from gas phase to the liquid phase is one of the main concerns of the ozonation processes. Mass transfer or the absorption of a gas from gaseous phase to liquid phase can be explained by Lewis and Whitman's two film theory which is demonstrated in Figure 2.3. According to this theory, there are two resistances in series that gas must penetrate through to reach the liquid phase. These resistances are liquid film and the gas film (Levenspiel, 1972). The driving force for ozone mass transfer to the liquid film is the difference between the concentration of the dissolved ozone and the equilibrium ozone concentration at the gas-liquid interface.

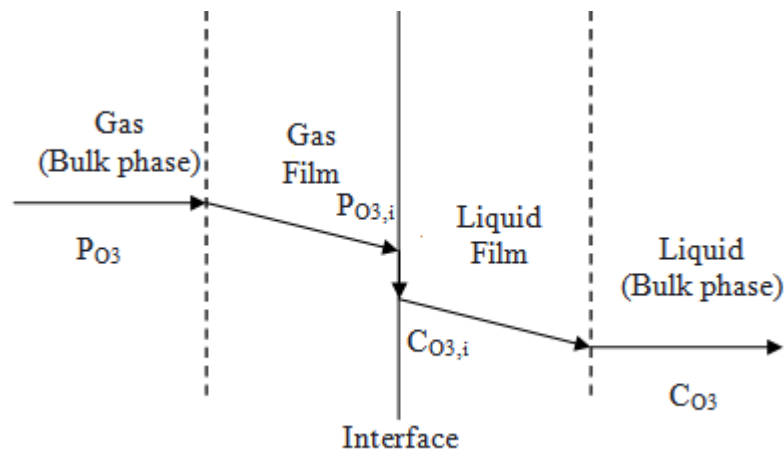


**Figure 2.2:** Mass transfer between phases.  $P_{O_3}$  is the partial pressure of ozone,  $P_{O_{3,i}}$  ( $P_{O_3}^*$ ) is the partial pressure of ozone at gas-liquid interface,  $C_{O_3}$  and  $C_{O_{3,i}}$  ( $C_{O_3}^*$ ) are ozone concentrations in bulk liquid and at gas-liquid interface, respectively.

Depending on the assumption of equilibrium at the interface, the relationship between the partial pressure of ozone and its concentration can be defined by Henry's Law;

$$P_{O_3}^* = H \times C_{O_3}^* \quad (2.8)$$

H: Henry's Law constant

Henry's Law constant for ozone-water system can be obtained from literature as (Farines et al., 2003);

$$H = 3.84 \times 10^7 \times [OH^-]^{0.035} \exp\left(\frac{-2428}{T}\right) \quad (2.9)$$

[OH<sup>-</sup>] is the hydroxide ion concentration in terms of mol/L (reflecting the effect of pH on the dissolution and amount of ozone in the liquid phase) and T is the temperature of water in Kelvin.

The concentration change of ozone in bulk liquid is proportional to the concentration driving force and the proportionality constant is the volumetric mass transfer coefficient of ozone. Also, since the solubility of ozone in water is very low, the resistances to mass transfer of ozone in gas phase and interface are negligible. Thus the concentration change of ozone in bulk liquid in a semi-batch reactor can be expressed as:

$$\frac{dC_{O_3}}{dt} = k_L a (C_{O_3}^* - C_{O_3}) \quad (2.10)$$

The concentration change of ozone in the liquid is also affected by the ozone decomposition rate. Thus, the decomposition rate should also be considered.

$$\frac{dC_{O_3}}{dt} = k_L a (C_{O_3}^* - C_{O_3}) - k_d C_{O_3}^m \quad (2.11)$$

The ' $k_d$ ' value is the self-decomposition rate constant for ozone; m is the decomposition reaction rate order. The  $k_L$  value is the mass transfer coefficient in the liquid film (m<sup>3</sup> liquid/ m<sup>2</sup> surface.s) and the value 'a' is m<sup>2</sup> surface area/ m<sup>3</sup> contactor.  $k_L a$  usually taken as one term in terms of m<sup>3</sup> liquid/ m<sup>3</sup> contactor.s or 1/s.

The volumetric mass transfer coefficient ( $k_L a$ ) which indicates the amount gas transferred from gaseous phase into aqueous phase depends significantly on some factors that can be grouped in two: physicochemical and hydrodynamic effects

(Levenspiel, 1972). ' $k_La$ ' depends on turbulent mixing, bubble diameter and bubble rise velocity hydrodynamically. Turbulent mixing in the contactor increases the contact between the two phases by decreasing bubble diameters. Bubbles with smaller diameters provide high interfacial area and enhance the mass transfer. Bubble rise velocity in the water also affects the mass transfer. While gas cannot find enough time to transfer to liquid when bubbles rise quickly, slowly rising bubbles provide time and more gas can diffuse to liquid before the bubbles reach to the surface. Physicochemical factors, on the other hand, are temperature, pressure and wastewater characteristics such as having different chemicals in its content (Levenspiel, 1972).

### 2.2.2.1 Mass Transfer in the Presence of Chemical Reactions

It has been reported that the formation of chemical reactions with the solute gas and liquid may enhance the mass transfer from gas phase into aqueous phase (Dankwerts, 1970). In wastewater treatment by ozonation process, ozone reacts with organic pollutants in water and many competition reactions involving ozone decomposition, molecular ozone and radical oxidation reactions take place in the reaction media. Depending on the kinetic models that Zhou and Smith (2000) proposed, it can be stated that for slower reactions (only ozone decomposition) occurring in the liquid bulk, mass transfer of ozone into liquid phase increases to a certain extent. However, as the rate of the reactions increases, ozone mass transfer increases very much; since the dissolved ozone starts to be consumed rapidly due to both of oxidation reactions and ozone decomposition reactions. As a result,  $k_La$  values increases in the presence of chemical reactions. This enhancement of  $k_La$  is described by an 'enhancement factor' ( $E$ ) being the ratio of actual rate of mass transfer in the presence of chemical reactions to the physical absorption of ozone without any chemical reaction and can be defined as follows (Levenspiel, 1972; Wu et al., 2000; Dankwerts, 1970):

$$E = \frac{(k_La)_E}{k_La} \quad (2.12)$$

where  $(k_La)_E$  : volumetric mass transfer coefficient with a chemical reaction

$k_La$ : physical absorption volumetric mass transfer coefficient

The two parameters needed to find the enhancement factor are named as the ‘instantaneous enhancement factor’ ( $E_i$ ), and ‘Hatta Modulus’ ( $M_H^2$ ) that is the maximum possible conversion in the film compared with the maximum transport through the film (Levenspiel, 1972):

$$E_i = 1 + \frac{D_B C_B}{b D_A C_{Ai}} \quad (2.13)$$

$$M_H^2 = \frac{D_A k C_B}{k_{Ai}^2} \quad (2.14)$$

where  $D_B$ : Diffusivity of reactant B (reactant in the liquid phase, dye or organic compound in the ozonation process.)

$C_B$ : Concentration of reactant B

$H_A$ : Henry’s law constant

$b$ : stoichiometric coefficient

$D_A$ : Diffusivity of reactant A (reactant that transfer from the gas phase, ozone in ozonation reactions.)

$k$ : reaction rate constant

$C_{Ai}$ : concentration of reactant A at the interface (since gas film resistance is neglected in ozonation reactions, concentration of ozone in the gas feed can be used.)

$k_{La}$ : mass transfer coefficient of reactant A through the liquid film

Van Krevelens et al. (1972) developed a good approximate expression for the enhancement factor in terms of  $E_i$  and ‘Hatta Number’ ( $M_H$ ) as follows:

$$E = \sqrt{M_H^2 \frac{E_i - E}{E_i - 1}} / \tanh \sqrt{M_H^2 \frac{E_i - E}{E_i - 1}} \quad (2.15)$$

The reaction medium for such kind of gas-liquid reactions may be the liquid film or the bulk of the liquid depending on the rates of the reactions. Fast reactions occur in the liquid film since they start to occur with mass transfer of the gas phase to the liquid film because of their high rates. In the intermediate case, reactions take place

both in liquid film and in the bulk of the liquid. On the other hand, very slow reactions occur in liquid bulk. The evaluation of where the reaction occurs is possible after the calculation of  $M_H$ . If  $M_H > 2$ , reaction occurs in the film and mass transfer rate become the rate determining step. On the other hand, if  $M_H < 0.2$ , reaction takes place in the bulk of the liquid giving the role of rate determination to the chemical reaction. If  $M_H$  is in between 0.2 and 2, reaction both occurs in the film and in the liquid bulk.

### 2.3 Advanced Oxidation Processes (AOPs)

Ozone in water treatment technology gains interest and becomes subject to many studies due to its high oxidation capacity. The uses of ozone in removing color, taste and other organics are its most widely used applications. Although ozone usage has advantages, the disadvantages cause the need for the improvement of ozonation process. Due to the high cost of ozone production, limited oxidation capacity of ozone for some organics such as inactivated aromatics (low TOC and COD removals) and relatively low solubility and stability of ozone in water, the new methods of advanced oxidation namely advanced oxidation processes (AOPs) are needed. These processes can be listed as the use of ozone together with some chemicals or combination with UV radiation and some chemicals [ $O_3/H_2O_2$ ,  $H_2O_2/Fe^{+2}$  (Fenton's reagent),  $O_3/UV$ ,  $H_2O_2/UV$ ,  $O_3/H_2O_2/UV$ ] and catalytic ozonation. One of the main purposes of the AOPs is the generation of hydroxyl radicals ( $HO^\bullet$ ) which are more powerful and active than ozone. In this case, ozone can decompose into these species which provide higher oxidation potential for organic pollutants and their by-products. The main AOPs based on the formation of radicals can be grouped in four as follows (Kasprzyk-Hordern et al., 2003):

- Homogeneous systems without irradiation:  $O_3/H_2O_2$ ,  $O_3/OH^-$ ,  $H_2O_2/Fe^{2+}$  (Fenton's reagent),
- Homogeneous systems with irradiation:  $O_3/UV$ ,  $H_2O_2/UV$ ,  $O_3/H_2O_2/UV$ , photo Fenton, electron beam, ultrasound, vacuum-UV
- Heterogeneous systems with irradiation:  $TiO_2/O_2/UV$
- Heterogeneous systems without irradiation: electro-Fenton.

Advanced oxidation processes have been used in removing different types of organics including textile effluents and synthetic dyed solutions in many studies. Fazzini and Young (1994) investigated the removal efficiencies of refractory organics by O<sub>3</sub>, UV, O<sub>3</sub>/UV processes. In comparison of them, an improvement was observed in the organic removal when O<sub>3</sub>/UV is used instead of O<sub>3</sub> only. Similarly, Gomez et al. (2000) obtained total mineralization of anilin and 4-cholorophenol by O<sub>3</sub>/UV system.

Besides the addition of UV light into the ozonation system, addition of H<sub>2</sub>O<sub>2</sub> to the system can increase the ozone decomposition rate. Acar and Özbelge (2006) investigated the effect of H<sub>2</sub>O<sub>2</sub> addition on ozonation process by changing the [H<sub>2</sub>O<sub>2</sub>]/[O<sub>3</sub>] concentration ratio and concluded that there appeared an increase in ozone decomposition rate at pHs between 2.5-10. Espulas et al. (2008) compared the efficiencies of different AOPs involving O<sub>3</sub>, O<sub>3</sub>/H<sub>2</sub>O<sub>2</sub>, UV, UV/O<sub>3</sub>, UV/H<sub>2</sub>O<sub>2</sub>, O<sub>3</sub>/UV/H<sub>2</sub>O<sub>2</sub>, Fe<sup>2+</sup>/H<sub>2</sub>O<sub>2</sub> and photocatalysis on phenol degradation. They found out that O<sub>3</sub>/H<sub>2</sub>O<sub>2</sub> process yielded the best removal efficiencies at neutral pH.

### **2.3.1 Catalytic Ozonation**

Catalytic ozonation being one of the AOPs can be examined in two headings. Homogeneous catalytic ozonation is based on the catalytic activity of metal ions in the solution. Heterogeneous catalytic ozonation, on the other hand, is performed using metal oxides or metals/metal oxides on supports (Kasprzyk-Hordern et al., 2003).

#### **2.3.1.1 Homogeneous Catalytic Ozonation**

The ions of transition metals have a catalytic activity on ozonation when added to the reaction media by affecting the rates of oxidation reactions. Mostly used metals for this purpose can be listed as Fe, Ni, Co, Ag, Zn, Mn, Cu, Cd, Cr. Using transition metal ions as catalysts improves ozone decomposition and thus radical formation. The ions found in the solution act as initiators for the ozone decomposition reactions by helping the formation of O<sub>2</sub><sup>•-</sup> and accelerating the formation of HO<sup>•</sup> (Kasprzyk-

Hordern et al., 2003). Besides catalyzing ozone degradation and hydroxyl radicals' formation, metal ions may also form complexes with organic molecules such as carboxylic acids. According to Pines and Reckhow (2002) in the ozonation process with Co(II) ion with oxalic acid, firstly a complex ion namely Co(II)-oxalate is generated and then it is oxidized to give Co(III)-oxalate.

Piera et al. (2003) investigated the removal of 2,4-dichlorophenoxyacetic acid at an acidic pH of 3 under the application of  $\text{Fe}^{2+}/\text{O}_3$  and  $\text{Fe}^{2+}/\text{UV}$  system and observed complete mineralization of 2,4-dichlorophenoxyacetic acid in the system of  $\text{O}_3/\text{Fe}^{2+}/\text{UV}$ . This system was also found out to be effective in the degradation of aniline and 2,4-chlorophenol in water. Oxidation of humic substances by ozone was investigated by both sole ozonation and using different metal sulphates (Gracia et al., 1996). Humic substances being the target organics in the reaction medium were easily oxidized by ozone and formed oxidation by-products which could not be go under further oxidized by ozone due to its selectivity towards inactivated aromatic organics. This is because Gracia and his colleagues (1996) could not reach above 33% of TOC removals applying ozonation alone. On the other hand, they obtained 62% and 61% TOC removals by using Mn(II) and Ag(I), respectively due to the generation of non-selective radicals due to ozone decomposition reactions. Similarly, Legube and Leitner (1999) found out addition of Fe, Mn, Ni and Co sulphate to the ozonation process provided an increase in TOC removals compared to sole ozonation. Solution pH may be considered as an effective parameter on catalytic ozonation enhancing the formation of radicals. Talapad et al. (2008) examined the catalytic activity of  $\text{Cu}(\text{NO}_3)_2$  catalyst on the ozonation of Congo Red at different pHs observing higher activity of the catalyst at neutral and alkaline pH and no activity at acidic pH. Andreozzi et al. (2000) performed experiments in order to investigate the ozonation of glyoxalic acid in the presence of  $\text{Mn}^{2+}$  ions by using  $\text{MnSO}_4$  solution and found out that at an acidic pH of 2, the removal of glyoxalic acid from the water was improved compared to that in sole ozonation. Also, they reported that the existence of  $\text{Mn}^{2+}$  ions in the solution changed the mechanism of oxidation reactions and enhanced the further oxidation of the organics to  $\text{CO}_2$  and water.

### 2.3.1.2 Heterogeneous Catalytic Ozonation

#### 2.3.1.2.1 Metal Oxides and Metals or Metal Oxides on Supports

Metal oxides (e.g.  $\text{Al}_2\text{O}_3$ ,  $\text{MnO}_2$ ,  $\text{TiO}_2$ ) and metals or metal oxides on metal oxide supports (such as  $\text{Cu-Al}_2\text{O}_3$ ,  $\text{Fe}_2\text{O}_3/\text{Al}_2\text{O}_3$ ) are the catalysts used efficiently in heterogeneous catalytic ozonation. Generally, these catalysts cause ozone to decompose to hydroxyl radicals and by this way, they provide a catalytic activity. The effective catalytic activity of these catalysts used in ozonation processes changes depending on the catalyst type and its surface properties, solution pH that affects the surface active sites on catalyst and ozone decomposition reactions occurring in liquid phase. Surface properties of metal oxide catalysts which can be grouped in two (physical and chemical) become important in understanding the mechanism of catalytic ozonation processes of different organics. Physical properties of the catalyst surface are surface area, pore volume, porosity, pore size distribution and mechanical strength. Chemical properties, on the other hand, are chemical stability and the existence of active surface sites which take an important role in the occurrence of catalytic reactions (Kasprzyk-Hordern et al., 2003).

Different mechanisms of catalytic ozonation may occur according to the catalyst. Although some catalysts provide the ozone dissolution on the catalyst surface in molecular form and reaction takes place on the surface, for some others the general idea for the mechanism is the transfer of electrons from supported metal to ozone molecules with the production of  $\text{O}_3^-$  and  $\cdot\text{OH}$  generation and their further reaction with organic compounds (Xin et al, 2006). The possible mechanisms that are observed in the experiments for the catalytic ozonation in heterogeneous system are three types. First one occurs by chemisorption of the ozone to the catalyst surface. Then, active species are formed from ozone and are released to solution where they give reaction with the organic molecule that is not chemisorbed. In the second type, the organic molecule is chemisorbed on the catalyst surface and gives reaction with gaseous or aqueous ozone on the catalyst surface. The ozone in gas phase is adsorbed on the catalyst through one of its terminal atomic oxygen (Kasprzyk-Hordern et al., 2003). In some cases, ozone does not remain in molecular form and turns into atomic or diatomic oxygen species and these are adsorbed on catalyst by production of

surface bound oxygen atoms. Ozone adsorption on the catalyst surface can take place in four forms; physical adsorption, the formation of weak hydrogen bonds with surface OH groups, molecular adsorption with coordinative bonding to weak Lewis acid sites and dissociative adsorption on interaction with strong Lewis sites, resulting in the formation of atomic oxygen atoms, which are intermediates in the catalytic reactions of ozone decomposition (Kasprzyk-Hordern et al., 2003). The third possible mechanism starts with the chemisorption of both organic molecule and ozone, and then the ozonation reactions take place on the surface of the catalyst. Depending on this information, it can be said that certain catalysts show different properties at certain conditions and for certain organic compounds (Kasprzyk-Hordern et al., 2003).

In addition, the acidity or basicity of the reaction medium is an important parameter that influences the heterogeneous catalytic ozonation. The pH of point zero charge ( $\text{pH}_{\text{ZPC}}$ ), is the pH at which the net surface charge is zero. This  $\text{pH}_{\text{ZPC}}$  value determines the surface charge of a metal oxide particle at a certain pH, and thus its adsorption capability of whether anions or cations to be absorbed. To be adsorbed can be adsorbed on the surface at pHs below  $\text{pH}_{\text{ZPC}}$ , the adsorption of cations occur at a pH value higher than  $\text{pH}_{\text{ZPC}}$  (Erol and Özbelge, 2007).

Alumina ( $\text{Al}_2\text{O}_3$ ) was reported to have high catalytic activity on the ozonation of 2-chlorophenol by Ni and Chen (2001). They obtained an increase of 83.7% TOC removal using alumina catalyst with ozonation when compared with that of sole ozonation in an acidic medium and an improvement of 17% in TOC degradation at alkaline pH, obviously because the oxidation efficiency is already higher. Similarly, Trapido et al. (2005) indicated the efficiency of alumina catalyst in the ozonation of m-dinitrobenzene among several metal oxide catalysts (such as  $\text{MnO}_2$ ,  $\text{Fe}_2\text{O}_3$ ) in terms of COD removals. Erol and Özbelge (2007) stated in their study on catalytic ozonation of aqueous dye solutions that at an alkaline pH of 13, alumina catalyst enhanced the ozone decomposition reactions yielding highest COD degradation. Moreover, Beltran et al. (2000) investigated the catalytic efficiency of  $\text{TiO}_2$  catalyst on ozonation of oxalic acid and observed a significant improvement in case of  $\text{TiO}_2/\text{O}_3$  system when compared to ozonation alone.

Hassan and his colleagues (2002) examined the effect of Ferral catalyst which is a combination of  $\text{Al}_2\text{O}_3$  and  $\text{Fe}_2\text{O}_3$  on ozonation for different dyes at different pHs and using different initial dye concentrations. They found that dye and COD removals using the catalyst increases at  $\text{pH} = 3$ , and also an increase in the catalyst amount improves the removal efficiencies. They indicate that while the COD reduction is about 7% in the sole ozonation process, it increases to 76% by using 488 mg/L Ferral catalyst.

Xin et al. (2006) investigated the catalytic efficiency of six different types of catalysts which were supported on  $\text{Al}_2\text{O}_3$ . The catalysts they used in their study were  $\text{Cu}/\text{Al}_2\text{O}_3$ ,  $\text{Ni}/\text{Al}_2\text{O}_3$ ,  $\text{Co}/\text{Al}_2\text{O}_3$ ,  $\text{Mn}/\text{Al}_2\text{O}_3$ ,  $\text{Al}/\text{Al}_2\text{O}_3$  and  $\text{Fe}/\text{Al}_2\text{O}_3$ . At the end of their study, they have compared the catalytic efficiencies of these catalysts on oxidation where ozone was used as the oxidizing agent. Their results indicated that the TOC removal efficiencies obtained by means of  $\text{Cu}/\text{Al}_2\text{O}_3$ ,  $\text{Ni}/\text{Al}_2\text{O}_3$ ,  $\text{Co}/\text{Al}_2\text{O}_3$  and  $\text{Mn}/\text{Al}_2\text{O}_3$  catalytic ozonation were greater than the corresponding ones obtained by the application of ozonation alone.  $\text{Cu}/\text{Al}_2\text{O}_3$  showed the removal efficiency among the tested catalysts,  $\text{Al}/\text{Al}_2\text{O}_3$  showed the same removal efficiency and  $\text{Fe}/\text{Al}_2\text{O}_3$  showed negative effect on the catalytic ozonation. Similarly, Qu et al. (2004) made a study on the  $\text{Cu}/\text{Al}_2\text{O}_3$  catalyzed ozonation for degrading alachlor, an endocrine disruptor, in water. They stated that  $\text{Cu}/\text{Al}_2\text{O}_3$  had very effective catalytic activity in the ozonation process. The use of  $\text{Cu}/\text{Al}_2\text{O}_3$  as an oxidation catalyst could have increased the TOC removal rates from 20 to 60%. Moreover, it was claimed that the by-product production was prevented by the use of  $\text{Cu}/\text{Al}_2\text{O}_3$  catalyst. The amount of free  $\cdot\text{OH}$  radicals increased with the application of the catalyst and the main pathway for the ozonation process could be considered as the indirect reaction of  $\cdot\text{OH}$  radicals and the alachlor (Qu et al., 2004).

#### **2.3.1.2.2 Ozonation with Non-polar Alumina Bonded Phases**

The non-selectivity of radicals during the oxidation reactions necessitates new studies on ozonation systems to enhance the selective molecular ozone solubility and stability in the reaction media. Perfluorinated hydrocarbons have already been reported as ozone stabilizers and found to be effective in terms of organic removals from water. There are two methods for the improvement in the organic matter

removals by using perfluorinated hydrocarbons being two phase ozonation with these hydrocarbons and catalytic ozonation with perfluorinated alumina bonded phases (Kasprzyk-Hordern et al., 2003). By the high absorption capacity of alumina especially toward perfluorinated surfactants, a monomolecular layer of non-polar perfluorinated alkyl chains can be formed on the surface of the alumina. This layer can act as an active layer that has the capability of extracting both molecular ozone and organic molecules from the aqueous phase (Kasprzyk-Hordern et al., 2003). This provides a reaction medium for molecular ozone and organics, and thus the target organics can be oxidized by selective ozone molecules instead of radicals in this organic phase (non-polar perfluorinated hydrocarbon solvent saturated with ozone) on alumina (Kasprzyk-Hordern et al., 2005). It is known that ozone solubility becomes to be ten times higher in fluorinated hydrocarbon solvents than that in water.

The catalytic activity of perfluorinated catalysts, mainly perfluorooctyl alumina (PFOA) catalyst, was reported to be due to its hydrophobicity and the length of perfluorinated alkyl chains on the surface of the catalyst. In Figure 2.3, the proposed mechanism of ozonation in the presence of non-polar alumina bonded phase can be seen and understood easily. According to Kasprzyk-Hordern et al. (2003) after the extraction of molecular ozone and organic molecules to non-polar phase, oxidation occurs on the catalyst surface, and then the hydrophilic by-products are desorbed from the surface providing the regeneration of the surface.

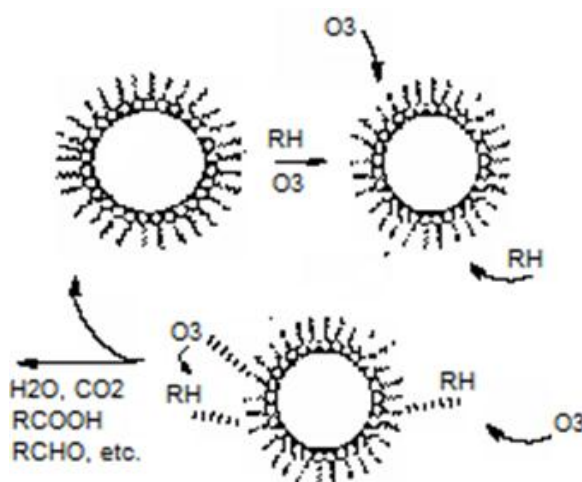


**Figure 2.3:** The proposed mechanism of ozonation in the presence of non-polar alumina bonded phase (Kasprzyk et al., 2003)

In order to form the organic phase on alumina mostly Perfluorooctanoic and perfluorooctadecanoic acids are used to produce PFOA catalysts (Kasprzyk-Hordern et al., 2003). In literature, ozonation with PFOA catalyst system was mostly seen in the studies of Kasprzyk-Hordern et al. (2004). They used PFOA as a catalyst in oxidation of aromatics like benzene, toluene; ethers like methyl tert-butyl; humic acids (HA) and natural organic matter (NOM) (Kasprzyk-Hordern et al., 2004). They reported an increase of 12.1% in the removal efficiency of methyl tert-butyl ether by ozonation with PFOA compared to that in sole ozonation (Kasprzyk-Hordern et al., 2004). Moreover, in one of their studies, they observed between 24% to 43% higher degradation rates of aromatics when using PFOA catalyst instead of ozonation alone (Kasprzyk-Hordern et al., 2003). Also, PFOA/O<sub>3</sub> system provided higher removal rates of Natural Organic Matter (NOM) resulting from the high attraction between NOM and PFOA (Kasprzyk-Hordern et al., 2004).

The stability of ozone was provided by the impregnation of perfluorooctanoic acid on alumina in the reaction medium (organic phase). Kasprzyk-Hordern et al. (2003) showed that at acidic pH, ozonation with PFOA catalyst provided high efficiencies in the removal of organics and no ozone decomposition was observed when PFOA catalysts exist in the system. They concluded that as a result of the occurrence of molecular ozone because of its high stability in the perfluorinated layer, direct ozonation mechanism took place during oxidation of the organic pollutants with PFOA/O<sub>3</sub> system. In addition to these, the use of PFOA catalyst during ozonation provided equal or higher removal efficiencies of the organic pollutants at the lower ozone dosages compared to those in the non-catalyzed ozonation. On the other hand, it was observed that high ozone dosages caused the PFOA sites to be blocked with by-products of ozonation. High O<sub>3</sub> dosages were determined to cause the occurrence of oxidation reactions in the bulk of the liquid producing some compounds such as carboxylic acids which had high affinity towards PFOA surface.

## CHAPTER 3

### EXPERIMENTAL

#### 3.1 Materials

##### 3.1.1 Industrial Textile Wastewater

The industrial textile wastewater was provided from AKSA Acrylic Plant which was established in Yalova-İstanbul/Turkey. AKSA now possesses the world's largest acrylic fiber production capacity. The WW is highly colored which provides the opportunity to observe the color removal more easily. The characterization experiments for the properties of the WW were done. The results of these experiments are given in Table 3.1.

**Table 3.1:** Properties of AKSA textile wastewater samples

Property	AKSA Textile Wastewater
COD (mg O <sub>2</sub> /L)	8750±10
TOC (mg C/L)	2869±10
TSS (mg/L)	36±5
Color (Pt-Co)	39300
pH	4
Metal Analysis	
Cu (mg/L)	0.4
Ni (mg/L)	0.5
Zr (mg/L)	-
Cr (mg/L)	1.0
Fe (mg/L)	-
Pb (mg/L)	-

As it can be seen, the TOC, COD and color values are very high. Moreover metal analysis was done on the sample by atomic absorption spectroscopy (AAS) and it was observed that WW contained different metals in small concentrations.

Depending on the information obtained from AKSA Acrylic Plant, the WW sample contained three different dyes which are blue, red and yellow in color. The preparation compositions of individual dye solutions were provided by private communication with Dr. İlhan Koşan; but their concentrations in the textile wastewater remained as unknowns, which could not be given. The provided information for each dye can be seen below (Koşan, 2009-2010):

Blue dye: CI Basic Blue 41 (BB 41), % 40-50

Acetic Acid, % 25-35

Yellow dye: CI Basic Yellow 28 (BY 28), % 35-45

Acetic Acid, % 20-30

Red dye: CI Basic Red 18.1 (BR 18.1), % 35-45

Acetic Acid, % 20-24

Caprolactam, % 3-7

The amount of acetic acid in the sample explained its low pH value. Moreover, in order to determine if there was any buffer in the medium, NaOH was added to the sample and it was observed that pH was changing easily explaining the absence of any buffer in the solution.

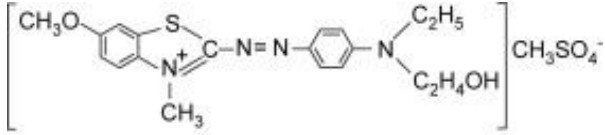
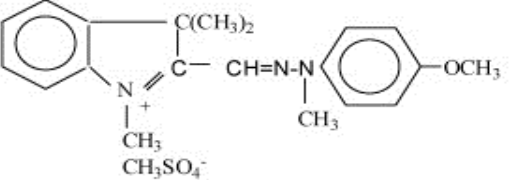
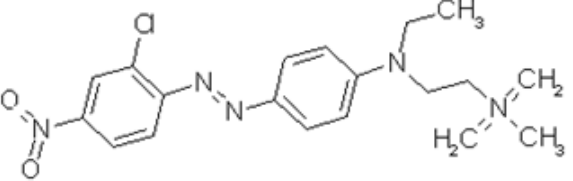
For the calibration of absorbance-concentration of dye mixtures and simulation of WW, dyes in WW (BB 41, BY 28 and BR 18.1) were obtained in powder form from AKSA Acrylic Plant. Dyes are all in basic class with characteristic properties shown in Table 3.2 (Koşan, 2009-2010).

The calibration of the three dyes by the relationship between concentration and absorbance at their maximum wavelengths were done for each dye separately and for their mixtures. The calibration curves for the dyes and their mixtures can be seen in Appendix A.

Other chemicals were used in determining the ozone concentration in the liquid and gas phases, adjusting pH, preparing PFOA catalyst. The water used in the reactions was distilled water and supplied from TKA water distillation unit. Alumina supplied from Damla Kimya (Ankara, Turkey) in the form of  $\gamma$ -alumina was used in the

preparation of PFOA catalyst as the support and also used as the catalyst. Alumina particles were obtained at different particle sizes, and then they were sieved to get uniform sizes. In the experiments, particles of 3 to 4 mm were used as the catalyst and support for the PFOA catalyst.

**Table 3.2:** The characteristic properties of dyes found in AKSA wastewater

Parameter	Characteristic Property
C.I. Name	Basic Blue 41
Chemical Formula	$C_{20}H_{26}N_4O_6S_2$
Class	Basic
Molecular Weight	482.57 g/mole
$\lambda_{max}$	617 nm
Molecular Structure	
C.I. Name	Basic Yellow 28
Chemical Formula	$C_{20}H_{14}N_3O-CH_3O_4S$
Class	Basic
Molecular Weight	433.57 g/mole
$\lambda_{max}$	437 nm
Molecular Structure	
C.I. Name	Basic Red 18.1
Chemical Formula	$C_{19}H_{25}ClN_5O_2$
Class	Basic
Molecular Weight	390.94 g/mole
$\lambda_{max}$	529 nm
Molecular Structure	

## 3.2 Experimental Set-up

In this study, the experiments were carried out in two types of reactors. They are a semi-batch reactor for the determination of catalyst activity on ozonation and kinetics of non-diluted real wastewater and a fluidized bed reactor for the continuous ozonation experiments.

### 3.2.1 Semi-Batch Reactor

Catalytic ozonation and ozonation experiments of non-diluted wastewater were conducted in a 1 L rounded bottom glass reactor (Figure 3.1). On the top of the reactor there are input ports for adding catalyst, for inserting a pH meter for feeding ozone gas and output ports for sampling. The reactor also has a mechanical stirrer for providing perfect mixing in the liquid phase during the reaction.

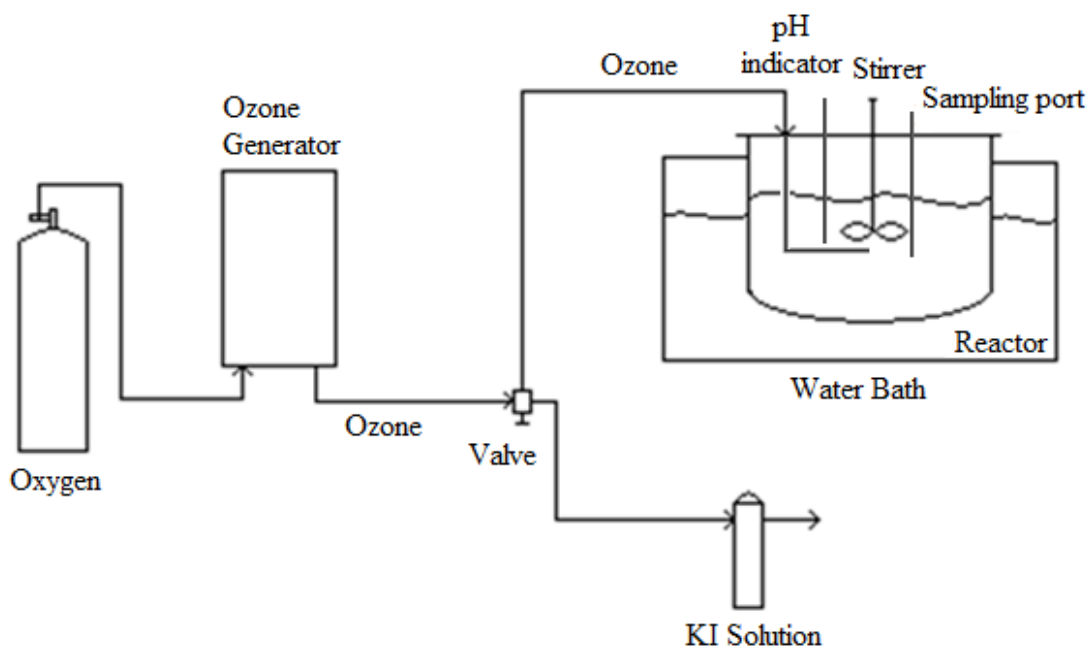


**Figure 3.1:** Semi-batch experimental set-up

Inlet Ozone was generated by an Ozomax OZO 2 VTTL ozone generator from pure oxygen and ozone-oxygen gas mixture comes to a three-way-valve. This valve helps ozone to be sent to a 2% KI washing bottle and then to the reactor. The gas flow rate of the inlet gas to the valve (ozone and oxygen gas mixture) from the generator was

measured by a flow meter on the generator. In order to determine the ozone concentration in this inlet gas, gas mixture was first fed to the KI washing bottle for two minutes; thus ozone concentration in it was obtained by KI method. Then the gas was sent to the reactor by changing the direction of flow via a three-way-valve. Ozone reached to the bottom of the reactor by a stainless steel tube and released to the liquid just under the mechanical stirrer at such a mixing rate that small gas bubbles to form in order to increase the mass transfer of ozone into liquid phase. The experiments were done at constant temperature of 25°C obtained by a water bath in which the reactor was placed. During the experiments, liquid phase stayed in the reactor and the gas was continuously fed to the reactor, and the oxidation of organics in the wastewater occurred by continuously increasing the amount of ozone in the reactor.

### **3.2.2 Three Phase Fluidized Bed Reactor**

The fluidized bed reactor system is a three phase reactor, where (ozone + O<sub>2</sub>) gas mixture and industrial wastewater co-currently and continuously flow upward and fluidize the catalyst particles of PFOA or alumina used. Fluidized bed reactor is a cylindrical plexiglass column with an inner diameter of 0.08 m and an effective height of 1 m and total height of 1.5 m. All of other connections and tubes are stainless steel or teflon in order to prevent the undesirable effects of ozone. Ozone is produced from pure oxygen by Ozomax OZO 2 VTLL ozone generator and is fed to the column from the bottom. The flow rate of the inlet gas is regulated and monitored by a flow meter on the generator. As in the semi-batch system, the inlet gas is sent to the KI bottles first to determine the ozone concentration in ozone-oxygen gas mixture and then to the column with the help of a three-way-valve. Unreacted ozone gas from the reactor is again sent to KI traps to determine ozone concentration in the outlet gas.

The inlet gas to the reactor is passed through a gas distributor which is composed of three glass discs (Figure 3.2). These discs are placed 9 cm above the liquid intake and equal distance from each other and column wall. The discs of 3 cm are porous fritted with a pore diameter of 40-50 µm. The inlet gas flow is separated to three parts before it enters the reactor and these three branches of flow are sent to the three discs which can be regulated by three valves. The distributor has an overall height of

4 cm in the column with its tubes and the discs. These discs and their places provide uniform distribution of the gas phase through the column.

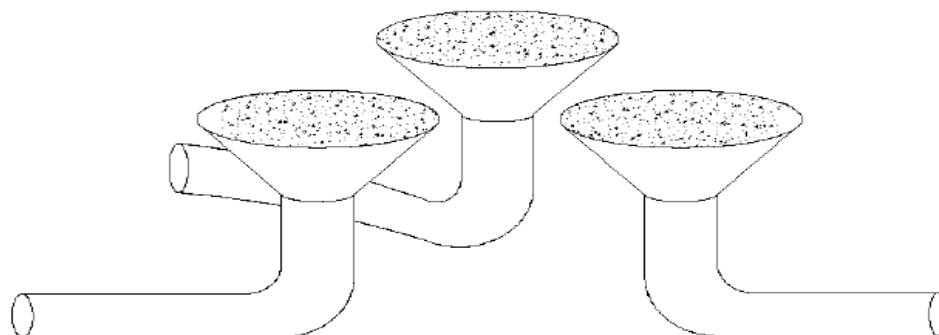


**Figure 3.2:** The configuration of porous fritted discs

The liquid phase is pumped from a storage tank of 65 L by a Baldor type centrifugal pump with a power of 5 hp at a pumping rate of 1725 rpm. A by-pass valve is placed after the pump in order to adjust the liquid flow rate. The flow rate of the liquid phase is regulated by a flow meter placed in front of the column and with the help of the by-pass valve. Liquid phase then reaches to the column and passes through a liquid distributor which is designed especially for its uniform distribution into the reactor. The liquid distributor which can be seen in Figure 3.3 is a triangular pitch type perforated stainless steel plate having distributed holes with 1 mm in diameter. It is placed 3.5 cm above the liquid intake to the reactor and has a thickness of 0.8 mm.

For the catalytic ozonation experiments, a stainless steel sieve is used to hold on the catalyst particles. The sieve has holes of 0.5 mm diameters and is placed 2 cm above the gas distributor.

Along the height of the column, six sampling ports are placed; three of which are on the right hand side and the other three are on the left hand side of the column. Two ports are on the opposite sides at equal heights. First two of them are 20 cm above gas distributors, second two are 50 cm above and the last ones are 80 cm above the gas entrance to the reactor.

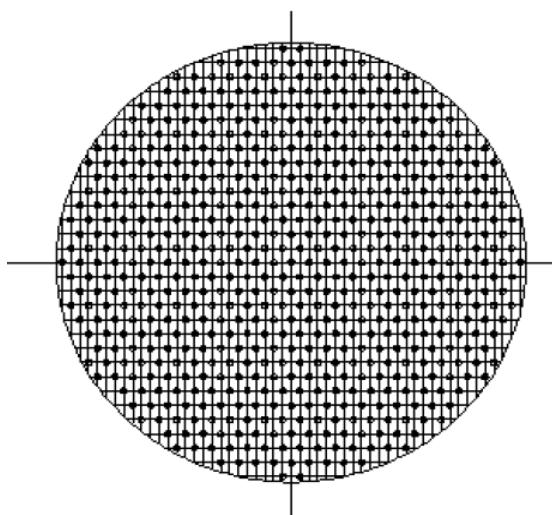


**Figure 3.3:** The schematic diagram of liquid distributor

The liquid stream leaves the reactor from an outlet at 100 cm above the liquid entrance and is sent to a 50 L storage tank. The rest 50 cm height of the column called ‘disengaging section’ is for only gas flow and prevents the overflow of liquid phase to the gas traps after the column. The unreacted ozone gas passes through this section and comes to the KI washing bottles. The schematic diagram of the overall system can be seen in Figure 3.4.

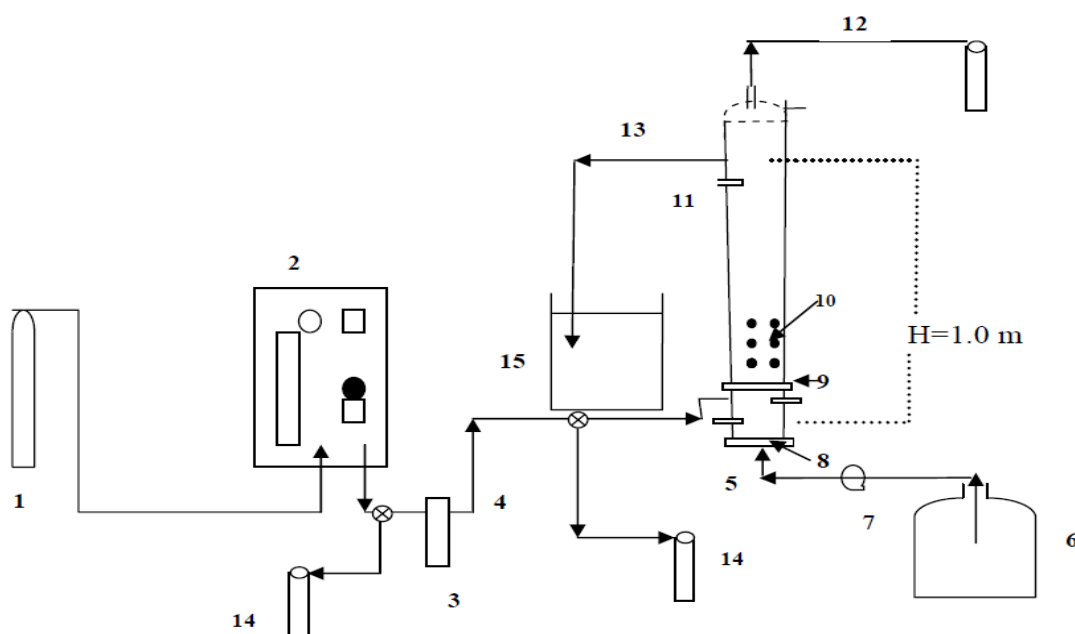


**Figure 3.4:** The schematic of the overall fluidized bed reactor system: 1-Dry air tube, 2-Ozone generator, 3-Gas flow-meter, 4-Ozone inlet, 5-Liquid inlet, 6-Liquid reservoir, 7-Centrifugal pump, 8-Liquid distributor, 9-Gas distributor, 10-PFOA catalyst, 11-Manometer taps, 12-Ozone outlet, 13-Liquid outlet, 14-KI traps, 15-Liquid outlet tank

### 3.3 Preparation and Characterization of the Catalysts

For the catalytic ozonation experiments, alumina particles supplied from Damla Kimya (Ankara, Turkey) were used as a catalyst and also as a support for PFO acid. The appropriately sized alumina particles between 3.0 and 4.0 mm were selected after the screen analysis of these particles was carried out. Alumina particles were calcined at 600°C in order to be sure the alumina particles were active  $\gamma$ -alumina particles. The PFOA catalyst was prepared by the impregnation of PFO acid (Aldrich Chemical Company, Milwaukee, USA) on the alumina particles. The catalyst was prepared by reacting 10 g of calcined alumina with 100 mL of 0.15 M PFO acid aqueous solution in a flask at 60°C for 4 h in a shaker according to the procedure described in the literature (Wieserman, 1991; Kasprzyk-Hordern et al., 2004). For the preparation of 0.15 M PFO acid solution, 6.48 g of PFO acid monohydrate (96% purity) was dissolved in 100 mL of deionized water. After the reaction, the mixture was cooled to room temperature. Then, 100 mL of 0.1 M sodium bicarbonate solution was prepared. After half an hour, catalyst was filtered under vacuum by washing with sodium bicarbonate solution and 200 mL of pure water in order to remove the unreacted PFO acid molecules from the surface of the particles. Finally, the catalyst was dried at 60°C in an incubator for about 2 h.

The surface characterization analyse of alumina and PFOA catalyst samples were made in order to find out the catalyst surface area and pore size distribution in the Central Laboratory of METU. Brunauer Emmett Teller (BET) method which involves the physical adsorption of nitrogen on the solid surface was used to determine the surface area of the catalysts. Average pore size, on the other hand, was determined by using the nitrogen adsorption/desorption method. The data obtained are given in Table 3.3. It can be seen that pore size decreases after the impregnation of PFO acid onto alumina with again a decrease in surface area.

**Table 3.3:** The surface area and pore size of alumina and PFOA catalysts

Type of Catalyst	$A_{BET}$ (m <sup>2</sup> /g)	$d_{pore}$ (Å <sup>o</sup> )
Alumina	289.8	38.20
PFOA	157.0	37.77

The density measurements of both types of the catalysts were also done. The bulk and true densities of alumina and PFOA catalyst particles were measured again in the Central Laboratory of METU. While for the determination of bulk density a mercury porosimeter was used, helium pycnometer method was applied to the particles for the measurement of true density and the results obtained are shown in Table 3.4.

**Table 3.4:** The bulk and true densities of alumina and PFOA catalysts

Type of Catalyst	Bulk Density (g/cm <sup>3</sup> )	True Density (g/cm <sup>3</sup> )
Alumina	1.0679	2.9624
PFOA	1.4226	2.7760

Moreover, for the characterization of alumina and PFOA catalysts, the fresh and several times used particles after ozonation process were analyzed by FT-IR Spectroscopy and XPS in the Central Lab of METU.

### 3.4 Semi-Batch Experiments

Ozonation and catalytic ozonation experiments of synthetic dye solutions prepared with BB 41, BY 28 and BR 18.1 were conducted in semi-batch reactor system in order to examine the degradation of the dyes in WW, separately. The total decolorisation of each dye was observed at different time intervals of the ozonation reactions due to the different structures of the dyes and their pH dependent ozonation mechanism. Data obtained from these experiments were analyzed and used in determining also the ozonation kinetics of wastewater in terms of color, TOC and COD removals.

In an experimental run, 1 L of synthetic dye solution was put into the reactor and ozone gas from the generator was continuously fed to the reactor for one and a half hours. During ozonation experiment, the samples were taken from the reactor more frequently at the beginning of the reaction (two to five minutes) then, at longer time intervals (fifteen to thirty minutes). At each time interval, two samples were withdrawn: One sample was taken into 50 mL erlenmeyer containing 1 mL of 0.025 M sodium thiosulfate (Na<sub>2</sub>S<sub>2</sub>O<sub>3</sub>) solution to quench the residual O<sub>3</sub> in the sample. This sample was analyzed for COD, TOC, dye concentrations and Pt-Co color unit.

The other sample was added into a 100-mL volumetric flask in which Indigo reagent was placed to determine the dissolved O<sub>3</sub> concentration in the sample was measured by the Indigo method (Rand, 1992; Bader and Hoigne, 1981). The ozone concentration in the inlet gas stream was determined by the KI method (Appendix B). Thus, the ozone consumption throughout the experiment can be calculated for each run. For the catalytic ozonation experiments, the desired amount of catalyst was weighed and added to the reactor just before the run started.

These experiments were conducted for two types of catalysts at pH of 4 and 10. The pH of the solution was monitored during the reaction by using a WTW 330i pH meter set. On the other hand, the gas flow rate, stirrer rate, temperature and ozone dosage were kept constant. The experimental parameters can be seen in Table 3.5 below.

**Table 3.5:** The semi-batch experimental parameters

<b>Parameter</b>	<b>Value</b>
$C_{d,i, BB\ 41}$ (mg/L)	300
$C_{d,i, BY\ 28}$ (mg/L)	300
$C_{d,i, BR\ 18.1}$ (mg/L)	300
pH	4, 10
Catalyst type	Alumina, PFOA
$Q_G$ (L/h)	150 L/h
Dye type	BB 41, BY 28, BR 18.1
$m_{cat}$ (g)	5
$C_{O_3, G, in}$	0.9±0.1 mmol/L gas

### 3.5 Experiments Conducted in a Fluidized Bed Reactor

Fluidized bed reactor system is a continuous system as described above. Ozonation and catalytic ozonation of textile wastewater were carried out in this system. The water used in the preparation of liquid phase is deionized water. Ozone gas was generated by Ozomax OZO 2 VTLL ozone generator as in semi-batch experiments from pure oxygen. The liquid phase was prepared at desired concentrations in a 65 L storage tank and pumped to the reactor. The ozone concentration in the inlet gas stream throughout the experiments was kept constant and adjusted by a dose adjusting button on the generator.

### 3.5.1 Wastewater Ozonation Experiments

The continuous ozonation experiments in the fluidized bed reactor were conducted by providing the gas and liquid streams to flow co-currently upward to fluidize the catalyst particles of PFOA or alumina used. The produced ozone gas was fed to the reactor from the bottom of the column. Wastewater solutions having different inlet COD values were prepared by diluting the stock solution of industrial textile wastewater in necessary amounts in a 65 L storage tank. For experiments conducted at different pHs, the basic medium (pH=10) was prepared by adding necessary amounts of 0.1 M NaOH solution, since the pH of the original wastewater is about 4; for the experiments at acidic medium, the pH was not adjusted.

The experiment was started by introducing ozone gas mixture to the system. The gas flow rate and the ozone dosage were regulated by the flow meters before they were sent to the reactor. The ozone concentration in the inlet gas was determined by sending the inlet gas into a washing bottle containing 200 mL of KI (2%) solution. Then, the gas flow was started into the column. After a while, the liquid was sent to the column by operating the pump and its flow rate was regulated. The outlet liquid stream from the top of the reactor was discharged to a second storage tank, and the outlet gas stream was sent to a train of washing bottles containing KI solutions, where excess ozone gas was trapped. Thus, the ozone concentration in the outlet gas stream was also determined by KI titration method. During each run, samples were withdrawn from the sampling ports at different column heights and at different time intervals until the steady state was reached. The steady state was reached in about 7.5 min after the beginning of the run, and the complete run was continued almost 20 min. At each sampling point, samples were withdrawn for the analyse of COD, TOC and dye concentrations and for the dissolved O<sub>3</sub> concentration in the sample. The samples taken for organic concentrations were put into 50 mL erlenmeyers each containing 1 mL of 0.025 M sodium thiosulfate (Na<sub>2</sub>S<sub>2</sub>O<sub>3</sub>) solution to quench the residual O<sub>3</sub> in the samples. The other samples were added into 100-mL volumetric flasks in each of which Indigo reagent was placed in order to use Indigo method for determining the dissolved O<sub>3</sub> concentration.

The wastewater ozonation experiments in the fluidized bed reactor were conducted at different inlet COD concentrations and different gas and liquid flow rates in order to investigate the effects of these parameters.

Moreover catalytic ozonation experiments were done by adding desired amount of catalysts (PFOA or alumina) were placed in the reactor and following the same procedure; but this time the received samples from the reactor were kept waiting for a while in order to provide the settling of tiny particles (forming because of catalyst) in the samples in order to obtain more accurate results in the analyses. The catalyst type (PFOA or alumina) and dosage were the experimental parameters in the catalytic ozonation experiments. In addition, the effect of pH on catalytic ozonation was examined conducting the experiments at different pHs (acidic or basic). The range of the parameters can be seen in Table 3.6.

**Table 3.6:** The fluidized bed experimental parameters

<b>Parameter</b>	<b>Value</b>
$COD_{in}$ (mg/L)	60, 120, 180, 300
pH	4, 10, 12
Catalyst type	Alumina, PFOA
$Q_G$ (L/h)	150, 170, 200, 227, 250, 283, 340
$Q_L$ (L/h)	70, 100, 150, 200, 250
Dye type	AKSA industrial wastewater
$m_{cat}$ (g)	0, 150, 300, 400
$C_{O_3,G,in}$	0.9±0.1 mmol/L gas

### 3.6 Analytical Methods

During this study, several analytical methods were used in the analyses of the samples obtained both from the semi-batch and the fluidized bed reactor. The analyses of TOC, COD, dye concentrations and dissolved ozone concentrations were done for each sample in order to examine the ozonation process.

The samples from the wastewater ozonation experiments were analyzed for color in terms of Pt-Co by a Hach DR-2010 type portable spectrophotometer. On the other hand, determining the concentration of each dye in the wastewater samples was

difficult by measuring their absorbances directly at their maximum wavelengths ( $\lambda_{\text{max}}$ ) because of the interaction of their wavelength spectra. Thus, in order to determine the dye removals of each dye in the sample and also to estimate the amount of colored dyes in the textile wastewater sample. “Absorbance vs. concentration” calibration correlations were developed. For this purpose, firstly wavelength spectra of the prepared synthetic dye solutions of each dye were examined and compared and a certain wavelength was chosen for each dye at which insignificant interference among the dyes occurred, when they were mixed in the solution. These chosen wavelengths are 380 nm for BY 28, 500 nm for BR 18.1 and 617 nm for BB 41. When the wavelength scans are again compared (Figure 3.5), it can be seen that at the chosen wavelength of BB 41 (617 nm), BR 18.1 and BY 28 do not give any absorbance, as BB 41 and BR 18.1 have no absorbance at 380 nm. Therefore, the amounts of BB 41 and BY 28 in the mixture can easily be determined by measuring the absorbance of the mixture and using single dye “absorbance vs. concentration” calibration curves (obtained at their chosen wavelengths) of BB 41 and BY 28. The uniformity of the single dye solution calibration curves of BB 41 and BY 28 with the ones obtained for the three dye mixture (Figure 3.6), could reveal the validity of dye concentrations found in the mixture. Since both of BB 41 and BY 28 have absorbances at 500 nm (chosen for BR 18.1), using calibration curve obtained for single BR 18.1 solution gives wrong results. Therefore, a new calibration curve was modified for BR 18.1 by subtracting the absorbances of BB 41 and BY 28 at 500 nm from the absorbance of the mixture of three dyes. As seen in Figure 3.6, this developed curve and single dye calibration curve for BR 18.1 are very close to each other proving that the new curve gives valid results for the concentration of BR 18.1 in the mixture.

The interaction between the wavelength spectra of the dyes brings the idea if the ozonation by-products have absorbances at the chosen wavelengths. Therefore, some of the organic acids (acetic acid, oxalic acid, formic acid and glyoxalic acid) that could be the main by-products of the ozonation process were supplied and checked if they have absorbance at chosen wavelengths. It was observed that most of the organic acids have their maximum wavelength near 210 nm and have no absorbance at chosen wavelengths for dye concentration determination.



respectively. Also the concentrations of each dye in the samples can be found out yielding the removal rates of each dye in the mixture during ozonation.

COD values of the samples were measured by adding 2 mL of each sample into a glass vial containing 3 mL of the COD solution prepared by dissolving 6 g  $K_2Cr_2O_7$ , 6 g  $Ag_2SO_4$  and 3.6 g  $HgSO_4$  in 500 mL of 95-98% concentrated  $H_2SO_4$  and digesting this mixture in a WTW Cr-3000 type thermo-reactor for 2 h at  $150^\circ C$  according to the standard methods (Rand, 1992). After each sample was cooled, its COD was determined directly by a Hach DR-2010 type spectrophotometer. Shimadzu  $V_{CPH}$  type TOC analyzer was used in determining TOC concentrations. High colored samples were diluted in order to protect the equipment.

The ozone concentrations in the inlet and outlet gas streams were determined by the KI method (Rand, 1992), explained in Appendix B. Indigo method (Rand, 1992) was used to measure the residual  $O_3$  concentration in the liquid phase using the Hitachi spectrophotometer.

## CHAPTER 4

### RESULTS AND DISCUSSION

#### 4.1 Ozonation Reaction Kinetics

The rate of dye ozonation reactions was shown to follow a second order reaction being first order both with respect to the dye and ozone concentrations (Zhao et al., 2006). Since the ozone concentration was assumed to be constant due to the excess ozone in the solution, the reaction rate appears to follow a pseudo first order. Ozonation rate expression was written by taking the ozone concentration term as constant and including it in the reaction rate constant expression as follows:

$$\frac{dC_d}{d\tau} = k \times C_{O_3} \times C_d \quad (4.1)$$

$$\frac{dC_d}{d\tau} = k' \times C_d \quad (4.2)$$

where  $C_d$ : dye concentration at any height

$\tau$ : relative residence time

$k$ : overall reaction kinetic constant

$k' = k \times C_{O_3}$  : pseudo first order kinetic constant

Assuming the reaction rate as pseudo first order with respect to dye concentration (as reported in literature) and integrating Eqn. (4.2), Eqn. (4.3) can be obtained:

$$\ln\left(\frac{C_d}{C_{d,in}}\right) = -k' \times \tau \quad (4.3)$$

where  $C_{d,in}$ : inlet dye concentration

This way, ' $\ln (C_d/C_{d,in})$  vs.  $\tau$ ' plots can be drawn to obtain the observed reaction rate constant ( $k'$ ).

On the other hand, in the case of semi-batch reactor since the samples were taken with respect to time, time ( $t$ ) could be used instead of relative residence time.

## **4.2 Effect of Operating Parameters on Ozonation of Wastewater in Fluidized Bed Reactor (FBR)**

### **4.2.1 Effect of Inlet COD ( $COD_{in}$ )**

In literature, many studies showed that initial organic concentration has an important effect on ozonation in terms of organic removal and also in terms of ozonation reaction kinetics (Soares et al., 2006). The initial concentration of organic pollutant was chosen as a parameter; because high amounts of organics necessitate high amounts of ozone to be degraded into by-products, and thus affects the efficiency of ozonation process. The sources of organic pollutants in a textile wastewater (WW) are dyeing agents (dyes, surfactants, organic acids, etc.) used in the dyeing and finishing steps of the textile preparation process. Since there are mixtures of dyes and many other organics in WW solutions, in order to examine the effect of initial organic loading on ozonation, solutions of different inlet COD values were prepared by diluting the stock solution supplied directly from AKSA Acrylic Plant (Yalova, İstanbul).

The non-catalytic ozonation experiments of WW solutions with different inlet COD values were performed. The dye concentrations of three dyes in WW were estimated by the developed concentration-absorbance calibration method, and also ozone concentrations in liquid phase along the column were measured at steady state. Dye concentrations were decreased with the distance along the column for three of the dyes (BB 41, BY 28, BR 18.1) (Figures 4.1, 4.2 and 4.3).

WW solution and ozone started to give reaction at the bottom of the reactor, since the gas and liquid streams both entered the reactor from the bottom. Dye concentration

decreased along the column, because ozone and dye molecules further reacted with each other since they traveled together to the top of the reactor. Ozone concentrations on the other hand, showed an increase through the column, since the higher amounts of ozone can be absorbed in the solution when gas and liquid phases remain longer in contact with each other.

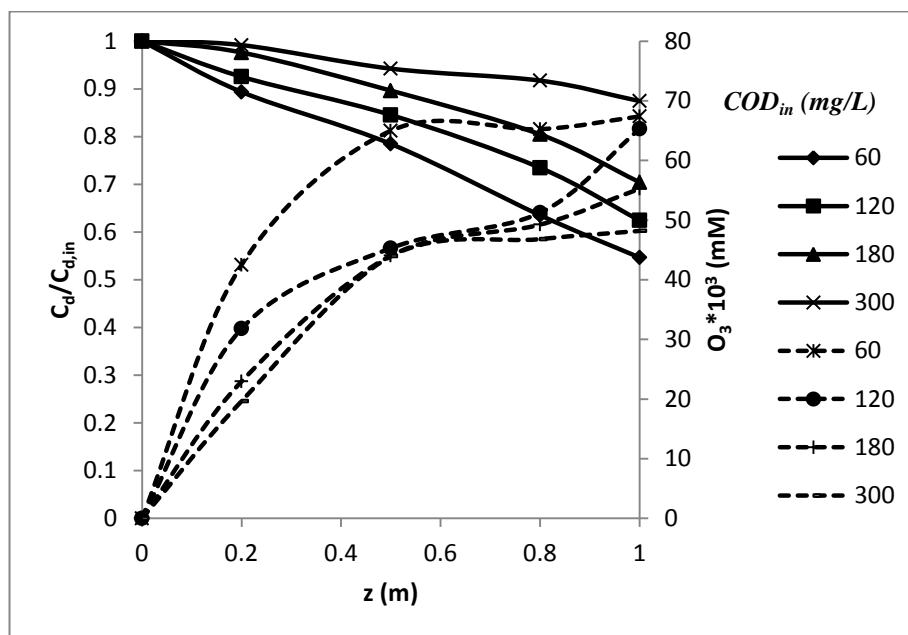


**Figure 4.1:** The effect of inlet COD value on blue dye degradation in WW solution,  $Q_G = 170$  L/h,  $Q_L = 150$  L/h, pH = free (4),  $C_{O_3,G,in} = 0.9 \pm 0.1$  mmol/L gas, catalyst: none, dye concentration is shown by line, and ozone concentration in liquid phase by dotted line (----).

The effect of inlet COD ( $COD_{in}$ ) value was also examined on the dye, TOC, COD removals and ozone consumption. It seemed that the increase in the  $COD_{in}$  caused smaller percent removals and higher ozone consumptions as can be seen in Figures 4.4(a) and 4.4(b) with Table 4.1. While  $COD_{in}$  is equal to 60 mg/L the percent dye removals were close to 100 % for red and yellow dyes and 45.3% for blue dye; increasing  $COD_{in}$  to 300 mg/L decreased the removals of BB 41 to 12.6% , BY 28 to 92.7% and BR 18.1 to 63.3%. Different operating conditions yields different removals obviously; but the decreasing trend of removals by the increase in inlet COD did not change (Figure 4.5). The smaller COD removal percentages mean that ozone firstly attacks aromatic structures (giving the dye its color) and degrades the

dye into its by-products (Table 4.2). Then, the mineralization of the by-products takes place and further COD removals are obtained after de-colorization.

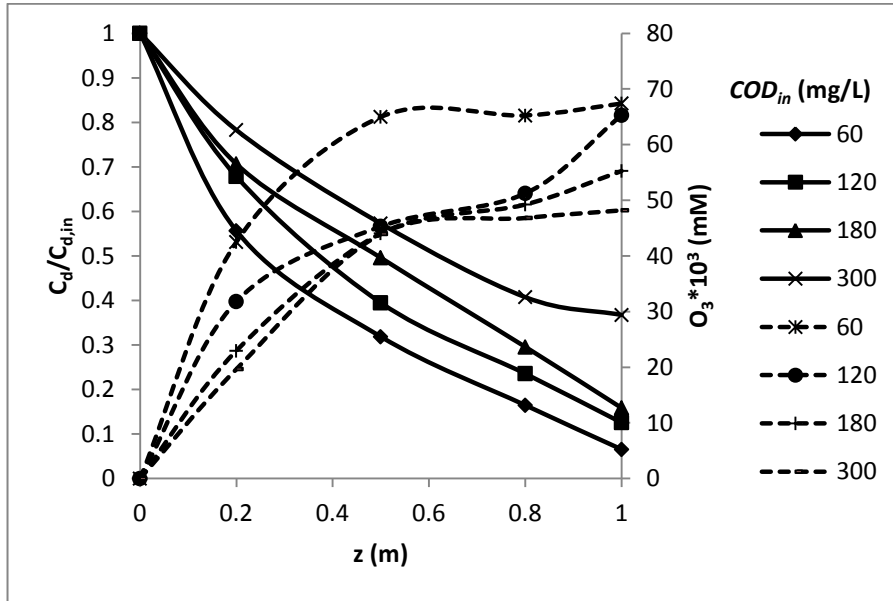


**Figure 4.2:** The effect of inlet COD value on red dye degradation in WW solution,  $Q_G = 170$  L/h,  $Q_L = 150$  L/h, pH = free (4),  $C_{O_3,G,in} = 0.9 \pm 0.1$  mmol/L gas, catalyst: none, dye concentration is shown by line, and ozone concentration in liquid phase by dotted line (----)

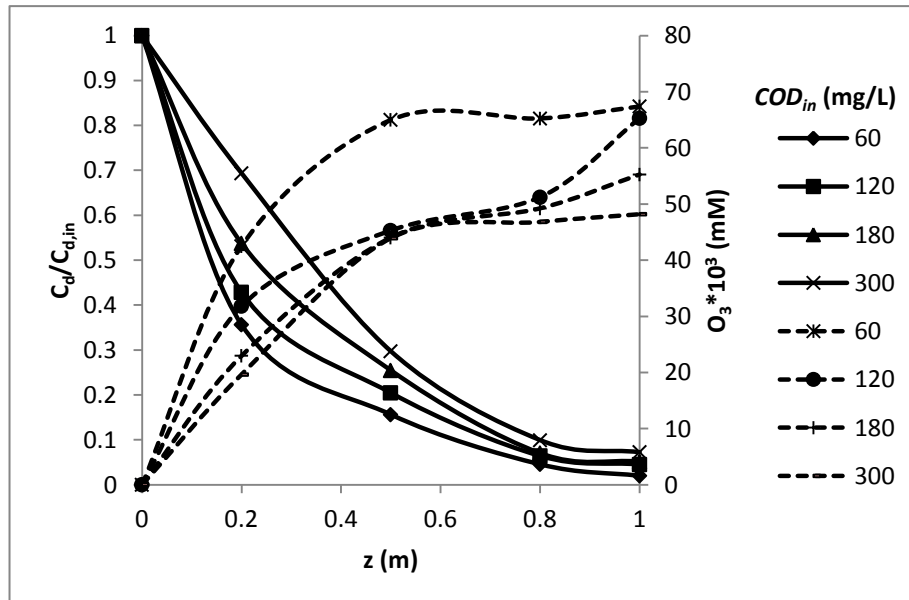
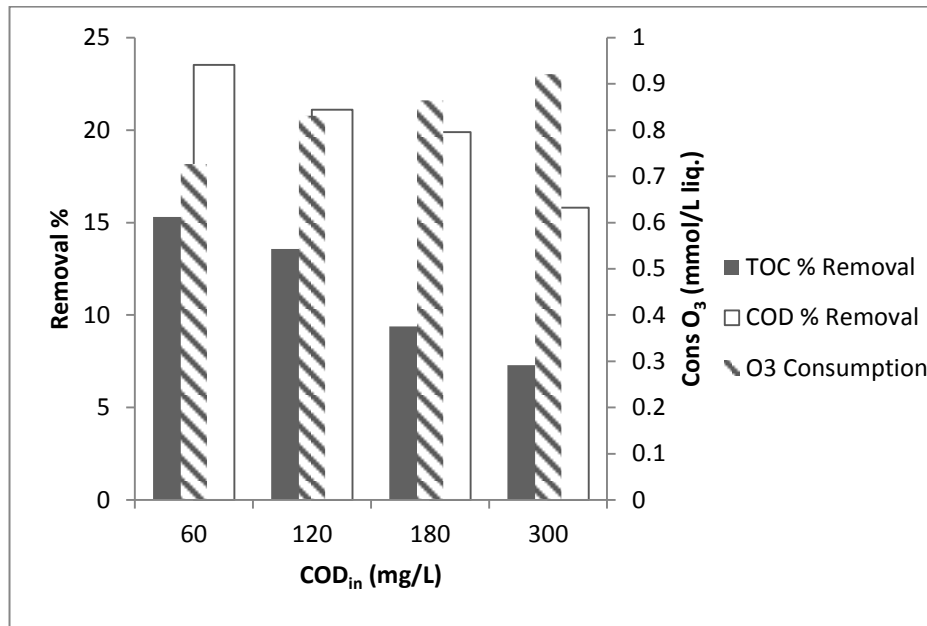
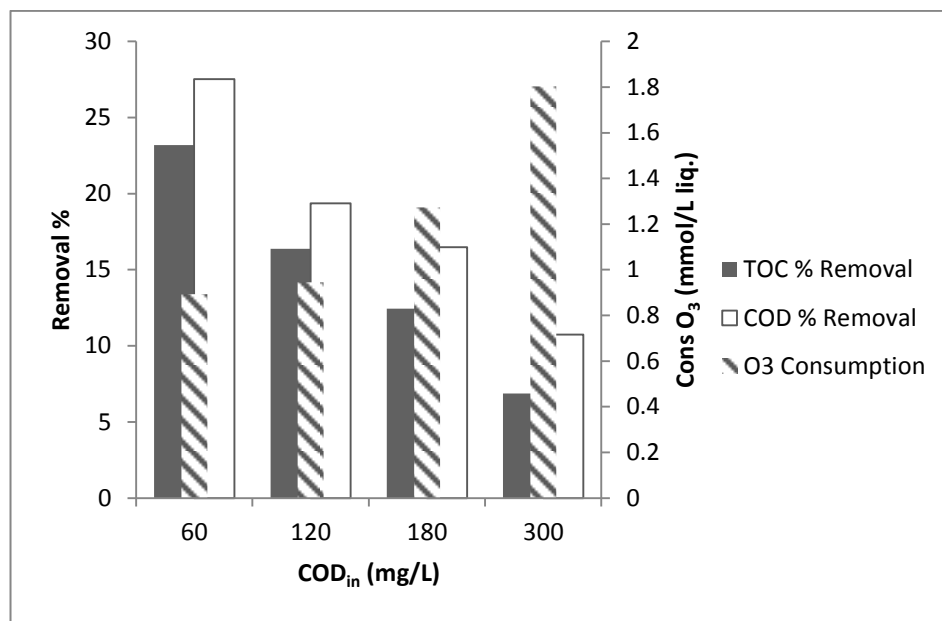


**Figure 4.3:** The effect of inlet COD value on yellow dye degradation in WW solution,  $Q_G = 170$  L/h,  $Q_L = 150$  L/h, pH = free (4),  $C_{O_3,G,in} = 0.9 \pm 0.1$  mmol/L gas, catalyst: none, dye concentration is shown by line, and ozone concentration in liquid phase by dotted line (----)



(a)



(b)

**Figure 4.4:** The effect of inlet COD value on overall TOC, COD removals and ozone consumption, (a)  $Q_G = 170$  L/h,  $Q_L = 150$  L/h, (b)  $Q_G = 340$  L/h,  $Q_L = 250$  L/h, pH = free (4),  $C_{O_3,G,in} = 0.9 \pm 0.1$  mmol/L gas, catalyst: none

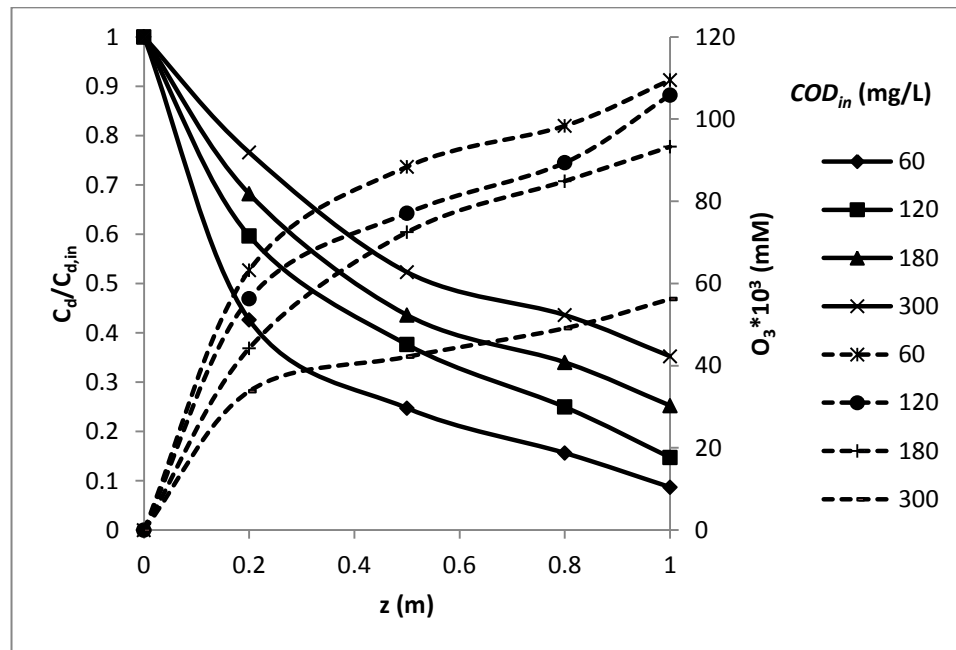


**Figure 4.5:** The effect of inlet COD value on dye degradation including all dyes in the WW in terms of Pt-Co color unit,  $Q_G = 340$  L/h,  $Q_L = 250$  L/h, pH = free (4),  $C_{O_3,G,in} = 0.9 \pm 0.1$  mmol/L gas, catalyst: none, dye concentration is shown by line, and ozone concentration in liquid phase by dotted line (----)

The decrease in the dye and COD removals at the highest inlet COD value can be explained by both the increase of by-product concentration in solution and the lower apparent reaction rate constants. The WW with a higher inlet COD (or with a higher dye concentration) required longer decolorization time (for the degradation of the dye molecules) thus leaving less time for the oxidation of by-products.

**Table 4.1:** The dye removals for different  $COD_{in}$ , pH = free (4),  $C_{O_3,G,in} = 0.9 \pm 0.1$  mmol/L gas, catalyst: none.

$Q_G$ (L/h)	$Q_L$ (L/h)	$COD_{in}$ (mg/L)	BB 41 Removal (%)	BR 18.1 Removal (%)	BY 28 Removal (%)
170	150	60	45.35	93.46	98.00
		120	37.57	87.46	95.47
		180	29.57	84.16	94.82
		300	12.57	63.27	92.75
340	250	60	50.37	97.28	100.00
		120	43.27	93.20	99.91
		180	35.70	88.81	99.82
		300	16.55	71.89	98.37

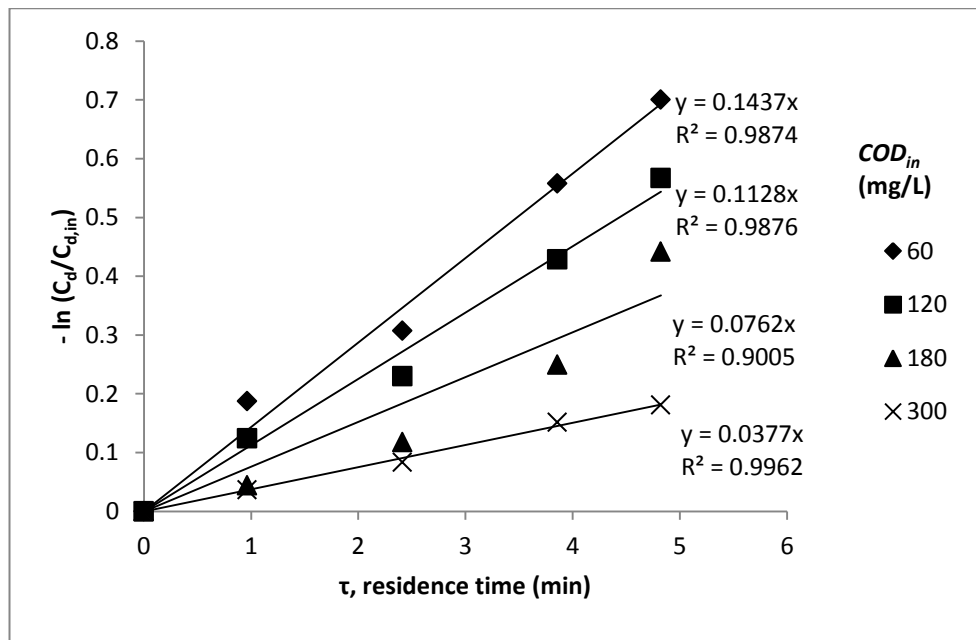
Moreover, the increase of the oxidation by-products of dyes enhances ozone consumption. Then, the available ozone will start to be consumed both for oxidation of intermediates and also for the continuing degradation of the original dye. In order to achieve higher degradation efficiencies at high inlet COD values, increasing gas flow rate providing higher dissolved ozone concentration to the reactor or lowering liquid flow rate providing longer gas-liquid contact time for decolorization and degradation of by-products would be useful. Also to increase the oxidation capacity of the system, increasing solution pH for the generation of HO• radicals at a higher concentrations would be beneficial.

**Table 4.2:** The COD and TOC removals with ozone consumption for different  $COD_{in}$ , pH = free (4),  $C_{O_3,G,in} = 0.9 \pm 0.1$  mmol/L gas, catalyst: none.

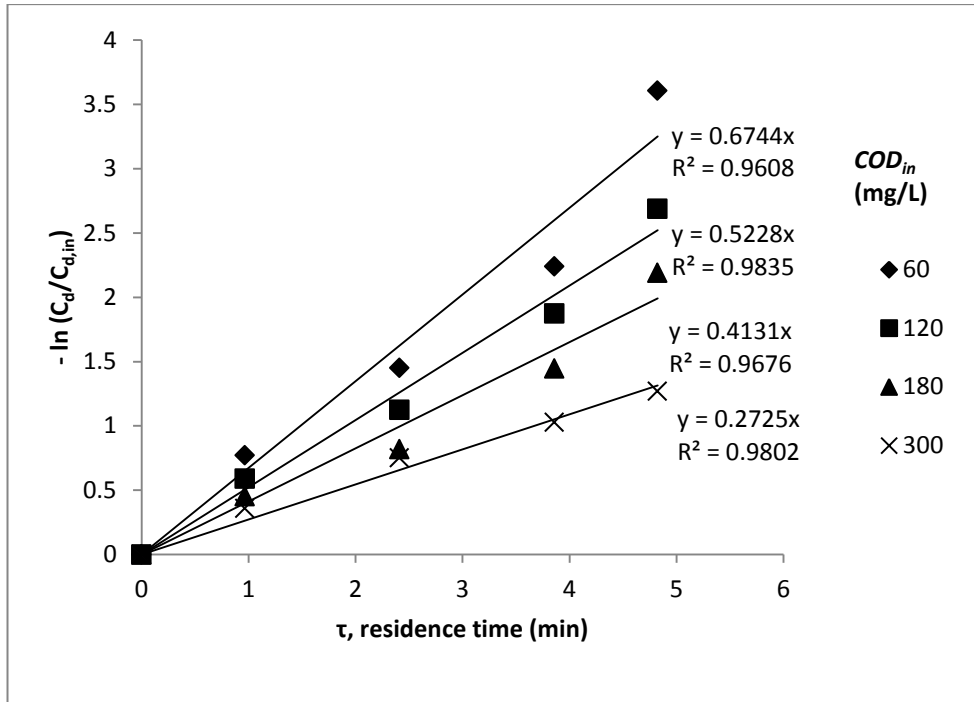
$Q_G$ (L/h)	$Q_L$ (L/h)	$COD_{in}$ (mg/L)	COD Removal (%)	TOC Removal (%)	$Cons_{O_3}$ (mmol/L liq.)
170	150	60	23.53	15.30	0.726
		120	21.09	13.57	0.831
		180	19.90	9.39	0.864
		300	15.81	7.29	0.921
340	250	60	27.53	23.19	0.893
		120	19.36	16.37	0.945
		180	16.49	12.45	1.273
		300	10.75	6.86	1.803

In addition to percent organic removals from WW solution; the decolorization kinetics of the dyes in the WW were analyzed and the pseudo first order behavior with respect to dye concentration was observed. The pseudo first order reaction rate constants ( $k'$ ) of the dyes in WW were estimated (Figures 4.6(a), 4.6(b) and 4.6(c)) and shown in Table 4.3. These estimated rate constants are the apparent ones which included the product of the dissolved ozone concentration with the intrinsic rate constant. The apparent rate constants were observed to decrease logarithmically with an increase in inlet COD concentration as it was stated in literature (Wu et al., 2008). Obviously, the changes in  $k'$  with the inlet COD concentration at constant temperature further verified that the estimated  $k'$  values are apparent ones; but not real, because the real rate constants are temperature dependent only.

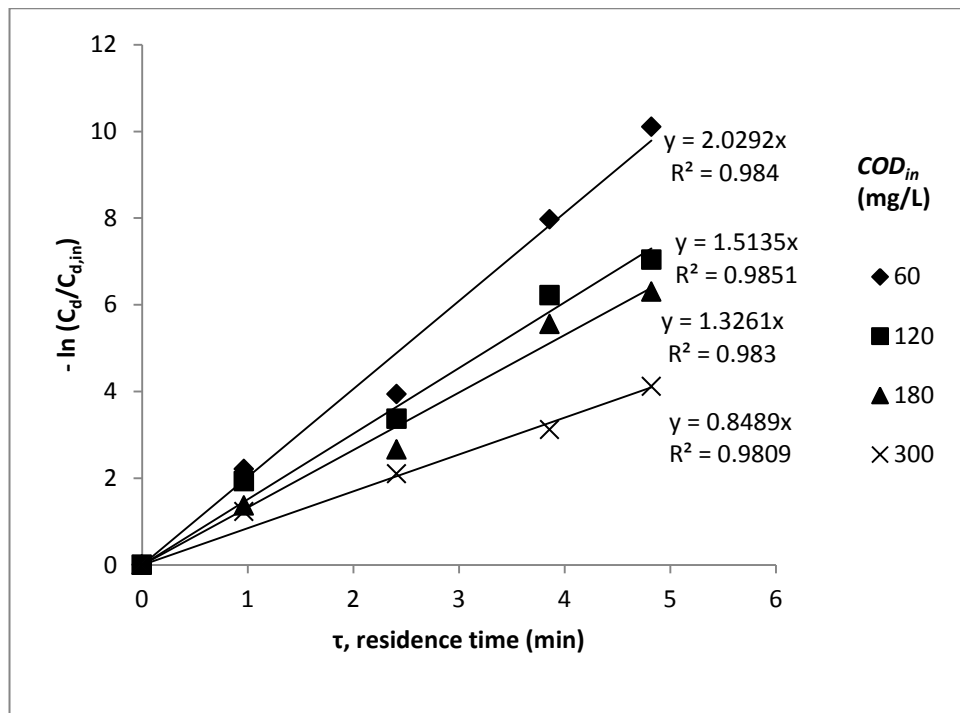
The decrease in the reaction rate constants with increasing inlet COD concentrations may be declared by the formation of oxidation by-products in higher amounts with the increase in  $COD_{in}$ . These by-products consumed more ozone and thus, dissolved ozone concentration in water was lower with higher  $COD_{in}$ . Consequently, the apparent rate constants for higher inlet COD concentrations decrease. Also the difference in the reaction rates were explained by the help of two film theory in some studies; because the reaction between the dye and ozone molecules occurs more rapidly in the liquid film during ozonation of the dye solutions having lower inlet dye concentrations (Low inlet COD value means low inlet dye concentration.). In other words, ozonation is controlled by chemical degradation reactions instead of mass transfer of ozone. On the other hand, the ozonation reaction of dye solutions having higher inlet COD values occurs both within the liquid film and also in the bulk liquid (Choi and Wiesman, 2004); because the same amount of ozone starts not to be enough for the degradation of all color at the boundary although the reaction becomes faster due to the inlet organic concentration and ozone mass transfer controlled. But, the increase in inlet organics causes a resistance for ozone to dissolve good enough and since the reaction is mass transfer controlled, the rate constants obtained for high  $COD_{in}$  were lower (Choi and Wiesman, 2004)



(a)



(b)



(c)

**Figure 4.6:** The kinetic analysis of the WW ozonation reaction for different  $COD_{in}$  concentrations in terms of dye concentrations (mg/L) in WW solution,  $Q_G = 340$  L/h,  $Q_L = 250$  L/h, pH = free (4),  $C_{O_3,G,in} = 0.9 \pm 0.1$  mmol/L gas, catalyst: none, (a) BB 41, (b) BR 18.1 and (c) BY 28.

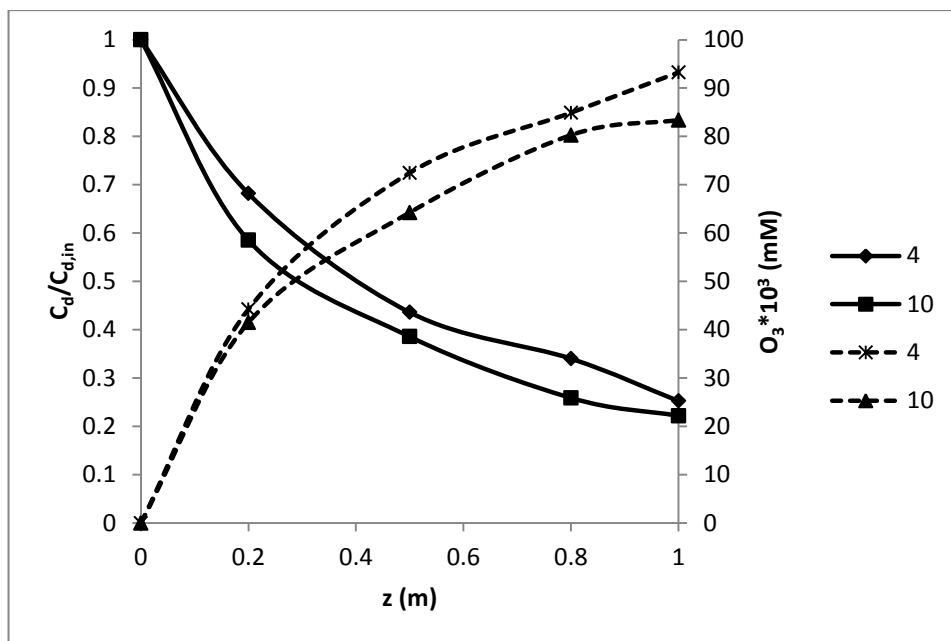
**Table 4.3:** The observed reaction rate constants in terms of dye concentrations,  $Q_G = 340$  L/h,  $Q_L = 250$  L/h, pH = free (4),  $C_{O_3,G,in} = 0.9 \pm 0.1$  mmol/L gas, catalyst: none

Dye	$COD_{in}$ (mg/L)	$C_{d,in}$ (mg/L)	$k'$ ( $\text{min}^{-1}$ )	$R^2$
BB 41	60	30.18	0.144	0.99
	120	60.36	0.113	0.99
	180	90.54	0.076	0.91
	300	150.9	0.038	0.99
BR 18.1	60	5.29	0.674	0.96
	120	10.58	0.523	0.98
	180	15.87	0.413	0.97
	300	26.4	0.273	0.98
BY 28	60	5.26	2.029	0.98
	120	10.51	1.514	0.99
	180	15.76	1.326	0.98
	300	26.2	0.849	0.98

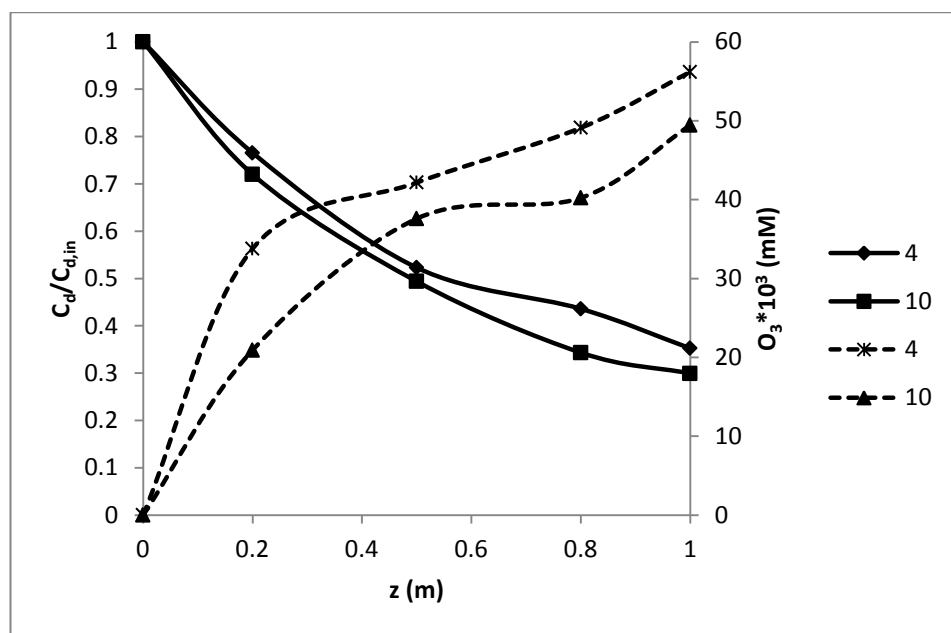
#### 4.2.2 Effect of pH

Many studies in the literature have revealed that pH of the dye solution is an important parameter in the ozonation of WWS (Soares et al., 2006). Therefore, ozonation experiments at different pH values were conducted in order to observe the effects of acidic and basic pH values on the ozonation reactions. In Figures 4.7(a) and 4.7(b), it can be easily seen that at high pH the color removals were higher for both inlet COD values of 180 mg/L and 300 mg/L.

It is believed that during ozonation, the oxidation of WW occurs by two ways. Ozone molecules can oxidize the dyehouse effluent directly or at the same time indirectly by hydroxyl radicals having higher oxidation potential, which result from the decomposition of ozone. In acidic media, due to the scarcity of hydroxyl ions, the decomposition of ozone does not occur significantly and ozone molecules take role in the oxidation of organics directly (direct ozonation mechanism). Conversely, in basic media ozone decomposes with the help of hydroxyl ions and generated hydroxyl radicals will oxidize organics indirectly (Chu and Chi, 1999).



(a)

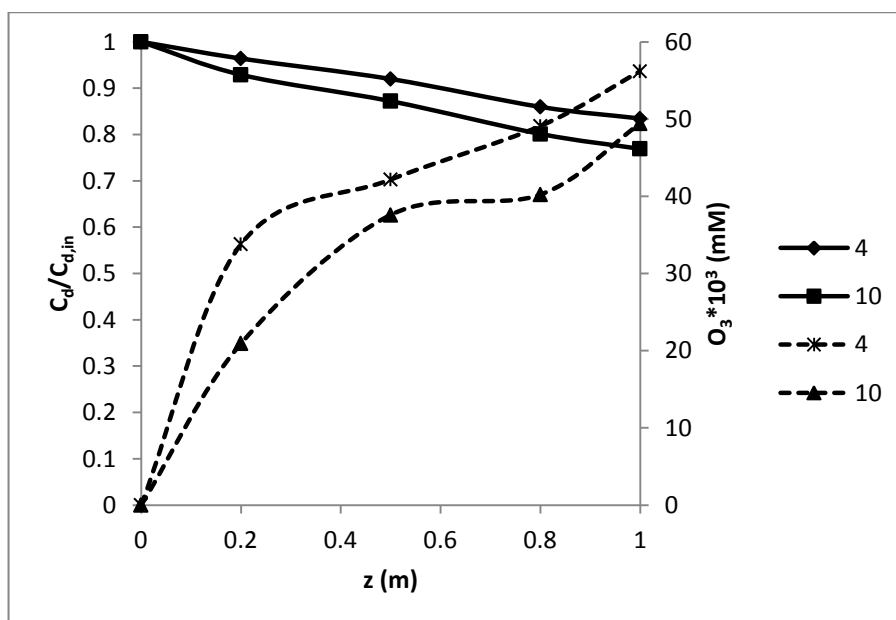


(b)

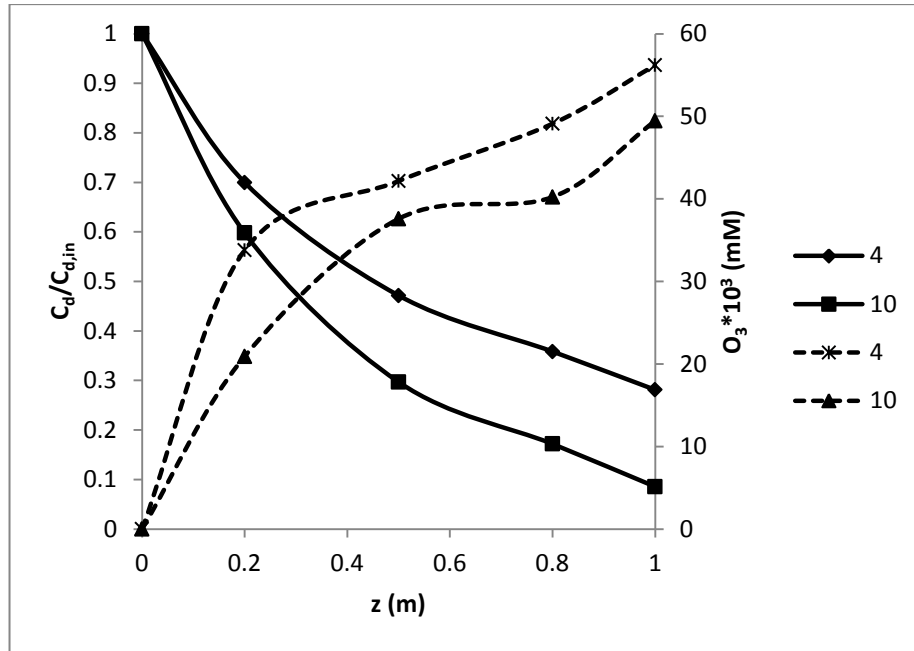
**Figure 4.7:** The effect of pH on dye removals (in terms of Pt-Co Color unit) and ozone concentration,  $Q_G = 340$  L/h,  $Q_L=250$  L/h,  $C_{O_3,G,in} = 0.9 \pm 0.1$  mmol/L gas, catalyst: none, (a)  $COD_{in} = 180$  mg/L; (b)  $COD_{in} = 300$  mg/L. In figures dye concentration is shown by line and ozone concentration in liquid phase by dotted line (----).

Since molecular ozone is selective for the destruction of aromatic chromophore groups present in some kinds of dyes, the decolorization of these dyes is favored at

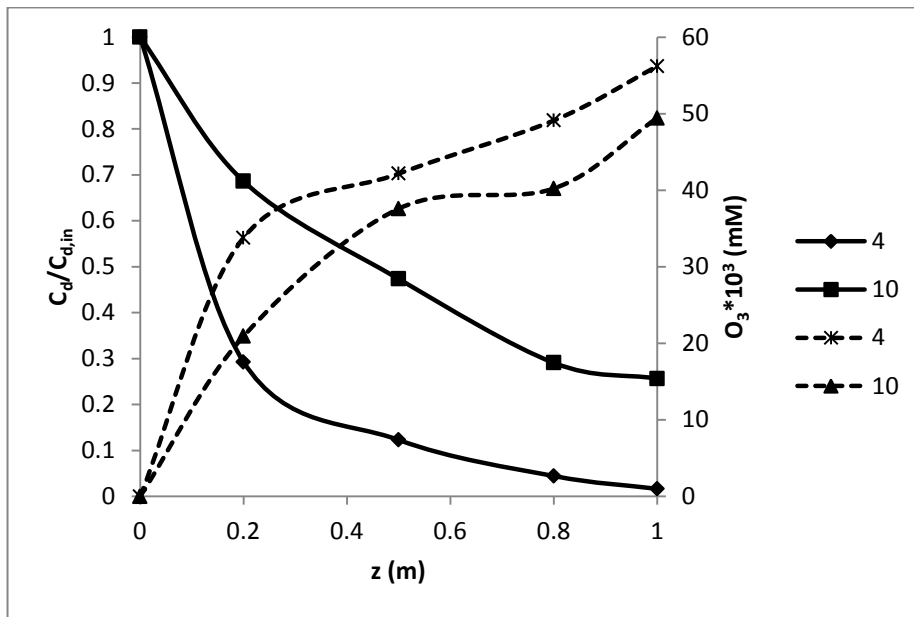
low pH values (Soares et al., 2006). This means that the decolorization mechanism is dependent on the structure and type of dyes. Depending on the dye type or structure, more selective molecular ozone or radicals may yield better dye removals. As it was stated, Figures 4.8(a), 4.8(b) and 4.8(c) showed the dye removals of each dye in the WW solution. Blue, red and yellow dyes (BB 41, BR 18.1 and BY 28) were observed to be degraded better at different pHs. While percent removals of blue and red dyes were higher at pH of 10, yellow dye removal was higher when solution pH is equal to 4 (Table 4.4). This observation may reveal that the direct oxidation of BY 28 by ozone molecules prevails against the indirect oxidation by hydroxyl radicals formed due to the decomposition of ozone at basic medium. According to many studies, molecular ozone prefers to react with aromatic type structures (Beltran et al., 2002). The aromatic structures found in BY 28 may attract the ozone molecules and cause them to attack the yellow dye first instead of red and blue dyes. The azo and sulphonic groups found in red and blue dyes make them more resistive to ozone oxidation and emerges the necessity of non-selective and more powerful oxidants, mainly hydroxyl radicals. This indicates the dominance of indirect oxidation for blue and red dye degradations against the direct oxidation by ozone molecule itself.



(a)



(b)



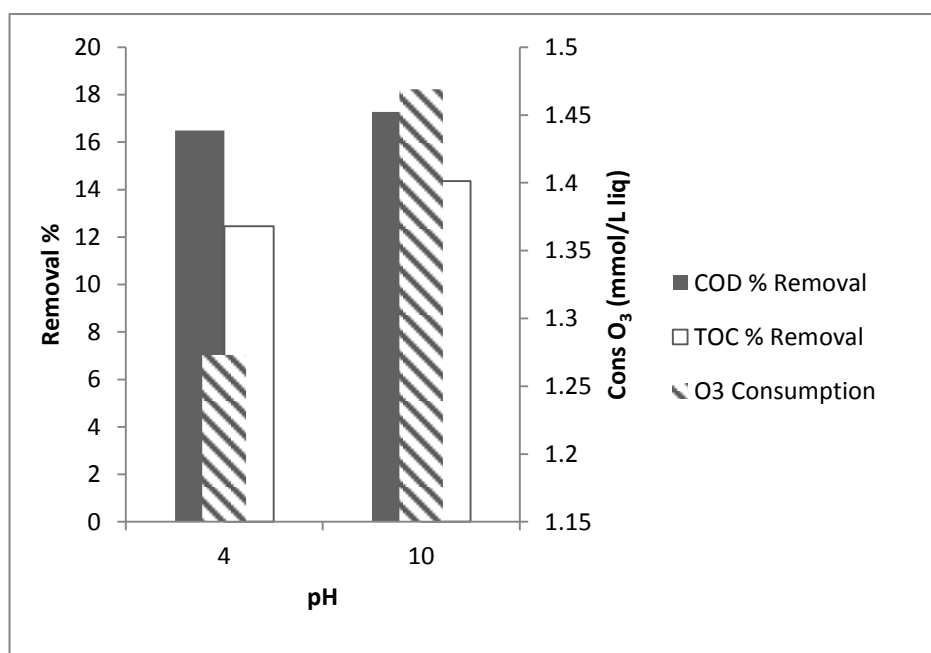
(c)

**Figure 4.8:** The effect of pH on dye removals (in terms dye concentrations for each dye in WW solution) and ozone concentrations,  $Q_G = 340$  L/h,  $Q_L = 250$  L/h,  $C_{O_3,G,in} = 0.9 \pm 0.1$  mmol/L gas, catalyst: none,  $COD_{in} = 300$  mg/L,  $C_{d,in,BB\ 41} = 150.9$  mg/L,  $C_{d,in,BR\ 18.1} = 26.4$  mg/L,  $C_{d,in,BY\ 28} = 26.2$  mg/L (a) BB 41, (b) BR 18.1, (c) BY 28. In figures dye concentration is shown by line and ozone concentration in liquid phase by dotted line (----).

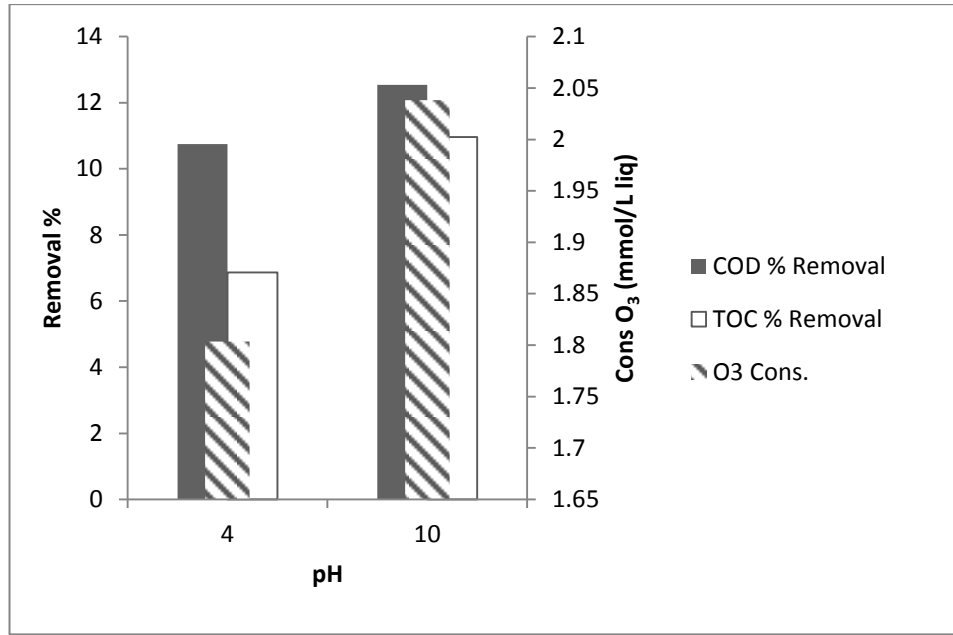
**Table 4.4:** The dye removals for different values of pH and  $COD_{in}$ ,  $C_{O_3,G,in} = 0.9 \pm 0.1$  mmol/L gas,  $Q_G = 340$  L/h,  $Q_L = 250$  L/h, catalyst: none.

$COD_{in}$ (mg/L)	pH	BB 41 Removal (%)	BR 18.1 Removal (%)	BY 28 Removal (%)
180	4	35.70	88.81	99.82
	10	42.63	98.85	91.05
300	4	16.55	71.88	98.37
	10	23.09	91.44	74.35

On the other hand, it is known that molecular ozone is insufficient in the oxidation of by-products, and thus the COD and TOC removals are lower. At high pH values, further mineralization occurs by the hydroxyl radicals being less selective than molecular ozone yielding higher TOC and COD removals in the runs conducted at basic conditions (Figures 4.9(a) and 4.9(b), Table 4.5).



(a)



(b)

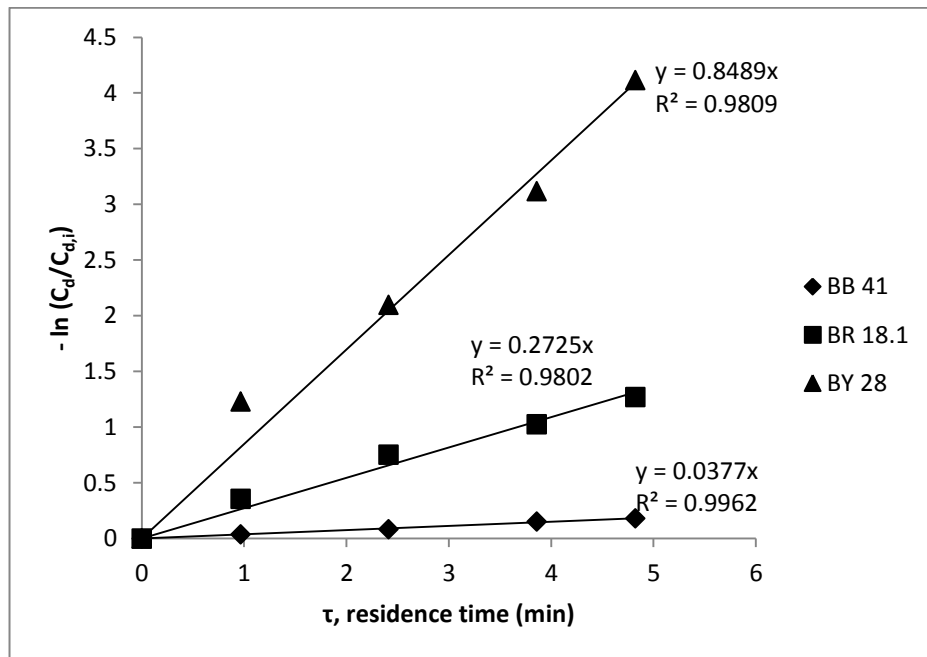
**Figure 4.9:** The effect of pH on TOC, COD removals and ozone consumption,  $Q_G = 340$  L/h,  $Q_L=250$  L/h,  $C_{O_3,G,in}=0.9 \pm 0.1$  mmol/L gas, catalyst: none, (a)  $COD_{in} = 180$  mg/L, (b)  $COD_{in} = 300$  mg/L.

**Table 4.5:** The TOC and COD removals with ozone consumptions for different values of pH and  $COD_{in}$ ,  $C_{O_3,G,in} = 0.9 \pm 0.1$  mmol/L gas,  $Q_G = 340$  L/h,  $Q_L=250$  L/h, catalyst: none.

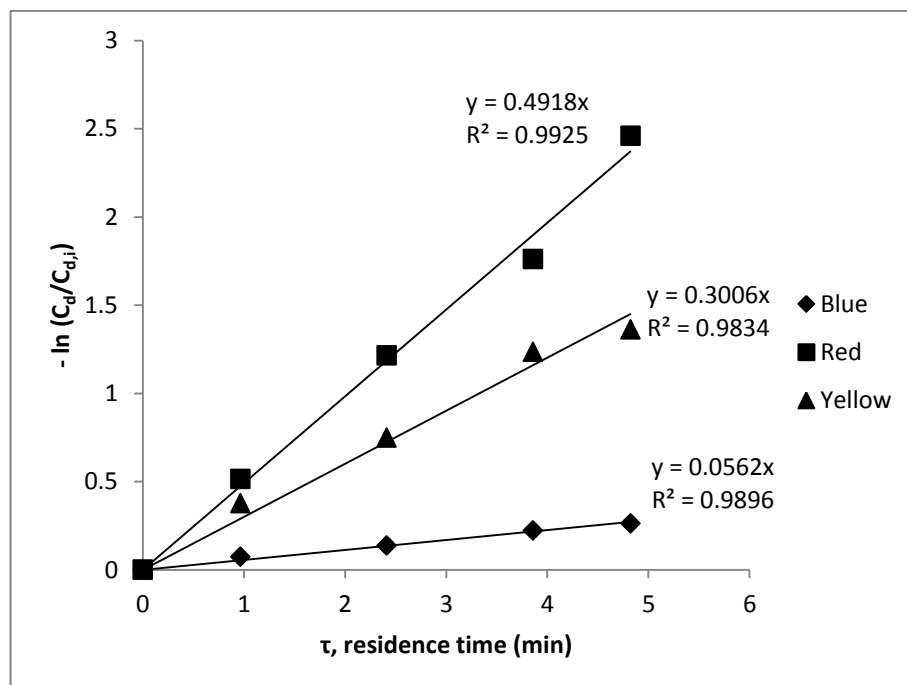
$COD_{in}$ (mg/L)	pH	TOC Removal (%)	COD Removal (%)	$Cons_{O_3}$ (mmol/L liq.)
180	4	12.45	16.49	1.273
	10	14.35	12.28	1.469
300	4	6.86	10.75	1.803
	10	10.97	12.54	2.038

The pseudo first order kinetic constants (apparent rate constants) for each dye were found in terms of each dye removal in the WW solution at different pHs by assuming that the ozone concentration was constant in aqueous phase (Figures 4.10(a) and 4.10(b)). Blue and red dye removal rates were found to be higher at basic solutions where generation of hydroxyl radicals was enhanced; on the other hand, at pH of 4, yellow dye removal rates were observed to be higher. As seen in Table 4.6, pseudo first order reaction rates showed an increasing trend with the increasing solution pH indicating the effect of radical reactions on ozonation kinetics for red and the blue

dyes. However, the reaction rates were found to be increased in the runs conducted with acidic dye solutions where molecular ozone was dominant for the yellow dye.



(a)



(b)

**Figure 4.10:** The kinetic analysis of the WW ozonation reaction in terms of dye concentrations (mg/L) in WW solution,  $Q_G = 340$  L/h,  $Q_L = 250$  L/h,  $COD_{in} = 300$  mg/L,  $C_{d,in, BB\ 41} = 150.9$  mg/L,  $C_{d,in, BR\ 18.1} = 26.4$  mg/L,  $C_{d,in, BY\ 28} = 26.2$  mg/L,  $C_{O_3, G, in} = 0.9 \pm 0.1$  mmol/L gas, catalyst: none (a) pH = free (4), (b) pH = 10.

**Table 4.6:** The observed reaction rate constants in terms of dye concentrations for different  $COD_{in}$  and pH values,  $Q_G = 340$  L/h,  $Q_L = 250$  L/h,  $C_{O_3,G,in} = 0.9 \pm 0.1$  mmol/L gas, catalyst: none

Dye	$COD_{in}$ (mg/L)	$C_{d,in}$ (mg/L)	pH	$k'$ ( $\text{min}^{-1}$ )	$R^2$
BB 41	180	90.54	4	0.076	0.90
BR 18.1		15.87		0.413	0.97
BY 28		15.76		1.326	0.98
BB 41	180	90.54	10	0.106	0.97
BR 18.1		15.87		0.895	0.99
BY 28		15.76		0.515	0.99
BB 41	300	150.9	4	0.038	0.99
BR 18.1		26.4		0.272	0.98
BY 28		26.2		0.849	0.98
BB 41	300	150.9	10	0.056	0.99
BR 18.1		26.4		0.492	0.98
BY 28		26.2		0.301	0.99

### 4.3 Catalytic Ozonation Experiments in FBR with Alumina or PFOA

The application of ozonation to larger scale systems becomes difficult because of the high operating costs. Moreover, it is known that sole ozonation is not very effective in oxidizing by-products of the recalcitrant organics and thus for high COD and TOC reductions. Therefore, catalytic ozonation being one of the advanced oxidation processes can be seen as a solution according to many researchers. In this study, firstly the catalysts were prepared and characterized then catalytic ozonation experiments were conducted by two types of catalysts (alumina and PFOA) and the results were compared with the ones obtained from sole ozonation experiments. In addition to these, catalytic ozonation experiments were done at different pH values and the effect of pH on catalyst efficiency was investigated. Catalyst dosage was also considered as an experimental parameter and its effect on ozonation was examined.

### 4.3.1 Catalyst Characterization

The alumina and PFOA particles used as the catalysts, were characterized after the preparation of the fresh catalysts. Moreover, characterization experiments were done after they were used once, three and five times in the ozonation experiments in order to determine whether any changes occurred in their physical and chemical properties.

#### 4.3.1.1 Surface Characterization Experiments

The surface characterization and BET surface area analyses of the catalyst particles were done by ‘Quantachrome Corporation, Autosorb-1-C/MS’ in METU Central Laboratory. Alumina, fresh PFOA and PFOA used once, three and five times in the experiments were analyzed in terms of their surface properties by BET method. The results obtained are shown in Table 4.7.

**Table 4.7:** The surface areas obtained by the BET method and the pore diameters of the catalyst particles

Catalyst	$A_{BET}$ (m <sup>2</sup> /g)	$d_p$ (Å <sup>o</sup> )
Alumina	289.8	38.20
PFOA	157.0	37.77
PFOA (1 time)	154.7	37.86
PFOA (3 times)	150.9	38.03
PFOA (5 times)	129.7	37.90

BET surface area results show that surface area of alumina particles the surface area is significantly greater than that of PFOA particles. PFOA catalyst is prepared by the impregnation of the PFO acid on to  $\gamma$ -alumina particles as it is explained before. It is obvious that during impregnation, PFO acid covers the particle surface and filled the pores on alumina particles decreases the surface area. This can also be seen from the pore diameter results. As it can be seen, after the synthesis of PFOA catalyst the pore diameter decreases from 38.20 Å<sup>o</sup> to 37.77 Å<sup>o</sup>. Instead of fresh PFOA and alumina particles, in the case of used PFOA particles, while surface areas for the once and three times used catalysts particles in the ozonation experiments are close to each other; the surface area of the particles used for five times is observed to be lower probably due to the adsorption of the dye molecules on to the catalyst particles,

filling the pores and thus causing the BET surface area to decrease. Since using the PFOA particles for five times in the ozonation experiments causes significant differences, catalyst particles are decided to be used three times at most in order to make use of them more efficiently.

#### 4.3.1.2 Density Analysis

The densities of the alumina and PFOA particles whose sizes are in the range between 2.4 mm and 3.3 mm were obtained and shown in Table 4.8.

The true densities of the particles are observed to be higher than the bulk densities as seen in Table 4.8. Since in the case of bulk density measurements, air in the pores of the particles is included; but, on the other hand, true density means the skeleton density of the material the particle composed of, it is expected to obtain lower bulk densities than the true densities. Moreover, the impregnation of PFO acid on to alumina causes the bulk density of the PFOA particles to increase. This may be due to the pores filled up with PFO acid during the impregnation step. When PFO acid fills the pores, it takes the place of air and thus increases the density. On the other hand, since the density of PFO acid ( $1.8 \text{ g/cm}^3$ ) is lower than the alumina density, the true density of the PFOA particles decreases.

**Table 4.8:** The bulk and true densities measured for alumina and PFOA particles

Catalyst	Bulk Density ( $\text{g/cm}^3$ )	True Density ( $\text{g/cm}^3$ )
Alumina	1.0679	2.9624
PFOA	1.4226	2.7760

#### 4.3.1.3 FT-IR Spectroscopic Studies

FT-IR studies were conducted in order to characterize the catalyst particles. These studies were performed on alumina, PFO acid and PFOA samples. Moreover, the PFOA particles used in the ozonation experiments more than once were also examined by the FT-IR studies in order to find out if any changes occurred and using the catalyst more than once if it was still efficient or not. The FT-IR spectrum of the

particles was obtained by using “Bruker IFS 66/S, FRA 106/S, HYPERION 2000, RAMANSCOPE” in METU Central Laboratory and choosing the spectrum range as MIR ( $400\text{ cm}^{-1}$  -  $7000\text{ cm}^{-1}$ ) for the spectroscopy. Figures 4.11 to 4.16 show the spectra of these particles obtained from FT-IR studies.

In Figure 4.11, the spectrum of alumina can be seen. The band at  $3315\text{ cm}^{-1}$  may be because of the presence of moisture in the sample. The intense band at  $466\text{ cm}^{-1}$ , on the other hand, indicates Al-O stretching vibrations.

The FT-IR spectrum of PFO acid is shown in Figure 4.12; as it can be seen there appear sharp bands at  $1132\text{ cm}^{-1}$ ,  $1144\text{ cm}^{-1}$ ,  $1196\text{ cm}^{-1}$  and  $1297\text{ cm}^{-1}$  indicating C-F stretching vibrations. The existence of O-H stretching vibrations can be understood from the band at  $3536\text{ cm}^{-1}$ , and the band at  $1692\text{ cm}^{-1}$  presents the appearance of C=O stretching vibrations. Moreover, the bands occurring between  $1500\text{--}700\text{ cm}^{-1}$  are responsible for C-C stretching vibrations.

The spectrum of PFOA can be seen in Figure 4.13. The sharp band at  $1662\text{ cm}^{-1}$  corresponds to C=O stretching vibrations as in the case of PFO acid. This band may indicate the adsorption of PFO acid arising from  $\text{-COOH}$  group reactions with  $\text{-OH}$  groups present on the alumina surface as it has been stated in the study of Kasprzyk et al (2003). The bands at  $1132\text{ cm}^{-1}$ ,  $1144\text{ cm}^{-1}$ ,  $1196\text{ cm}^{-1}$  and  $1297\text{ cm}^{-1}$  observed in the spectra of PFO acid are also present in the spectra of PFOA catalyst confirming an interaction of PFO acid with the alumina surface. In addition it is observed that the band at  $3536\text{ cm}^{-1}$  showing O-H stretching band in the spectra of PFO acid has shifted to  $3323\text{ cm}^{-1}$  in the case of PFOA.

In Figures 4.14, 4.15 and 4.16, the spectra of PFOA particles used once and more than once in the ozonation experiments can easily be examined. It was observed from the figures that no changes occur on the surface of alumina. Also it is found out that ozone gas does not deactivate the PFOA phase by oxidizing C-F bonds of PFO acid which is adsorbed on alumina surface.

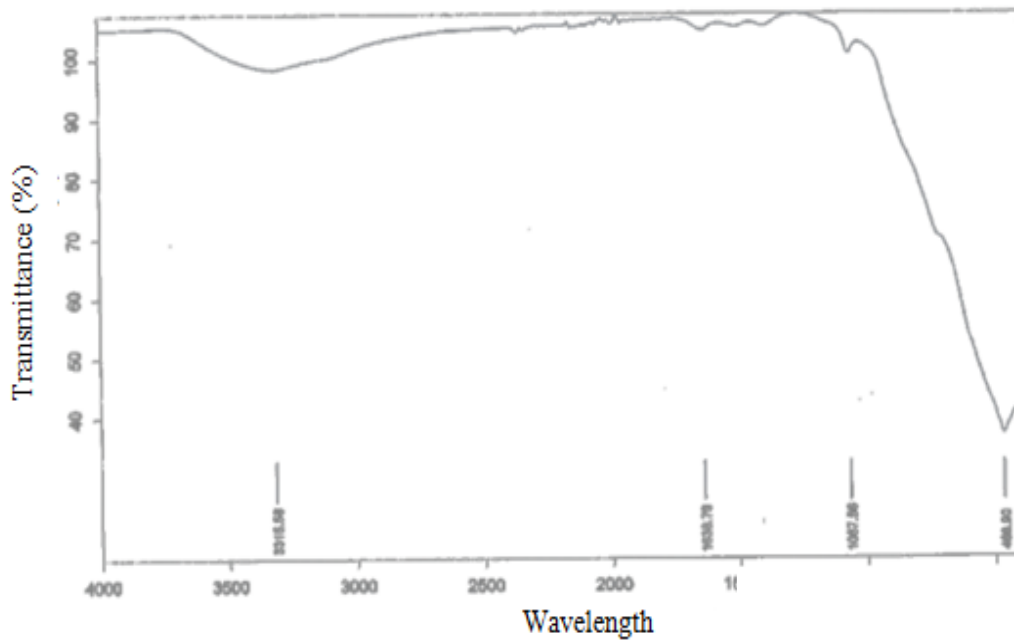


**Figure 4.11:** FT-IR Spectrum of Alumina

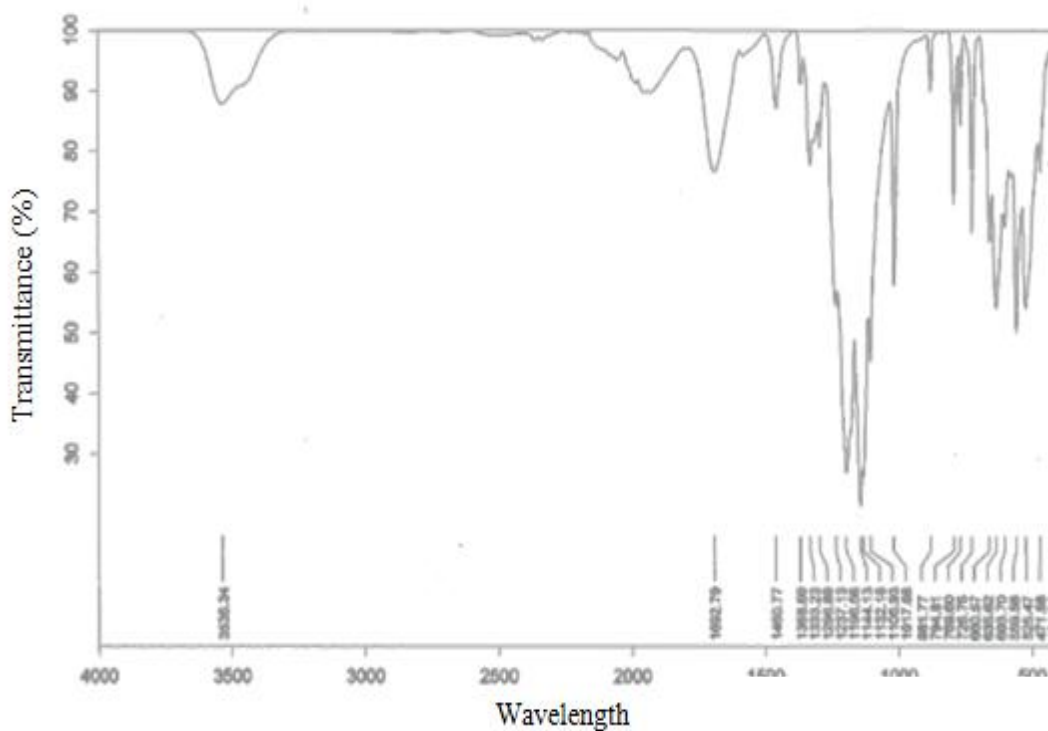


**Figure 4.12:** FT-IR Spectrum of PFO Acid

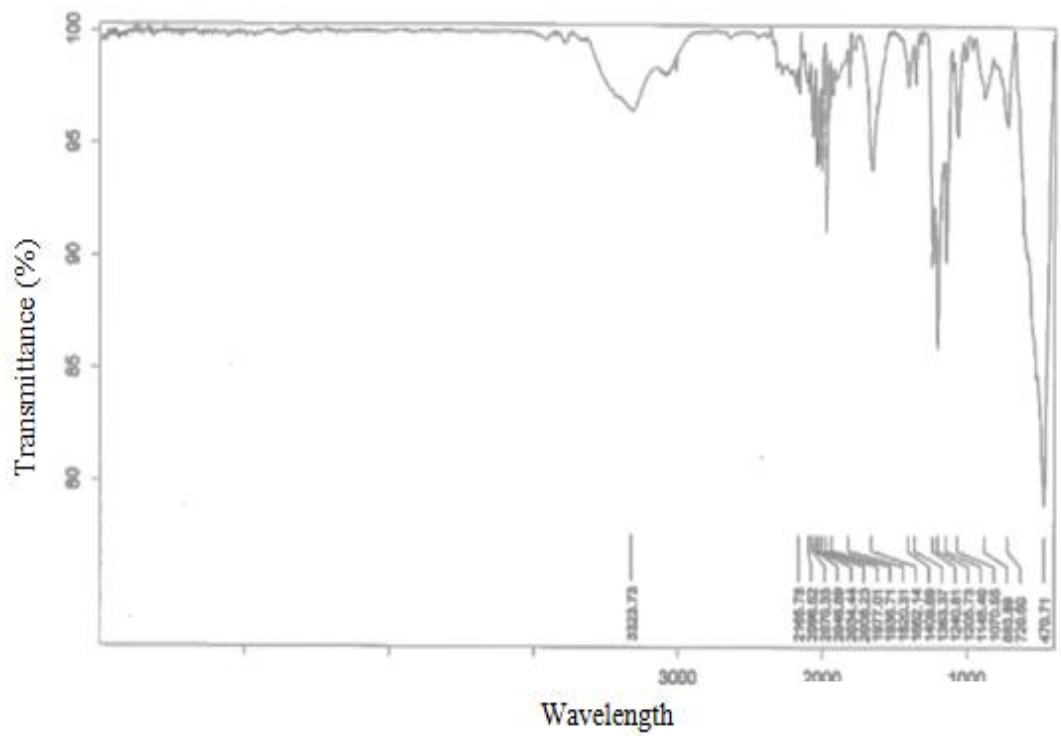


**Figure 4.13:** FT-IR Spectrum of PFOA catalyst

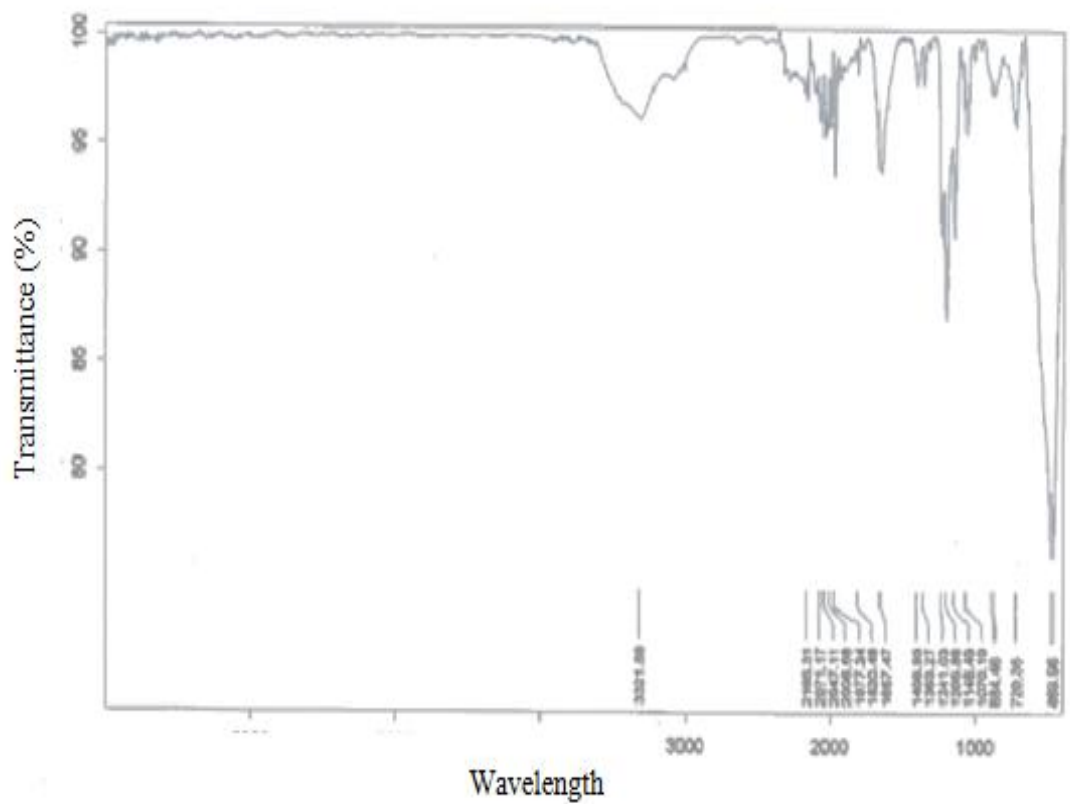


**Figure 4.14:** FT-IR Spectrum of PFOA catalyst used once

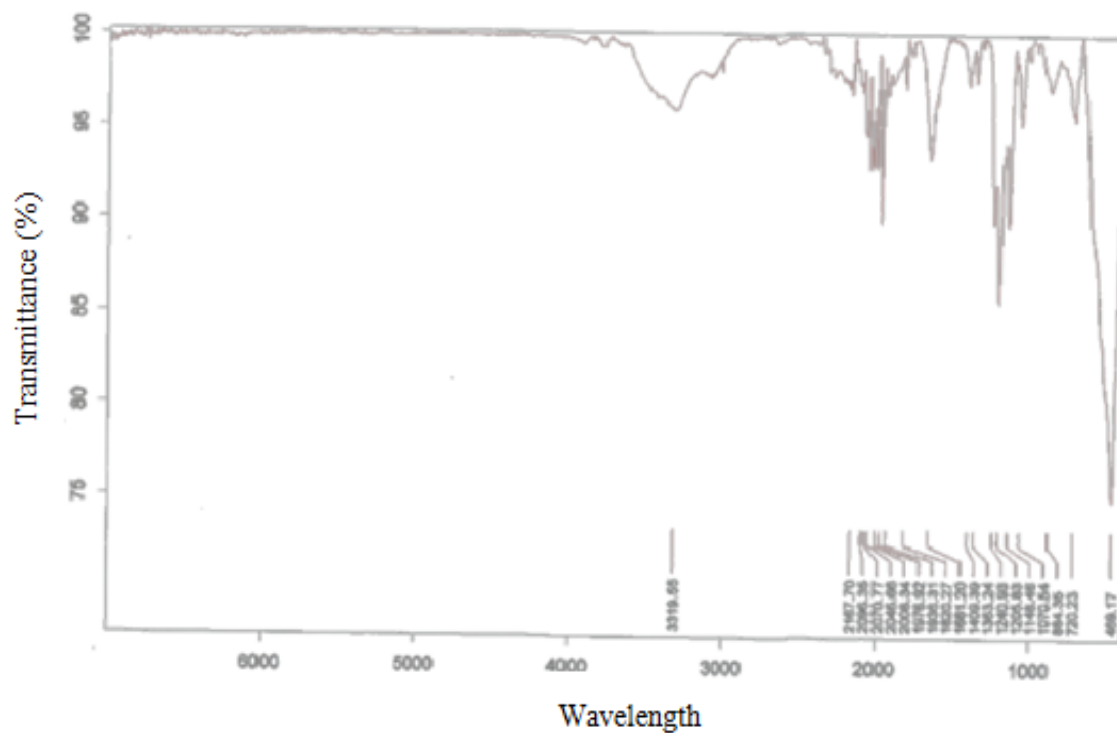


Figure 4.15: FT-IR Spectrum of PFOA catalyst used three times

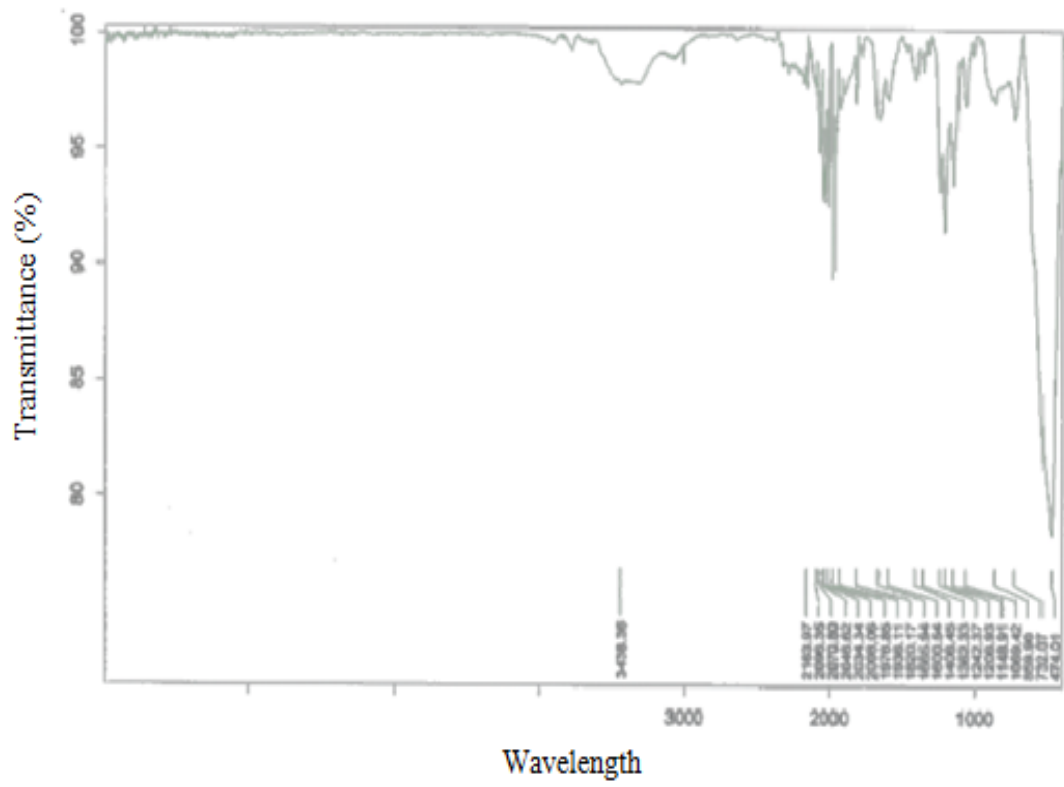


Figure 4.16: FT-IR Spectrum of PFOA catalyst used five times

#### 4.3.1.4 ESCA (XPS) Analysis

The chemical elemental composition on the surface of PFOA catalyst particles were determined by XPS analysis in METU Central Laboratory. Electron Spectroscopy for Chemical Analysis (ESCA), which is also called as XPS, is a surface analysis method which gives information about the chemical composition on the surfaces of solid materials. This method provides the emission of photoelectrons by using an X-ray beam to excite the solid samples. The spectra obtained from ESCA analysis can give information about the chemical environment and oxidation states of the elements. Atoms associated with different chemical environments produce peaks with slightly different binding energies which are called chemical shifts. Distinct chemical states which are close in energy can be separated from each other by using peak fitting programs which can give the composition of each state in percent amounts.

Also catalyst particle samples are further bombarded with 5000 eV for 2 min, in order to obtain information about the elemental composition below the surface instead of only the surface of the particles. For this purpose, an argon ion gun which lets depth profiling of the sample surface is used with the combination of the ESCA spectrometer. These analyses were conducted with 'SPECS' type electron spectroscopy in METU Central Laboratory.

Table 4.9 and 4.10 show the results obtained from ESCA analyses. As it can be seen, the fluorine amounts are lower for all of the particles exposed to bombardment stage. This can be due to the fact that instead of going further into the catalyst, PFO acid which is the main source of fluorine adsorbs on to the alumina. It is understood that the percent of elemental fluorine does not change significantly for the fresh PFOA and PFOA particles used once or three times verifying the results obtained from FT-IR studies. But, in the case of PFOA particles used for five times, the fluorine amounts are observed to decrease proving the leaching of the organic acid (PFO acid) into the water during the ozonation experiments. These results also verify that using of the catalyst three times at most provides an efficient catalytic ozonation process, and also is not harmful to the environment, because leaching of organics in to the water does not occur.

Moreover, smaller amounts of sulfur and nitrogen atoms are observed on the surface of the catalyst particles used once or more than once due to the adsorption of the dye molecules on the catalyst surface.

**Table 4.9:** Elemental compositions of the fresh PFOA catalyst particles before and after bombardment

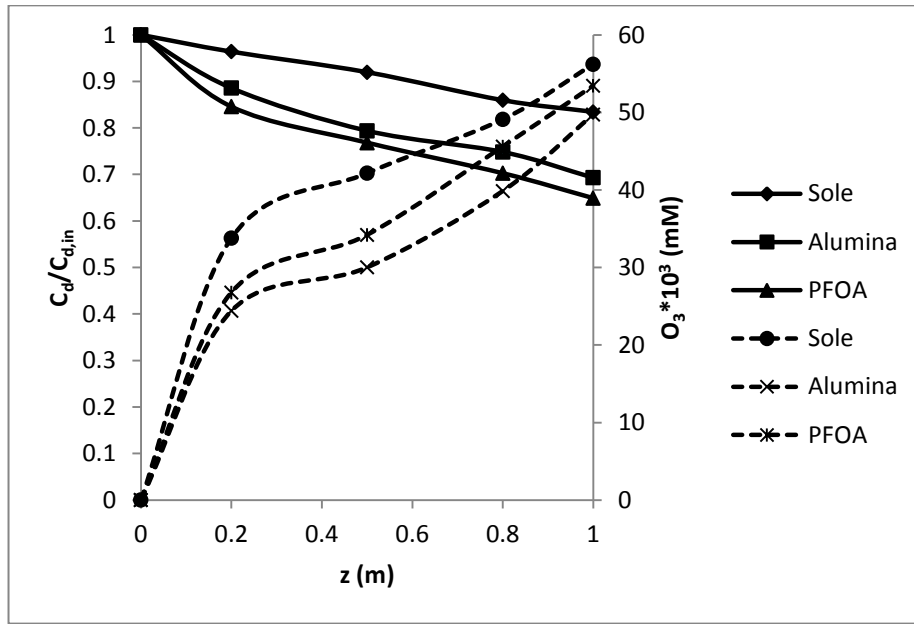
Element	Before Bombardment	After Bombardment
	Atom %	Atom %
C	14.1	15.9
O	40	45.4
F	31	18.9
Al	14.9	19.8
N	0	0
S	0	0

**Table 4.10:** Elemental percentages of the PFOA catalyst particles used for one, three and five times before and after bombardment

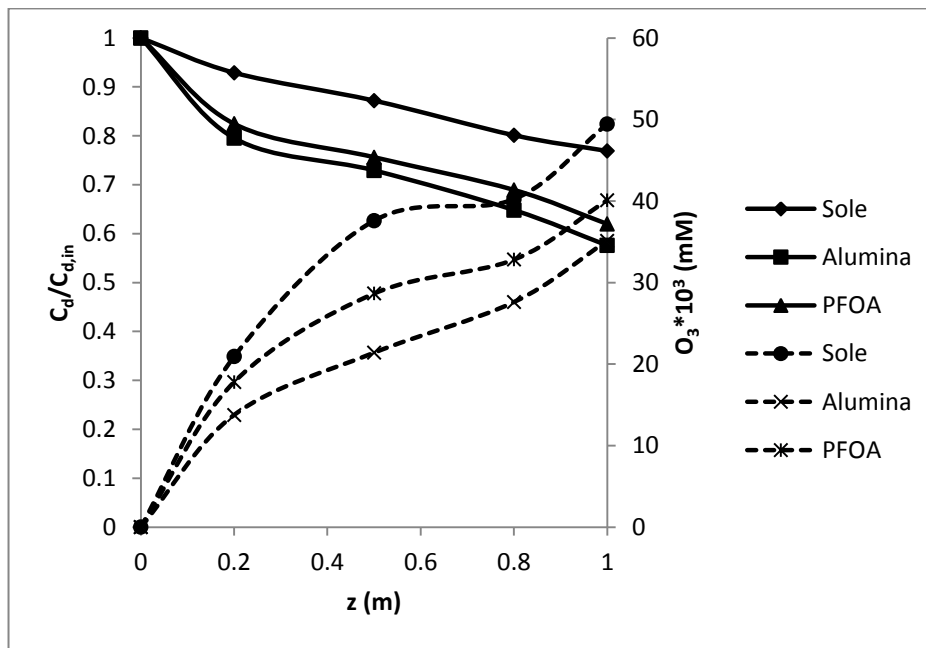
Element	PFOA (one time)		PFOA (three times)		PFOA (five times)	
	Bombardment		Bombardment		Bombardment	
	Before	After	Before	After	Before	After
	Atom %	Atom %	Atom %	Atom %	Atom %	Atom %
C	13.8	13.6	12.6	11	15	19.7
O	40	44.3	42.4	46.8	44.9	48.7
F	31.6	21.5	28.6	20.2	21.6	9.5
Al	14.5	20.3	16.4	21.9	18.4	22.2
N	0.1	0.3	0.1	0.2	0	0
S	0	0	0	0	0.1	0

### 4.3.2 Effect of pH on Catalytic Ozonation

The effect of pH on catalytic ozonation process becomes important because of its effect on the possible radical reactions occurring during ozonation. In Figures 4.17, 4.18 and 4.19, it is observed that both of the catalysts have a positive effect on the color removals. Alumina catalyst provides high removals in basic media because of its catalytic activity on the decomposition reactions of ozone into hydroxyl radicals with hydroxyl ions being available at higher pH values (Thomas et al., 1997).

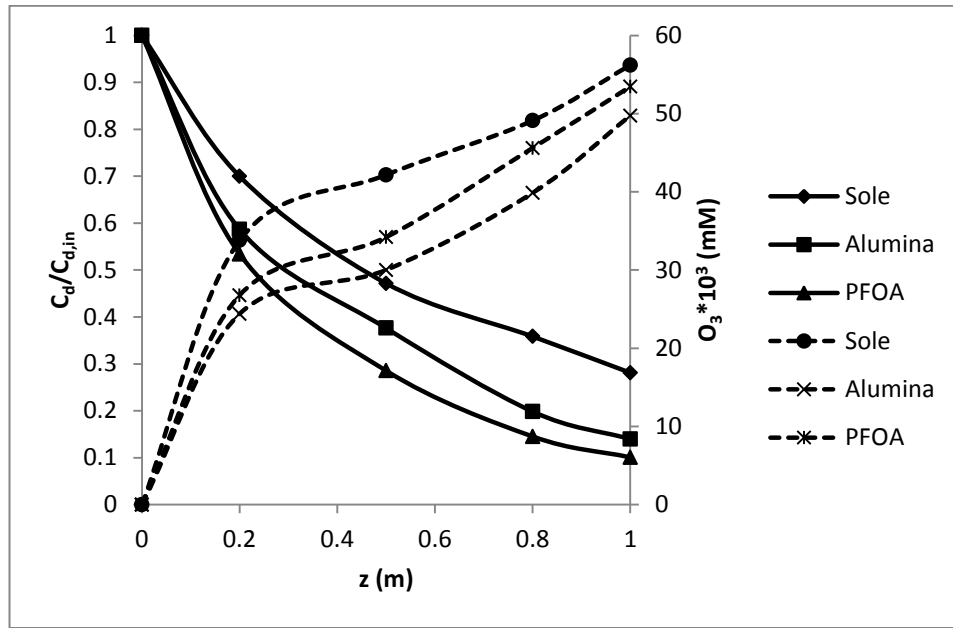


(a)

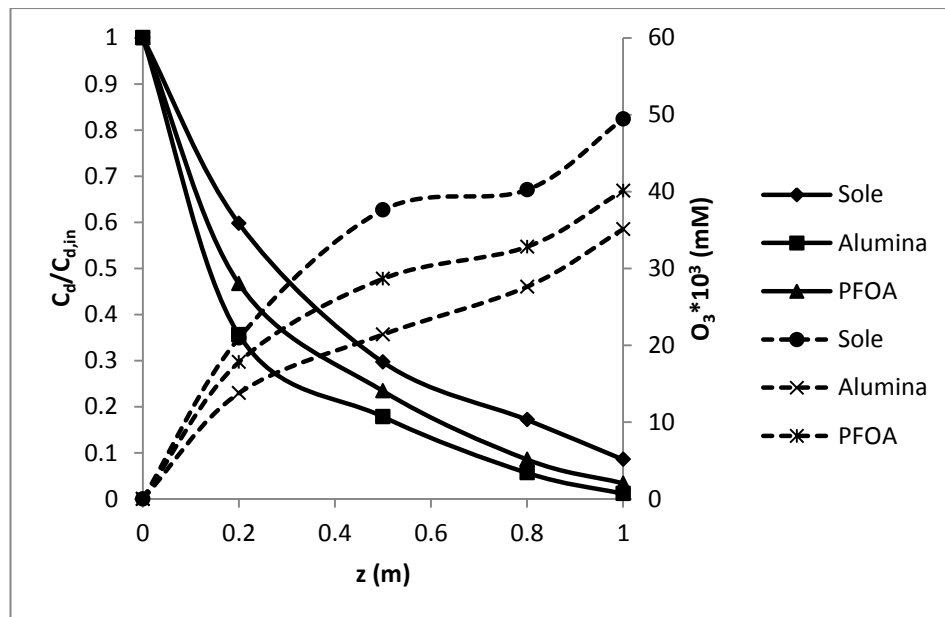


(b)

**Figure 4.17:** The effect of catalyst addition on blue dye (BB 41) removal (in terms dye concentrations for each dye in WW solution) and ozone concentration,  $Q_G = 340$  L/h,  $Q_L = 250$  L/h,  $C_{O_3,G,in} = 0.9 \pm 0.1$  mmol/L gas,  $COD_{in} = 300$  mg/L,  $C_{d,in, BB\ 41} = 150.9$  mg/L,  $C_{d,in, BR\ 18.1} = 26.4$  mg/L,  $C_{d,in, BY\ 28} = 26.2$  mg/L,  $m_{cat} = 300$  g, (a) pH = 4, (b) pH = 10, In figures dye concentration is shown by line and ozone concentration in liquid phase by dotted line (----).

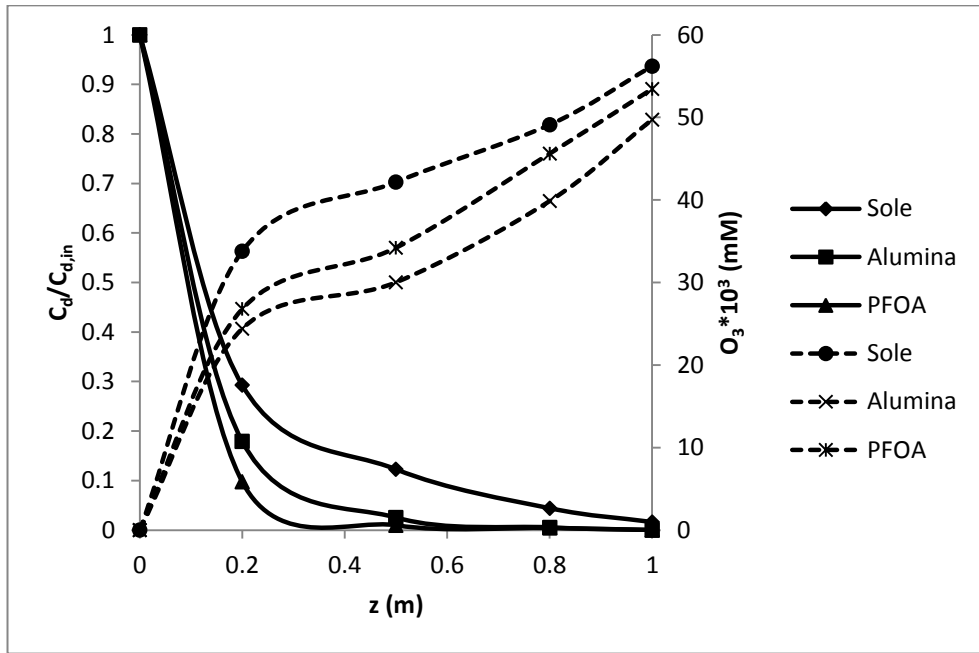


(a)

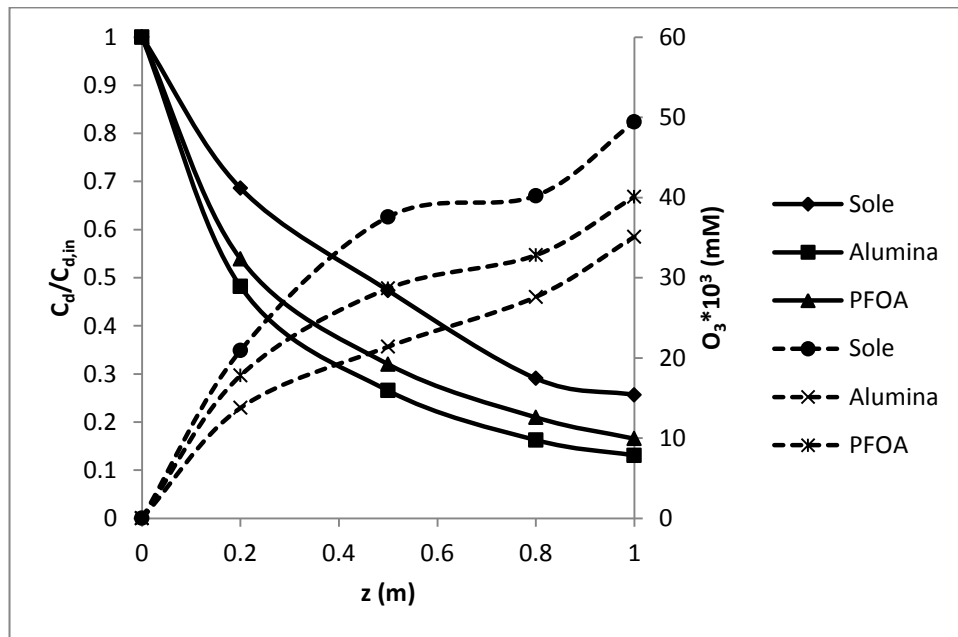


(b)

**Figure 4.18:** The effect of catalyst addition on red dye (BR 18.1) removal (in terms dye concentrations for each dye in WW solution) and ozone concentration,  $Q_G=340$  L/h,  $Q_L=250$  L/h,  $C_{O_3,G,in}=0.9 \pm 0.1$  mmol/L gas,  $COD_{in}=300$  mg/L,  $C_{d,in,BB\ 41}=150.9$  mg/L,  $C_{d,in,BR\ 18.1}=26.4$  mg/L,  $C_{d,in,BY\ 28}=26.2$  mg/L,  $m_{cat}=300$  g, (a) pH = 4, (b) pH = 10, In figures dye concentration is shown by line and ozone concentration in liquid phase by dotted line (----).



(a)



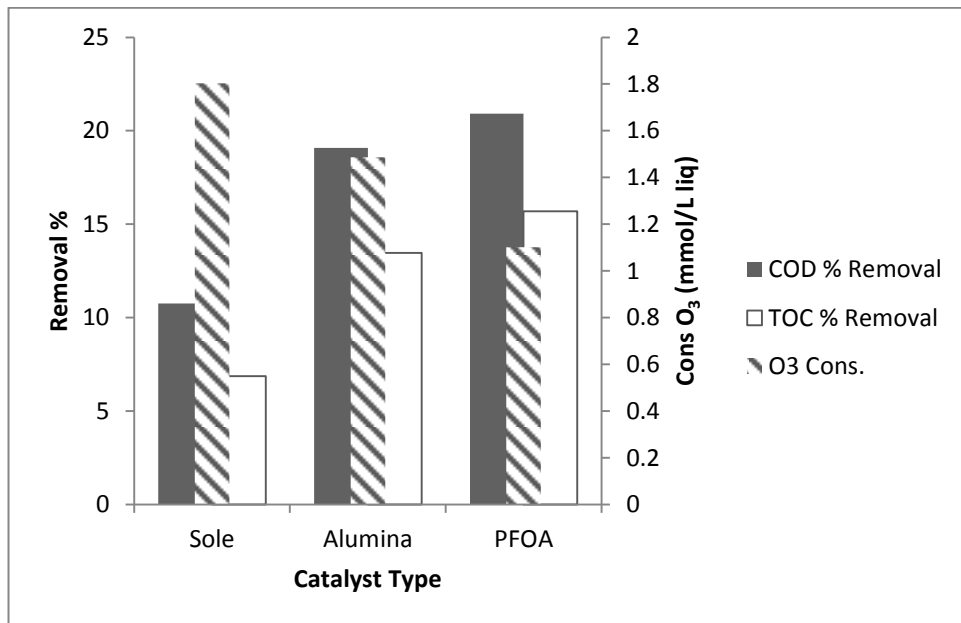
(b)

**Figure 4.19:** The effect of catalyst addition on yellow dye (BY 28) removal (in terms dye concentrations for each dye in WW solution) and ozone concentration,  $Q_G = 340$  L/h,  $Q_L = 250$  L/h,  $C_{O_3,G,in} = 0.9 \pm 0.1$  mmol/L gas,  $COD_{in} = 300$  mg/L,  $C_{d,in, BB 41} = 150.9$  mg/L,  $C_{d,in, BR 18.1} = 26.4$  mg/L,  $C_{d,in, BY 28} = 26.2$  mg/L,  $m_{cat} = 300$  g, (a) pH = 4, (b) pH = 10, In figures dye concentration is shown by line and ozone concentration in liquid phase by dotted line (----).

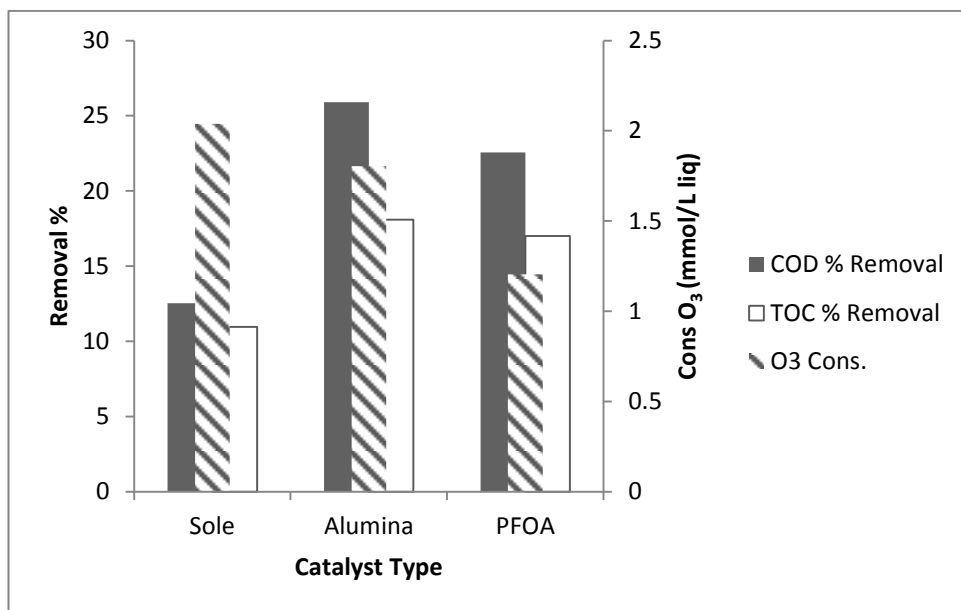
Moreover, in the catalytic ozonation, the effect of adsorption of dye molecules on catalyst surface should not be ignored. The adsorption capability of the catalyst depends on its type, properties, groups on its surface and solution pH (Erol and Özbelge, 2008). The pH of point zero charge ( $\text{pH}_{\text{PZC}}$ ) at which the net surface charge is zero determines the surface charge of Alumina particles at a known pH. At acidic pH where the pH is less than the  $\text{pH}_{\text{PZC}}$  value, surface of alumina is positive and therefore anions could easily be adsorbed on its surface. Conversely, at basic pH ( $\text{pH} > \text{pH}_{\text{PZC}}$ ), the surface is negative and let cations to be adsorbed (Kasprzyk-Hordern et al., 2003). A basic dye such as the dyes found in AKSA ITWW, is positively charged in the solution and is adsorbed on the surface of alumina at basic pH. Easily adsorbed dye molecules on the surface can be degraded by remaining ozone and radicals on the surface of the catalyst as well as in the liquid phase. On the other hand, in the case of PFOA catalyst, instead of surface acidity or basicity, the hydrophobic character becomes important for the adsorption due to the formation of perfluorinated alkyl chains on the surface. Organic molecules which are hydrophobic in character could easily be adsorbed on the surface of PFOA catalyst. Depending on the results, it is found out that PFOA reveals higher removals in acidic medium (Figures 4.17(a), 4.18(a) and 4.19(a)). As it is discussed above, at low pH values, molecular ozone oxidizes the organic pollutants by direct ozonation mechanism. Therefore, at low pHs it is important to keep molecular ozone and to increase its solubility in the reaction medium to get higher efficiencies. In the alkyl phase (reaction medium where both ozone and organic pollutants diffuse and give reaction) on surface of PFOA catalyst, the solubility of ozone is about ten times higher than its value in water (Kasprzyk-Hordern et al., 2004). This may also reveal the dependency of PFOA catalytic activity on the length of perfluorinated alkyl chains on the surface of the catalyst (Kasprzyk-Hordern et al., 2003). Moreover, at acidic pHs, due to the low hydroxyl ion concentrations, the decomposition rate of ozone into hydroxyl radicals ( $\text{OH}^\bullet$ ) is very low. Therefore, it becomes reasonable to obtain high removals in acidic medium by PFOA catalyst.

Figures 4.20(a) and 4.20(b) showed that for the studied pHs, the COD and TOC removals increased with the addition of each type of catalyst. As it can be seen in Table 4.12, while low pH enhances the activity of PFOA, alumina provides higher COD removal percentage at high pH. Moreover while at high pH, alumina increases

the TOC removal from 6.86 % to 15.68 %; alumina can also cause an increase of 7.38 % (from 6.8 % to 13.46 %) in the COD removal at high pH.



(a)



(b)

**Figure 4.20:** The effect of Alumina and PFOA catalysts on TOC and COD removals with ozone consumptions.  $Q_G=340$  L/h,  $Q_L=250$  L/h,  $C_{O_3,G,in}=0.9 \pm 0.1$  mmol/L gas, catalyst:  $Al_2O_3$  and PFOA,  $m_{cat}=300$  g,  $COD_{in}=300$  mg/L, (a) pH = 4; (b) pH = 10, for  $Al_2O_3$   $H_E = 17$  cm, for PFOA  $H_E = 18.3$  cm,  $H_S = 5$  cm.

The high efficiency of PFOA catalyst on COD removals may be due to the adsorption of by-products on PFOA catalyst. Because of the adsorption of the dye molecules on alumina, dye molecules and ozonation by-products would compete among themselves for the surface active sites. For the alumina catalyst, adsorption of dye is more dominant than the by-products causing lower COD removals. PFOA catalyst, on the other hand, preferred the adsorption of ozonation by-products due to its non-polar nature (Erol and Özbelge, 2008).

**Table 4.11:** The dye removals for different pH,  $COD_{in}$  and catalyst type  $C_{O_3,G,in} = 0.9 \pm 0.1$  mmol/L gas,  $Q_G = 340$  L/h,  $Q_L = 250$  L/h,  $m_{cat} = 300$  g, for  $Al_2O_3$   $H_E = 17$  cm, for PFOA  $H_E = 18.3$  cm,  $H_S = 5$  cm.

Catalyst	pH	$COD_{in}$ (mg/L)	BB 41 Removal (%)	BR 18.1 Removal (%)	BY 28 Removal (%)
sole	4	180	35.70	88.81	99.82
	10		42.63	98.85	91.05
	4	300	16.55	71.88	98.37
	10		23.09	91.44	74.35
Alumina	4	180	49.91	98.98	98.99
	10		59.07	99.87	98.88
	4	300	30.71	86.02	99.98
	10		42.39	98.86	86.92
PFOA	4	180	51.47	99.11	99.9
	10		53.09	99.56	95.64
	4	300	35.09	89.91	99.98
	10		38.01	96.59	83.45

Moreover, catalytic ozonation can be accepted as a more efficient oxidation process economically since using catalysts during ozonation decreases the ozone consumption. In Figure 4.20 and Table 4.12 it can be easily seen that PFOA catalyst decreases the amount of ozone consumptions compared to those in the sole ozonation for the required treatment efficiency by increasing the utilization ratio. In other words, the catalyst provides an efficient usage of ozone by organics in the solution by increasing the stability of ozone in the alkyl phase.

**Table 4.12:** The TOC, COD removals with ozone consumptions for different pH,  $COD_{in}$  and catalyst type  $C_{O_3,G,in} = 0.9 \pm 0.1$  mmol/L gas,  $Q_G = 340$  L/h,  $Q_L = 250$  L/h,  $m_{cat} = 300$  g, for  $Al_2O_3$   $H_E = 17$  cm, for PFOA  $H_E = 18.3$  cm,  $H_S = 5$  cm.

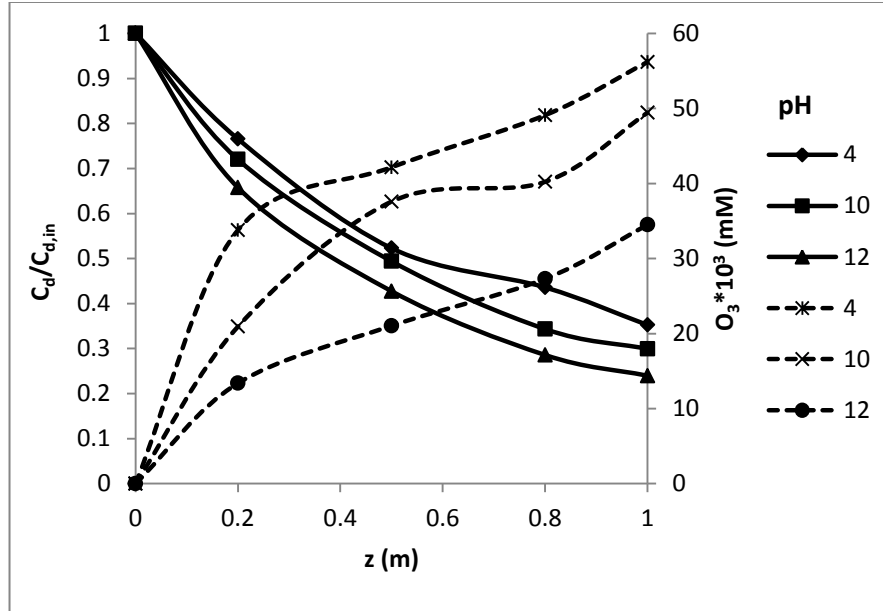
Catalyst	pH	$COD_{in}$ (mg/L)	TOC Removal (%)	COD Removal (%)	$Cons_{O_3}$ (mmol/L liq.)
sole	4	180	12.45	16.49	1.273
	10		14.35	12.28	1.469
	4	300	6.86	10.75	1.803
	10		10.97	12.54	2.038
Alumina	4	180	20.57	25.83	0.904
	10		26.55	30.71	1.264
	4	300	13.47	19.08	1.487
	10		18.09	25.9	1.803
PFOA	4	180	22.98	27.9	0.726
	10		23.19	28.09	0.901
	4	300	15.69	20.92	1.102
	10		17.02	22.56	1.205

### 4.3.3 Higher pH Effect on Catalytic Ozonation

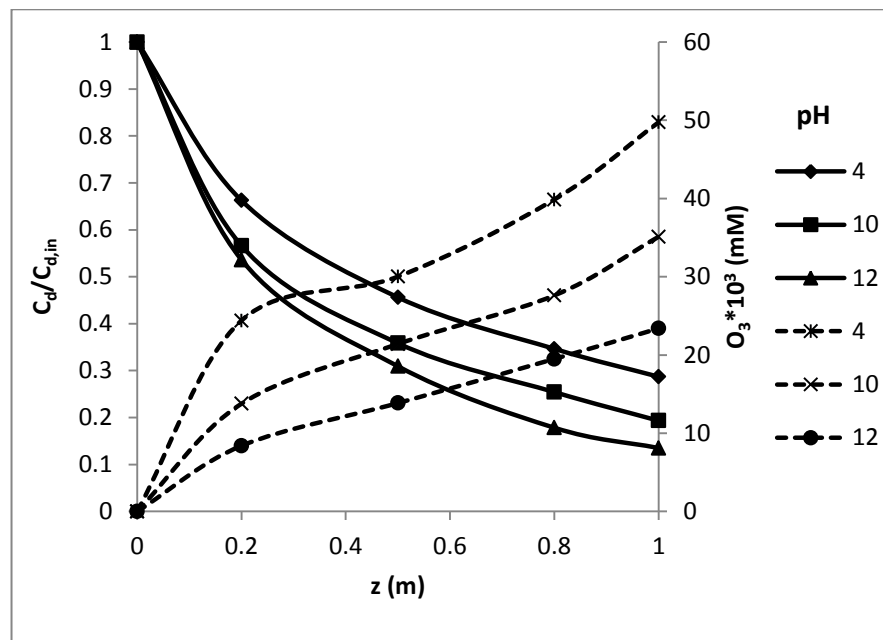
The experimental results found showed that increasing pH from pH of 4 to pH of 10 provided higher dye (in terms of Pt-Co unit), TOC and COD removals in the ozonation of wastewater. This gave the idea if increasing pH further yields can increase the removals further or not. In order to find out the optimum parameters for the ozonation of wastewater taken from AKSA Acrylic Plant, it makes sense to investigate the ozonation reaction at pH of 12 by using both alumina and PFOA particles.

Figures 4.21(a), 4.21(b) and 4.21(c) showed the results obtained for pH of 12 with pHs 4 and 10. The overall color removals (in terms of Pt-Co unit) seemed to follow an increasing trend with increasing pH. On the other hand, when the dyes in the WW solution investigated separately blue and red dyes were observed to degrade higher at high pH of 12; but yellow dye were examined to show higher removal at pH of 4 (Table 4.13). The different effects of hydroxyl radicals and molecular ozone on different types of dyes cause these changes in the degradation of dye molecules, as expected. The use of different catalyst particles, alumina and PFOA, enhances the ozonation reaction both at alkaline and acidic pH; but again the overall color

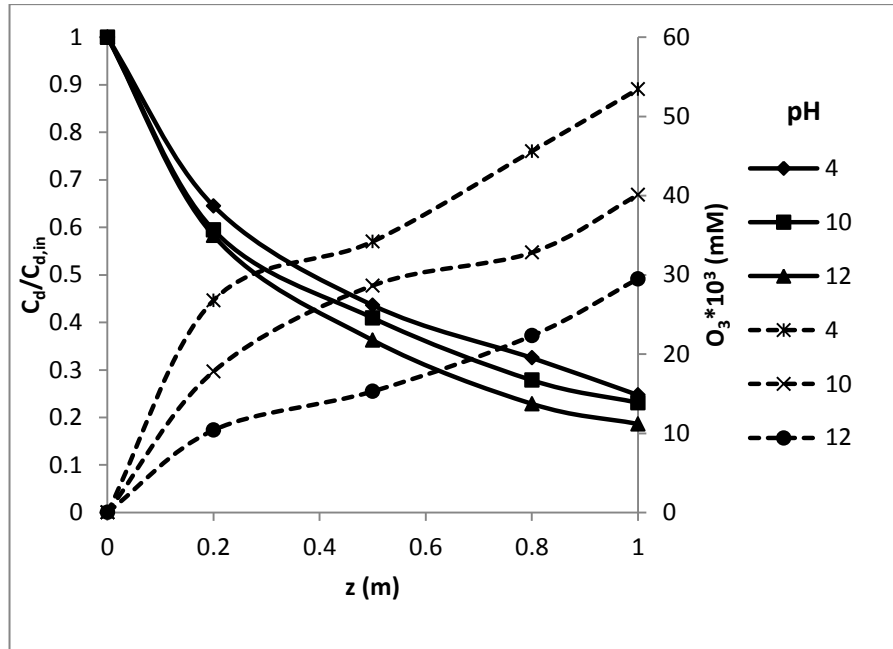
removals showed their maximum at alkaline pH of 12 with alumina particles. Moreover, the highest TOC and COD removals were obtained again at pH of 12 with alumina particles (Figures 4.22(a), 4.22(b) and 4.22(c) and Table 4.14).



(a)



(b)



(c)

**Figure 4.21:** The effect of pH on overall color removals (in terms of Pt-Co unit) and ozone concentration,  $Q_G = 340$  L/h,  $Q_L=250$  L/h,  $C_{O_3,G,in} = 0.9 \pm 0.1$  mmol/L gas, catalyst: (a) none, (b) Alumina, (c) PFOA,  $COD_{in} = 300$  mg/L ( $C_{d,in} = 1570$  Pt-Co),  $m_{cat} = 300$  g. In figures dye concentration is shown by line and ozone concentration in liquid phase by dotted line (----).

**Table 4.13:** The dye removals for different pH, and catalyst type,  $COD_{in} = 300$  mg/L ( $C_{d,in,BB\ 41} = 150.9$  mg/L,  $C_{d,in,BR\ 18.1} = 26.4$  mg/L,  $C_{d,in,BY\ 28} = 26.2$  mg/L,  $C_{d,in} = 1570$  Pt-Co),  $C_{O_3,G,in} = 0.9 \pm 0.1$  mmol/L gas,  $Q_G = 340$  L/h,  $Q_L=250$  L/h,  $m_{cat} = 300$  g, for  $Al_2O_3$   $H_E = 17$  cm, for PFOA  $H_E = 18.3$  cm,  $H_S = 5$  cm.

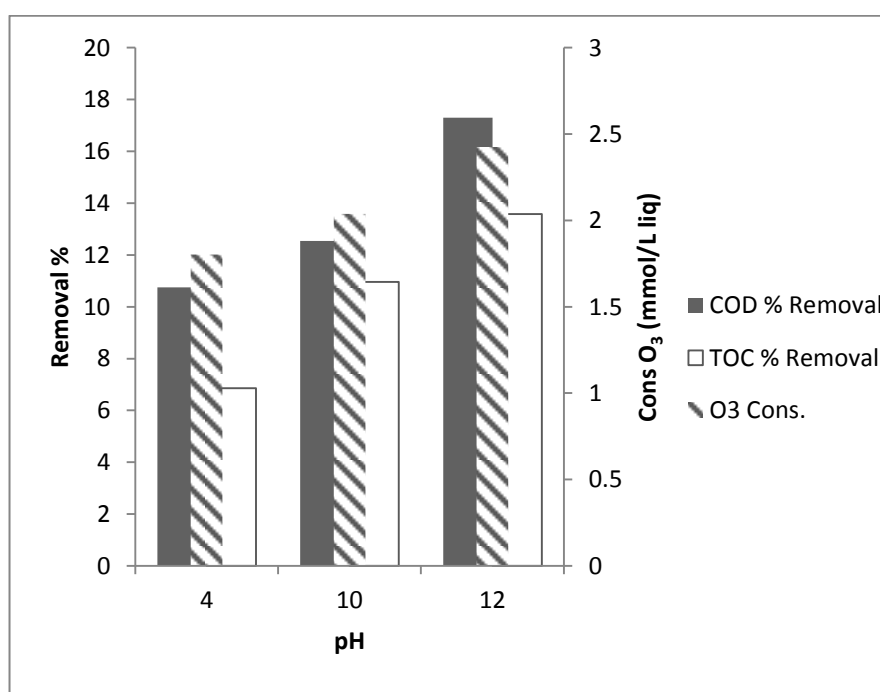
Catalyst	pH	BB 41 Removal (%)	BR 18.1 Removal (%)	BY 28 Removal (%)
Sole	4	16.55	71.88	98.37
	10	23.09	91.44	74.35
	12	30.19	97.38	70.23
Alumina	4	30.71	86.02	99.98
	10	42.40	98.86	86.92
	12	48.49	99.00	82.39
PFOA	4	35.09	89.91	99.99
	10	38.02	96.59	83.45
	12	43.49	98.15	74.28

The low concentration of yellow dye in WW solution and the higher overall color, TOC and COD removals at higher pH (pH = 12) makes the pH parameter of 12 more preferable for the ozonation of WW taken from AKSA. Moreover, the addition of alumina particles into the reaction medium yields most efficient organic removals at

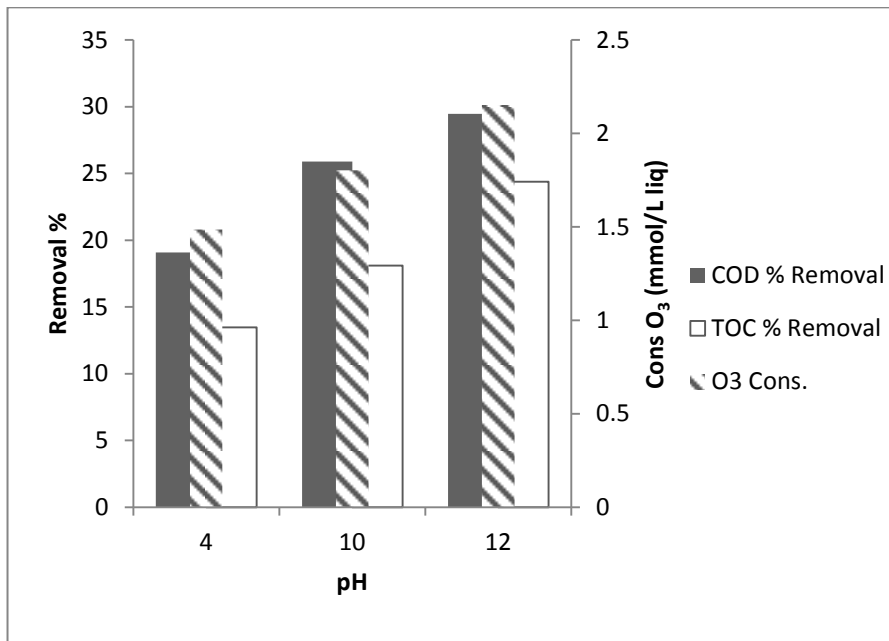
pH of 12. As alumina particles were known to enhance the ozone decomposition reactions; it can be concluded that for the ozonation of WW taken from AKSA the role of hydroxyl radicals is more important than the molecular ozone.

**Table 4.14:** The TOC, COD and color removals with ozone consumptions for different pH, and catalyst type,  $COD_{in} = 300$  mg/L ( $C_{d,in,BB\ 41} = 150.9$  mg/L,  $C_{d,in,BR\ 18.1} = 26.4$  mg/L,  $C_{d,in,BY\ 28} = 26.2$  mg/L,  $C_{d,in} = 1570$  Pt-Co),  $C_{O_3,G,in} = 0.9 \pm 0.1$  mmol/L gas,  $Q_G = 340$  L/h,  $Q_L = 250$  L/h,  $m_{cat} = 300$  g, for  $Al_2O_3$   $H_E = 17$  cm, for PFOA  $H_E = 18.3$  cm,  $H_S = 5$  cm.

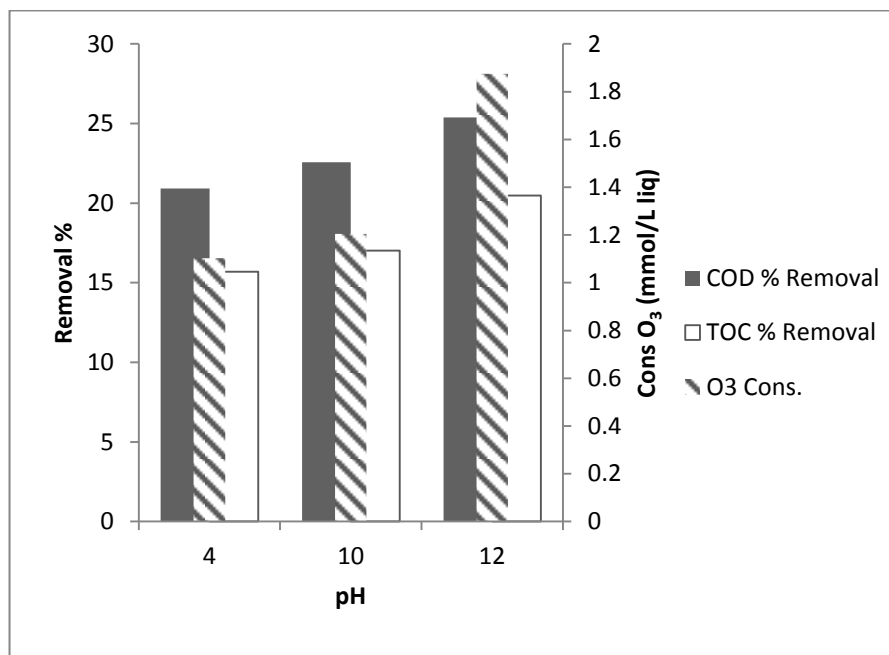
Catalyst	pH	TOC Removal (%)	COD Removal (%)	Color Removal (%)	Cons <sub>O<sub>3</sub></sub> (mmol/L liq.)
Sole	4	6.86	10.75	64.75	1.803
	10	10.97	12.54	70.05	2.038
	12	13.58	17.30	76.03	2.427
Alumina	4	13.47	19.08	71.30	1.487
	10	18.10	25.90	80.67	1.804
	12	24.38	29.48	86.49	2.153
PFOA	4	15.69	20.92	75.28	1.102
	10	17.02	22.56	76.90	1.205
	12	20.49	25.38	81.37	1.875



(a)



(b)

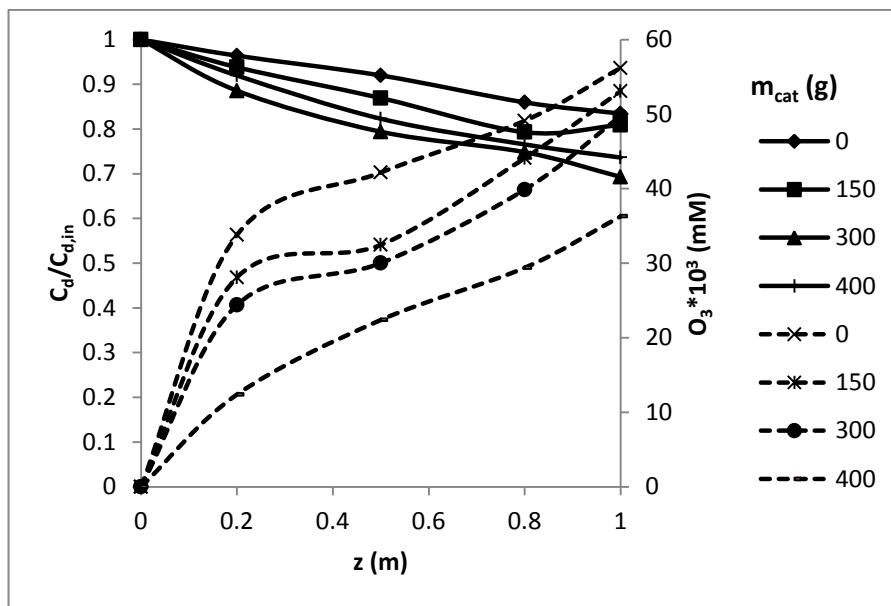


(c)

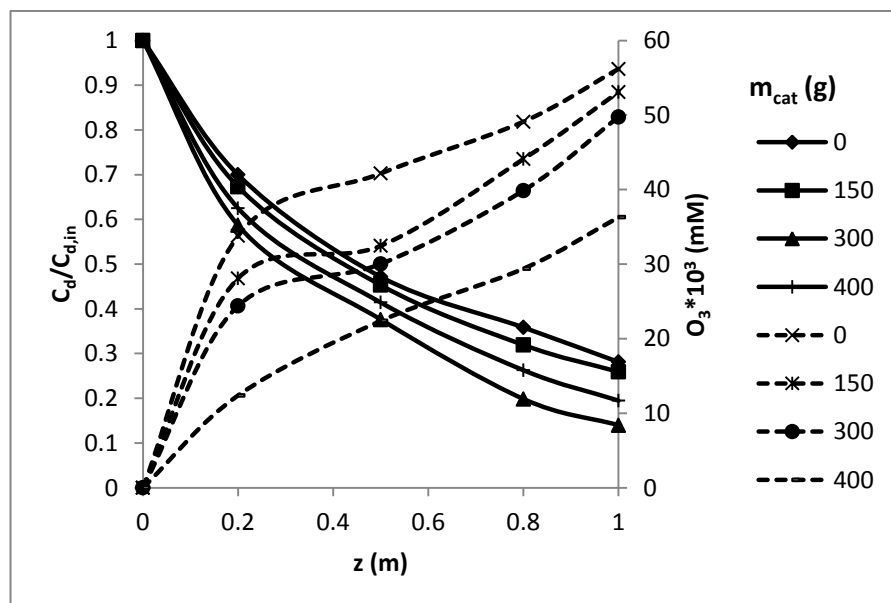
**Figure 4.22:** The effect of pH on TOC, COD removals and ozone consumption,  $Q_G = 340$  L/h,  $Q_L=250$  L/h,  $C_{O_3,G,in} = 0.9 \pm 0.1$  mmol/L gas, catalyst: (a) none, (b) Alumina, (c) PFOA,  $COD_{in} = 300$  mg/L ( $C_{d,in,BB 41} = 150.9$  mg/L,  $C_{d,in,BR 18.1} = 26.4$  mg/L,  $C_{d,in,BY 28} = 26.2$  mg/L,  $C_{d,in} = 1570$  Pt-Co),  $m_{cat} = 300$  g.

### 4.3.4 Effect of Catalyst Dosage

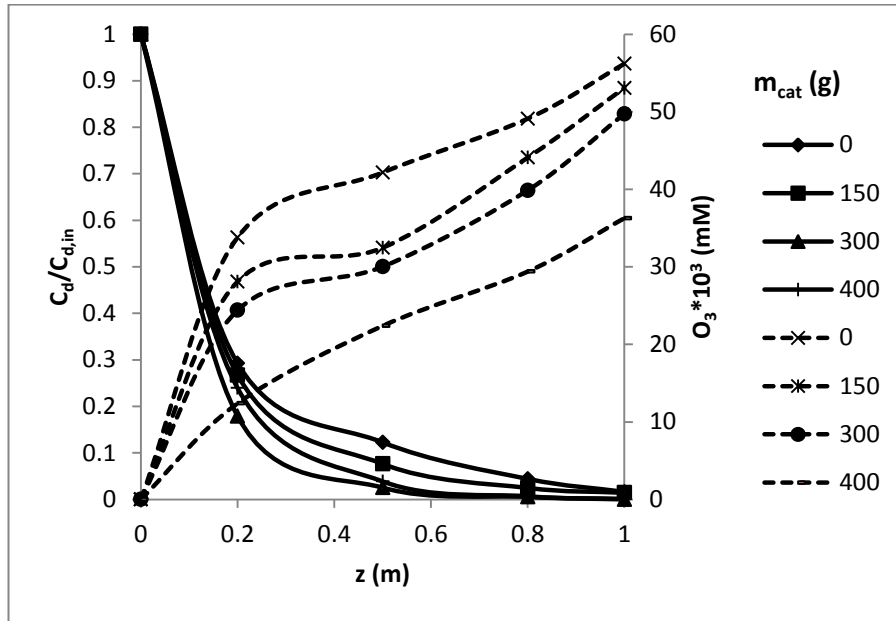
In order to investigate if the catalyst loading to reactor has an effect on ozonation, the catalysts at different dosages were added to the reaction media. Experiments were performed by using 150 g, 300 g and 400 g of alumina and PFOA catalysts and the results were shown in terms of dye, TOC and COD removals with ozone consumptions in Figures 4.23 and 4.24 and in Table 4.15.



(a)

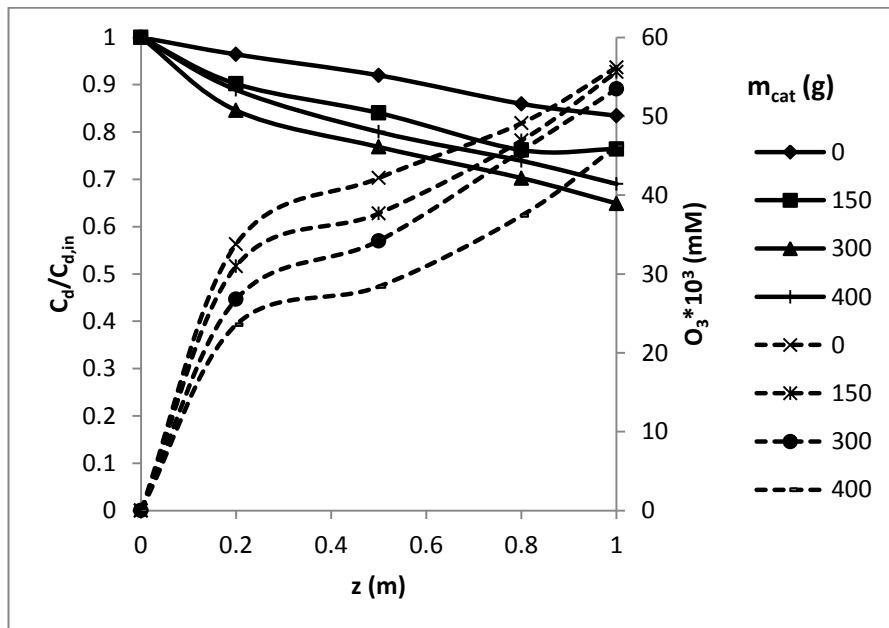


(b)

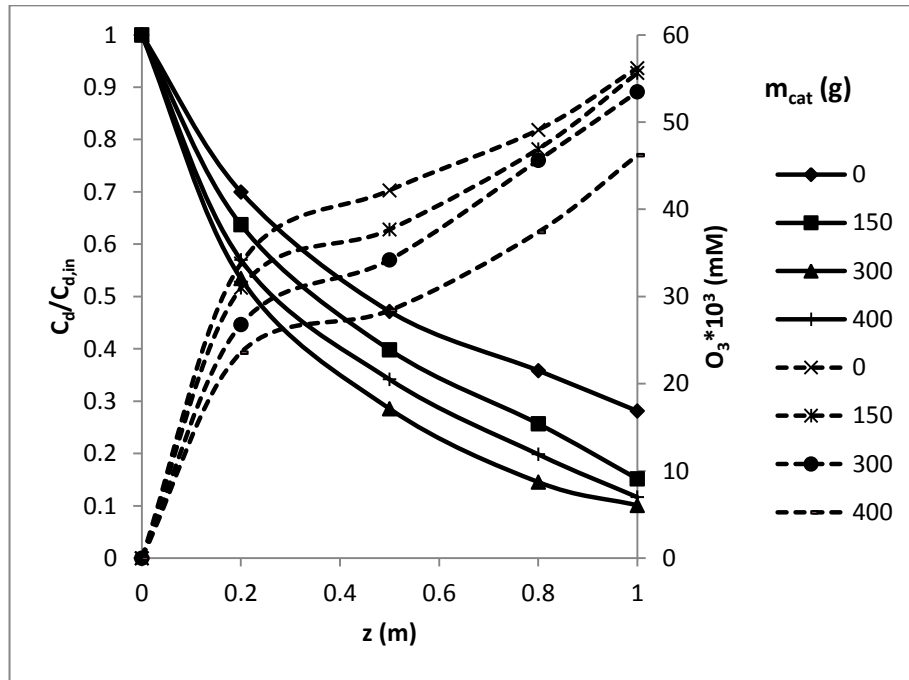


(c)

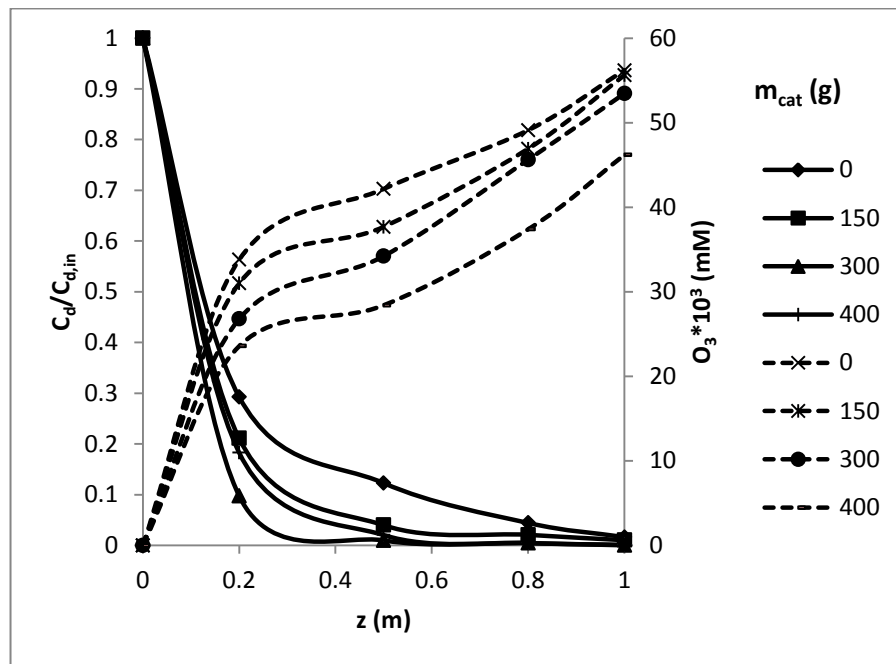
**Figure 4.23:** The effect of catalyst dosage on dye removals (in terms dye concentrations for each dye in WW solution) and ozone concentration,  $Q_G = 340$  L/h,  $Q_L = 250$  L/h,  $C_{O_3,G,in} = 0.9 \pm 0.1$  mmol/L gas, catalyst: Alumina, pH = 4,  $COD_{in} = 300$  mg/L, ( $C_{d,in,BB\ 41} = 150.9$  mg/L,  $C_{d,in,BR\ 18.1} = 26.4$  mg/L,  $C_{d,in,BY\ 28} = 26.2$  mg/L), (a) BB 41, (b) BR 18.1, (c) BY 28. In figures dye concentration is shown by line and ozone concentration in liquid phase by dotted line (----).



(a)



(b)



(c)

**Figure 4.24:** The effect of catalyst dosage on dye removals (in terms dye concentrations for each dye in WW solution) and ozone concentration,  $Q_G = 340$  L/h,  $Q_L = 250$  L/h,  $C_{O_3,G,in} = 0.9 \pm 0.1$  mmol/L gas, catalyst: PFOA, pH = 4,  $COD_{in} = 300$  mg/L, ( $C_{d,in,BB\ 41} = 150.9$  mg/L,  $C_{d,in,BR\ 18.1} = 26.4$  mg/L,  $C_{d,in,BY\ 28} = 26.2$  mg/L), (a) BB 41, (b) BR 18.1, (c) BY 28. In figures dye concentration is shown by line and ozone concentration in liquid phase by dotted line (----).

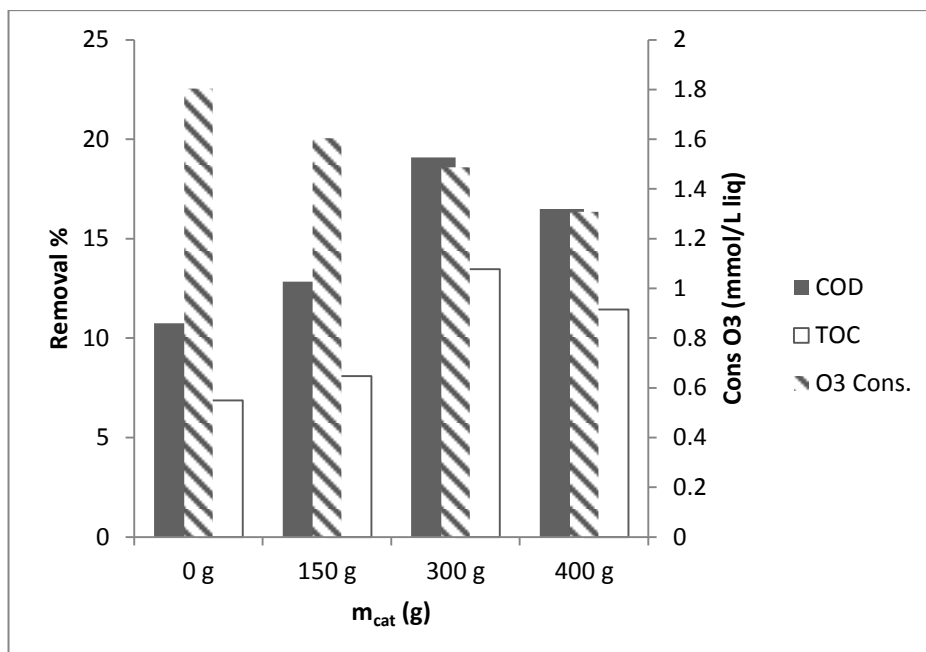


**Figure 4.25:** The effect of catalyst dosage on TOC, COD removals with ozone consumptions,  $Q_G = 340$  L/h,  $Q_L=250$  L/h,  $C_{O_3,G,in} = 0.9 \pm 0.1$  mmol/L gas, catalyst: Alumina, pH = 4,  $COD_{in} = 300$  mg/L.

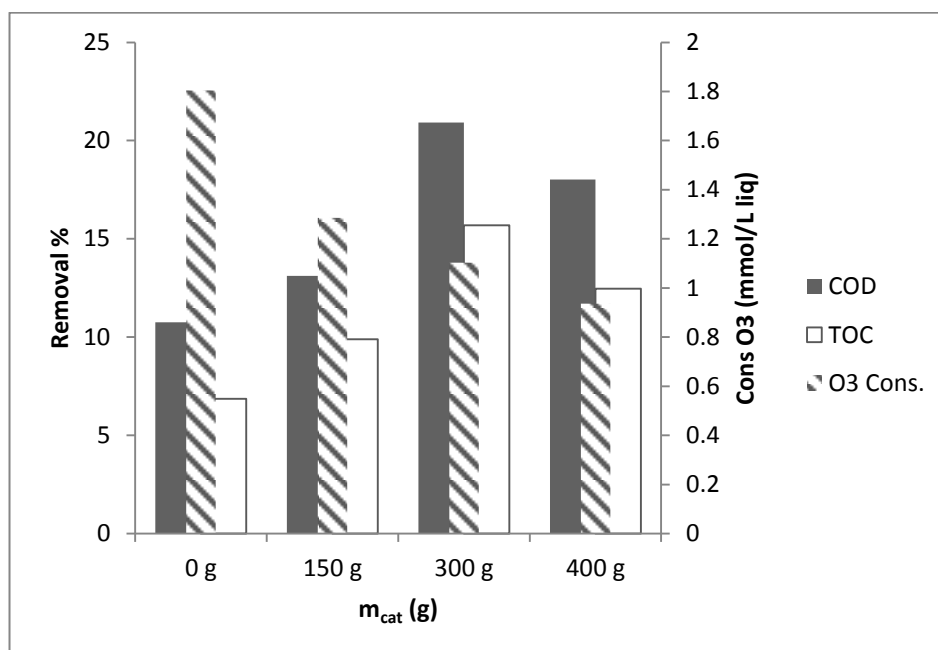


**Figure 4.26:** The effect of catalyst dosage on TOC, COD removals with ozone consumptions,  $Q_G = 340$  L/h,  $Q_L=250$  L/h,  $C_{O_3,G,in} = 0.9 \pm 0.1$  mmol/L gas, catalyst: PFOA, pH = 4,  $COD_{in} = 300$  mg/L.

As it can be seen from the Figures 4.25 and 4.26, increasing the catalyst loading to 300 g had an important influence on the degradation efficiencies of all of the dyes

and also on TOC and COD removals. Since the active sites on the surfaces of both of the catalysts have a great importance on the ozonation reactions, increasing the catalyst dosage yields higher degradation because of the increased number of the active sites and surface area by adding high dosages of catalysts to the reaction medium.

Adding 300 g of PFOA showed increments from 16.4% to 27.9% in COD removals at q pH of 4 when the inlet COD concentrations are 180 mg/L and 300 mg/L, respectively. On the other hand, alumina provided higher increments of 13% (17.2% to 30.2%) and 13.4% (12.5% to 25.9%) at a pH of 10 for the 180 mg/L and 300 mg/L inlet COD concentrations.

Dissolved ozone concentrations in the liquid phase were observed to decrease when the catalyst loading to the reactor was increased (Figures 4.23 and 4.24). As it was stated before, alumina catalyst was responsible for the radical formation reactions emerging from the decomposition of ozone in the medium. Thus, it is expected that increasing the amount of catalyst provides more active alumina sites that enhance the ozone decomposition reactions. Moreover, as in the case of alumina catalyzed experiments, PFOA also caused lower ozone concentration in the liquid. Since PFOA increases the solubility of ozone on the alkyl phase on itself, enhances the molecular ozone reactions with the organics in the medium and causes more ozone to be consumed in the reactions emerging the lower amounts of ozone in the solution.

Ozone consumptions for each of the experiments conducted in order to see the effect of catalyst dosage were calculated for the gas phase per liter of liquid. As Figures 4.25 and 4.26 with Table 4.16 showed that the consumed amounts of ozone gas was lowered by increasing the catalyst dosage for both of the catalysts.

The WW solution to be ozonated required less ozone for the degradation of dye molecules and even for the TOC removal in the presence of catalysts. Low WW treatment efficiency with a high amount of ozone gas consumption means ozone mass transfer from the gas phase to the liquid phase is very low; as a result, most of the ozone gas cannot pass to the liquid phase to be used in the oxidation reactions and is wasted from the gas phase. However, using a catalyst enhances ozone mass

transfer to the liquid phase due to the better mixing in the reactor, enhances ozone decomposition reactions and thus formation of radicals having higher oxidative potentials and provides a faster reaction on the active sites of the catalyst surface.

**Table 4.15:** The effect of catalyst dosage on dye removals (in terms dye concentrations for each dye in WW solution) for different pH and  $COD_{in}$ ,  $Q_G = 340$  L/h,  $Q_L = 250$  L/h,  $C_{O_3,G,in} = 0.9 \pm 0.1$  mmol/L gas.

Catalyst	$m_{cat}$ (g)	pH	$COD_{in}$ (mg/L)	BB 41 Removal (%)	BR 18.1 Removal (%)	BY 28 Removal (%)	
sole	-	4	180	35.70	88.81	99.82	
		10		42.63	98.85	91.05	
		4	300	16.55	71.88	98.37	
		10		23.09	91.44	74.35	
Alumina	150	4	180	38.02	90.17	99.79	
		10		50.86	99.25	95.90	
		4	300	19.10	74.09	98.57	
		10		34.10	95.08	80.95	
PFOA		150	4	180	43.01	97.82	99.83
			10		46.08	99.13	92.81
			4	300	23.59	84.85	98.97
			10		31.09	93.71	79.03
Alumina	300		4	180	49.91	98.98	98.99
			10		59.07	99.87	98.88
			4	300	30.71	86.02	99.98
			10		42.39	98.86	86.92
PFOA		300	4	180	51.47	99.11	99.90
			10		53.09	99.56	95.64
			4	300	35.09	89.91	99.98
			10		38.01	96.59	83.45
Alumina	400		4	180	44.18	98.68	99.99
			10		55.69	99.27	91.89
			4	300	26.38	80.53	99.87
			10		37.93	97.26	83.29
PFOA		400	4	180	45.92	98.92	99.99
			10		47.80	99.08	93.72
			4	300	30.97	88.36	99.89
			10		34.98	95.60	80.47

**Table 4.16:** The effect of catalyst dosage on TOC, COD removals with ozone consumptions for different pH and  $COD_{in}$ ,  $Q_G = 340$  L/h,  $Q_L=250$  L/h,  $C_{O_3,G,in} = 0.9 \pm 0.1$  mmol/L gas.

Catalyst	$m_{cat}$ (g)	pH	$COD_{in}$ (mg/L)	TOC Removal (%)	COD Removal (%)	$Cons_{O_3}$ (mmol/L liq.)	
sole	-	4	180	12.45	16.49	1.273	
		10		14.35	12.28	1.469	
		4	300	6.86	10.75	1.803	
		10		10.97	12.54	2.038	
Alumina	150	4	180	14.50	18.06	1.106	
		10		20.93	24.08	1.264	
		4	300	8.09	12.84	1.604	
		10		14.02	20.81	1.804	
PFOA		150	4	180	17.13	19.96	0.887
			10		18.86	20.39	1.115
			4	300	9.89	13.12	1.286
			10		12.10	14.56	1.502
Alumina	300		4	180	20.57	25.83	0.904
			10		26.55	30.71	1.264
			4	300	13.47	19.08	1.487
			10		18.09	25.90	1.803
PFOA		300	4	180	22.98	27.90	0.726
			10		23.19	28.09	0.901
			4	300	15.69	20.92	1.102
			10		17.02	22.56	1.205
Alumina	400		4	180	18.16	22.11	0.762
			10		23.49	27.03	1.104
			4	300	11.44	16.50	1.308
			10		15.36	22.90	1.684
PFOA		400	4	180	20.08	24.50	0.614
			10		20.86	25.96	0.735
			4	300	12.46	18.02	0.935
			10		14.02	19.98	1.094

On the other hand, increasing the catalyst dosage further to 400 g causes a decrease in the dye removals decrease to 37.93%, 97.26% and 83.29% for blue, red and yellow dyes, respectively at pH of 10 for alumina and to 34.98%, 95.6% and 80.47% for PFOA catalysts. Also, the TOC and COD percent removals are lower when compared with the previous ones as expected, because of the lower dye removals.

Although high treatment efficiencies were expected due to the increasing catalyst dosage further by increasing the surface active sites, observations on the hydrodynamic behavior of the phases in the reactor may explain these lower organic removals. When 400 g of catalyst was put in the reactor, gas bubbles formed channels through the catalyst particles and cannot separate and spread the catalyst particles homogeneously. As a result, gas bubbles in larger sizes form in the reactor causing decreases in mass transfer of ozone into the liquid phase due to the smaller interfacial area between the gas and liquid phases. Adding as high as 400 g of catalyst to the reactor affects the fluidization behavior of catalyst particles; then the gas and liquid flow rates used may not be enough to fluidize the catalyst particles. Increasing the gas or liquid flow rate with this amount of catalyst dosage might yield higher treatment efficiencies again due to creating more turbulence in the reactor.

#### **4.3.5 Effect of $Q_G/Q_L$ on Catalytic Ozonation**

Operating conditions of the three phase fluidized bed reactor, namely gas and liquid flow rates could be important parameters for both non-catalytic and catalytic ozonation reactions. In order to examine the effects of these parameters, different ratios of gas to liquid flow rates ( $Q_G/Q_L$ ) were obtained with different gas and liquid flow rates and ozonation experiments were conducted under these conditions. In Figures 4.27 and 4.28 with Table 4.17, the treatment efficiencies can be seen in terms of dye, TOC and COD removals at different values of  $Q_G/Q_L$ .

Figures 4.27 and 4.28 show that with increasing  $Q_G/Q_L$  ratio, the percent organic removals increases. In these figures dispersion coefficients ( $D_L$ ) and mass transfer coefficients ( $k_{La}$ ) which were estimated by the correlations obtained for this experimental set-up in the previous study of Erol and Özbelge (Erol and Özbelge, 2009) were also shown. As it can be seen, high  $Q_G/Q_L$  ratio was obtained by increasing the  $Q_G$  to 283 L/h and decreasing the  $Q_L$  to 70 L/h. Since an increase in the gas flow rate, keeping ozone dosage ( $C_{O_3,G,in}$ ) in the gas constant, increases the applied ozone amount to the system per liter of liquid. Therefore, it is expected to obtain higher removals at high gas flow rates.

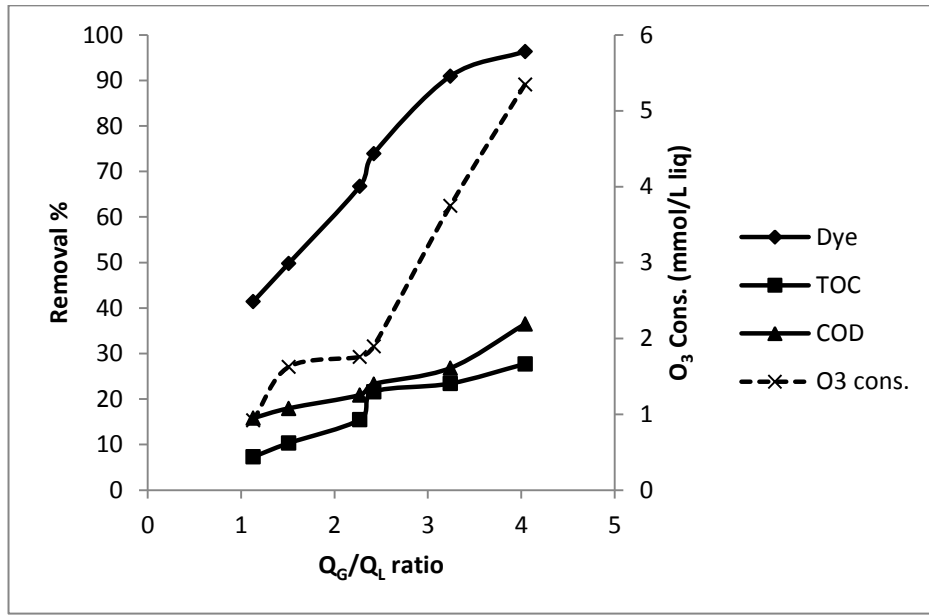


**Figure 4.27:** The effect of  $Q_G/Q_L$  ratio on TOC and COD removals with ozone consumptions (dye removals are in terms of Pt-Co Color unit),  $T = 22^\circ\text{C}$ ,  $COD_{in} = 300 \text{ mg/L}$ ,  $C_{d,in,BB 41} = 150.9 \text{ mg/L}$ ,  $C_{d,in,BR 18.1} = 26.4 \text{ mg/L}$ ,  $C_{d,in,BY 28} = 26.2 \text{ mg/L}$ ,  $C_{O_3,G,in} = 0.9 \pm 0.1 \text{ mmol/L gas}$ ,  $\text{pH} = 4$ , catalyst: none. In figures percent removals are shown by line and ozone consumption by dotted line (----).

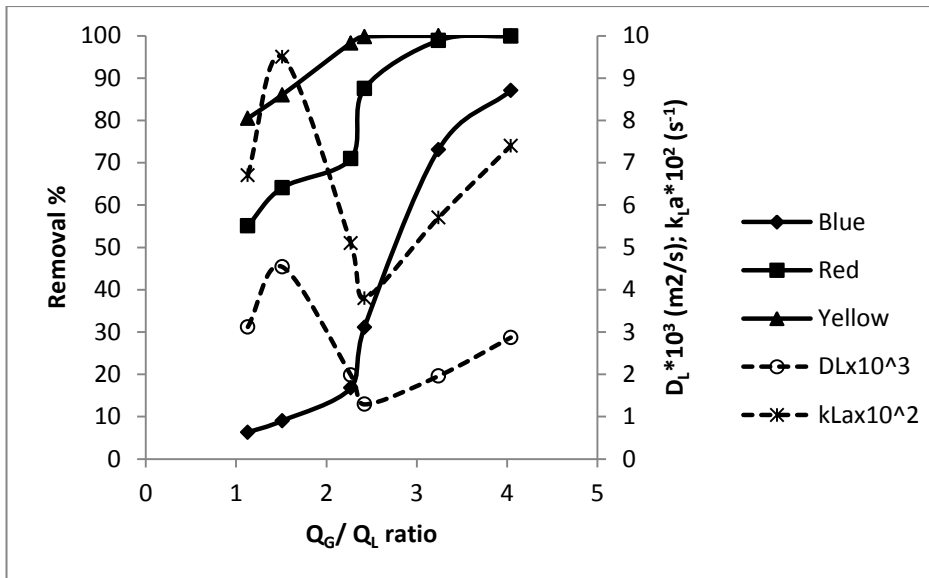


**Figure 4.28:** The effect of  $Q_G/Q_L$  ratio on dye removals (in terms dye concentrations for each dye in WW solution) with  $D_L$  and  $k_{La}$  values,  $T = 22^\circ\text{C}$ ,  $COD_{in} = 300 \text{ mg/L}$ ,  $C_{d,in,BB 41} = 150.9 \text{ mg/L}$ ,  $C_{d,in,BR 18.1} = 26.4 \text{ mg/L}$ ,  $C_{d,in,BY 28} = 26.2 \text{ mg/L}$ ,  $C_{O_3,G,in} = 0.9 \pm 0.1 \text{ mmol/L gas}$ ,  $\text{pH} = 4$ , catalyst: none. In figures percent removals are shown by line and  $D_L$  and  $k_{La}$  by dotted line (----).

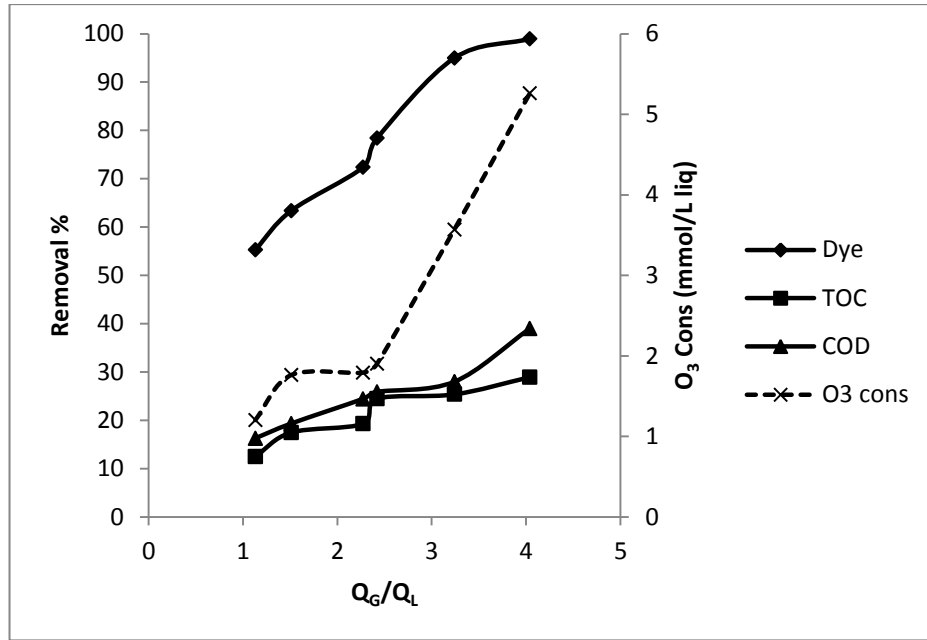


**Figure 4.29:** The effect of  $Q_G/Q_L$  ratio on TOC and COD removals with ozone consumptions (dye removals are in terms of Pt-Co Color unit),  $T = 22^\circ\text{C}$ ,  $COD_{in} = 300 \text{ mg/L}$ ,  $C_{d,in,BB\ 41} = 150.9 \text{ mg/L}$ ,  $C_{d,in,BR\ 18.1} = 26.4 \text{ mg/L}$ ,  $C_{d,in,BY\ 28} = 26.2 \text{ mg/L}$ ,  $C_{O_3,G,in} = 0.9 \pm 0.1 \text{ mmol/L gas}$ ,  $\text{pH} = 4$ , catalyst: alumina. In figures percent removals are shown by line and ozone consumption by dotted line (----).

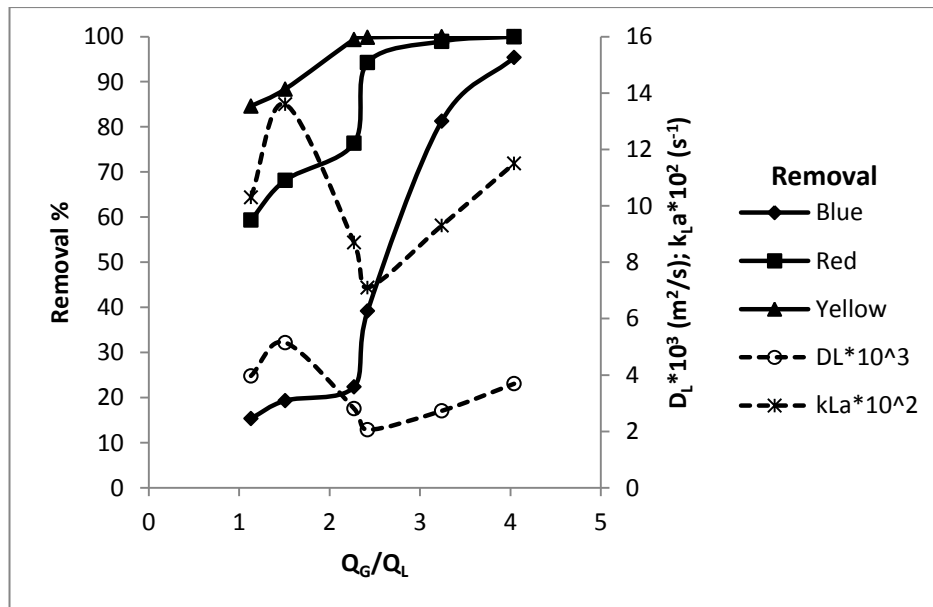


**Figure 4.30:** The effect of  $Q_G/Q_L$  ratio on dye removals (in terms dye concentrations for each dye in WW solution) with  $D_L$  and  $k_{La}$  values,  $T = 22^\circ\text{C}$ ,  $COD_{in} = 300 \text{ mg/L}$ ,  $C_{d,in,BB\ 41} = 150.9 \text{ mg/L}$ ,  $C_{d,in,BR\ 18.1} = 26.4 \text{ mg/L}$ ,  $C_{d,in,BY\ 28} = 26.2 \text{ mg/L}$ ,  $C_{O_3,G,in} = 0.9 \pm 0.1 \text{ mmol/L gas}$ ,  $\text{pH} = 4$ , catalyst: alumina. In figures percent removals are shown by line and  $D_L$  and  $k_{La}$  by dotted line (----).

Moreover, increasing the gas flow rate causes more turbulence and mixing in the reactor yielding better contact among the phases; thus efficiency of the system increases. On the other hand, decreasing the liquid flow rate yielded higher dye, TOC and COD removals, because when liquid flow rate decreases, contact time of gas and liquid phases increases and ozone finds more time to degrade the organics in the WW solution.

Apart from  $Q_G/Q_L$  ratio, considering gas and liquid flow rates separately; as it can be seen in Table 4.17 for the same gas flow rate of 170 L/h the dye removals of 41.41%, 66.7% and 73.91% (in terms of Pt-Co color unit) were achieved for 150 L/h, 100 L/h and 70 L/h liquid flow rates, respectively. Moreover, for a constant  $Q_L$  value of 70 L/h, the dye removals of 73.91%, 90.93% and 96.36% (again in terms of Pt-Co color unit) were obtained when  $Q_G$  is equal to 170 L/h, 227 L/h and 283 L/h, respectively.

**Table 4.17:** The dye, TOC and COD removals with dispersion coefficients and  $k_{La}$  values (dye removals are in terms of Pt-Co color unit),  $T = 22^\circ\text{C}$ ,  $COD_{in} = 300 \text{ mg/L}$ ,  $C_{O_3,G,in} = 0.9 \pm 0.1 \text{ mmol/L}$  gas,  $m_{cat} = 150 \text{ g}$ , for alumina  $H_E = 15 \text{ cm}$ , for PFOA  $H_E = 16.4 \text{ cm}$ ,  $H_S = 3 \text{ cm}$ .

Catalyst	$Q_G/Q_L$	$Q_G$ (L/h)	$Q_L$ (L/h)	Dye Rem %	TOC Rem %	COD Rem %	$D_L \times 10^3$ ( $\text{m}^2/\text{s}$ )	$k_{La} \times 10^2$ ( $\text{s}^{-1}$ )
Sole	1.13	170	150	41.41	7.29	15.81	3.12	6.7
	1.51	227	150	49.8	10.31	17.97	4.54	9.5
	2.27	170	100	66.7	15.47	20.89	1.98	5.1
	2.42	170	70	73.91	21.58	23.31	1.29	3.8
	3.24	227	70	90.93	23.41	26.81	1.96	5.7
	4.04	283	70	96.36	27.72	36.49	2.87	7.4
Alumina	1.13	170	150	55.27	12.48	16.29	3.97	10.3
	1.51	227	150	63.36	17.48	19.33	5.15	13.6
	2.27	170	100	72.34	19.28	24.44	2.81	8.7
	2.42	170	70	78.38	24.47	25.9	2.06	7.1
	3.24	227	70	94.98	25.37	27.99	2.73	9.3
	4.04	283	70	98.96	28.93	38.83	3.69	11.5
PFOA	1.13	170	150	58.38	15.82	20.47	3.97	10.6
	1.51	227	150	67.09	20.47	22.48	5.15	12.9
	2.27	170	100	74.57	21.37	28.37	2.81	9.2
	2.42	170	70	81.35	26.56	28.45	2.06	6.7
	3.24	227	70	96.47	27.62	30.24	2.73	8.8
	4.04	283	70	99.06	30.25	40.05	3.69	10.9

In addition to these, the  $D_L$  and  $k_{La}$  estimations provided an idea about the degree of mixing and turbulence in the reactor. As seen in Figures 4.28 and 4.30 with Table 4.17, both  $D_L$  and  $k_{La}$  reached a maximum when the  $Q_G/Q_L$  ratio was equal to 1.51, then they decreased and started to increase again after the  $Q_G/Q_L$  ratio of 2.42. This brought the idea that not only the gas to liquid flow rate ratio was important, but the gas and liquid flow rates separately are also important parameters on dispersion and mass transfer coefficients. When the values are examined, it can easily be seen that  $D_L$  and  $k_{La}$  values increase when both the gas and liquid flow rates are increased due to the high turbulence formation in the reactor. Moreover, addition of solid catalyst particles to the reactor causes an increase in turbulence.

However, as seen again in Figures 4.28 and 4.30, although increases in  $D_L$  and  $k_{La}$  values meant higher turbulence and higher mass transfer efficiency, respectively, in the column, the operating conditions where these coefficients were maximum could not provide the best treatment efficiencies. This can be because of the high flow rate of liquid phase when the  $Q_G/Q_L$  ratio was equal to 1.51. WW solution could flow very fast that ozone gas could not find time to react with organics and oxidize them even though high mixing provided the enhancement of ozone mass transfer. Thus, in order to fully examine the effects of dispersion and mass transfer coefficients on the treatment efficiency, the dye, TOC and COD degradations were investigated after increasing both the gas and liquid flow rates keeping the  $Q_G/Q_L$  ratio constant.

Keeping  $Q_G/Q_L$  ratio equal to 1, WW ozonation experiments were performed for  $Q_G$  and  $Q_L$  values of 150 L/h, 200 L/h and 250 L/h. Figures 4.31, 4.32 and 4.33 show the results obtained from these experiments. It was found out that increasing gas and liquid flow rates in the same ratio, increased the degradation rates of all dyes, TOC and COD. Although increasing liquid flow rate decreased the contact time between the gas and liquid phases, increments observed in  $D_L$  and  $k_{La}$  values showed better mixing in the reactor enhancing the ozone mass transfer and yielding higher percent removals. This showed that the mass transfer coefficient of ozone into liquid phase was mainly affected by the gas flow rate and the liquid flow rate had a minor effect on mass transfer. In other words, the change in the gas flow rate had greater influence on performance of the system than the change in liquid flow rate in terms of ozone mass transfer. Analyzing the results obtained by using Yate's algorithm

(Box et al., 1978) should explain the higher effect of gas flow rate on the system performance (Tables 4.18 and 4.19). On the other hand, increase in the gas flow rate meant as stated before; more ozone was applied to the column and more ozone oxidized more dye and by-products yielding again higher removals.

**Table 4.18:** The Yate's algorithm analysis for the effect of  $Q_G$  and  $Q_L$  on  $k_{LA}$ ,  $COD_{in} = 300$  mg/L,  $C_{d,in,BB\ 41} = 150.9$  mg/L,  $C_{d,in,BR\ 18.1} = 26.4$  mg/L,  $C_{d,in,BY\ 28} = 26.2$  mg/L, pH = 4,  $C_{O_3,G,in} = 0.9 \pm 0.1$  mmol/L gas, catalyst: none.

Exp.	$Q_G$ (L/h)	$Q_L$ (L/h)	$k_{LA} \times 10^2$ (s <sup>-1</sup> )	1	2	divisor	effect	variable
1	150	150	6.3	15.4	30	4	7.5	average
2	250	150	9.1	14.6	6.6	2	3.3	$Q_G$
3	150	250	5.4	2.8	-0.8	2	-0.4	$Q_L$
4	250	250	9.2	3.8	1	2	0.5	$Q_G-Q_L$

**Table 4.19:** The Yate's algorithm analysis for the effect of  $Q_G$  and  $Q_L$  on percent dye removals (in terms of Pt-Co),  $COD_{in} = 300$  mg/L,  $C_{d,in,BB\ 41} = 150.9$  mg/L,  $C_{d,in,BR\ 18.1} = 26.4$  mg/L,  $C_{d,in,BY\ 28} = 26.2$  mg/L, pH = 4,  $C_{O_3,G,in} = 0.9 \pm 0.1$  mmol/L gas, catalyst: none.

Exp.	$Q_G$ (L/h)	$Q_L$ (L/h)	Dye Rem (%)	1	2	divisor	effect	variable
1	150	150	38.2	95.54	184.6	4	46.15	average
2	250	150	57.34	89.06	29.78	2	14.89	$Q_G$
3	150	250	39.21	19.14	-6.48	2	-3.24	$Q_L$
4	250	250	49.85	10.64	-8.5	2	-4.25	$Q_G-Q_L$

Addition of catalyst particles to the reaction medium was observed to increase the degradation efficiencies due to their catalytic activity and also their contributions to the mixing in the column (Tables 4.20 and 4.21).

Ozone consumptions obtained in the reactions were higher when the gas and liquid flow rates are high due to the more efficient use of ozone in the oxidation reactions. Thus, increasing the gas and liquid flow rates by keeping the  $Q_G/Q_L$  ratio constant and equal to 1 provided the efficient use of ozone gas by enhancing mass transfer and prevented the escape of ozone in the waste gas. But still ozone consumptions were lower in the catalytic ozonation experiments compared to those in sole ozonation although the percent removals are higher in the former.

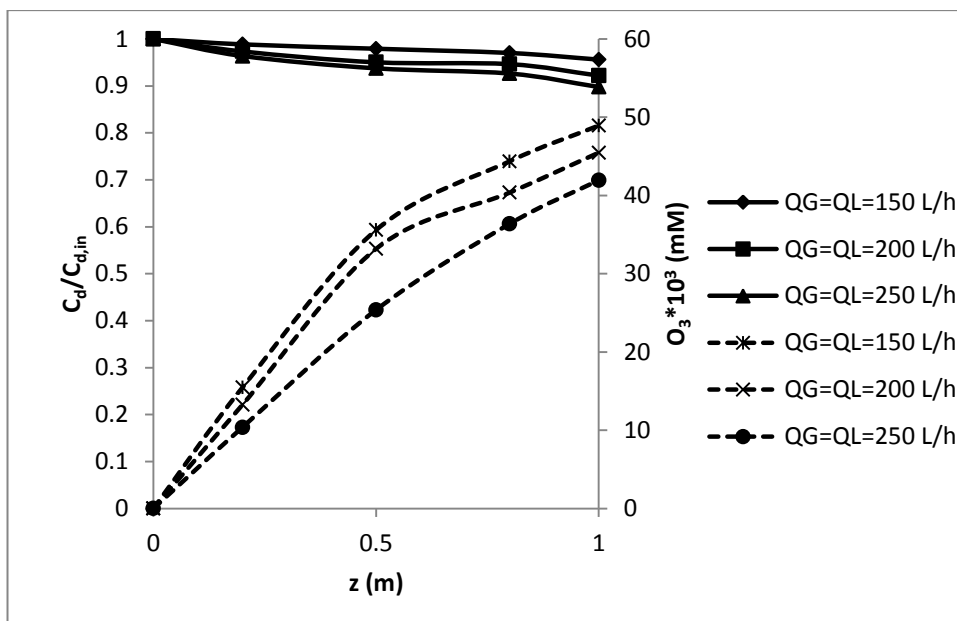


**Figure 4.31:**  $C_d/C_{d,in}$  for different  $Q_G$  and  $Q_L$  on blue dye (BB 41) removals (in terms dye concentrations in WW solution) and ozone concentration in liquid phase,  $Q_G/Q_L = 1$   $C_{O_3,G,in} = 0.9 \pm 0.1$  mmol/L gas, catalyst: none, pH = 4,  $COD_{in} = 300$  mg/L,  $C_{d,in, BB41} = 150.9$  mg/L,  $C_{d,in, BR 18.1} = 26.4$  mg/L,  $C_{d,in, BY 28} = 26.2$  mg/L. In figures dye concentration is shown by line and ozone concentration in liquid phase by dotted line (----).

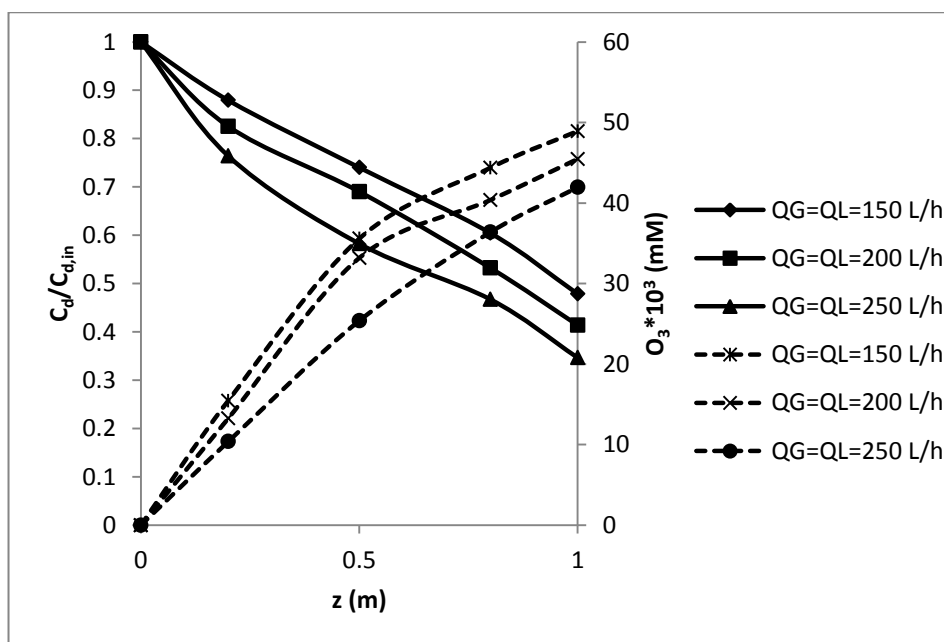


**Figure 4.32:**  $C_d/C_{d,in}$  for different  $Q_G$  and  $Q_L$  on red dye (BR 18.1) removals (in terms dye concentrations in WW solution) and ozone concentration in liquid phase,  $Q_G/Q_L = 1$   $C_{O_3,G,in} = 0.9 \pm 0.1$  mmol/L gas, catalyst: none, pH = 4,  $COD_{in} = 300$  mg/L,  $C_{d,in, BB41} = 150.9$  mg/L,  $C_{d,in, BR 18.1} = 26.4$  mg/L,  $C_{d,in, BY 28} = 26.2$  mg/L. In figures dye concentration is shown by line and ozone concentration in liquid phase by dotted line (----).

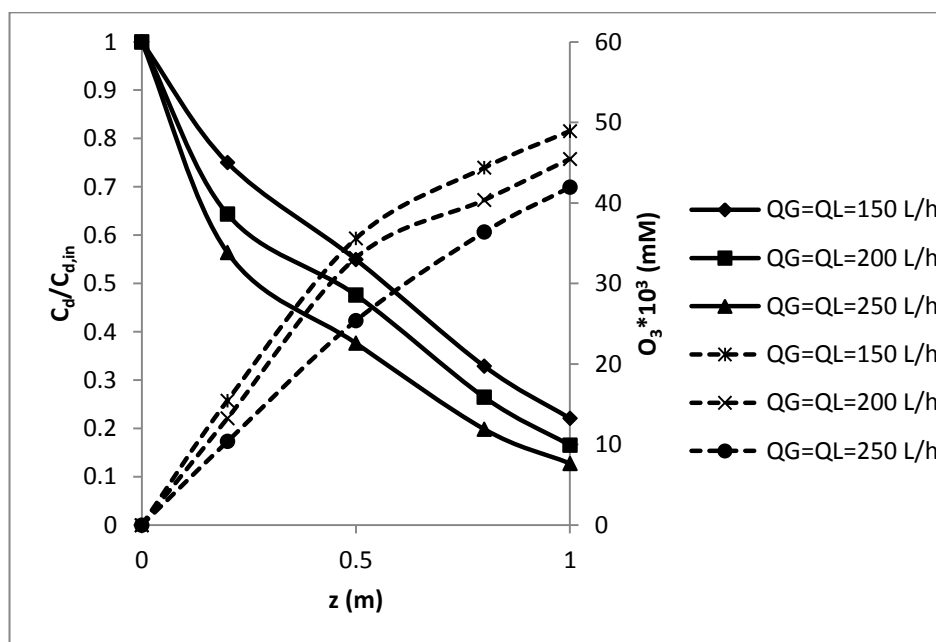


**Figure 4.33:**  $C_d/C_{d,in}$  for different  $Q_G$  and  $Q_L$  on yellow dye (BY 28) removals (in terms dye concentrations in WW solution) and ozone concentration in liquid phase,  $Q_G/Q_L = 1$   $C_{O_3,G,in} = 0.9 \pm 0.1$  mmol/L gas, catalyst: none, pH = 4,  $COD_{in} = 300$  mg/L,  $C_{d,in,BB\ 41} = 150.9$  mg/L,  $C_{d,in,BR\ 18.1} = 26.4$  mg/L,  $C_{d,in,BY\ 28} = 26.2$  mg/L. In figures dye concentration is shown by line and ozone concentration in liquid phase by dotted line (----).

**Table 4.20:** The TOC, COD removals with ozone consumption for different  $Q_G$  and  $Q_L$ ,  $COD_{in} = 300$  mg/L,  $C_{d,in,BB\ 41} = 150.9$  mg/L,  $C_{d,in,BR\ 18.1} = 26.4$  mg/L,  $C_{d,in,BY\ 28} = 26.2$  mg/L, pH = 4,  $m_{cat} = 300$  g, for alumina  $H_E = 17$  cm, for PFOA  $H_E = 18.3$  cm,  $H_S = 5$  cm  $C_{O_3,G,in} = 0.9 \pm 0.1$  mmol/L gas.

Catalyst	$Q_G$ (L/h)	$Q_L$ (L/h)	TOC Removal (%)	COD Removal (%)	$Cons_{O_3}$ (mmol/L liq.)
Sole	150	150	5.15	12.45	0.846
	200	200	7.92	16.47	1.198
	250	250	9.17	18.36	1.963
PFOA	150	150	7.13	13.98	0.692
	200	200	9.34	18.65	0.838
	250	250	11.25	21.53	1.238
Alumina	150	150	6.63	13.02	0.762
	200	200	8.45	17.63	0.968
	250	250	10.56	19.04	1.732

**Table 4.21:** The dye removals with  $D_L$  and  $k_La$  for different  $Q_G$  and  $Q_L$  (dye removals are in terms of Pt-Co Color unit),  $COD_{in} = 300$  mg/L,  $C_{d,in,BB\ 41} = 150.9$  mg/L,  $C_{d,in,BR\ 18.1} = 26.4$  mg/L,  $C_{d,in,BY\ 28} = 26.2$  mg/L, pH = 4,  $m_{cat} = 300$  g, for alumina  $H_E = 17$  cm, for PFOA  $H_E = 18.3$  cm,  $H_S = 5$  cm  $C_{O_3,G,in} = 0.9 \pm 0.1$  mmol/L gas.

Catalyst	$Q_G$ (L/h)	$Q_L$ (L/h)	Dye Removal (%)	$D_L \times 10^3$ (m <sup>2</sup> /s)	$k_L a \times 10^2$ (s <sup>-1</sup> )
Sole	150	150	38.2	3.15	6.3
	200	200	45.6	4.8	8.6
	250	250	49.85	6.87	9.2
PFOA	150	150	43.45	4.01	11.0
	200	200	49.52	5.72	13.2
	250	250	52.98	8.03	14.8
Alumina	150	150	40.46	4.01	11.2
	200	200	47.56	5.72	12.9
	250	250	51.12	8.03	14.1

## 4.4 Reactor Hydrodynamics

Catalyst particles forming the solid phase in the three phase reactor are fluidized with liquid and gas phases flowing co-currently from the bottom to the top of the reactor. Due to the change in hydrodynamic properties of the reactor at different operating conditions, the performance of the reactor was obviously expected to be affected. Therefore, in order to determine the minimum fluidization velocity ( $u_{L,min}$ ) and the hold-up values of gas, liquid and solid phases, the hydrodynamic characteristics of the three phase reactor were investigated.

### 4.4.1 Minimum Fluidization Velocity in the Column

The minimum fluidization velocity is the value of superficial water velocity at which the particles begin to fluidize at a constant superficial air velocity. The  $u_{L,min}$  values at different gas flow rates were determined in the column filled with catalyst particles. Alumina and PFOA particles have different densities causing the minimum fluidization velocities to differ from each other. Therefore, the  $u_{L,min}$  values at different  $Q_G$  values were determined for both catalyst types separately. The obtained results can be seen in Tables 4.22 and 4.23.

**Table 4.22:** Minimum fluidization velocities at the studied gas velocities; catalyst: PFOA,  $m_{cat} = 150$  g,  $d_{cat} = 3.0$  mm.

$u_G \times 10^3$ (m/s)	$Q_G$ (L/h)	$u_{L,min} \times 10^3$ (m/s)	$Q_{L,min}$ (L/h)	$H_E$ (cm)
9.40	170	5.81	105	13.5
12.55	227	5.53	100	17.2
15.65	283	5.25	90	18.0
18.80	340	4.97	85	18.7

As the gas velocity increased, the  $u_{L,min}$  values were observed to be decreased, because higher gas velocities enabled the fluidization of particles giving additional force to fluidize them. Comparison of the values obtained for PFOA and alumina catalyst particles showed that for a given gas velocity ( $u_G$ ), minimum fluidization velocity was increased in the case of alumina compared to those for PFOA and higher liquid flow rates were needed to fluidize alumina.

**Table 4.23:** Minimum fluidization velocities at the studied gas velocities; catalyst: alumina,  $m_{cat} = 150$  g,  $d_{cat} = 3.0$  mm.

$u_G \times 10^3$ (m/s)	$Q_G$ (L/h)	$u_{L,min} \times 10^3$ (m/s)	$Q_{L,min}$ (L/h)	$H_E$ (cm)
9.40	170	6.08	100	12.0
12.55	227	5.80	105	15.2
15.65	283	5.25	95	17.0
18.80	340	4.98	90	17.5

#### 4.4.2 Determination of Hold-up Values for Gas, Liquid and Solid Phases

In the column, the gas hold-up was evaluated with the height measurement from Equations (4.4) and (4.5).

$$A.h(1 - \varepsilon_G) = A.h_0 \quad (4.4)$$

$$\varepsilon_G = 1 - \frac{h_0}{h} \quad (4.5)$$

where,  $h$  is the height of the aerated liquid in the column and  $h_0$  is the original liquid height before the gas flow. For the gas-liquid system, the total of gas and liquid hold-up values is equal to one, as shown in Eqn. (4.6).

$$\varepsilon_G + \varepsilon_L = 1 \quad (4.6)$$

Similarly the hold-up values were found for the three phase system according to Equation (4.7). Now, the solid hold-up (loading) was found from the relationship given in Equation (4.8) between the catalyst loading amount ( $m_{cat}$ ), catalyst density ( $\rho_{cat}$ ), reactor cross-sectional area ( $A$ ) and expanded bed height ( $H_E$ ).

$$\varepsilon_G + \varepsilon_L + \varepsilon_S = 1 \quad (4.7)$$

$$\varepsilon_S = \frac{m_{cat}}{\rho_{cat} \cdot A \cdot H_E} \quad (4.8)$$

For the gas hold-up measurement, the reactor was filled with the distilled water in the absence of gas flow. Then, the liquid flow was stopped and the static (original) liquid height was measured. Afterwards, the gas was sent to the reactor at a constant flow rate; the aerated liquid height due to the gas flow was determined. For the reactor filled with the catalyst particles, the same procedure was applied; however in that case, 300 g of the particles were fed to the reactor and then, the liquid heights before and after the gas flow were measured. The solid hold-up was found from Equation (4.7) by measuring the expanded bed height during the experiment.

The gas, liquid and solid phase hold-up values were obtained for different values of gas and liquid flow rates. Table 4.24 and 4.25 presents the hold-up values for the gas-liquid-solid three phase system.

At a constant liquid flow rate, the gas hold-up increased with the increase of gas flow rate. It was observed that the bubble velocity and the number of bubbles per unit reactor volume increased with the increase of  $Q_G$  resulting in higher  $\varepsilon_G$ . Increasing  $Q_L$  decreased  $\varepsilon_G$ . Addition of catalyst particles to the medium decreased the gas and liquid hold-up values as expected. That was due to the increase of turbulence with the higher amount of solids in the reactor. The increase of turbulence in the column probably caused the increase of interaction between gas, liquid and solid phases

leading improvements in the performance of the reactor. In the three phase system, increasing  $Q_G$  positively affected the gas hold-up.

**Table 4.24:** The calculated gas, liquid and solid-phase hold-up values under different operating conditions, catalyst: alumina,  $m_{cat} = 300$  g

$Q_G$ (L/h)	$Q_L$ (L/h)	$\varepsilon_G$	$\varepsilon_L$	$\varepsilon_S$
150	150	0.020	0.932	0.048
170	70	0.051	0.901	0.048
	100	0.039	0.913	0.048
	150	0.027	0.915	0.048
200	200	0.043	0.909	0.048
227	70	0.062	0.890	0.048
	150	0.058	0.894	0.048
250	250	0.071	0.881	0.048
283	70	0.080	0.872	0.048
340	250	0.086	0.866	0.048

**Table 4.25:** The calculated gas, liquid and solid-phase hold-up values under different operating conditions, catalyst: PFOA,  $m_{cat} = 300$  g

$Q_G$ (L/h)	$Q_L$ (L/h)	$\varepsilon_G$	$\varepsilon_L$	$\varepsilon_S$
150	150	0.026	0.938	0.036
170	70	0.060	0.904	0.036
	100	0.043	0.921	0.036
	150	0.028	0.936	0.036
200	200	0.049	0.915	0.036
227	70	0.067	0.897	0.036
	150	0.063	0.901	0.036
250	250	0.077	0.887	0.036
283	70	0.079	0.885	0.036
340	250	0.092	0.872	0.036

It was observed that the flow in the studied two or three phase reactor fitted to the “homogeneous bubbling regime” and at all the studied gas and liquid flow rates, the gas phase uniformly flowed through the liquid phase with homogeneous bubbles. The distribution of particles in the column was uniform while gas and liquid were flowing. At high gas and liquid velocities, a small amount of particles was carried to the top of the column (1 m), but most of them distributed homogeneously in the fluidized bed section.

The increase of gas flow rate at constant liquid flow rate increased the expansion of the bed and similarly increasing liquid flow rate keeping the gas flow rate constant also provided higher bed expansions. At the constant liquid flow rate of 150 L/h, the expanded bed height ( $H_E$ ) was 13.0 and 14.6 cm for  $Q_G=170$  L/h; whereas at a flow rate of  $Q_G=227$  L/h, 22.0 and 23.6 cm of  $H_E$  were observed for alumina and PFOA, respectively. The increase in the bed expansions provided by the higher liquid and gas flow rates would be expected to increase the reactor performance because particles can be carried to the higher sections in the reactor and become more effective throughout the reactor. Moreover, the distance among the particles increases and this can give a chance to gas and liquid phases for a better interaction with each other, and also with the solid phase leading a higher performance for the reactor.

## **4.5 Experiments Conducted in Semi-Batch Reactor**

### **4.5.1 Single Synthetic Dye Solution Experiments**

The ozonation of BB 41, BR 18.1 and BY 28 separately was examined in a semi-batch reactor in the presence and absence each of alumina and PFOA particles. The dye, COD and TOC removals were determined at the end of 90 min ozonation of the dye solutions. In addition, the kinetics of ozonation and catalytic ozonation processes were investigated. The stirrer rate was regulated to 300 rpm in the semi-batch experiments.

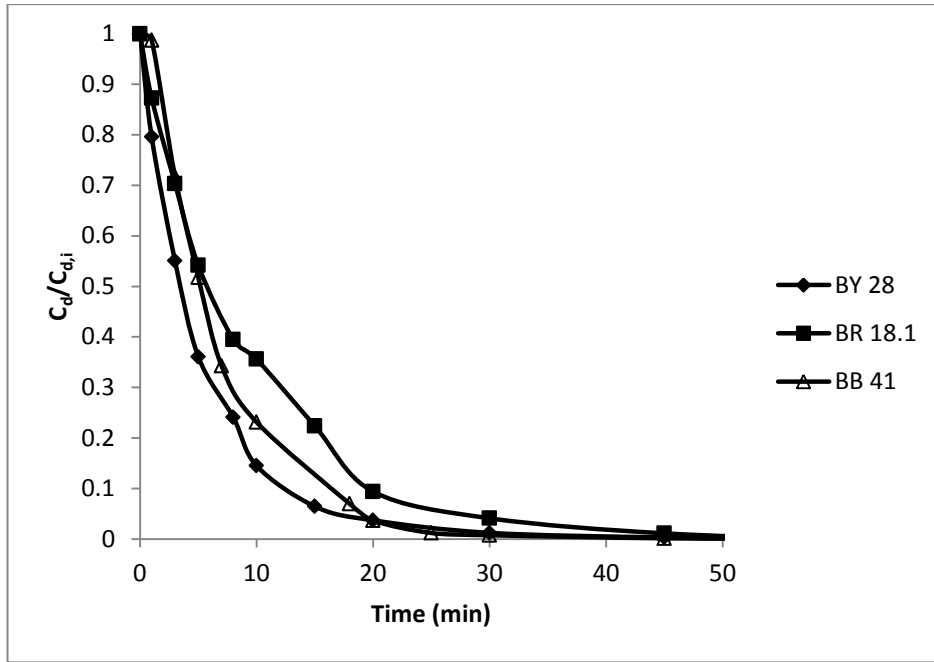
#### **4.5.1.1 Ozonation Experiments**

Experiments of the ozonation of the prepared single dye solutions were conducted without using catalyst particles at different pH values of 4 (acidic medium) and 10 (basic medium). As it was stated in the literature (Chu and Chi, 1999), at the acidic pH the direct oxidation of the organics in dye solutions with molecular ozone prevails because of the low concentration of  $\text{HO}^-$ , one of most important initiators of radical reactions. At an alkaline pH, ozone decomposition reactions occur because of

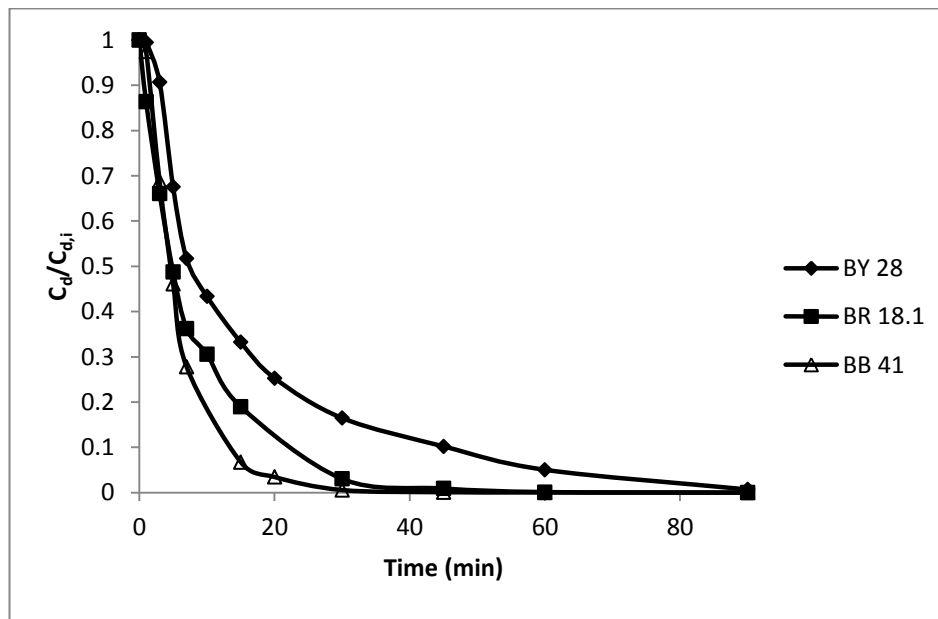
high HO<sup>•</sup> concentration and thus, indirect oxidation by radicals predominate over direct oxidation reactions.

After 30 min ozonation of each of the three different dye solutions, more than 85% of dye removals were obtained at both the acidic and alkaline pHs as shown in Figures 4.34(a) and 4.34(b). The dye removals and the initial rates of ozonation reactions showed differences at different pHs for different dye solutions. While for BY 28 the initial reaction rate was higher at acidic pH of 4, for BB 41 and BR 18.1 rates were found to be higher at alkaline pH of 10. This showed that molecular ozone took role in the oxidation of yellow dye with direct oxidation reactions; but it could not be powerful enough for the oxidation of blue and red dyes. For the oxidation of blue and red dyes, it was realized that radicals, non-selective and more powerful oxidants, were responsible. The aromatic structures found in the yellow dye might attract ozone molecules more strongly, and thus ozone might oxidize these aromatic chromophore groups first yielding higher dye removals at the lower pH values for this dye. On the other hand, the oxidation power of molecular ozone might not be sufficiently high for the red and blue dyes containing azo and sulphonic groups in their structures. However, increasing the pH of the solution yielded the higher color removals of the latter two dyes due to the formation of more powerful hydroxyl radicals.

Moreover, when the dye removals of BB 41 and BR 18.1 were compared it was observed that at the same operating conditions percent removals of BR 18.1 were lower than those of BB 41. This may be attributed to the presence of the more azo bonds in the molecular structure of BR 18.1. Also, an auxochrome (-Cl) found in the structure could improve the substantivity of BR 18.1 and could cause a more difficult dye degradation than BB 41. On the other hand, it was found out that while in order to oxidize one mole of BB 41 7.20 moles of ozone was required, 5.22 moles of ozone was necessary to oxidize one mole of BR 18.1 (Table 4.26). The high molecular weight of BB 41 may explain the difference in the amounts of ozone required for the oxidation of these two dyes ( $M_{w, BB\ 41} = 482.57$  g/mole,  $M_{w, BR\ 18.1} = 390.94$  g/mole,  $M_{w, BY\ 28} = 433.57$  g/mole).



(a)



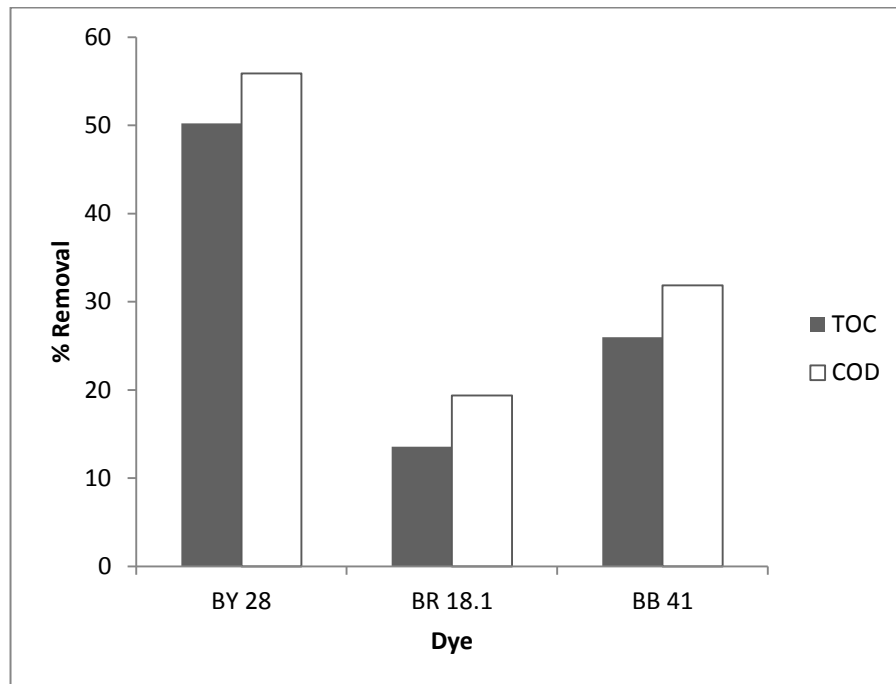
(b)

**Figure 4.34:** Dye removals with ozonation for BB 41, BY 28 and BR 18.1,  $C_{d,i} = 300$  mg/L (for each dye), stirrer rate = 300 rpm,  $Q_G = 150$  L/h,  $C_{O_3,G,in} = 0.9 \pm 0.1$  mmol/L gas, catalyst: none, (a) pH = 4, (b) pH = 10

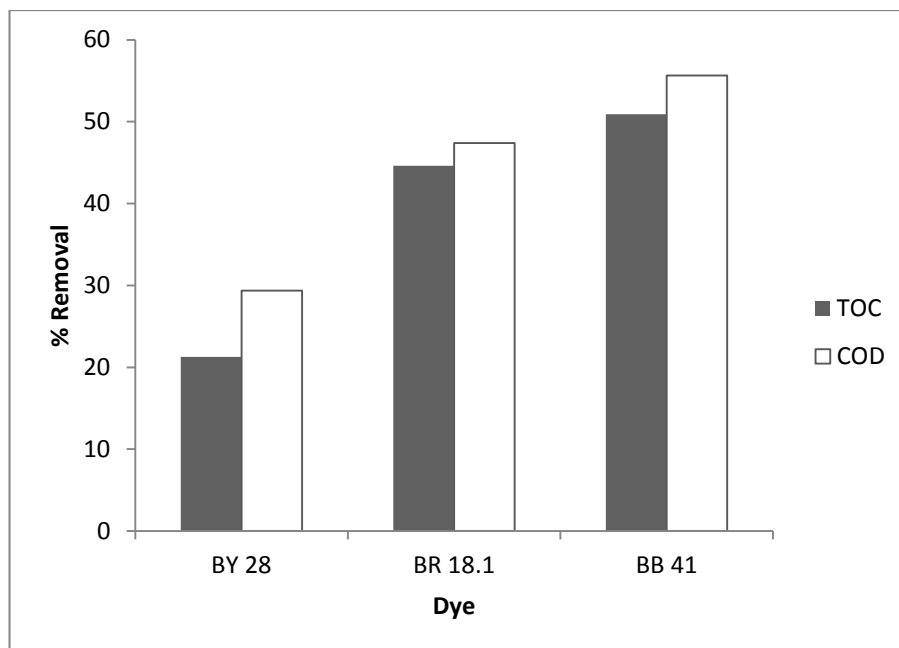
**Table 4.26:** Moles of ozone required to oxidize one mole of dye for each dye,  $C_{d,in} = 250$  mg/L (for each dye),  $Q_G = 150$  L/h, pH = 4,  $C_{O_3,G,in} = 0.9 \pm 0.1$  mmol/L gas, catalyst: none

Dye	Moles of ozone required to oxidize one mole of dye
Basic Blue 41	7.20
Basis Yellow 18	6.11
Basic Red 18.1	5.22

Figures 4.35(a) and 4.35(b) showed the effects of acidic and alkaline pHs on the COD removals. For BR 18.1 and BB 41, higher COD removals of 47.4% and 55.6% were achieved at alkaline pH of 10, respectively. For BY 28 on the other hand, increasing pH from 4 to 10 decreased the COD removal from 55.9% to 29.4%. The COD removals normally indicated the removals of the oxidation by-products.



(a)



(b)

**Figure 4.35:** COD and TOC removals after 90 min ozonation for BB 41, BY 28 and BR 18.1,  $C_{d,i} = 300$  mg/L (for each dye), stirrer rate = 300 rpm,  $Q_G = 150$  L/h,  $C_{O_3,G,in} = 0.9 \pm 0.1$  mmol/L gas, catalyst: none, (a) pH = 4, (b) pH = 10

Actually, it was stated in the literature that the by-product removals were higher at the high pHs; but it was also known that by-product removals started to occur after the degradation of chromophoric structures in the dyes giving their colors. Since for BY 28, dye removals were very low at the pH of 10, by-product formation occurred very slowly causing the lower COD reductions. Thus, starting the ozonation process at a low pH and above 90% dye removal was obtained increasing the pH to 10 or higher, most probably could yield COD removals higher than 55.9% for BY 28.

#### 4.5.1.2 Catalytic Ozonation Experiments

Alumina and PFOA particles were used as catalysts in the catalytic ozonation experiments with BB 41, BY 28 and BR 18.1. The results were compared and most efficient conditions for each dye were obtained in terms of dye, TOC and COD removals. Catalytic ozonation of each dye showed different efficiencies depending on solution pH and catalyst type (Table 4.27).

**Table 4.27:** Dye removal percentages for BB 41, BY 28 and BR 18.1 for different pH values and catalyst types,  $C_{d,i} = 300$  mg/L (for each dye), stirrer rate = 300 rpm,  $Q_G = 150$  L/h,  $C_{O_3,G,in} = 0.9 \pm 0.1$  mmol/L gas, reaction time = 30 min.

Ozonation Process	pH	Dye Removal %		
		BB 41	BY 28	BR 18.1
Sole	4	98.74	99.29	96.05
	10	99.46	84.46	97.13
With Alumina	4	98.91	99.79	98.25
	10	99.97	96.31	99.61
With PFOA	4	99.53	99.84	99.12
	10	99.95	94.43	99.23

Similar to the results of sole ozonation experiment, yellow dye showed higher dye and COD removals in the acidic medium in the presence of each of the catalysts, PFOA yielding higher efficiency than that of the alumina catalyst. As it was discussed earlier, PFOA catalyst keeps the ozone in molecular form helping the direct oxidation reactions to occur and since it is known that molecular ozone is responsible for the oxidation of yellow dye, obtaining higher removal efficiencies for yellow dye with PFOA catalyst is an expected result. On the other hand, alumina catalyst provided higher dye removals in a shorter period of time for BB 41 and BR 18.1. It was found out that hydroxyl radicals were dominant in the oxidation of these dyes. According to several studies (Thomas et al., 1997; Ni and Chen, 2001), the active sites on the alumina particles took charge in the decomposition of ozone into hydroxyl radicals with the help of hydroxyl ions found at basic medium. Thus, again it was reasonable to observe higher degradation at the basic pH of 10 with alumina particles.

In the catalytic ozonation, the effect of adsorption on to the catalyst particles could be important and should be considered in the examination and discussion of the obtained results. In the case of alumina particles, the adsorption capability of the catalyst depends on the acidity or basicity of the sites on alumina and of the dye molecule. In basic medium, the surface of alumina is negative because pH is higher than the  $pH_{PZC}$  of alumina. This provides cations to be adsorbed on the surface. A basic dye, on the other hand, is cationic at alkaline pHs. Thus, the basic red and blue dyes can easily be adsorbed onto alumina with hydroxyl radicals at basic conditions. This could also help the easy oxidation of red and blue dyes with alumina particles.

Yellow dye is also a basic dye and can be adsorbed onto the surface; but the scarcity of the molecular ozone at high pH could prevent high level of dye degradation.

As seen in Figures 4.36, 4.37 and 4.38, the addition of each type of catalysts improved the COD and TOC removals at both acidic pH of 4 and alkaline pH of 10. Table 4.28 shows that while low pH enhances the activity of PFOA, alumina provides a higher COD removal at the high pH of 10.

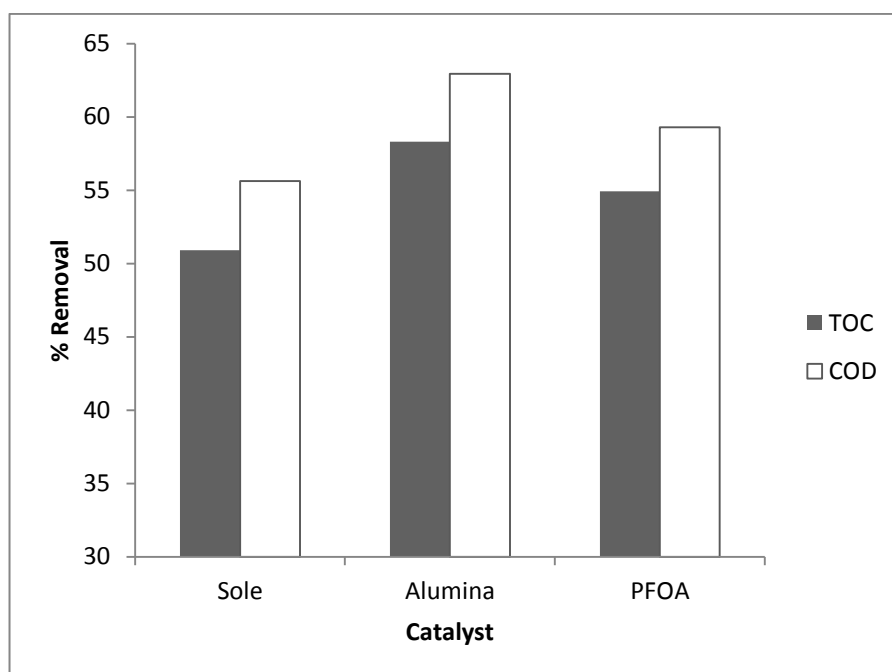


**Figure 4.36:** COD and TOC removals after 90 min ozonation for BB 41,  $C_{d,i} = 300$  mg/L, stirrer rate = 300 rpm,  $Q_G = 150$  L/h,  $C_{O_3,G,in} = 0.9 \pm 0.1$  mmol/L gas, pH = 10

The high efficiency of PFOA catalyst on COD removals might be due to the adsorption of by-products on PFOA catalyst. Because of the adsorption of the dye molecules on alumina, dye molecules and ozonation by-products might compete among themselves for the surface active sites. For the alumina catalyst, adsorption of the dyes was probably more dominant than those of the by-products causing lower COD removals. PFOA catalyst, on the other hand, preferred the adsorption of ozonation by-products on itself due to its non-polar nature (Erol and Özbelge, 2008).

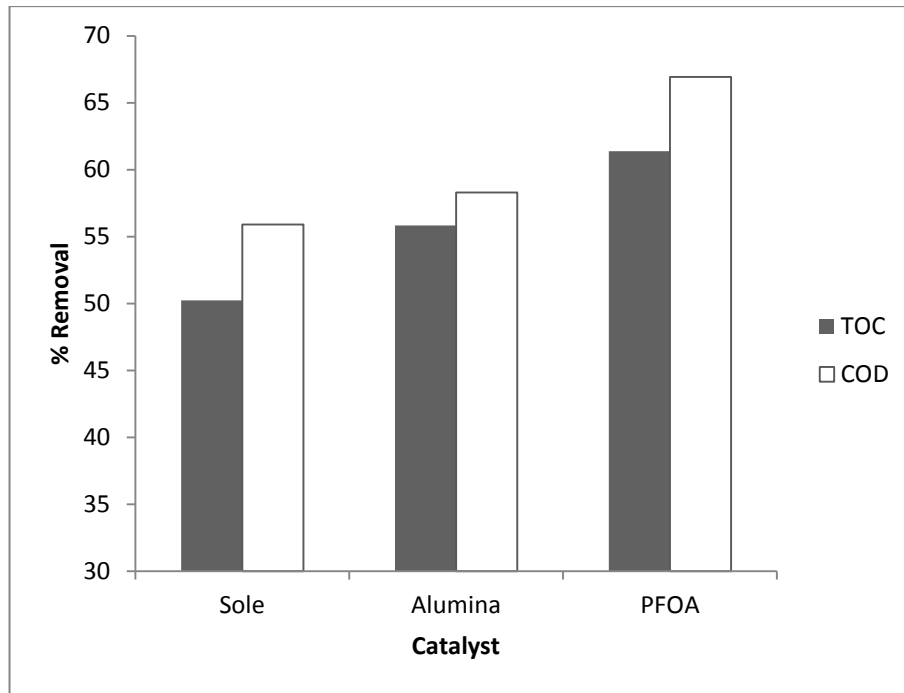


**Figure 4.37:** COD and TOC removals after 90 min ozonation for BY 28,  $C_{d,i} = 300$  mg/L, stirrer rate = 300 rpm,  $Q_G = 150$  L/h,  $C_{O_3,G,in} = 0.9 \pm 0.1$  mmol/L gas, pH = 4

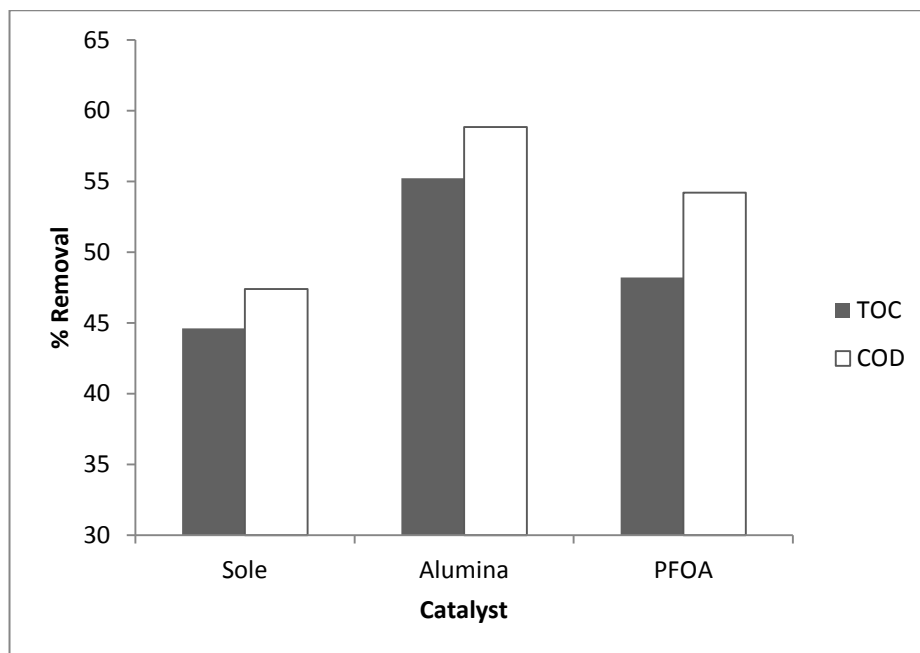


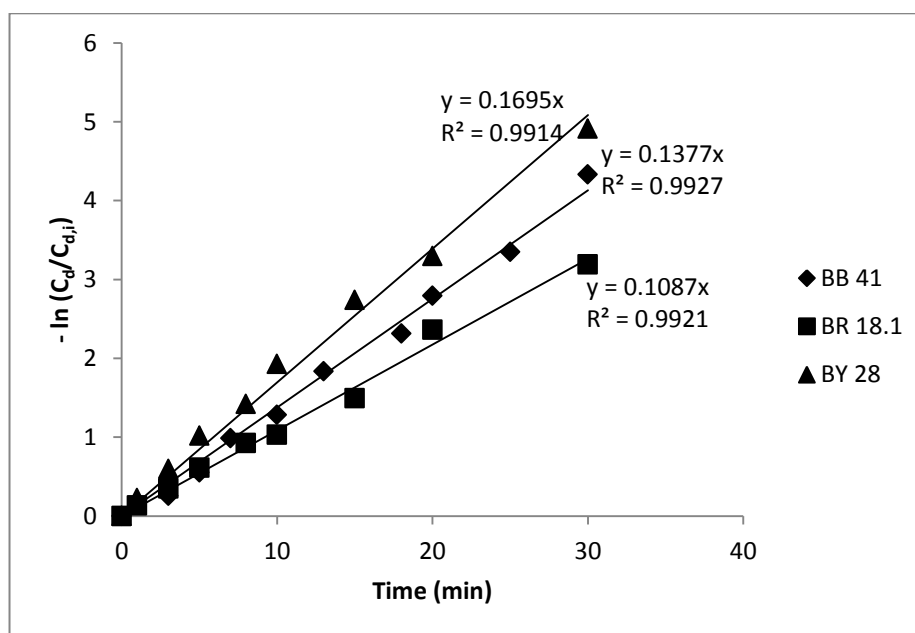
**Figure 4.38:** COD and TOC removals after 90 min ozonation for BR 18.1,  $C_{d,i} = 300$  mg/L, stirrer rate = 300 rpm,  $Q_G = 150$  L/h,  $C_{O_3,G,in} = 0.9 \pm 0.1$  mmol/L gas, pH = 10

**Table 4.28:** TOC and COD removal percentages for BB 41, BY 28 and BR 18.1 for different pH values and catalyst types,  $C_{d,i} = 300$  mg/L (for each dye), stirrer rate = 300 rpm,  $Q_G = 150$  L/h,  $C_{O_3,G,in} = 0.9 \pm 0.1$  mmol/L gas, reaction time = 90 min.

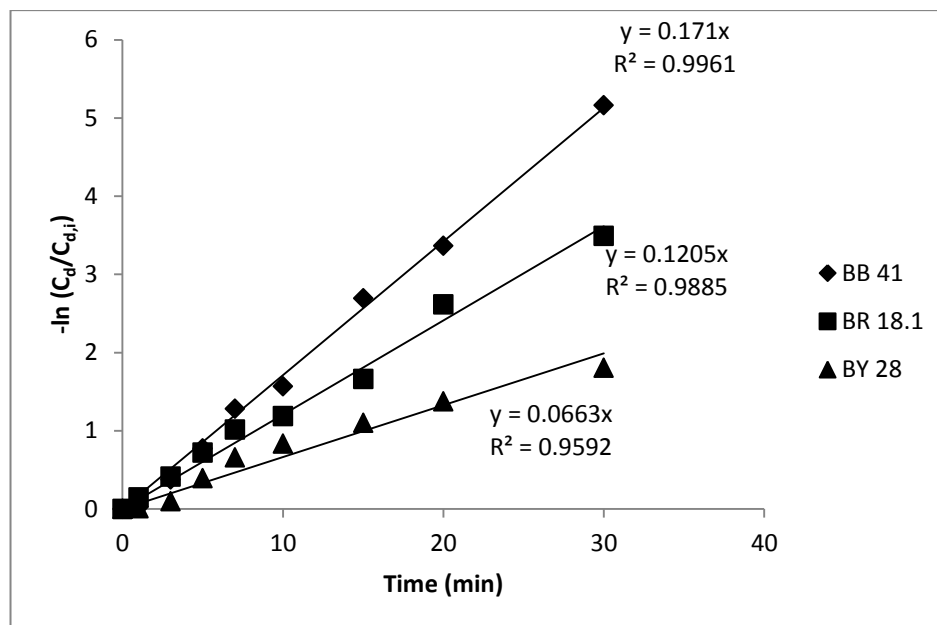
Ozonation Process	pH	BB 41 Removal %		BY 28 Removal %		BR 18.1 Removal %	
		TOC	COD	TOC	COD	TOC	COD
Sole	4	25.98	31.85	50.24	55.89	13.56	19.37
	10	50.91	55.63	21.27	29.37	44.60	47.38
With Alumina	4	28.49	33.96	55.83	58.29	19.48	23.96
	10	58.30	62.93	35.48	40.83	55.21	58.84
With PFOA	4	35.30	39.20	61.38	66.93	27.49	36.18
	10	54.93	59.29	26.47	30.19	48.20	54.20

#### 4.5.1.3 Kinetics of Non-Catalytic and Catalytic Ozonations

The ozonation reaction kinetics were examined for three of the dyes separately at pH of 4 and 10. At the equilibrium concentration of ozone in the aqueous phase,  $\ln(C_d/C_{d,i})$  versus time data showed a linear trend indicating a pseudo-first order reaction for each of the dyes at the acidic and alkaline media (Figures 4.39(a) and 4.39(b)).



(a)

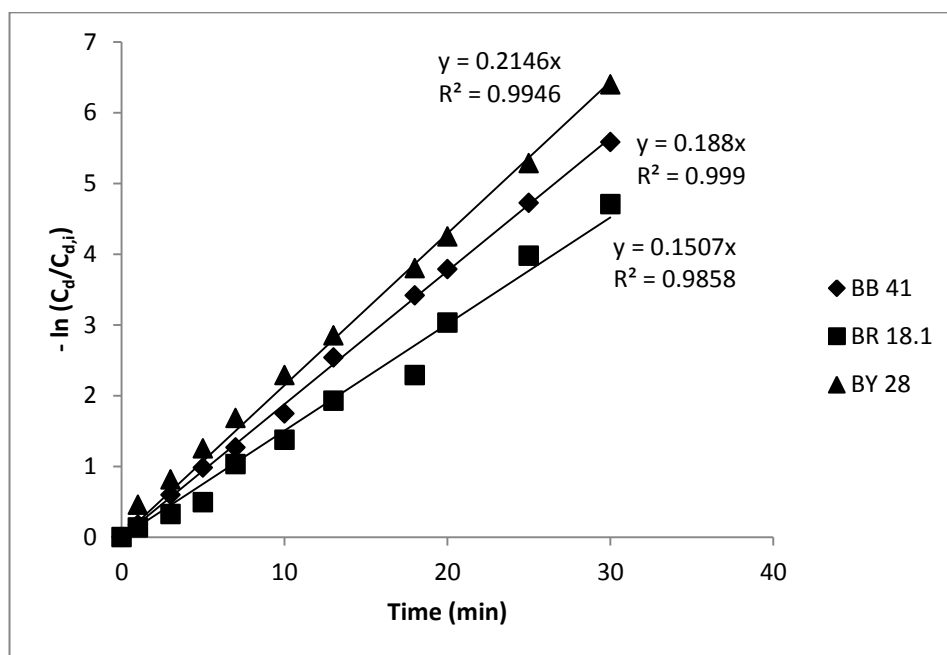


(b)

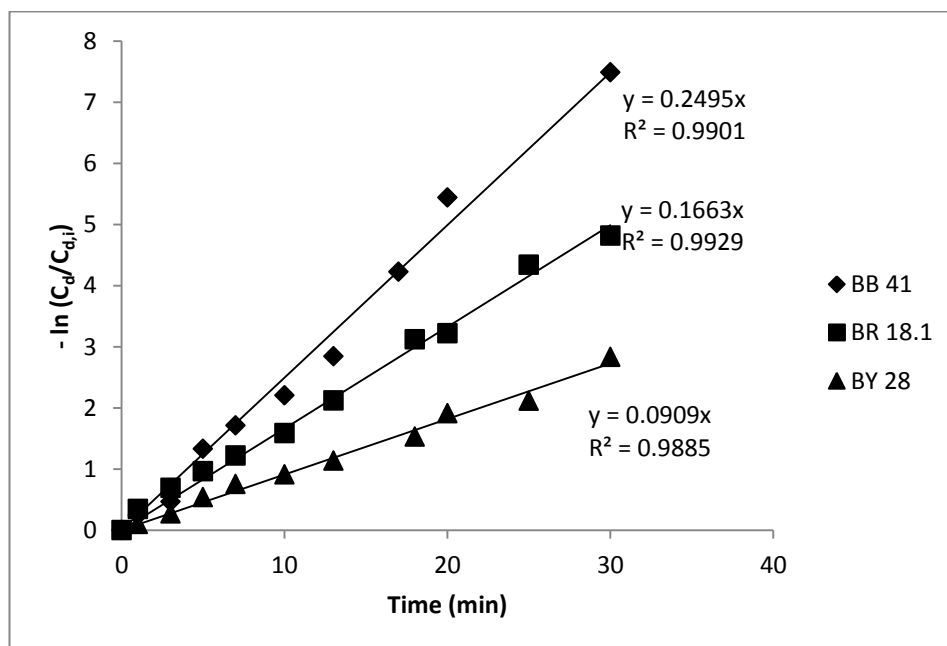
**Figure 4.39:** The pseudo-first order kinetic analysis,  $C_{d,i} = 300$  mg/L (for each dye), stirrer rate = 300 rpm,  $Q_G = 150$  L/h,  $C_{O_3,G,in} = 0.9 \pm 0.1$  mmol/L gas, catalyst: none; (a) pH = 4, (b) pH = 10

The pseudo-first order reaction rate constants in other words apparent rate constants were determined and shown in Table 4.29 for each dye at different pHs. The kinetic rate constants were observed to increase by increasing the pH from 4 to 10 for the red and blue dyes denoting the effect of radicals on the kinetics.

In addition to sole ozonation, catalytic ozonation kinetic data were also analyzed in terms kinetic analysis. Similar to sole ozonation, the change of the natural logarithm of  $C_d/C_{d,i}$  with time was observed to be linear showing that catalytic ozonation also followed a pseudo-first order reaction; but as seen in Table 4.23, pseudo-first order rate constants show differences when catalyst particles are added. The change in these constants is observed to depend on the pH and dye type. Adding PFOA increased the rate constant of the yellow dye at acidic pH showing the effect of molecular ozone on yellow dye degradation (Figures 4.40(a) and 4.40(b)). Alumina, on the other hand, caused a higher increase in the rate constants of the red and blue dyes and also a slight increase in rate constant of the yellow dye at a high pH of 10 indicating the effect of adsorption of basic dye on to the surface (Figures 4.41(a) and 4.41(b)). This also indicates the effect of hydroxyl ions on the decomposition of ozone by radical formation.

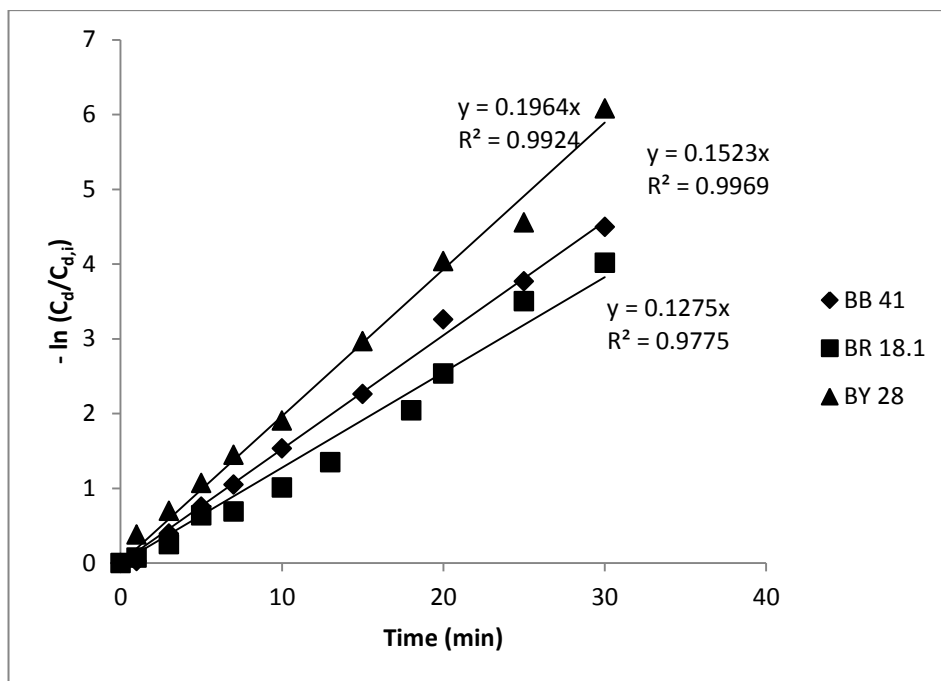


(a)

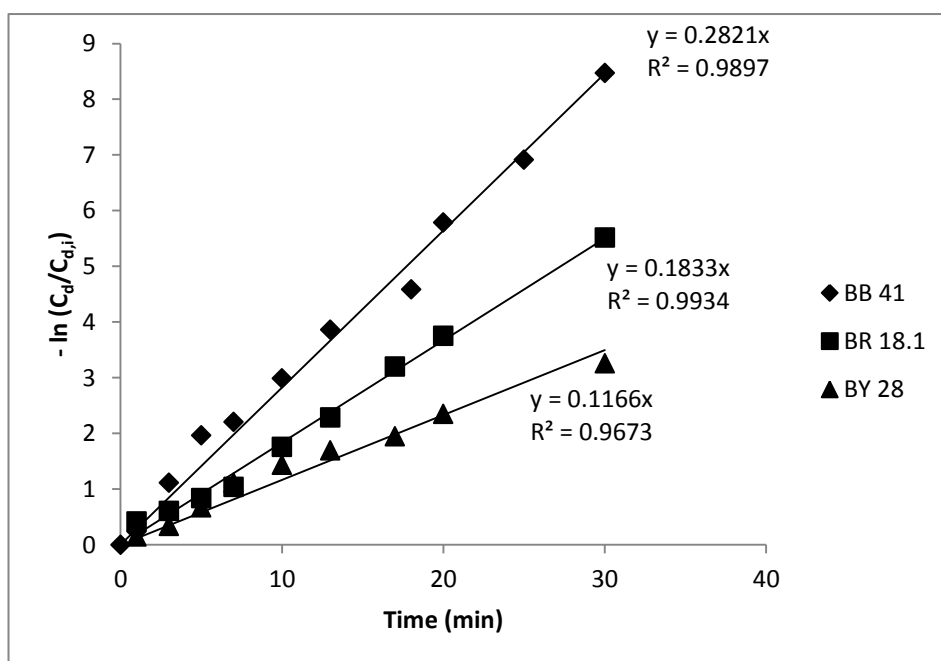


(b)

**Figure 4.40:** The pseudo-first order kinetic analysis,  $C_{d,i} = 300$  mg/L (for each dye), stirrer rate = 300 rpm,  $Q_G = 150$  L/h,  $C_{O_3,G,in} = 0.9 \pm 0.1$  mmol/L gas, catalyst: PFOA; (a) pH = 4, (b) pH = 10



(a)



(b)

**Figure 4.41:** The pseudo-first order kinetic analysis,  $C_{d,i} = 300$  mg/L (for each dye), stirrer rate = 300 rpm,  $Q_G = 150$  L/h,  $C_{O_3,G,in} = 0.9 \pm 0.1$  mmol/L gas, catalyst: alumina; (a) pH = 4, (b) pH = 10

**Table 4.29:** The pseudo-first order kinetic rate (apparent) constants for BB 41, BY 28 and BR 18.1 for sole and catalytic ozonation,  $C_{d,i} = 300$  mg/L (for each dye), stirrer rate = 300 rpm,  $Q_G = 150$  L/h,  $C_{O_3,G,in} = 0.9 \pm 0.1$  mmol/L gas

Dye	pH	Process	$k'$ (min <sup>-1</sup> )
BB 41	4	Sole	0.138
		Alumina/O <sub>3</sub>	0.152
		PFOA/O <sub>3</sub>	0.188
	10	Sole	0.171
		Alumina/O <sub>3</sub>	0.282
		PFOA/O <sub>3</sub>	0.249
BY 28	4	Sole	0.169
		Alumina/O <sub>3</sub>	0.196
		PFOA/O <sub>3</sub>	0.215
	10	Sole	0.066
		Alumina/O <sub>3</sub>	0.117
		PFOA/O <sub>3</sub>	0.091
BR 18.1	4	Sole	0.109
		Alumina/O <sub>3</sub>	0.127
		PFOA/O <sub>3</sub>	0.151
	10	Sole	0.120
		Alumina/O <sub>3</sub>	0.183
		PFOA/O <sub>3</sub>	0.166

## CHAPTER 5

### CONCLUSIONS

In this study, catalytic ozonation of the real WW from AKSA A.Ş. was examined at different operating conditions with or without alumina and perfluorooctyl alumina (PFOA) particles in a fluidized bed reactor. Moreover, the dyes included in this WW solution (BB 41, BR 18.1 and BY 28) were obtained separately and synthetic solutions of these dyes were also ozonated in a semi-batch reactor in the presence and absence of alumina and PFOA catalyst particles in order to examine the dyes separately. The effect of operating conditions like gas and liquid flow rates,  $COD_{in}$ , pH of WW solution, catalyst type and dosage on dye, COD and TOC removals and ozone consumption were investigated.

Experiments conducted in semi-batch reactor introduced the following conclusions:

- The ozonation of Basic Blue 41 (BB41), Basic Red 18.1 (BR 18.1) and Basic Yellow 28 (BY 28) synthetic dye solutions were performed and above 85% of color removals were achieved after 30 min. ozonation time for all of dye solutions. Addition of alumina or PFOA particles into the reaction medium was observed to increase the removal efficiencies.
- The dye removals show differences at different pHs for different dye solutions. While for BY 28 the dye removal was higher at acidic pH of 4, for BB 41 and BR 18.1 removals were found to be higher at alkaline pH of 10.
- Alumina catalyst enhances the ozone decomposition reactions and thus helps radical formation yielding higher TOC and COD removals for both of BB 41 and BR 18.1 at pH of 10. On the other hand, for BY 28 PFOA catalyst was found to be more efficient at pH of 4 in terms of TOC and COD removals.
- Kinetic analysis of both non-catalytic and catalytic ozonation processes showed that ozonation reaction followed pseudo-first order reaction kinetics with respect to dye concentration. The pseudo-first order reaction rate constants were

determined for each dye. While increasing pH from 4 to 10 provides an increase in the rate constants of BB 41 and BR 18.1 indicating the effect of radicals on the kinetics, at a low pH of 4 the rate constant of BY 28 was found to be higher denoting the role of molecular ozone on BY 28 dye degradation. Moreover, catalyst addition to the reaction medium generally was observed to increase the rate constants obtained for all of the dyes.

- Molecular ozone was found to be more important for the degradation of BY 28 occurred by direct oxidation reactions; while on the other hand, hydroxyl radicals took charge in the degradation of both BB 41 and BR 18.1 formed due to the indirect oxidation reactions depending on the structures and types of the dyes.

Conclusions obtained from the results of the experiments conducted in fluidized bed reactor can be listed as follows:

- A new “absorbance vs. concentration” calibration method was developed in order to determine the concentration of each dye in the mixture. By using this method, the color removals for each dye in the mixture can be obtained and examined separately. By using these calibrations, the amount of each dye in the WW sample obtained from AKSA Acrylic Plant was found as 4175 mg/L, 727 mg/L and 732 mg/L for BB 41, BY 28 and BR 18.1, respectively.
- The effect of inlet COD concentration ( $COD_{in}$ ) of the wastewater solution was investigated and increasing  $COD_{in}$  was found to decrease the color removals of each dye in WW solution also the TOC and COD removals. Moreover, ozone consumption increased with  $COD_{in}$ . At  $Q_G = 340$  L/h,  $Q_L = 250$  L/h, ozonation without catalyst yielded 50.37% dye removal of BB 41, 97.28% of BR 18.1 and 100% of BY 28 for the lowest  $COD_{in}$  of 60 mg/L while at same conditions for  $COD_{in}$  is equal to 300 mg/L, dye removals of 16.55%, 71.89% and 98.37% were achieved for BB 41, BR 18.1 and BY 28, respectively.
- After the kinetic analysis of the dye decolorization in the WW, the pseudo first order behavior with respect to dye concentration was observed and the pseudo first order reaction rate constants ( $k'$ ) of the dyes in WW were estimated. These rate constants were observed to decrease logarithmically with an increase in  $COD_{in}$  indicating that the estimated constants are apparent; but not intrinsic reaction rate constants.

- Removals of BB 41 and BR 18.1 were observed to increase at a higher pH of 12; but the removal of BY 28 was higher at an acidic pH of 4. At  $Q_G = 340$  L/h,  $Q_L = 250$  L/h, sole ozonation provided 98.37% removal for BY 28 at pH of 4, 30.19% and 97.38% removals for BB 41 and BR 18.1, respectively.
- Dye, TOC and COD removals were found to be higher at basic pH when using alumina catalyst due to the higher decomposition rate of ozone with alumina and higher adsorption of WW on alumina catalyst. On the other hand, at acidic pH PFOA catalyst yields higher removals due to the high stability of molecular ozone in the alkyl phase on the catalyst.
- Indirect oxidation reactions were determined to take charge in the oxidation of BB 41 and BR 18.1 and direct oxidation reactions in the oxidation of BY 28 indicating the effect of radicals and molecular ozone on the degradation of blue, red and yellow dyes.
- The low concentration of yellow dye in WW solution and the higher overall color, TOC and COD removals at higher pH (pH = 12) makes the pH parameter of 12 more preferable for the ozonation of WW taken from AKSA. Moreover, the addition of alumina particles into the reaction medium yields most efficient organic removals at pH of 12.
- The experiments done in order to investigate the effect of catalyst dosage showed that increasing the catalyst amount to 300 g increased the dye, TOC and COD removal efficiencies; but increasing the catalyst amount further to 400 g caused decreases in the removal efficiencies due to the formation gas bubbles in larger sizes and thus smaller interfacial area between the gas and liquid phases.
- Increasing  $Q_G/Q_L$  ratio from 1.13 to 4.04 provided the percent organic removals to increase almost two times.
- Dispersion coefficients ( $D_L$ ) and mass transfer coefficients ( $k_La$ ) were estimated by the correlations obtained in the previous study done by Erol and Özbelge, (2009) and these coefficients reached a maximum when the  $Q_G/Q_L$  ratio is equal to 1.51 bringing the idea that not only  $Q_G/Q_L$  ratio is important; but the  $Q_G$  and  $Q_L$  separately are also important parameters on  $D_L$  and  $k_La$ .
- Keeping  $Q_G/Q_L$  ratio constant and increasing the gas and liquid flow rates yielded higher organic removals due to the increase in  $D_L$  and  $k_La$  values and thus turbulence in the reactor.

## CHAPTER 6

### RECOMMENDATIONS

The main aim of this study was to investigate the catalytic ozonation of an industrial textile wastewater supplied from AKSA A.Ş. in the presence of alumina and PFOA catalysts and to determine the most efficient operating parameters of the treatment process of wastewater ozonation in terms of higher dye removal, higher TOC and COD removals and lower ozone consumption. The following studies can be recommended as the further examinations on this subject:

In order to optimize the operating parameters, in the future the experiments at pH of 7 could be performed. This can provide to investigate the effect of hydroxyl radicals on the ozonation reactions further.

In the analysis of reaction kinetics, the rate constants found in this study are apparent ones including the ozone and hydroxyl radical concentrations, the intrinsic rate constants could be found out using scavengers in the reaction medium to determine radical concentration. Thus, the effect of temperature can be investigated on the intrinsic rate constant of the ozonation reactions.

Ozonation side products could be investigated in order to fully determine and understand the mechanism of the ozonation process. HPLC analysis could be done near TOC and COD analysis in order to find out which organic acids, aldehydes or ketones as the by-products.

Although the lower  $Q_L$  values were found out to increase the dye, TOC and COD removals, in case of catalytic operations, the degree of fluidization and mixing were also determined to be important; thus in order to reach higher liquid velocities for

lower  $Q_L$  values, reactors with smaller inside diameter could be designed and used for wastewater ozonation processes.

It was found out that ozone behaves selective and yields higher removals in color removals; but on the other hand, sole ozonation was not efficient enough for TOC and COD removals. Since ozone firstly attacked to the chromophore groups and resulted color to disappear and then by-products were degraded; designing a reactor that has two segments would be useful. The segment at which gas and liquid flows enters the reactor could be the two phase region where dye can be ozonated easily and the segment above this first segment could be three phase including catalyst particles and thus providing the degradation of by-products after dye removal.

## REFERENCES

- Acar E., Özbelge T. (2006). Oxidation of Acid Red 151 aqueous solutions by the peroxone process and its kinetic evaluation. *Ozone Sci. Eng.* 28, 155-164.
- Alaton, İ.A., Balcıoğlu, İ.A., Bahnemann, D.W. (2002). Advanced oxidation of a reactive dyebath effluent: Comparison of O<sub>3</sub>, H<sub>2</sub>O<sub>2</sub>/UV-C and TiO<sub>2</sub>/UV-A processes. *Water Res.*, 36(5), 1143-1154.
- Andreozzi, R., Marotta, R., Sanchirico, R. (2000). Manganese-Catalysed Ozonation of Glyoxalic Acid in Aqueous Solutions. *J. Chem. Technol. Biot.*, 75, 59-65.
- Arslan, I., Balcıoğlu, I.A. (2001). Degradation of Remazol Black B Dye and Its Simulated Dyebath Wastewater by Advanced Oxidation Processes in Heterogeneous and Homogeneous Media. *Color. Technol.*, 117, 38-42.
- Bader H., Hoigne J., (1981), Determination of Ozone in Water by the Indigo Method, *Water Res.* 15, 449–455.
- Balcıoğlu, I.A., Arslan, İ. (2001) Partial oxidation of Reactive Dyestuffs and Synthetic Textile Dye-Bath by the O<sub>3</sub> and O<sub>3</sub>/H<sub>2</sub>O<sub>2</sub> Processes. *Water Sci. Technol.*, 43(2), 221-228.
- Beltran, F.J., Rivas, F.J., Espinoza, R.M. (2002). Catalytic ozonation of oxalic acid in an aqueous TiO<sub>2</sub> slurry reactor. *Appl. Catal. B: Environ.*, 39, 221-231.
- Box, G.E.P., Hunter, W.G., Hunter J.S. (1978). Statistics for Experimenters. John Wiley and Sons. 323-325.
- Buxton, G.V., Greenstock, C.L., Helman, W.P., Ross, A.B. (1988). Critical review of rate constants for reaction of hydrated electrons, hydrogen atoms and hydroxyl radicals (/O•HO-) in aqueous solution. *J. Phys. Chem. Ref. Data* 17, 513-886.
- Carbajo M., Beltran F.J., Gimeno O., Acedo B., Rivas F.J. (2007). Ozonation of phenolic wastewaters in the presence of a perovskite type catalyst. *Appl. Catal. B: Environ.* 74(3-4), 203-210.
- Carriere, J., Jones, P., Broadbent, A.D. (1993). Decolorization of textile dye solutions. *Ozone Sci. Eng.*, 15, 189-200.
- Choi I.S., Wiesmann U., (2004), Influence of Mass Transfer and Chemical Reaction on Ozonation of Azo Dyes, *Water Sci. Technol.*, 49, 37-43.

- Chu W. and Chi-Wai M. (1999). Quantitative prediction of direct and indirect dye ozonation kinetics. *Water Res.* 34 (12), 3153-3160.
- Ciardelli, G., Ranieri, N. (2001). The treatment and reuse of wastewater in the textile industry by means of ozonation and electroflocculation. *Water Res.* 35(2), pp. 567-572.
- Cooper, Sydney G. (1978) The textile industry: environmental control and energy conservation. Park Ridge, N.J.: Noyes Data Corp
- Dankwerts, P. (1970). Gas-liquid Reaction. Mc-Graw Hill, New York.
- Eriksson, M. (2005). Ms. Thesis. Ozone chemistry in aqueous solution-ozone decomposition and stabilization, Department of Chemistry, Royal Institute of Technology, Sweden.
- Erol F. (2008). Ph.D. Thesis. Advanced oxidation techniques for the removal of refractory organics from textile wastewaters, Graduate School of Natural Sciences, Middle East Technical University.
- Erol F. and Özbelge T. (2009). Effects of pH, Initiator, Scavenger and Surfactant on the Ozonation Mechanism of an Azo Dye (Acid Red-151) in a Batch Reactor. *Chem. Eng. Commun.* 196, 1-2, 39-55.
- Erol F. and Özbelge T. (2007). Catalytic ozonation with non-polar bonded alumina phases for treatment of aqueous dye solutions in a semi-batch reactor. *Chem. Eng. J.* 139, 272-283.
- Farines V., Baig S., Albet J., Molinier J. & Legay C. (2003). Ozone transfer from gas to water in a co-current upflow packed bed reactor containing silica gel. *Chem. Eng. J.* 91, 67-73
- Fazzini, L., Young, J.C. (1994). Use of ozone and ultraviolet oxidation to enhance the biological degradation of refractory organics in Landfill Leachate. *49th Purdue Industrial Waste Conference Proceedings.* 253-262.
- Gomes de Moraes, S., Freire, R.S., Duran, N. (2000). Degradation and toxicity reduction of textile effluent by combined photocatalytic and ozonation processes. *Chemosphere*, 40, 369-373.
- Gracia J., Aragües J.L., Ovelleiro J.L. (1996). Study of the Catalytic Ozonation of Humic Substances in Water and Their Ozonation Byproducts. *Ozone Sci. Eng.* 18(3), 195-208.
- Hassan M. M., and Hawkyard C.J. (2002). Decolourisation of aqueous dyes by sequential oxidation treatment with ozone and Fenton' s reagent , *J. Chem. Technol. Biot.*, 77, 834-841.

- Hassan M. M., Hawkyard C. J. and Barratt P. A. (2006). Decolourisation of dyes and dyehouse effluent in a bubble-column reactor by ozonation in the presence of H<sub>2</sub>O<sub>2</sub>, KMnO<sub>4</sub> or ferral. *J. Chem. Technol. Biot.*, 81, 158-166
- Hoigné, J. and Bader, H. (1983). Rate Constants of Reactions of Ozone with Organic and Inorganic Compounds in Water-I. *Water Res.*, 17, 173-183.
- Hoigné, J., and Bader, H. (1976). The Role of Hydroxyl Radical Reactions in Ozonation Process in Aqueous Solutions. *Water Res.*, Vol. 10, 377-385.
- Hsing H., Chiang P., Chang E. & Chan M. (2006). The decolorization and mineralization of Acid Orange 6 Azo Dye in aqueous solution by Advanced Oxidation. *Water Res.* 19 (5).
- Hsu, Y.C., Chen, J.T., Yang, H.C., Chen, J.H., Fang, C.F. (2001). Ozone Decolorization of Mixed-Dye Solutions in a Gas-Induced Reactor. *Water Environ. Res.*, 73(4), 494-503.
- Kasprzyk-Hordern, B., Andrzejewski, P., Dabrowska, A., Czaczyk, K., Nawrocki, J. (2004). MTBE, DIPE, ETBE and TAME Degradation in Water Using Perfluorinated Phases as Catalysts for Ozonation Process. *Appl. Catal. B: Environ.*, 51, 51-66.
- Kasprzyk-Hordern B., Andrzejewski P., Nawrocki J. (2005). Catalytic ozonation of gasoline compounds in model and natural water in the presence of perfluorinated alumina bonded phases. *Ozone Sci. Eng.* 27:4, 301-310
- Kasprzyk-Hordern, B., Dabrowska, A., Swietlik, J., Nawrocki, J. (2004). The Application of the Perfluorinated Bonded Alumina Phase for Natural Organic Matter Catalytic Ozonation. *J. Environ. Eng. Sci.*, 3, 41-50.
- Kasprzyk-Hordern B., Swietlik J., Dabrowska A., Nawrocki J., (2004). Ozonation enhancement with non-polar bonded phases. *Ozone Sci. Eng.* 26, 367-380.
- Kasprzyk-Hordern B., Ziolek M. and Nawrocki J. (2003). Catalytic ozonation and methods of enhancing molecular ozone reactions in water treatment. *Appl. Catal. B: Environ.* 46, 639-669.
- Konsowa, A.H. (2003). Decolorisation of wastewater containing direct dye by ozonation in a batch bubble column reactor, *Desalination*, 158, 233-240.
- Kornmüller, A., Karcher, S., Jekel, M. (2001). Cucurbituril for water treatment. Part II: Ozonation and oxidative regeneration of cucurbituril. *Water Res.*, 35(14), 3317-3324.
- Kos L. and Perkowski J. (2003). Decolouration of real textile wastewater with advanced oxidation processes. *Fiber. Text.* Vol. 11, 4(43).

- Koşan, İ. (2009, 2010). Private communication
- Koyuncu, İ., Afşar, H. (1996). Decomposition of dyes in the textile wastewater with ozone. *J. Environ. Sci. Heal. A* 31(5), 1035-1041.
- Kulkarni S.V., Blackwell C.D., Blackard A.L., Stackhouse C.W., Alexander M.W. (1985). Textile Dyes and Dying Equipment: Classification, Properties and Environmental Aspects. *EPA's Project Summary*, 1-5.
- Legube B., Leitner N.K. (1999). Catalytic ozonation: a promising advanced oxidation technology for water treatment. *Catal. Today*, 53(1), 61-72.
- Levenspiel O. (1972). Chemical Reaction Engineering. Wiley, New York, pp. 418-419
- Liakou S., Pavlou S., Lyberatos G. (1997). Ozonation of azo dyes. *Water Sci. Technol.* 35(4), pp. 279 – 286.
- Lopez-Lopez, A., Pic, J.S., Debellefontaine, H. (2007). Ozonation of azo dye in a semi-batch reactor: A determination of the molecular and radical contributions, *Chemosphere*, 66(11), 2120-2126.
- Moussavi G. and Mahmoudi M. (2009). Removal of azo and anthraquinone reactive dyes from industrial wastewaters using MgO nanoparticles. *J. Hazard. Mater.* 168 (2-3), 806-812.
- Muthukumar, M., Selvakumar, N. (2004). Studies on the Effect of Inorganic Salts on Decolorization of Acid Dye Effluents by Ozonation. *Dyes. Pigments.*, 62, 221-228.
- Ni C.H., Chen J.N. (2001). Heterogeneous catalytic ozonation of 2-chlorophenol aqueous solution with alumina as a catalyst. *Water Sci. Technol.* 43(2), 213-220.
- Oyama, S.T. (2000). Chemical and Catalytic Properties of Ozone. *Catal. Today*, 42(3), 279-322.
- Park J.S., Choi H., Cho J. (2004). Kinetic decomposition of ozone and para-chlorobenzoic acid (p-CBA) during catalytic ozonation. *Water Res.* 38(9), 2285-2292.
- Pines D. S., Reckow D.A. (2002). Effect of Dissolved Cobalt(II) on the Ozonation of Oxalic Acid. *Environ. Sci. Technol.* 36(19), 4046-4051.
- Pirgalioglu S. (2008). Ms. Thesis. Catalytic ozonation of dye solutions in a semi-batch reactor, Graduate School of Natural Sciences, Middle East Technical University.

- Qu J., Li H., Liu H. and He H. (2004). Ozonation of alachlor catalyzed by Cu/Al<sub>2</sub>O<sub>3</sub> in water. *Catal. Today*. 90, 291-296.
- Rand M.C., Greenberg A.E., Taras M.J., (1992), Standard Methods for the Examination of Water and Wastewater, 18<sup>th</sup> ed., APHA, Washington, DC, pp. 455–460.
- Rice R. G. & Netzer A. (1982). Handbook of Ozone Technology and Applications. Ann Arbor Science, Michigan, pp. 2-4
- Salome O., Soares G.P., Faria P.C.C., Orfao J.J.M. and Pereira M.F.R. (2007). Ozonation of textile effluents and dye solutions in the presence of activated carbon under continuous operation. *Separ. Sci. Technol.* 42, 1477-1492.
- Sarayu, K., Swaminathan, K., Sandhya, S. (2007). Assessment of degradation of eight commercial reactive azo dyes individually and in mixture in aqueous solution by ozonation. *Dyes. Pigments.*, 75, 362-368.
- Slokar, Y.M., Marechal, A.M.L. (1998). Methods of Decoloration of Textile Wastewaters. *Dyes. Pigments.*, 37(4), 335-356.
- Soares G.P., Saloma O., Orfao J.J.M., Portela D., Vieira A., Pereira M.R., (2006), Ozonation of Textile Effluents and Dye Solutions under Continuous Operation: Influence of Operating Parameters. *J. Hazard. Mater.* B137, 1664-1673.
- Srisukphun T. (2002). Fouling mechanism of reverse osmosis membrane in textile wastewater reuse plant. Retrieved March 29, 2008 from the World Wide Web [www.cv.titech.ac.jp/~jsps/activity\\_report/2006/Thirdphong\\_research\\_report.pdf](http://www.cv.titech.ac.jp/~jsps/activity_report/2006/Thirdphong_research_report.pdf)
- Staehelin, J. and Hoigne, J. (1985). Decomposition of Ozone in Water in the Presence of Organic Solutes Acting as Promoters and Inhibitors of Radical Chain Reactions. *Environ. Sci. Technol.*, 19(12), 1206-1213.
- Talapad, T., Neramittagapong, A., Neramittagapong, S. (2008). Degradation of Congo Red Dye by Ozonation. *Chiang Mai J. Sci.* 35(1), 63-68.
- Talarposhti A. M., Donnely T and Anderson G.K. (2001). Color removal from a simulated dye wastewater using a two-phase anaerobic packed bed reactor. *Water Res.* 35(2), 425-432.
- Thomas K., Hoggan P.E., Mariey L., Lamote J., Lavalley J.C. (1997). Experimental and Theoretical Study of Ozone Adsorption on Alumina. *Catal. Lett.* 46, 77-82.
- Trapido, M., Veressinina, Y., Munter, R., Kallas, J. (2005). Catalytic Ozonation of m-Dinitrobenzene. *Ozone Sci. Eng.*, 27, 359-363.

- Vandevivere, P.C., Bianchi, R., Verstraete, W. (1998). Treatment and reuse of wastewater from the textile wet-processing industry: review of emerging technologies. *J. Chem. Technol. Biot.* 72, 289-302.
- Wang, C., Yediler, A., Lienert, D., Wang, Z., Kettrup, M. (2003). Ozonation of an azo dye C.I. Remazol Black 5 and toxicological assessment of its oxidation products. *Chemosphere*, 52(7), 1225-1232.
- Wu J. and Wang T. (2000). Ozonation of aqueous azo dye in a semi-batch reactor. *Water Res.* 35 (4), 1093-1099
- Wu J., Doan H., Upreti S. (2008). Decolorization of aqueous reactive textile dye by ozone, *Chem. Eng. J.* 142, 156-160.
- Xin L., Yao J. and Qi J. (2006). Degradation of organic pollutants in water by catalytic ozonation. *Chem. Res. Chinese U.* 23 (3), 273-275.
- Yong K., Wu J., and Andrews S. (2005), Heterogeneous catalytic ozonation of aqueous reactive dye, *Ozone Sci. Eng.*, 27, 257-263 (2005).
- Yurteri, C., and Gürol, M.D. (1988). Ozone Consumption in Natural Waters: Effects of Background Organic Matter, pH and Carbonate Species. *Ozone Sci. Eng.*, 10, 272- 282.
- Zhao W., Wu Z. and Wang D. (2006). Ozone direct oxidation kinetics of Cationic Red X-GRL in aqueous solution. *J. Hazard. Mater.*, B137, 1859-1865
- Zhou, H., Smith, D.W. (2000). Ozone mass transfer in water and wastewater treatment: Experimental observations using a 2D-laser particle dynamics analyzer. *Water Res.*, 34, 909-921.

## APPENDIX A

### CALIBRATION CURVES OF BB 41, BR 18.1 AND BY 28 DYES

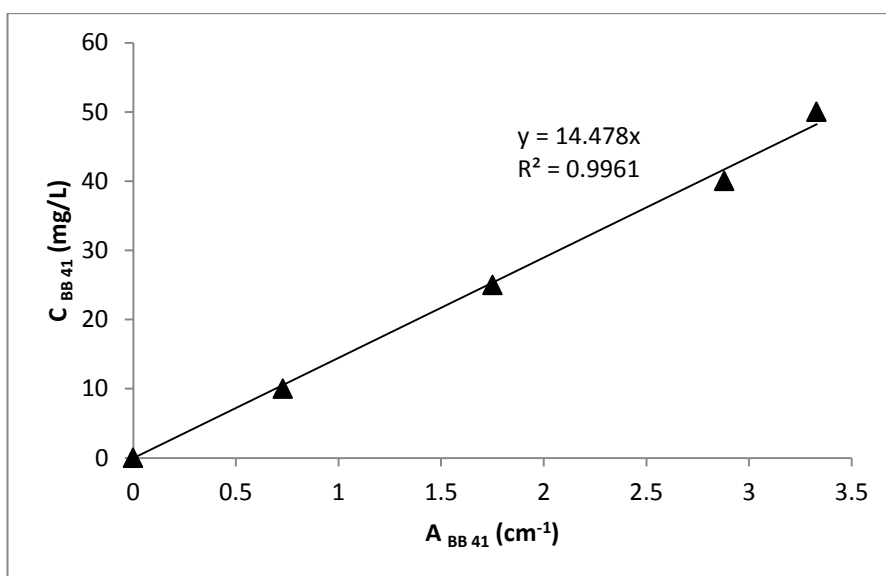


**Figure A.1.** The concentration versus absorbance values for BB 41 at pH = 4, 10 and 12 at 617 nm.

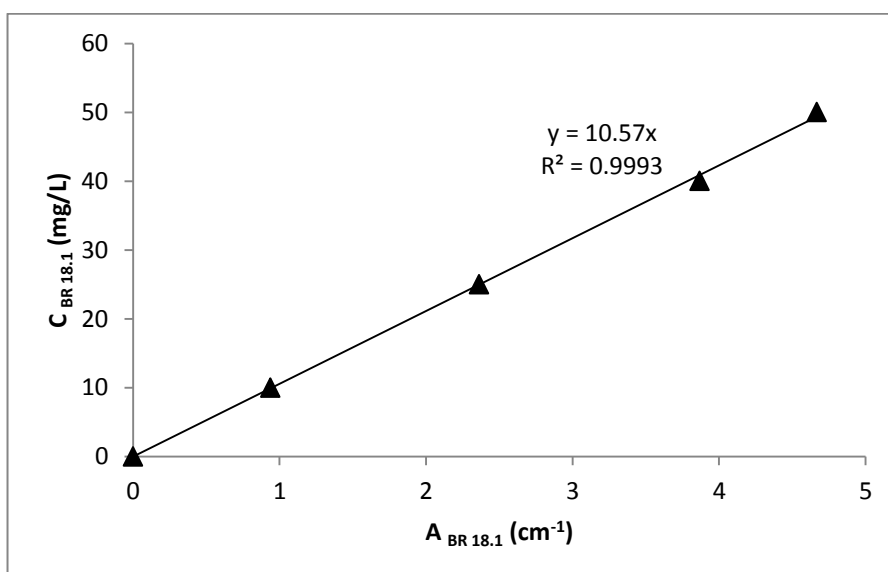


**Figure A.2.** The concentration versus absorbance values for BR 18.1 at pH = 4, 10 and 12 at 529 nm.

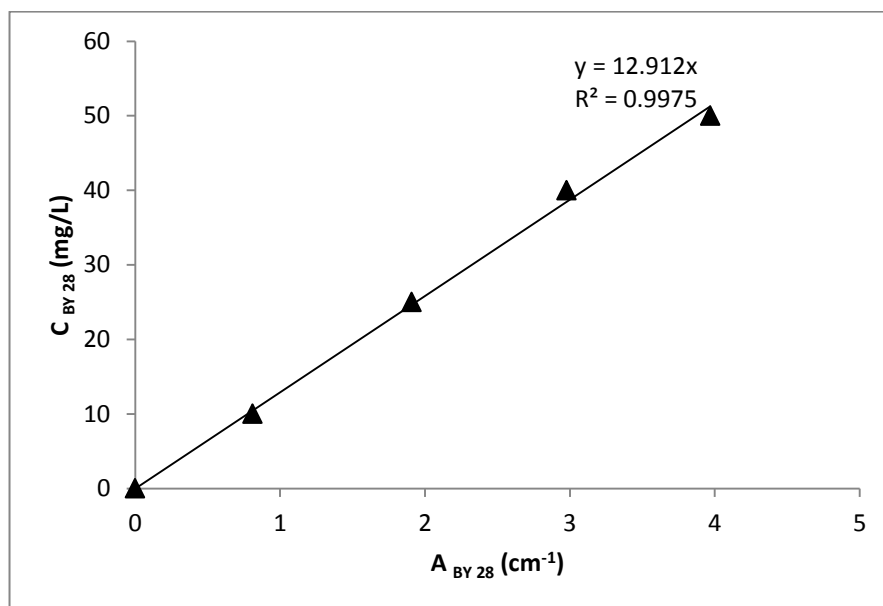


**Figure A.3.** The concentration versus absorbance values for BY 28 at pH = 4, 10 and 12 at 437 nm.

## APPENDIX B

### ANALYTICAL METHODS

#### B.1 KI Method for Ozone

The determination of ozone concentration in the gas phase

KI method can be used for the determination of ozone in air by adsorption of ozone in iodide solution. Ozone liberates iodine from 2% potassium iodide (KI) solution. After immediate acidification, the liberated iodine (Rxn. B1) is titrated with standard 0.1 M sodium thiosulfate ( $\text{Na}_2\text{S}_2\text{O}_3$ ) using starch indicator.



#### Calculation Procedure

Let's take the molarity of  $\text{Na}_2\text{S}_2\text{O}_3$  as M. The volume of thiosulfate solution spent for the determination of ozone is

$$\Delta V = V_{\text{thio}} - V_{\text{thio,blank}} \quad (\text{B.3})$$

where  $V_{\text{thio,inlet}}$  is the titrant spent for the sample and  $V_{\text{thio,blank}}$  is the titrant for the blank.

The amount of  $\text{S}_2\text{O}_3^{-2}$  as mole:

$$n_{S_2O_3^{-2}} = M_{thio} [\text{mole/L}] \times (V_{thio} - V_{thio,blank}) [\text{mL}] \times \frac{1L}{1000mL} = (V_{thio} - V_{thio,blank}) \times M \times 10^{-3} \text{ mole} \quad (\text{B.4})$$

Since 1 mole of ozone spends 2 moles of  $S_2O_3^{-2}$  in the reaction, the amount of ozone in the sample is,

$$n_{O_3,G} = \frac{1}{2} \times (V_{thio} - V_{thio,blank}) \times M_{thio} \times 10^{-3} \text{ mole ozone} \quad (\text{B.5})$$

The ozone dose is calculated for  $t$  (min) of ozonation:

$$D_{O_3} = \frac{n_{O_3,G}}{t} = \frac{(1/2) \times (V_{thio} - V_{thio,blank}) \times M_{thio} \times 10^{-3}}{t(\text{min})} \times \frac{60 \text{ min}}{1 \text{ h}} \quad (\text{B.6})$$

$$D_{O_3} = 0.03 \times (V_{thio} - V_{thio,blank}) \times M_{thio} \text{ mole } O_3/h \quad (\text{B.7})$$

Equation (B.7) is multiplied by  $10^3$  to convert the unit of  $D_{O_3}$  from mole  $O_3/h$  to mmol  $O_3/h$ .

$$D_{O_3} = \frac{30 \times (V_{thio} - V_{thio,blank}) \times M_{thio}}{t(\text{min})} \text{ mmol } O_3/h \quad (\text{B.8})$$

Inlet ozone concentration (mmol  $O_3/L$  gas) in the gas can be calculated from ozone dose and volumetric gas flow rate:

$$C_{O_3,G} = \frac{D_{O_3}(\text{mmol } O_3/h)}{Q_G(\text{L gas/h})} \quad (\text{B.9})$$

Ozone concentration in the inlet gas can be calculated by determining the inlet ozone dose with Equation (B.8).

$$C_{O_3,G,in} = \frac{D_{O_3,in} (mmol O_3/h)}{Q_G (L gas/h)} \quad (B.10)$$

Ozone concentration in the outlet gas can be calculated by determining the outlet ozone dose with Equation (B.8).

$$C_{O_3,G,out} = \frac{D_{O_3,out} (mmol O_3/h)}{Q_G (L gas/h)} \quad (B.11)$$

### **Sample Calculation**

For the ozonation experiment in the fluidized bed reactor at pH = 4,  $COD_{in} = 300$  mg/L,  $Q_G = 227$  L/h,  $Q_L = 70$  L/h, no catalyst, ozone concentrations in the inlet gas and outlet gas were calculated:

Inlet gas;

$$M_{thio} = 0.3 \text{ M}$$

$$V_{thio} = 74.1 \text{ mL}$$

$$V_{thio,blank} = 0.1 \text{ mL}$$

$$t = 2 \text{ min}$$

$$D_{O_3} = \frac{30 \times (V_{thio} - V_{thio,blank}) \times M_{thio}}{t(\text{min})} = \frac{30 \times (74.1 - 0.1) \times 0.3}{2} = 306 \text{ mmol O}_3/\text{h}$$

Ozone concentration in the inlet gas:

$$C_{O_3,G,in} = \frac{D_{O_3,in} (mmol O_3/h)}{Q_G (L gas/h)} = \frac{306 \text{ mmol/h}}{227 \text{ L gas/h}} = 1.348 \text{ mmol O}_3/\text{L gas}$$

Outlet gas;

$$M_{thio} = 0.3 \text{ M}$$

$$V_{thio} = 107.1 \text{ mL}$$

$$V_{thio,blank} = 0.1 \text{ mL}$$

$t = 20 \text{ min}$

$$D_{O_3} = \frac{30 \times (V_{thio} - V_{thio,blank}) \times M_{thio}}{t(\text{min})} = \frac{30 \times (107.1 - 0.1) \times 0.3}{20} = 48.15 \text{ mmol O}_3/\text{h}$$

Ozone concentration in the outlet gas:

$$C_{O_3,G,out} = \frac{D_{O_3,out}(\text{mmol O}_3/\text{h})}{Q_G(\text{L gas}/\text{h})} = \frac{48.15 \text{ mmol}/\text{h}}{227 \text{ L gas}/\text{h}} = 0.212 \text{ mmol O}_3/\text{L gas}$$

## **B.2 Indigo Method for Dissolved O<sub>3</sub> Concentration in the Liquid Phase**

Method for dissolved ozone measurements based on the decolorization of indigotrisulfonate at acidic conditions. This method was found by H.Bader and J.Hoigné (1981) with their work “Determination of Ozone in Water by the Indigo Method”. They stated that it can be assumed that one mole of ozone undergoes reaction with one mole of sulfonated indigo. They also determined a constant sensitivity factor which reflects the change in absorbance with the amount of ozone added as  $\Delta A = 20\,000 \text{ cm}^{-1}(\text{mol}\cdot\text{L}^{-1})^{-1}$ . They stated that the factor given does not vary with ozone concentration, small changes in temperature of reaction or with the chemical composition of the water unless pH is below 4. In this work dissolved ozone amount was measured by using the sensitivity factor given by Bader et al. (1981). UV absorbance measurements were conducted at wavelength of 600 nm.

### Reagent Preparation

Stock Solution (1 L)

500 mL water + 1mL dose Phosphoric acid + 770 mg potassium indigo phosphate + fill to mark

Indigo Reagent I (1 L)

20 mL stock + 10 g NaH<sub>2</sub>PO<sub>4</sub> + 7 mL conc phosphoric acid + dilute to mark

Indigo Reagent II (1 L)

100 mL stock + 10 g NaH<sub>2</sub>PO<sub>4</sub> + 7 mL conc phosphoric acid + dilute to mark

### Application

10 mL Reagent II + 10 mL sample → 100 mL and read absorbance at 600 nm against the blank

Use formula to calculate the oxygen amount:

$$mg\ O_3/L = \frac{100 \times \Delta A}{f \times b \times V} \quad (B.12)$$

$\Delta A$  = absorbance difference between the blank and the sample  $f = 0.42$  (factor depends on the sensitivity factor in order to obtain a result in terms of mg/L).

$b$  = pathway length of the cell (1)

$V$  = sample volume (90 mL) (found value must be corrected by a correction factor according to the dilution (10 mL of sample added))

### **Sample Calculation**

In most of the cases that ozone was measured, it was measured in WW solutions which have maximum absorptions at 617 nm which resulted interference in measurements. That interference problem was handled by taking the difference between the absorbance of the dye solution at that particular height which sample was taken in indigo solution and the absorbance of the sample taken in indigo solution. A sample calculation is given below:

For the ozonation experiment in the fluidized bed reactor at pH = 4,  $COD_{in} = 300$  mg/L,  $Q_G = 227$  L/h,  $Q_L = 70$  L/h, no catalyst, the sample taken at  $z = 0.5$  m when the reactor is at steady state.

$$V_{\text{indigo sample}} = 19 \text{ mL}$$

$$V_{\text{sample}} = 19 - 10 = 9 \text{ mL since there is 10 mL of indigo solution.}$$

Keeping in mind the dilution of the indigo samples before the measurement, this absorbance value must also be multiplied by the dilution factor:

$$\text{Indigo-Sample Abs.} = 0.149 \text{ (measured for indigo solution)}$$

$$\text{Sample Abs.} = 0.35$$

$$\text{Dilution} = \frac{V_{\text{sample}}}{V_{\text{dil}}(100 \text{ mL})} = \frac{9}{100} = 0.09 \quad (B.13)$$

$$\text{Abs.} = 0.35 \times 0.09 = 0.0315$$

True absorbance of the indigo solution was found by subtracting the correction value calculated from the absorbance measured for the indigo sample.

$$\text{True Abs.} = 0.149 - 0.0315 = 0.1175$$

$$\text{mg O}_3/\text{L} = \frac{100 \times \Delta A}{f \times b \times V}$$

$$\Delta A = \text{Blank Abs.} - \text{True Abs.} = 0.233 - 0.1175 = 0.1155$$

$$\text{mg O}_3/\text{L} = \frac{100 \times 0.1155}{0.42 \times 1 \times 9} = 3.055 \text{ mg/L} = 63.657 \times 10^{-3} \text{ mM O}_3$$

### B.3 The Calculation of Concentrations of BB 41, BR 18.1 and BY 28 Dyes in WW Solution

As it was discussed in Section 3.6, in order to determine the dye removals of each dye in the sample and also to estimate the amount of colored dyes in the textile wastewater sample, “absorbance vs. concentration” calibration correlations were developed. The calibration curves for BB 41 and BY 28 at their chosen wavelengths of 617 nm and 380 nm and also at 500 nm were shown in Figures B.1 and B.2.

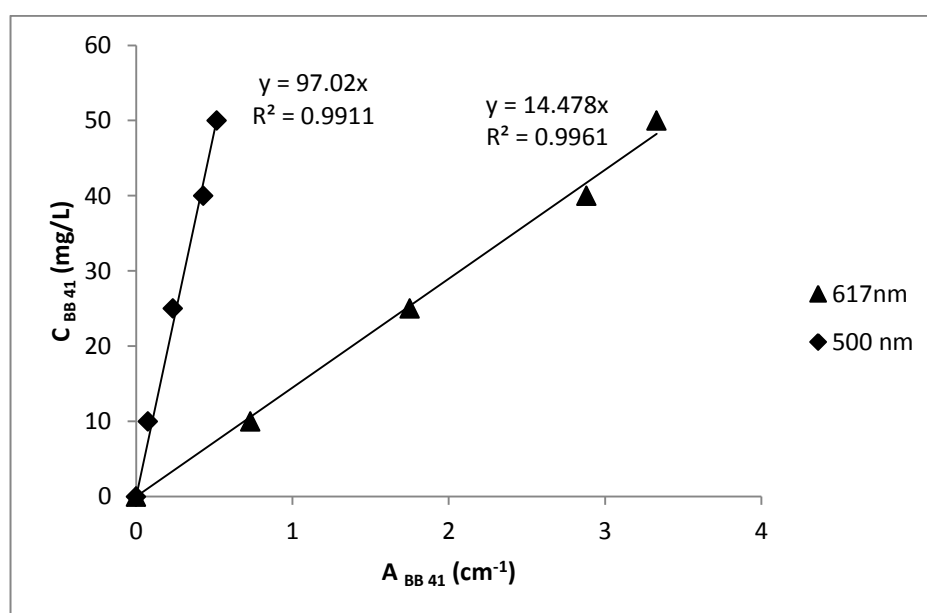


**Figure B.1.** The concentration versus absorbance values for BB 41 at pH = 4, 10 and 12 at 617 nm and 500 nm.

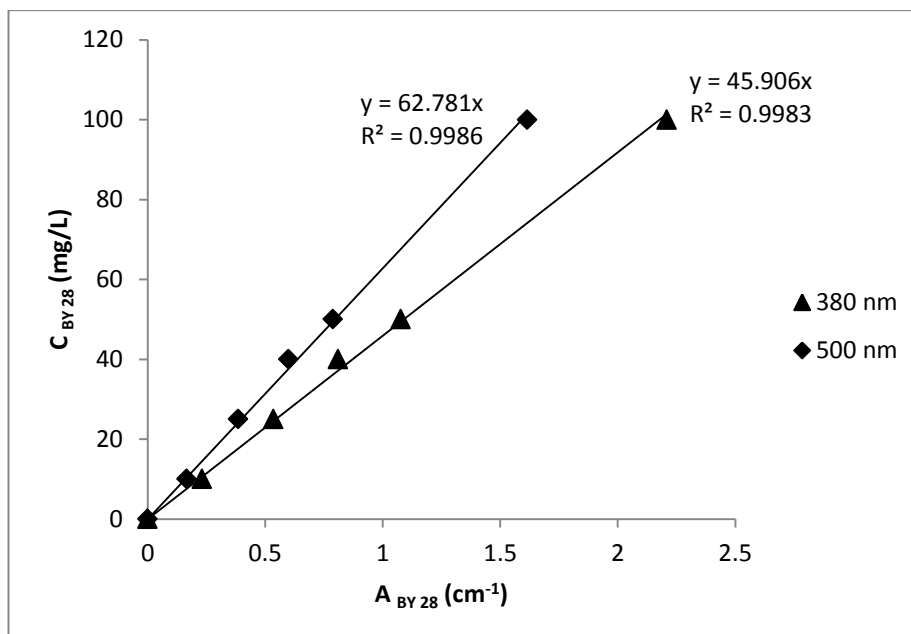


**Figure B.2.** The concentration versus absorbance values for BY 28 at pH = 4, 10 and 12 at 380 nm and 500 nm.

The absorbances of samples were measured at 380 nm and 617 nm for BB 41 and BY 28. Then by using their calibration curves at 500 nm their absorbances were found out at 500 nm and subtracted the absorbance of WW sample in order to find out only the absorbance of BR 18.1. Then by using the calibration curve for BR 18.1 at 500 nm (Figure B.3), its concentration can be found out.

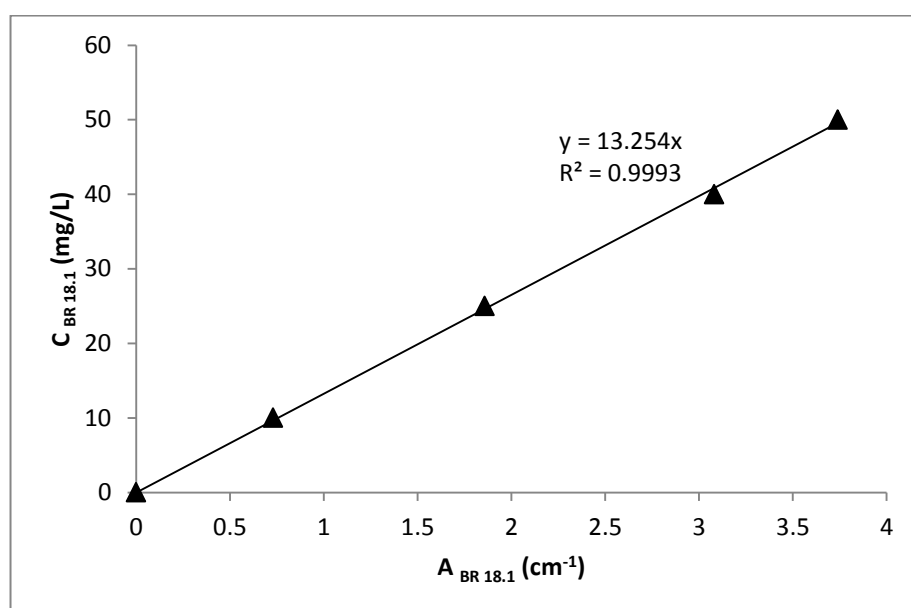


**Figure B.3.** The concentration versus absorbance values for BR 18.1 at pH = 4, 10 and 12 at 500 nm

### Sample Calculation

For the ozonation experiment in the fluidized bed reactor at pH = 4,  $COD_{in} = 300$  mg/L,  $Q_G = 340$  L/h,  $Q_L = 250$  L/h, no catalyst, the dye concentrations for the sample taken from the reactor at  $z = 0.5$  m:

$$A_{\text{sample}} \text{ (at 617 nm)} = 0.957 \text{ (with 10 times dilution)}$$

$$V_{\text{sample}} = 34 \text{ mL including 1 mL Na}_2\text{S}_2\text{O}_3$$

$$V_{\text{WW, sample}} = 34 - 1 = 33 \text{ mL}$$

Thus the true absorbance becomes:

$$A_{\text{true}} \text{ (at 617 nm)} = \frac{0.957 \times 10 \times 34}{33} = 9.86$$

$$C_{BB\ 41} = 9.86 \times 14.478 = 137.45 \text{ mg/L}$$

$$A_{\text{sample}} \text{ (at 380 nm)} = 0.563$$

$$A_{\text{true}} \text{ (at 380 nm)} = \frac{0.563 \times 34}{33} = 0.580$$

$$C_{BY\ 28} = 0.580 \times 45.91 = 3.26 \text{ mg/L}$$

$$A_{\text{sample}} \text{ (at 500 nm)} = 2.616$$

$$A_{BB\ 41} \text{ (at 500 nm)} = \frac{137.45}{97.02} = 1.416$$

$$A_{BY\ 28} \text{ (at 500 nm)} = \frac{3.26}{62.781} = 0.0519$$

$$A_{BR\ 18.1} \text{ (at 500 nm)} = 2.616 \quad (1.416 + 0.0519) = 1.4181$$

$$C_{BR\ 18.1} = 1.481 \times 13.254 = 12.28 \text{ mg/L}$$

### **B.4 Calculation of Dye, TOC removals, O<sub>3</sub> Consumption and O<sub>3</sub> Consumption Rate**

The dye and TOC removals as the percentage are calculated from Equations (B.14) and (B.15).

$$\text{Dye removal (\%)} = \frac{C_{D,in} - C_{D,out}}{C_{D,in}} \times 100 \quad (\text{B.14})$$

$$\text{TOC removal (\%)} = \frac{TOC_{in} - TOC_{out}}{TOC_{in}} \times 100 \quad (\text{B.15})$$

Then, the consumption of ozone and consumption rate (%) are calculated from the inlet and outlet gaseous ozone concentrations found in Section B.1. Also the applied ozone is calculated from inlet gaseous O<sub>3</sub> concentration.

$$Cons_{O_3} \text{ (mmol/L liq)} = (C_{O_3,G,in} - C_{O_3,G,out}) \times \frac{Q_G}{Q_L} \quad (\text{B.16})$$

$$R_{cons,O_3} = \frac{(C_{O_3,G,in} - C_{O_3,G,out})}{C_{O_3,G,in}} \times 100 \quad (\text{B.17})$$

$$\text{Applied } O_3 \text{ (mmol/L liq)} = \frac{C_{O_3,G,in} \times Q_G}{Q_L} \quad (\text{B.18})$$

### **Sample calculation**

For the ozonation experiment in the fluidized bed reactor with pH = 4,  $C_{d,in} = 1580$  Pt-Co color unit,  $Q_G = 227$  L/h,  $Q_L = 70$  L/h, no catalyst, the values were calculated for  $t = 20$  min,  $z = 1.0$  m:

$$C_{d,in} = 1570 \text{ Pt-Co unit}$$

$$C_{d,out} = 138 \text{ Pt-Co unit}$$

$$TOC_{in} = 83.13 \text{ mg/L}$$

$$TOC_{out} = 70.02 \text{ mg/L}$$

$$C_{O_3,G,in} = 1.348 \text{ mmol O}_3/\text{L gas}$$

$$C_{O_3,G,out} = 0.212 \text{ mmol O}_3/\text{L gas}$$

$$\text{Dye removal (\%)} = \frac{C_{d,in} - C_{d,out}}{C_{d,in}} \times 100 = \frac{1570 - 138}{1570} \times 100 = 91.21\%$$

$$\text{TOC removal (\%)} = \frac{TOC_{in} - TOC_{out}}{TOC_{in}} \times 100 = \frac{83.13 - 70.02}{83.13} \times 100 = 15.8\%$$

$$Cons_{O_3} = (C_{O_3,G,in} - C_{O_3,G,out}) \times \frac{Q_G}{Q_L} = (1.348 - 0.212) \times \frac{227}{70} = 4.069 \text{ mmol/L liq}$$

$$R_{cons,O_3} = \frac{(C_{O_3,G,in} - C_{O_3,G,out})}{C_{O_3,G,in}} \times 100 = \frac{(1.348 - 0.212)}{1.348} \times 100 = 84.27\%$$

$$\text{Applied } O_3 = \frac{C_{O_3,G,in} \times Q_G}{Q_L} = \frac{1.348 \times 227}{70} = 4.37 \text{ mmol/L liq}$$

## APPENDIX C

### AKSA WASTEWATER OZONATION EXPERIMENTS DATA

**Experiment:**

Conditions: pH=4,  $Q_G=170$  L/h,  $Q_L=150$  L/h,  $t=20$  min,  $COD_{,in}=60$  mg/L,  $C_{d,in,BB41} = 30.18$  mg/L,  $C_{d,in,BR18.1} = 5.26$  mg/L,  $C_{d,in,BY28} = 5.29$  mg/L,  $C_{d,in} = 315$  Pt-Co,  $C_{O_3,G,in} = 0.9 \pm 0.1$  mmol/L gas  $TOC_{in}=20.73$  mg/L, no catalyst.

**Table C.1:** Dye concentration change at steady state

z (m)	Abs <sub>380nm</sub> (cm <sup>-1</sup> )	Abs <sub>500nm</sub> (cm <sup>-1</sup> )	Abs <sub>617nm</sub> (cm <sup>-1</sup> )	$C_{d,BB41}$ (mg/L)	$C_{d,BY28}$ (mg/L)	$C_{d,BR18.1}$ (mg/L)
0	0.219	0.794	2.165	30.18	5.25	5.29
0.2	0.158	0.530	1.934	26.97	1.87	2.94
0.5	0.120	0.384	1.699	23.68	0.82	1.69
0.8	0.087	0.267	1.375	19.17	0.24	0.87
1	0.067	0.198	1.183	16.49	0.11	0.35

**Table C.2:** Dissolved O<sub>3</sub> concentration in liquid change at steady state

z (m)	V <sub>sample</sub> (mL)	Abs <sub>Ind</sub> (cm <sup>-1</sup> )	$C_{O_3,L} \times 10^3$ (mmol/L)
0			0
0.2	10	0.341	42.5
0.5	14	0.287	64.9
0.8	12	0.240	65.2
1	11	0.214	67.4

**Table C.3:** TOC and COD change at steady state

z (m)	TOC (mg/L)	COD (mg/L)
0	20.73	58
0.2	20.01	54
0.5	19.23	51
0.8	18.59	47
1	17.55	44

**Experiment:**

Conditions: pH=4,  $Q_G=170$  L/h,  $Q_L=150$  L/h,  $t=20$  min,  $COD_{in}=120$  mg/L,  $C_{d,in,BB41} = 60.3$  mg/L,  $C_{d,in,BR18.1} = 10.51$  mg/L,  $C_{d,in,BY28} = 10.58$ mg/L,  $C_{d,in} = 628$  Pt-Co,  $C_{O_3,G,in} = 0.9 \pm 0.1$  mmol/L gas  $TOC_{in}=43.03$  mg/L, no catalyst.

**Table C.4:** Dye concentration change at steady state

z (m)	Abs <sub>380nm</sub> (cm <sup>-1</sup> )	Abs <sub>500nm</sub> (cm <sup>-1</sup> )	Abs <sub>617nm</sub> (cm <sup>-1</sup> )	$C_{d,BB41}$ (mg/L)	$C_{d,BY28}$ (mg/L)	$C_{d,BR18.1}$ (mg/L)
0	0.438	1.588	4.330	60.36	10.51	10.58
0.2	0.351	1.189	4.007	55.85	4.50	7.18
0.5	0.271	0.875	3.660	51.02	2.15	4.18
0.8	0.212	0.656	3.181	44.33	0.68	2.49
1	0.814	2.849	2.703	37.68	0.48	32.51

**Table C.5:** Dissolved O<sub>3</sub> concentration in liquid change at steady state

z (m)	V <sub>sample</sub> (mL)	Abs <sub>Ind</sub> (cm <sup>-1</sup> )	$C_{O_3,L} \times 10^3$ (mmol/L)
0			0
0.2	15	0.738	31.8
0.5	13	0.590	45.3
0.8	18	0.620	51.2
1	12	0.399	65.3

**Table C.6:** TOC and COD change at steady state

z (m)	TOC (mg/L)	COD (mg/L)
0	43.03	118
0.2	42.14	112
0.5	40.28	106
0.8	38.76	101
1	37.19	93

**Experiment:**

Conditions: pH=4,  $Q_G=170$  L/h,  $Q_L=150$  L/h,  $t=20$  min,  $COD_{in}=180$  mg/L,  $C_{d,in,BB41} = 90.54$  mg/L,  $C_{d,in,BR18.1} = 15.76$  mg/L,  $C_{d,in,BY28} = 15.87$  mg/L,  $C_{d,in} = 942$  Pt-Co,  $C_{O_3,G,in} = 0.9 \pm 0.1$  mmol/L gas  $TOC_{in}=60.49$  mg/L, no catalyst.

**Table C.7:** Dye concentration change at steady state

z (m)	Abs <sub>380nm</sub> (cm <sup>-1</sup> )	Abs <sub>500nm</sub> (cm <sup>-1</sup> )	Abs <sub>617nm</sub> (cm <sup>-1</sup> )	$C_{d,BB41}$ (mg/L)	$C_{d,BY28}$ (mg/L)	$C_{d,BR18.1}$ (mg/L)
0	0.657	2.382	6.495	90.54	15.76	15.87
0.2	0.552	1.892	6.340	88.38	8.47	11.21
0.5	0.456	1.494	5.821	81.15	4.01	7.87
0.8	0.360	1.122	5.225	72.84	1.11	4.69
1	0.282	0.860	4.575	63.77	0.82	2.51

**Table C.8:** Dissolved O<sub>3</sub> concentration in liquid change at steady state

z (m)	V <sub>sample</sub> (mL)	Abs <sub>Ind</sub> (cm <sup>-1</sup> )	$C_{O_3,L} \times 10^3$ (mmol/L)
0			0
0.2	18	1.291	22.9
0.5	13	0.874	44.0
0.8	14	0.826	49.2
1	19	0.891	55.3

**Table C.9:** TOC and COD change at steady state

z (m)	TOC (mg/L)	COD (mg/L)
0	60.49	176
0.2	58.67	167
0.5	57.82	158
0.8	55.99	150
1	54.8	141

**Experiment:**

Conditions: pH=4,  $Q_G=170$  L/h,  $Q_L=150$  L/h,  $t=20$  min,  $COD_{in}=300$  mg/L,  $C_{d,in,BB41} = 150.9$  mg/L,  $C_{d,in,BR18.1} = 26.4$  mg/L,  $C_{d,in,BY28} = 26.2$  mg/L,  $C_{d,in} = 1570$  Pt-Co,  $C_{O_3,G,in} = 0.9 \pm 0.1$  mmol/L gas  $TOC_{in}=94.01$  mg/L, no catalyst.

**Table C.10:** Dye concentration change at steady state

$z$ (m)	Abs <sub>380nm</sub> (cm <sup>-1</sup> )	Abs <sub>500nm</sub> (cm <sup>-1</sup> )	Abs <sub>617nm</sub> (cm <sup>-1</sup> )	$C_{d,BB41}$ (mg/L)	$C_{d,BY28}$ (mg/L)	$C_{d,BR18.1}$ (mg/L)
0	1.094	3.965	10.825	150.9	26.20	26.402
0.2	0.970	3.391	10.734	149.64	18.17	20.66
0.5	0.827	2.730	10.201	142.19	7.79	15.10
0.8	0.723	2.280	9.929	138.41	2.61	10.75
1	0.677	2.122	9.465	131.94	1.90	9.69

**Table C.11:** Dissolved O<sub>3</sub> concentration in liquid change at steady state

$z$ (m)	$V_{sample}$ (mL)	Abs <sub>Ind</sub> (cm <sup>-1</sup> )	$C_{O_3,L} \times 10^3$ (mmol/L)
0			0
0.2	17	1.990	19.7
0.5	15	1.630	43.9
0.8	18	1.850	46.8
1	13	1.337	48.2

**Table C.12:** TOC and COD change at steady state

$z$ (m)	TOC (mg/L)	COD (mg/L)
0	94.01	310
0.2	92.38	298
0.5	90.24	285
0.8	88.59	273
1	87.15	261

**Experiment:**

Conditions: pH=4,  $Q_G=340$  L/h,  $Q_L=250$  L/h,  $t=20$  min,  $COD_{,in}=60$  mg/L,  $C_{d,in,BB41} = 30.18$  mg/L,  $C_{d,in,BR18.1} = 5.26$  mg/L,  $C_{d,in,BY28} = 5.29$  mg/L,  $C_{d,in} = 315$  Pt-Co,  $C_{O_3,G,in} = 0.9 \pm 0.1$  mmol/L gas  $TOC_{in}=21.42$  mg/L, no catalyst.

**Table C.13:** Dye concentration change at steady state

z (m)	Abs <sub>380nm</sub> (cm <sup>-1</sup> )	Abs <sub>500nm</sub> (cm <sup>-1</sup> )	Abs <sub>617nm</sub> (cm <sup>-1</sup> )	$C_{d,BB41}$ (mg/L)	$C_{d,BY28}$ (mg/L)	$C_{d,BR18.1}$ (mg/L)
0	0.220	0.796	2.166	30.20	5.23	5.32
0.2	0.141	0.453	1.796	25.04	0.58	2.46
0.5	0.106	0.325	1.593	22.20	0.10	1.25
0.8	0.074	0.221	1.240	17.29	0.002	0.57
1	0.057	0.165	1.075	14.99	0.000	0.14

**Table C.14:** Dissolved O<sub>3</sub> concentration in liquid change at steady state

z (m)	V <sub>sample</sub> (mL)	Abs <sub>Ind</sub> (cm <sup>-1</sup> )	$C_{O_3,L} \times 10^3$ (mmol/L)
0			0
0.2	12	0.296	63.2
0.5	13	0.208	88.4
0.8	9	0.166	98.3
1	11	0.109	109.4

**Table C.15:** TOC and COD change at steady state

z (m)	TOC (mg/L)	COD (mg/L)
0	21.42	63
0.2	20.37	59
0.5	19.03	55
0.8	17.84	50
1	16.46	46

**Experiment:**

Conditions: pH=4,  $Q_G=340$  L/h,  $Q_L=250$  L/h,  $t=20$  min,  $COD_{in}=120$  mg/L,  $C_{d,in,BB41} = 60.3$  mg/L,  $C_{d,in,BR18.1} = 10.51$  mg/L,  $C_{d,in,BY28} = 10.58$ mg/L,  $C_{d,in} = 628$  Pt-Co,  $C_{O_3,G,in} = 0.9 \pm 0.1$  mmol/L gas  $TOC_{in}=42.89$  mg/L, no catalyst.

**Table C.16:** Dye concentration change at steady state

z (m)	Abs <sub>380nm</sub> (cm <sup>-1</sup> )	Abs <sub>500nm</sub> (cm <sup>-1</sup> )	Abs <sub>617nm</sub> (cm <sup>-1</sup> )	$C_{d,BB41}$ (mg/L)	$C_{d,BY28}$ (mg/L)	$C_{d,BR18.1}$ (mg/L)
0	0.441	1.600	4.382	61.09	10.70	10.60
0.2	0.317	1.025	3.870	53.94	1.56	5.88
0.5	0.247	0.766	3.482	48.54	0.37	3.45
0.8	0.177	0.533	2.855	39.79	0.02	1.63
1	0.140	0.412	2.486	34.65	0.009	0.72

**Table C.17:** Dissolved O<sub>3</sub> concentration in liquid change at steady state

z (m)	V <sub>sample</sub> (mL)	Abs <sub>Ind</sub> (cm <sup>-1</sup> )	$C_{O_3,L} \times 10^3$ (mmol/L)
0			0
0.2	16	0.671	56.3
0.5	13	0.484	77.1
0.8	18	0.422	89.4
1	13	0.279	105.8

**Table C.18:** TOC and COD change at steady state

z (m)	TOC (mg/L)	COD (mg/L)
0	42.89	124
0.2	40.38	119
0.5	38.69	113
0.8	37.21	107
1	35.89	100

**Experiment:**

Conditions: pH=4,  $Q_G=340$  L/h,  $Q_L=250$  L/h,  $t=20$  min,  $COD_{in}=180$  mg/L,  $C_{d,in,BB41} = 90.54$  mg/L,  $C_{d,in,BR18.1} = 15.76$  mg/L,  $C_{d,in,BY28} = 15.87$  mg/L,  $C_{d,in} = 942$  Pt-Co,  $C_{O_3,G,in} = 0.9 \pm 0.1$  mmol/L gas  $TOC_{in}=61.18$  mg/L, no catalyst.

**Table C.19:** Dye concentration change at steady state

z (m)	Abs <sub>380nm</sub> (cm <sup>-1</sup> )	Abs <sub>500nm</sub> (cm <sup>-1</sup> )	Abs <sub>617nm</sub> (cm <sup>-1</sup> )	$C_{d,BB41}$ (mg/L)	$C_{d,BY28}$ (mg/L)	$C_{d,BR18.1}$ (mg/L)
0	0.656	2.377	6.499	90.59	15.83	15.79
0.2	0.522	1.717	6.219	86.69	4.04	10.06
0.5	0.435	1.373	5.777	80.52	1.10	6.96
0.8	0.332	1.009	5.063	70.58	0.06	3.72
1	0.247	0.734	4.178	58.24	0.03	1.77

**Table C.20:** Dissolved O<sub>3</sub> concentration in liquid change at steady state

z (m)	V <sub>sample</sub> (mL)	Abs <sub>Ind</sub> (cm <sup>-1</sup> )	$C_{O_3,L} \times 10^3$ (mmol/L)
0			0
0.2	11	0.819	44.2
0.5	11	0.708	72.5
0.8	11	0.602	84.9
1	10	0.463	93.3

**Table C.21:** TOC and COD change at steady state

z (m)	TOC (mg/L)	COD (mg/L)
0	61.18	188
0.2	60.20	181
0.5	58.20	174
0.8	55.76	163
1	53.56	157

**Experiment:**

Conditions: pH=4,  $Q_G=340$  L/h,  $Q_L=250$  L/h,  $t=20$  min,  $COD_{in}=300$  mg/L,  $C_{d,in,BB41} = 150.9$  mg/L,  $C_{d,in,BR18.1} = 26.4$  mg/L,  $C_{d,in,BY28} = 26.2$  mg/L,  $C_{d,in} = 1570$  Pt-Co,  $C_{O_3,G,in} = 0.9 \pm 0.1$  mmol/L gas  $TOC_{in}=93.76$  mg/L, no catalyst.

**Table C.22:** Dye concentration change at steady state

$z$ (m)	Abs <sub>380nm</sub> (cm <sup>-1</sup> )	Abs <sub>500nm</sub> (cm <sup>-1</sup> )	Abs <sub>617nm</sub> (cm <sup>-1</sup> )	$C_{d,BB41}$ (mg/L)	$C_{d,BY28}$ (mg/L)	$C_{d,BR18.1}$ (mg/L)
0	1.094	3.959	10.857	151.34	25.97	26.31
0.2	0.909	3.014	10.465	145.88	7.60	18.41
0.5	0.760	2.422	9.986	139.19	3.19	12.41
0.8	0.665	2.071	9.332	130.09	1.15	9.43
1	0.609	1.867	9.060	126.29	0.43	7.39

**Table C.23:** Dissolved O<sub>3</sub> concentration in liquid change at steady state

$z$ (m)	$V_{sample}$ (mL)	Abs <sub>Ind</sub> (cm <sup>-1</sup> )	$C_{O_3,L} \times 10^3$ (mmol/L)
0			0
0.2	18	1.994	33.8
0.5	10	1.147	42.2
0.8	11	1.151	49.1
1	14	1.343	56.2

**Table C.24:** TOC and COD change at steady state

$z$ (m)	TOC (mg/L)	COD (mg/L)
0	93.76	307
0.2	92.25	299
0.5	90.87	289
0.8	89.28	281
1	87.33	274

**Experiment:**

Conditions: pH=10,  $Q_G=340$  L/h,  $Q_L=250$  L/h,  $t=20$  min,  $COD_{,in}=180$  mg/L,  $C_{d,in,BB41} = 90.54$  mg/L,  $C_{d,in,BR18.1} = 15.76$  mg/L,  $C_{d,in,BY28} = 15.87$  mg/L,  $C_{d,in} = 945$  Pt-Co,  $C_{O_3,G,in} = 0.9 \pm 0.1$  mmol/L gas  $TOC_{in}=52.50$  mg/L, no catalyst.

**Table C.25:** Dye concentration change at steady state

z (m)	Abs <sub>380nm</sub> (cm <sup>-1</sup> )	Abs <sub>500nm</sub> (cm <sup>-1</sup> )	Abs <sub>617nm</sub> (cm <sup>-1</sup> )	$C_{d,BB41}$ (mg/L)	$C_{d,BY28}$ (mg/L)	$C_{d,BR18.1}$ (mg/L)
0	0.640	2.320	6.450	89.91	15.68	15.15
0.2	0.406	1.379	5.679	79.17	7.86	5.81
0.5	0.308	0.984	5.210	72.63	4.09	2.25
0.8	0.233	0.709	4.426	61.70	2.19	0.51
1	0.189	0.567	3.700	51.58	1.40	0.17

**Table C.26:** Dissolved O<sub>3</sub> concentration in liquid change at steady state

z (m)	V <sub>sample</sub> (mL)	Abs <sub>Ind</sub> (cm <sup>-1</sup> )	$C_{O_3,L} \times 10^3$ (mmol/L)
0			0
0.2	15	0.959	41.5
0.5	13	0.742	64.3
0.8	12	0.570	80.3
1	14	0.516	83.4

**Table C.27:** TOC and COD change at steady state

z (m)	TOC (mg/L)	COD (mg/L)
0	52.50	191
0.2	50.67	180
0.5	48.51	173
0.8	46.55	161
1	44.97	158

**Experiment:**

Conditions: pH=10,  $Q_G=340$  L/h,  $Q_L=250$  L/h,  $t=20$  min,  $COD_{in}=300$  mg/L,  $C_{d,in,BB41} = 150.9$  mg/L,  $C_{d,in,BR18.1} = 26.4$  mg/L,  $C_{d,in,BY28} = 26.2$  mg/L,  $C_{d,in} = 1570$  Pt-Co,  $C_{O_3,G,in} = 0.9 \pm 0.1$  mmol/L gas  $TOC_{in}=93.23$  mg/L, no catalyst.

**Table C.28:** Dye concentration change at steady state

$z$ (m)	Abs <sub>380nm</sub> (cm <sup>-1</sup> )	Abs <sub>500nm</sub> (cm <sup>-1</sup> )	Abs <sub>617nm</sub> (cm <sup>-1</sup> )	$C_{d,BB41}$ (mg/L)	$C_{d,BY28}$ (mg/L)	$C_{d,BR18.1}$ (mg/L)
0	1.084	3.938	10.689	149.0	26.52	26.24
0.2	0.826	2.900	9.929	138.41	18.19	15.69
0.5	0.630	2.127	9.320	129.92	12.56	7.79
0.8	0.524	1.693	8.564	119.38	7.71	4.51
1	0.459	1.459	8.220	114.58	6.80	2.25

**Table C.29:** Dissolved O<sub>3</sub> concentration in liquid change at steady state

$z$ (m)	$V_{sample}$ (mL)	Abs <sub>Ind</sub> (cm <sup>-1</sup> )	$C_{O_3,L} \times 10^3$ (mmol/L)
0			0
0.2	17	1.849	20.9
0.5	18	1.774	37.6
0.8	11	1.086	40.2
1	15	1.316	49.4

**Table C.30:** TOC and COD change at steady state

$z$ (m)	TOC (mg/L)	COD (mg/L)
0	93.23	287
0.2	90.58	279
0.5	87.85	266
0.8	84.92	258
1	83.01	251

**Experiment:**

Conditions: pH=12,  $Q_G=340$  L/h,  $Q_L=250$  L/h,  $t=20$  min,  $COD_{in}=300$  mg/L,  $C_{d,in,BB41} = 150.9$  mg/L,  $C_{d,in,BR18.1} = 26.4$  mg/L,  $C_{d,in,BY28} = 26.2$  mg/L,  $C_{d,in} = 1580$  Pt-Co,  $C_{O_3,G,in} = 0.9 \pm 0.1$  mmol/L gas  $TOC_{in}=92.36$  mg/L, no catalyst.

**Table C.31:** Dye concentration change at steady state

$z$ (m)	Abs <sub>380nm</sub> (cm <sup>-1</sup> )	Abs <sub>500nm</sub> (cm <sup>-1</sup> )	Abs <sub>617nm</sub> (cm <sup>-1</sup> )	$C_{d,BB41}$ (mg/L)	$C_{d,BY28}$ (mg/L)	$C_{d,BR18.1}$ (mg/L)
0	1.085	3.936	10.755	149.93	26.29	26.13
0.2	0.725	2.578	9.544	133.04	19.96	11.78
0.5	0.561	1.920	8.980	125.19	14.43	5.30
0.8	0.450	1.462	8.062	112.38	8.87	2.16
1	0.391	1.255	7.508	104.66	7.83	0.68

**Table C.32:** Dissolved O<sub>3</sub> concentration in liquid change at steady state

$z$ (m)	$V_{sample}$ (mL)	Abs <sub>Ind</sub> (cm <sup>-1</sup> )	$C_{O_3,L} \times 10^3$ (mmol/L)
0			0
0.2	13	1.439	13.4
0.5	12	1.260	21.0
0.8	11	1.059	27.3
1	12	1.051	34.5

**Table C.33:** TOC and COD change at steady state

$z$ (m)	TOC (mg/L)	COD (mg/L)
0	92.36	297
0.2	88.29	287
0.5	85.46	274
0.8	82.34	266
1	79.82	255

**Experiment:**

Conditions: pH=4,  $Q_G=340$  L/h,  $Q_L=250$  L/h,  $t=20$  min,  $COD_{in}=180$  mg/L,  $C_{d,in,BB41} = 90.54$  mg/L,  $C_{d,in,BR18.1} = 15.76$  mg/L,  $C_{d,in,BY28} = 15.87$  mg/L,  $C_{d,in} = 940$  Pt-Co,  $C_{O_3,G,in} = 0.9 \pm 0.1$  mmol/L gas  $TOC_{in}=59.83$  mg/L, catalyst: alumina,  $m_{cat} = 300$  g.

**Table C.34:** Dye concentration change at steady state

z (m)	Abs <sub>380nm</sub> (cm <sup>-1</sup> )	Abs <sub>500nm</sub> (cm <sup>-1</sup> )	Abs <sub>617nm</sub> (cm <sup>-1</sup> )	$C_{d,BB41}$ (mg/L)	$C_{d,BY28}$ (mg/L)	$C_{d,BR18.1}$ (mg/L)
0	0.639	2.322	6.417	89.45	16.04	15.17
0.2	0.403	1.300	5.145	71.72	2.23	6.96
0.5	0.285	0.868	4.375	60.98	0.29	3.12
0.8	0.201	0.593	3.540	49.34	0.02	1.12
1	0.165	0.476	3.233	45.07	0.002	0.15

**Table C.35:** Dissolved O<sub>3</sub> concentration in liquid change at steady state

z (m)	V <sub>sample</sub> (mL)	Abs <sub>Ind</sub> (cm <sup>-1</sup> )	$C_{O_3,L} \times 10^3$ (mmol/L)
0			0
0.2	14	0.845	38.3
0.5	15	0.730	52.7
0.8	17	0.600	68.5
1	18	0.524	80.1

**Table C.36:** TOC and COD change at steady state

z (m)	TOC (mg/L)	COD (mg/L)
0	59.83	183
0.2	56.23	169
0.5	53.24	158
0.8	50.21	147
1	47.52	136

**Experiment:**

Conditions: pH=10,  $Q_G=340$  L/h,  $Q_L=250$  L/h,  $t=20$  min,  $COD_{,in}=180$  mg/L,  $C_{d,in,BB41} = 90.54$  mg/L,  $C_{d,in,BR18.1} = 15.76$  mg/L,  $C_{d,in,BY28} = 15.87$  mg/L,  $C_{d,in} = 940$  Pt-Co,  $C_{O_3,G,in} = 0.9 \pm 0.1$  mmol/L gas  $TOC_{in}=62.10$  mg/L, catalyst: alumina,  $m_{cat} = 300$  g.

**Table C.37:** Dye concentration change at steady state

z (m)	Abs <sub>380nm</sub> (cm <sup>-1</sup> )	Abs <sub>500nm</sub> (cm <sup>-1</sup> )	Abs <sub>617nm</sub> (cm <sup>-1</sup> )	$C_{d,BB41}$ (mg/L)	$C_{d,BY28}$ (mg/L)	$C_{d,BR18.1}$ (mg/L)
0	0.646	2.336	6.468	90.17	15.24	15.42
0.2	0.285	0.931	4.604	64.17	4.69	2.58
0.5	0.208	0.630	3.870	53.96	1.50	0.66
0.8	0.153	0.456	2.970	41.40	0.95	0.18
1	0.133	0.385	2.648	36.91	0.17	0.02

**Table C.38:** Dissolved O<sub>3</sub> concentration in liquid change at steady state

z (m)	V <sub>sample</sub> (mL)	Abs <sub>Ind</sub> (cm <sup>-1</sup> )	$C_{O_3,L} \times 10^3$ (mmol/L)
0			0
0.2	18	0.953	29.9
0.5	13	0.642	36.0
0.8	18	0.605	44.7
1	12	0.412	57.3

**Table C.39:** TOC and COD change at steady state

z (m)	TOC (mg/L)	COD (mg/L)
0	62.1	175
0.2	57.23	162
0.5	53.26	148
0.8	49.45	134
1	45.61	121

**Experiment:**

Conditions: pH=4,  $Q_G=340$  L/h,  $Q_L=250$  L/h,  $t=20$  min,  $COD_{in}=300$  mg/L,  $C_{d,in,BB41} = 150.9$  mg/L,  $C_{d,in,BR18.1} = 26.4$  mg/L,  $C_{d,in,BY28} = 26.2$  mg/L,  $C_{d,in} = 1570$  Pt-Co,  $C_{O_3,G,in} = 0.9 \pm 0.1$  mmol/L gas  $TOC_{in}=92.35$  mg/L, catalyst: alumina,  $m_{cat} = 300$  g.

**Table C.40:** Dye concentration change at steady state

z (m)	Abs <sub>380nm</sub> (cm <sup>-1</sup> )	Abs <sub>500nm</sub> (cm <sup>-1</sup> )	Abs <sub>617nm</sub> (cm <sup>-1</sup> )	$C_{d,BB41}$ (mg/L)	$C_{d,BY28}$ (mg/L)	$C_{d,BR18.1}$ (mg/L)
0	1.094	3.962	10.830	150.97	26.03	26.39
0.2	0.804	2.621	9.591	133.71	4.67	15.48
0.5	0.639	1.995	8.597	119.85	0.66	9.93
0.8	0.516	1.562	8.104	112.96	0.14	5.24
1	0.454	1.357	7.504	104.61	0.004	3.69

**Table C.41:** Dissolved O<sub>3</sub> concentration in liquid change at steady state

z (m)	V <sub>sample</sub> (mL)	Abs <sub>Ind</sub> (cm <sup>-1</sup> )	$C_{O_3,L} \times 10^3$ (mmol/L)
0			0
0.2	11	1.234	24.4
0.5	12	1.192	30.0
0.8	11	1.036	39.9
1	11	0.948	49.7

**Table C.42:** TOC and COD change at steady state

z (m)	TOC (mg/L)	COD (mg/L)
0	92.35	301
0.2	88.49	290
0.5	85.34	272
0.8	81.23	253
1	77.86	238

**Experiment:**

Conditions: pH=10,  $Q_G=340$  L/h,  $Q_L=250$  L/h,  $t=20$  min,  $COD_{in}=300$  mg/L,  $C_{d,in,BB41} = 150.9$  mg/L,  $C_{d,in,BR18.1} = 26.4$  mg/L,  $C_{d,in,BY28} = 26.2$  mg/L,  $C_{d,in} = 1570$  Pt-Co,  $C_{O_3,G,in} = 0.9 \pm 0.1$  mmol/L gas  $TOC_{in}=93.45$  mg/L, catalyst: alumina,  $m_{cat} = 300$  g.

**Table C.43:** Dye concentration change at steady state

$z$ (m)	Abs <sub>380nm</sub> (cm <sup>-1</sup> )	Abs <sub>500nm</sub> (cm <sup>-1</sup> )	Abs <sub>617nm</sub> (cm <sup>-1</sup> )	$C_{d,BB41}$ (mg/L)	$C_{d,BY28}$ (mg/L)	$C_{d,BR18.1}$ (mg/L)
0	1.072	3.877	10.847	151.21	25.83	25.28
0.2	0.621	2.117	8.627	120.27	12.44	9.00
0.5	0.491	1.586	7.912	110.29	6.85	4.51
0.8	0.383	1.185	7.032	98.02	4.20	1.43
1	0.320	0.973	6.248	87.10	3.38	0.29

**Table C.44:** Dissolved O<sub>3</sub> concentration in liquid change at steady state

$z$ (m)	$V_{sample}$ (mL)	Abs <sub>Ind</sub> (cm <sup>-1</sup> )	$C_{O_3,L} \times 10^3$ (mmol/L)
0			0
0.2	12	1.235	13.8
0.5	13	1.205	21.4
0.8	13	1.075	27.6
1	15	1.064	35.1

**Table C.45:** TOC and COD change at steady state

$z$ (m)	TOC (mg/L)	COD (mg/L)
0	93.45	273
0.2	89.17	257
0.5	85.67	241
0.8	81.23	226
1	77.55	211

**Experiment:**

Conditions: pH=4,  $Q_G=340$  L/h,  $Q_L=250$  L/h,  $t=20$  min,  $COD_{in}=180$  mg/L,  $C_{d,in,BB41} = 90.54$  mg/L,  $C_{d,in,BR18.1} = 15.76$  mg/L,  $C_{d,in,BY28} = 15.87$  mg/L,  $C_{d,in} = 943$  Pt-Co,  $C_{O_3,G,in} = 0.9 \pm 0.1$  mmol/L gas  $TOC_{in}=60.92$  mg/L, catalyst: PFOA,  $m_{cat} = 300$  g.

**Table C.46:** Dye concentration change at steady state

z (m)	Abs <sub>380nm</sub> (cm <sup>-1</sup> )	Abs <sub>500nm</sub> (cm <sup>-1</sup> )	Abs <sub>617nm</sub> (cm <sup>-1</sup> )	$C_{d,BB41}$ (mg/L)	$C_{d,BY28}$ (mg/L)	$C_{d,BR18.1}$ (mg/L)
0	0.647	2.361	6.543	91.21	16.83	15.28
0.2	0.370	1.174	5.050	70.40	1.58	5.61
0.5	0.258	0.781	4.093	57.05	0.15	2.53
0.8	0.195	0.571	3.521	49.09	0.02	0.86
1	0.162	0.466	3.175	44.26	0.00	0.14

**Table C.47:** Dissolved O<sub>3</sub> concentration in liquid change at steady state

z (m)	V <sub>sample</sub> (mL)	Abs <sub>Ind</sub> (cm <sup>-1</sup> )	$C_{O_3,L} \times 10^3$ (mmol/L)
0			0
0.2	19	1.031	42.1
0.5	9	0.500	55.9
0.8	12	0.479	73.1
1	11	0.389	87.0

**Table C.48:** TOC and COD change at steady state

z (m)	TOC (mg/L)	COD (mg/L)
0	60.92	183
0.2	57.72	165
0.5	54.19	154
0.8	50.54	143
1	46.91	132

**Experiment:**

Conditions: pH=10,  $Q_G=340$  L/h,  $Q_L=250$  L/h,  $t=20$  min,  $COD_{in}=180$  mg/L,  $C_{d,in,BB41} = 90.54$  mg/L,  $C_{d,in,BR18.1} = 15.76$  mg/L,  $C_{d,in,BY28} = 15.87$  mg/L,  $C_{d,in} = 944$  Pt-Co,  $C_{O_3,G,in} = 0.9 \pm 0.1$  mmol/L gas  $TOC_{in}=61.04$  mg/L, catalyst: PFOA,  $m_{cat} = 300$  g.

**Table C.49:** Dye concentration change at steady state

$z$ (m)	Abs <sub>380nm</sub> (cm <sup>-1</sup> )	Abs <sub>500nm</sub> (cm <sup>-1</sup> )	Abs <sub>617nm</sub> (cm <sup>-1</sup> )	$C_{d,BB41}$ (mg/L)	$C_{d,BY28}$ (mg/L)	$C_{d,BR18.1}$ (mg/L)
0	0.656	2.372	6.496	90.55	15.28	15.84
0.2	0.325	1.071	4.866	67.84	5.05	3.86
0.5	0.238	0.733	4.239	59.09	1.98	1.23
0.8	0.170	0.510	3.237	45.12	1.13	0.36
1	0.154	0.454	3.047	42.47	0.67	0.07

**Table C.50:** Dissolved O<sub>3</sub> concentration in liquid change at steady state

$z$ (m)	$V_{sample}$ (mL)	Abs <sub>Ind</sub> (cm <sup>-1</sup> )	$C_{O_3,L} \times 10^3$ (mmol/L)
0			0
0.2	13	0.764	38.8
0.5	13	0.667	44.6
0.8	15	0.546	57.0
1	12	0.426	71.4

**Table C.51:** TOC and COD change at steady state

$z$ (m)	TOC (mg/L)	COD (mg/L)
0	61.04	176
0.2	56.73	163
0.5	52.01	151
0.8	49.56	139
1	46.88	127

**Experiment:**

Conditions: pH=4,  $Q_G=340$  L/h,  $Q_L=250$  L/h,  $t=20$  min,  $COD_{in}=300$  mg/L,  $C_{d,in,BB41} = 150.9$  mg/L,  $C_{d,in,BR18.1} = 26.4$  mg/L,  $C_{d,in,BY28} = 26.2$  mg/L,  $C_{d,in} = 1570$  Pt-Co,  $C_{O_3,G,in} = 0.9 \pm 0.1$  mmol/L gas  $TOC_{in}=91.24$  mg/L, catalyst: PFOA,  $m_{cat} = 300$  g.

**Table C.52:** Dye concentration change at steady state

$z$ (m)	Abs <sub>380nm</sub> (cm <sup>-1</sup> )	Abs <sub>500nm</sub> (cm <sup>-1</sup> )	Abs <sub>617nm</sub> (cm <sup>-1</sup> )	$C_{d,BB41}$ (mg/L)	$C_{d,BY28}$ (mg/L)	$C_{d,BR18.1}$ (mg/L)
0	1.085	3.937	10.826	150.91	26.43	25.98
0.2	0.749	2.404	9.154	127.61	2.58	13.88
0.5	0.572	1.759	8.318	115.95	0.26	7.42
0.8	0.461	1.380	7.607	106.04	0.12	3.78
1	0.407	1.207	7.027	97.95	0.003	2.62

**Table C.53:** Dissolved O<sub>3</sub> concentration in liquid change at steady state

$z$ (m)	$V_{sample}$ (mL)	Abs <sub>Ind</sub> (cm <sup>-1</sup> )	$C_{O_3,L} \times 10^3$ (mmol/L)
0			0
0.2	12	1.267	26.8
0.5	11	1.072	34.2
0.8	12	1.035	45.6
1	14	1.066	53.5

**Table C.54:** TOC and COD change at steady state

$z$ (m)	TOC (mg/L)	COD (mg/L)
0	91.24	291
0.2	87.71	274
0.5	84.22	261
0.8	80.78	245
1	77.26	230

**Experiment:**

Conditions: pH=10,  $Q_G=340$  L/h,  $Q_L=250$  L/h,  $t=20$  min,  $COD_{in}=300$  mg/L,  $C_{d,in,BB41} = 150.9$  mg/L,  $C_{d,in,BR18.1} = 26.4$  mg/L,  $C_{d,in,BY28} = 26.2$  mg/L,  $C_{d,in} = 1570$  Pt-Co,  $C_{O_3,G,in} = 0.9 \pm 0.1$  mmol/L gas  $TOC_{in}=92.86$  mg/L, catalyst: PFOA,  $m_{cat} = 300$  g.

**Table C.55:** Dye concentration change at steady state

z (m)	Abs <sub>380nm</sub> (cm <sup>-1</sup> )	Abs <sub>500nm</sub> (cm <sup>-1</sup> )	Abs <sub>617nm</sub> (cm <sup>-1</sup> )	$C_{d,BB41}$ (mg/L)	$C_{d,BY28}$ (mg/L)	$C_{d,BR18.1}$ (mg/L)
0	1.090	3.941	10.836	151.05	25.69	26.17
0.2	0.703	2.427	8.934	124.55	13.85	12.23
0.5	0.539	1.771	8.195	114.23	8.23	6.13
0.8	0.422	1.328	7.470	104.14	5.39	2.24
1	0.356	1.100	6.716	93.63	4.25	0.89

**Table C.56:** Dissolved O<sub>3</sub> concentration in liquid change at steady state

z (m)	V <sub>sample</sub> (mL)	Abs <sub>Ind</sub> (cm <sup>-1</sup> )	$C_{O_3,L} \times 10^3$ (mmol/L)
0			0
0.2	15	1.519	17.8
0.5	11	1.071	28.6
0.8	10	0.914	32.8
1	10	0.824	40.1

**Table C.57:** TOC and COD change at steady state

z (m)	TOC (mg/L)	COD (mg/L)
0	92.86	305
0.2	88.37	286
0.5	85.64	269
0.8	82.13	252
1	77.05	236

**Experiment:**

Conditions: pH=12,  $Q_G=340$  L/h,  $Q_L=250$  L/h,  $t=20$  min,  $COD_{in}=300$  mg/L,  $C_{d,in,BB41} = 150.9$  mg/L,  $C_{d,in,BR18.1} = 26.4$  mg/L,  $C_{d,in,BY28} = 26.2$  mg/L,  $C_{d,in} = 1570$  Pt-Co,  $C_{O_3,G,in} = 0.9 \pm 0.1$  mmol/L gas  $TOC_{in}=91.24$  mg/L, catalyst: alumina,  $m_{cat} = 300$  g.

**Table C.58:** Dye concentration change at steady state

$z$ (m)	Abs <sub>380nm</sub> (cm <sup>-1</sup> )	Abs <sub>500nm</sub> (cm <sup>-1</sup> )	Abs <sub>617nm</sub> (cm <sup>-1</sup> )	$C_{d,BB41}$ (mg/L)	$C_{d,BY28}$ (mg/L)	$C_{d,BR18.1}$ (mg/L)
0	1.104	3.998	10.849	151.23	25.98	26.8
0.2	0.579	2.016	8.328	116.09	14.90	7.71
0.5	0.452	1.514	7.460	103.99	10.17	3.72
0.8	0.339	1.086	6.344	88.43	6.23	1.00
1	0.286	0.896	5.588	77.90	4.58	0.27

**Table C.59:** Dissolved O<sub>3</sub> concentration in liquid change at steady state

$z$ (m)	$V_{sample}$ (mL)	Abs <sub>Ind</sub> (cm <sup>-1</sup> )	$C_{O_3,L} \times 10^3$ (mmol/L)
0			0
0.2	10	1.049	8.4
0.5	11	1.023	13.8
0.8	12	0.947	19.5
1	11	0.796	23.4

**Table C.60:** TOC and COD change at steady state

$z$ (m)	TOC (mg/L)	COD (mg/L)
0	91.24	307
0.2	86.04	281
0.5	79.92	263
0.8	74.52	239
1	68.99	217

**Experiment:**

Conditions: pH=12,  $Q_G=340$  L/h,  $Q_L=250$  L/h,  $t=20$  min,  $COD_{in}=300$  mg/L,  $C_{d,in,BB41} = 150.9$  mg/L,  $C_{d,in,BR18.1} = 26.4$  mg/L,  $C_{d,in,BY28} = 26.2$  mg/L,  $C_{d,in} = 1570$  Pt-Co,  $C_{O_3,G,in} = 0.9 \pm 0.1$  mmol/L gas  $TOC_{in}=90.91$  mg/L, catalyst: PFOA,  $m_{cat} = 300$  g.

**Table C.61:** Dye concentration change at steady state

$z$ (m)	Abs <sub>380nm</sub> (cm <sup>-1</sup> )	Abs <sub>500nm</sub> (cm <sup>-1</sup> )	Abs <sub>617nm</sub> (cm <sup>-1</sup> )	$C_{d,BB41}$ (mg/L)	$C_{d,BY28}$ (mg/L)	$C_{d,BR18.1}$ (mg/L)
0	1.086	3.938	10.777	150.23	26.24	26.13
0.2	0.631	2.237	8.604	119.94	17.68	9.54
0.5	0.496	1.692	7.851	109.44	12.21	4.90
0.8	0.382	1.250	6.997	97.54	8.36	1.48
1	0.316	1.019	6.090	84.89	6.75	0.49

**Table C.62:** Dissolved O<sub>3</sub> concentration in liquid change at steady state

$z$ (m)	$V_{sample}$ (mL)	Abs <sub>Ind</sub> (cm <sup>-1</sup> )	$C_{O_3,L} \times 10^3$ (mmol/L)
0			0
0.2	11	1.156	10.4
0.5	10	0.987	15.3
0.8	12	1.019	22.3
1	13	0.947	29.5

**Table C.63:** TOC and COD change at steady state

$z$ (m)	TOC (mg/L)	COD (mg/L)
0	90.91	304
0.2	86.39	285
0.5	81.86	266
0.8	77.02	246
1	72.29	227

**Experiment:**

Conditions: pH=4,  $Q_G=340$  L/h,  $Q_L=250$  L/h,  $t=20$  min,  $COD_{in}=180$  mg/L,  $C_{d,in,BB41} = 90.54$  mg/L,  $C_{d,in,BR18.1} = 15.76$  mg/L,  $C_{d,in,BY28} = 15.87$  mg/L,  $C_{d,in} = 945$  Pt-Co,  $C_{O_3,G,in} = 0.9 \pm 0.1$  mmol/L gas  $TOC_{in}=62.95$  mg/L, catalyst: alumina,  $m_{cat} = 150$  g.

**Table C.64:** Dye concentration change at steady state

z (m)	Abs <sub>380nm</sub> (cm <sup>-1</sup> )	Abs <sub>500nm</sub> (cm <sup>-1</sup> )	Abs <sub>617nm</sub> (cm <sup>-1</sup> )	$C_{d,BB41}$ (mg/L)	$C_{d,BY28}$ (mg/L)	$C_{d,BR18.1}$ (mg/L)
0	0.642	2.311	6.545	91.24	14.92	15.01
0.2	0.467	1.520	5.696	79.41	2.96	8.68
0.5	0.395	1.241	5.196	72.43	0.55	6.44
0.8	0.285	0.863	4.475	62.38	0.05	2.91
1	0.234	0.695	4.057	56.55	0.03	1.48

**Table C.65:** Dissolved O<sub>3</sub> concentration in liquid change at steady state

z (m)	V <sub>sample</sub> (mL)	Abs <sub>Ind</sub> (cm <sup>-1</sup> )	$C_{O_3,L} \times 10^3$ (mmol/L)
0			0
0.2	10	0.722	40.1
0.5	11	0.674	58.9
0.8	19	0.795	75.1
1	13	0.530	88.1

**Table C.66:** TOC and COD change at steady state

z (m)	TOC (mg/L)	COD (mg/L)
0	62.95	183
0.2	60.45	173
0.5	58.21	165
0.8	56.04	158
1	53.82	150

**Experiment:**

Conditions: pH=10,  $Q_G=340$  L/h,  $Q_L=250$  L/h,  $t=20$  min,  $COD_{,in}=180$  mg/L,  $C_{d,in,BB41} = 90.54$  mg/L,  $C_{d,in,BR18.1} = 15.76$  mg/L,  $C_{d,in,BY28} = 15.87$  mg/L,  $C_{d,in} = 945$  Pt-Co,  $C_{O_3,G,in} = 0.9 \pm 0.1$  mmol/L gas  $TOC_{in}=63.07$  mg/L, catalyst: alumina,  $m_{cat} = 150$  g.

**Table C.67:** Dye concentration change at steady state

z (m)	Abs <sub>380nm</sub> (cm <sup>-1</sup> )	Abs <sub>500nm</sub> (cm <sup>-1</sup> )	Abs <sub>617nm</sub> (cm <sup>-1</sup> )	$C_{d,BB41}$ (mg/L)	$C_{d,BY28}$ (mg/L)	$C_{d,BR18.1}$ (mg/L)
0	0.655	2.366	6.471	90.21	15.27	15.81
0.2	0.360	1.216	5.108	71.21	6.76	4.96
0.5	0.236	0.743	4.221	58.84	3.08	1.16
0.8	0.188	0.568	3.500	48.79	1.19	0.60
1	0.162	0.476	3.180	44.3	0.63	0.12

**Table C.68:** Dissolved O<sub>3</sub> concentration in liquid change at steady state

z (m)	V <sub>sample</sub> (mL)	Abs <sub>Ind</sub> (cm <sup>-1</sup> )	$C_{O_3,L} \times 10^3$ (mmol/L)
0			0
0.2	11	0.721	33.5
0.5	10	0.570	42.1
0.8	13	0.541	56.1
1	11	0.436	66.3

**Table C.69:** TOC and COD change at steady state

z (m)	TOC (mg/L)	COD (mg/L)
0	63.07	179
0.2	59.02	168
0.5	55.92	158
0.8	52.36	147
1	49.87	136

**Experiment:**

Conditions: pH=4,  $Q_G=340$  L/h,  $Q_L=250$  L/h,  $t=20$  min,  $COD_{in}=300$  mg/L,  $C_{d,in,BB41} = 150.9$  mg/L,  $C_{d,in,BR18.1} = 26.4$  mg/L,  $C_{d,in,BY28} = 26.2$  mg/L,  $C_{d,in} = 1570$  Pt-Co,  $C_{O_3,G,in} = 0.9 \pm 0.1$  mmol/L gas  $TOC_{in}=91.23$  mg/L, catalyst: alumina,  $m_{cat} = 150$  g.

**Table C.70:** Dye concentration change at steady state

z (m)	Abs <sub>380nm</sub> (cm <sup>-1</sup> )	Abs <sub>500nm</sub> (cm <sup>-1</sup> )	Abs <sub>617nm</sub> (cm <sup>-1</sup> )	$C_{d,BB41}$ (mg/L)	$C_{d,BY28}$ (mg/L)	$C_{d,BR18.1}$ (mg/L)
0	1.083	3.932	10.854	151.31	26.81	25.78
0.2	0.873	2.886	10.183	141.96	7.17	17.35
0.5	0.717	2.269	9.435	131.50	2.05	11.68
0.8	0.604	1.868	8.606	119.91	0.67	8.23
1	0.580	1.772	8.781	122.41	0.39	6.68

**Table C.71:** Dissolved O<sub>3</sub> concentration in liquid change at steady state

z (m)	V <sub>sample</sub> (mL)	Abs <sub>Ind</sub> (cm <sup>-1</sup> )	$C_{O_3,L} \times 10^3$ (mmol/L)
0			0
0.2	12	1.387	28.1
0.5	13	1.375	32.5
0.8	15	1.391	44.1
1	17	1.544	53.1

**Table C.72:** TOC and COD change at steady state

z (m)	TOC (mg/L)	COD (mg/L)
0	91.23	303
0.2	89.45	293
0.5	87.13	284
0.8	85.52	273
1	83.84	264

**Experiment:**

Conditions: pH=10,  $Q_G=340$  L/h,  $Q_L=250$  L/h,  $t=20$  min,  $COD_{in}=300$  mg/L,  $C_{d,in,BB41} = 150.9$  mg/L,  $C_{d,in,BR18.1} = 26.4$  mg/L,  $C_{d,in,BY28} = 26.2$  mg/L,  $C_{d,in} = 1570$  Pt-Co,  $C_{O_3,G,in} = 0.9 \pm 0.1$  mmol/L gas  $TOC_{in}=92.04$  mg/L, catalyst: alumina,  $m_{cat} = 150$  g.

**Table C.73:** Dye concentration change at steady state

z (m)	Abs <sub>380nm</sub> (cm <sup>-1</sup> )	Abs <sub>500nm</sub> (cm <sup>-1</sup> )	Abs <sub>617nm</sub> (cm <sup>-1</sup> )	$C_{d,BB41}$ (mg/L)	$C_{d,BY28}$ (mg/L)	$C_{d,BR18.1}$ (mg/L)
0	1.084	3.926	10.819	150.81	26.14	25.92
0.2	0.745	2.595	9.148	127.53	15.43	13.72
0.5	0.558	1.858	8.471	118.08	10.12	6.36
0.8	0.444	1.413	7.784	108.50	6.41	2.55
1	0.384	1.200	7.129	99.39	4.98	1.28

**Table C.74:** Dissolved O<sub>3</sub> concentration in liquid change at steady state

z (m)	V <sub>sample</sub> (mL)	Abs <sub>Ind</sub> (cm <sup>-1</sup> )	$C_{O_3,L} \times 10^3$ (mmol/L)
0			0
0.2	11	1.204	16.1
0.5	10	1.031	24.4
0.8	11	1.016	33.0
1	12	0.989	41.3

**Table C.75:** TOC and COD change at steady state

z (m)	TOC (mg/L)	COD (mg/L)
0	92.04	294
0.2	89.23	278
0.5	85.78	263
0.8	82.45	248
1	79.14	233

**Experiment:**

Conditions: pH=4,  $Q_G=340$  L/h,  $Q_L=250$  L/h,  $t=20$  min,  $COD_{in}=180$  mg/L,  $C_{d,in,BB41} = 90.54$  mg/L,  $C_{d,in,BR18.1} = 15.76$  mg/L,  $C_{d,in,BY28} = 15.87$  mg/L,  $C_{d,in} = 945$  Pt-Co,  $C_{O_3,G,in} = 0.9 \pm 0.1$  mmol/L gas  $TOC_{in}=62.12$  mg/L, catalyst: PFOA,  $m_{cat} = 150$  g.

**Table C.76:** Dye concentration change at steady state

z (m)	Abs <sub>380nm</sub> (cm <sup>-1</sup> )	Abs <sub>500nm</sub> (cm <sup>-1</sup> )	Abs <sub>617nm</sub> (cm <sup>-1</sup> )	$C_{d,BB41}$ (mg/L)	$C_{d,BY28}$ (mg/L)	$C_{d,BR18.1}$ (mg/L)
0	0.661	2.400	6.538	91.14	16.12	15.96
0.2	0.458	1.492	5.494	76.58	2.69	8.74
0.5	0.343	1.059	4.987	69.52	0.45	4.44
0.8	0.232	0.689	3.949	55.04	0.03	1.61
1	0.194	0.562	3.726	51.94	0.03	0.35

**Table C.77:** Dissolved O<sub>3</sub> concentration in liquid change at steady state

z (m)	V <sub>sample</sub> (mL)	Abs <sub>Ind</sub> (cm <sup>-1</sup> )	$C_{O_3,L} \times 10^3$ (mmol/L)
0			0
0.2	10	0.694	43.7
0.5	12	0.677	64.0
0.8	10	0.471	77.9
1	12	0.475	84.9

**Table C.78:** TOC and COD change at steady state

z (m)	TOC (mg/L)	COD (mg/L)
0	62.12	184
0.2	59.51	177
0.5	56.84	165
0.8	54.13	156
1	51.48	147

**Experiment:**

Conditions: pH=10,  $Q_G=340$  L/h,  $Q_L=250$  L/h,  $t=20$  min,  $COD_{in}=180$  mg/L,  $C_{d,in, BB41} = 90.54$  mg/L,  $C_{d,in, BR18.1} = 15.76$  mg/L,  $C_{d,in, BY28} = 15.87$  mg/L,  $C_{d,in} = 945$  Pt-Co,  $C_{O_3,G,in} = 0.9 \pm 0.1$  mmol/L gas  $TOC_{in}=62.23$  mg/L, catalyst: PFOA,  $m_{cat} = 150$  g.

**Table C.79:** Dye concentration change at steady state

$z$ (m)	Abs <sub>380nm</sub> (cm <sup>-1</sup> )	Abs <sub>500nm</sub> (cm <sup>-1</sup> )	Abs <sub>617nm</sub> (cm <sup>-1</sup> )	$C_{d, BB41}$ (mg/L)	$C_{d, BY28}$ (mg/L)	$C_{d, BR18.1}$ (mg/L)
0	0.644	2.337	6.474	90.25	15.88	15.29
0.2	0.388	1.324	5.192	72.37	7.45	6.09
0.5	0.273	0.873	4.492	62.62	3.55	2.26
0.8	0.200	0.610	3.709	51.71	1.76	0.65
1	0.178	0.530	3.491	48.67	1.14	0.13

**Table C.80:** Dissolved O<sub>3</sub> concentration in liquid change at steady state

$z$ (m)	$V_{sample}$ (mL)	Abs <sub>Ind</sub> (cm <sup>-1</sup> )	$C_{O_3,L} \times 10^3$ (mmol/L)
0			0
0.2	11	0.717	39.1
0.5	12	0.648	51.2
0.8	13	0.535	68.8
1	11	0.452	74.6

**Table C.81:** TOC and COD change at steady state

$z$ (m)	TOC (mg/L)	COD (mg/L)
0	61.23	177
0.2	58.14	168
0.5	55.63	160
0.8	52.35	150
1	49.68	141

**Experiment:**

Conditions: pH=4,  $Q_G=340$  L/h,  $Q_L=250$  L/h,  $t=20$  min,  $COD_{in}=300$  mg/L,  $C_{d,in,BB41} = 150.9$  mg/L,  $C_{d,in,BR18.1} = 26.4$  mg/L,  $C_{d,in,BY28} = 26.2$  mg/L,  $C_{d,in} = 1570$  Pt-Co,  $C_{O_3,G,in} = 0.9 \pm 0.1$  mmol/L gas  $TOC_{in}=91.23$  mg/L, catalyst: PFOA,  $m_{cat} = 150$  g.

**Table C.82:** Dye concentration change at steady state

z (m)	Abs <sub>380nm</sub> (cm <sup>-1</sup> )	Abs <sub>500nm</sub> (cm <sup>-1</sup> )	Abs <sub>617nm</sub> (cm <sup>-1</sup> )	$C_{d,BB41}$ (mg/L)	$C_{d,BY28}$ (mg/L)	$C_{d,BR18.1}$ (mg/L)
0	1.103	3.996	10.839	151.09	26.08	26.81
0.2	0.847	2.781	9.774	136.24	5.50	17.08
0.5	0.680	2.130	9.107	126.94	1.04	10.68
0.8	0.558	1.714	8.258	115.12	0.54	6.88
1	0.500	1.501	8.282	115.45	0.27	4.06

**Table C.83:** Dissolved O<sub>3</sub> concentration in liquid change at steady state

z (m)	V <sub>sample</sub> (mL)	Abs <sub>Ind</sub> (cm <sup>-1</sup> )	$C_{O_3,L} \times 10^3$ (mmol/L)
0			0
0.2	12	1.331	30.9
0.5	13	1.318	37.7
0.8	11	1.037	46.9
1	14	1.235	55.6

**Table C.84:** TOC and COD change at steady state

z (m)	TOC (mg/L)	COD (mg/L)
0	91.23	298
0.2	88.83	288
0.5	86.67	279
0.8	84.43	268
1	82.21	259

**Experiment:**

Conditions: pH=10,  $Q_G=340$  L/h,  $Q_L=250$  L/h,  $t=20$  min,  $COD_{in}=300$  mg/L,  $C_{d,in,BB41} = 150.9$  mg/L,  $C_{d,in,BR18.1} = 26.4$  mg/L,  $C_{d,in,BY28} = 26.2$  mg/L,  $C_{d,in} = 1570$  Pt-Co,  $C_{O_3,G,in} = 0.9 \pm 0.1$  mmol/L gas  $TOC_{in}=90.45$  mg/L, catalyst: PFOA,  $m_{cat} = 150$  g.

**Table C.85:** Dye concentration change at steady state

z (m)	Abs <sub>380nm</sub> (cm <sup>-1</sup> )	Abs <sub>500nm</sub> (cm <sup>-1</sup> )	Abs <sub>617nm</sub> (cm <sup>-1</sup> )	$C_{d,BB41}$ (mg/L)	$C_{d,BY28}$ (mg/L)	$C_{d,BR18.1}$ (mg/L)
0	1.091	3.943	10.826	150.92	25.67	26.23
0.2	0.779	2.723	9.450	131.73	16.56	14.60
0.5	0.607	2.026	8.977	125.14	10.67	7.51
0.8	0.482	1.560	7.905	110.20	7.18	4.10
1	0.409	1.280	7.460	103.99	5.27	1.65

**Table C.86:** Dissolved O<sub>3</sub> concentration in liquid change at steady state

z (m)	V <sub>sample</sub> (mL)	Abs <sub>Ind</sub> (cm <sup>-1</sup> )	$C_{O_3,L} \times 10^3$ (mmol/L)
0			0
0.2	11	1.232	18.0
0.5	12	1.237	30.1
0.8	11	1.018	38.1
1	11	0.949	47.0

**Table C.87:** TOC and COD change at steady state

z (m)	TOC (mg/L)	COD (mg/L)
0	90.45	301
0.2	88.41	290
0.5	85.02	279
0.8	82.34	268
1	79.51	257

**Experiment:**

Conditions: pH=4,  $Q_G=340$  L/h,  $Q_L=250$  L/h,  $t=20$  min,  $COD_{in}=180$  mg/L,  $C_{d,in,BB41} = 90.54$  mg/L,  $C_{d,in,BR18.1} = 15.76$  mg/L,  $C_{d,in,BY28} = 15.87$  mg/L,  $C_{d,in} = 945$  Pt-Co,  $C_{O_3,G,in} = 0.9 \pm 0.1$  mmol/L gas  $TOC_{in}=61.34$  mg/L, catalyst: alumina,  $m_{cat} = 400$  g.

**Table C.88:** Dye concentration change at steady state

z (m)	Abs <sub>380nm</sub> (cm <sup>-1</sup> )	Abs <sub>500nm</sub> (cm <sup>-1</sup> )	Abs <sub>617nm</sub> (cm <sup>-1</sup> )	$C_{d,BB41}$ (mg/L)	$C_{d,BY28}$ (mg/L)	$C_{d,BR18.1}$ (mg/L)
0	0.645	2.348	6.531	91.04	16.57	15.19
0.2	0.438	1.422	5.392	75.17	2.61	8.02
0.5	0.342	1.070	4.635	64.60	0.46	5.26
0.8	0.242	0.729	3.905	54.43	0.03	2.21
1	0.187	0.539	3.645	50.81	0.002	0.20

**Table C.89:** Dissolved O<sub>3</sub> concentration in liquid change at steady state

z (m)	V <sub>sample</sub> (mL)	Abs <sub>Ind</sub> (cm <sup>-1</sup> )	$C_{O_3,L} \times 10^3$ (mmol/L)
0			0
0.2	10	0.711	30.5
0.5	16	0.822	47.2
0.8	13	0.577	62.3
1	12	0.493	73.2

**Table C.90:** TOC and COD change at steady state

z (m)	TOC (mg/L)	COD (mg/L)
0	61.34	186
0.2	58.87	177
0.5	56.03	166
0.8	53.42	156
1	50.2	145

**Experiment:**

Conditions: pH=10,  $Q_G=340$  L/h,  $Q_L=250$  L/h,  $t=20$  min,  $COD_{,in}=180$  mg/L,  $C_{d,in,BB41} = 90.54$  mg/L,  $C_{d,in,BR18.1} = 15.76$  mg/L,  $C_{d,in,BY28} = 15.87$  mg/L,  $C_{d,in} = 939$  Pt-Co,  $C_{O_3,G,in} = 0.9 \pm 0.1$  mmol/L gas  $TOC_{in}=62.03$  mg/L, catalyst: alumina,  $m_{cat} = 400$  g.

**Table C.91:** Dye concentration change at steady state

z (m)	Abs <sub>380nm</sub> (cm <sup>-1</sup> )	Abs <sub>500nm</sub> (cm <sup>-1</sup> )	Abs <sub>617nm</sub> (cm <sup>-1</sup> )	$C_{d,BB41}$ (mg/L)	$C_{d,BY28}$ (mg/L)	$C_{d,BR18.1}$ (mg/L)
0	0.645	2.338	6.504	90.67	15.83	15.26
0.2	0.330	1.113	4.944	68.92	6.79	3.90
0.5	0.215	0.676	3.966	55.29	3.03	0.76
0.8	0.172	0.526	3.313	46.1	1.77	0.28
1	0.147	0.443	2.882	40.17	1.28	0.11

**Table C.92:** Dissolved O<sub>3</sub> concentration in liquid change at steady state

z (m)	V <sub>sample</sub> (mL)	Abs <sub>Ind</sub> (cm <sup>-1</sup> )	$C_{O_3,L} \times 10^3$ (mmol/L)
0			0
0.2	11	0.720	25.8
0.5	12	0.631	32.1
0.8	14	0.586	39.2
1	15	0.520	48.1

**Table C.93:** TOC and COD change at steady state

z (m)	TOC (mg/L)	COD (mg/L)
0	62.03	178
0.2	58.53	167
0.5	54.61	155
0.8	51.05	143
1	47.46	130

**Experiment:**

Conditions: pH=4,  $Q_G=340$  L/h,  $Q_L=250$  L/h,  $t=20$  min,  $COD_{in}=300$  mg/L,  $C_{d,in,BB41} = 150.9$  mg/L,  $C_{d,in,BR18.1} = 26.4$  mg/L,  $C_{d,in,BY28} = 26.2$  mg/L,  $C_{d,in} = 1570$  Pt-Co,  $C_{O_3,G,in} = 0.9 \pm 0.1$  mmol/L gas  $TOC_{in}=93.61$  mg/L, catalyst: alumina,  $m_{cat} = 400$  g.

**Table C.94:** Dye concentration change at steady state

$z$ (m)	Abs <sub>380nm</sub> (cm <sup>-1</sup> )	Abs <sub>500nm</sub> (cm <sup>-1</sup> )	Abs <sub>617nm</sub> (cm <sup>-1</sup> )	$C_{d,BB41}$ (mg/L)	$C_{d,BY28}$ (mg/L)	$C_{d,BR18.1}$ (mg/L)
0	1.084	3.933	10.780	150.28	26.45	26.01
0.2	0.837	2.752	9.915	138.21	6.34	16.25
0.5	0.670	2.104	8.872	123.67	1.02	10.77
0.8	0.557	1.704	8.253	115.05	0.18	6.83
1	0.504	1.523	7.937	110.64	0.03	5.06

**Table C.95:** Dissolved O<sub>3</sub> concentration in liquid change at steady state

$z$ (m)	$V_{sample}$ (mL)	Abs <sub>Ind</sub> (cm <sup>-1</sup> )	$C_{O_3,L} \times 10^3$ (mmol/L)
0			0
0.2	10	1.200	12.3
0.5	13	1.328	22.4
0.8	11	1.076	29.4
1	11	1.026	36.3

**Table C.96:** TOC and COD change at steady state

$z$ (m)	TOC (mg/L)	COD (mg/L)
0	93.61	315
0.2	90.72	301
0.5	88.11	289
0.8	85.53	276
1	82.9	263

**Experiment:**

Conditions: pH=10,  $Q_G=340$  L/h,  $Q_L=250$  L/h,  $t=20$  min,  $COD_{in}=300$  mg/L,  $C_{d,in, BB41} = 150.9$  mg/L,  $C_{d,in, BR18.1} = 26.4$  mg/L,  $C_{d,in, BY28} = 26.2$  mg/L,  $C_{d,in} = 1570$  Pt-Co,  $C_{O_3,G,in} = 0.9 \pm 0.1$  mmol/L gas  $TOC_{in}=89.35$  mg/L, catalyst: alumina,  $m_{cat} = 400$  g.

**Table C.97:** Dye concentration change at steady state

z (m)	Abs <sub>380nm</sub> (cm <sup>-1</sup> )	Abs <sub>500nm</sub> (cm <sup>-1</sup> )	Abs <sub>617nm</sub> (cm <sup>-1</sup> )	$C_{d, BB41}$ (mg/L)	$C_{d, BY28}$ (mg/L)	$C_{d, BR18.1}$ (mg/L)
0	1.091	3.948	10.850	151.25	25.92	26.19
0.2	0.703	2.432	8.859	123.49	14.05	12.39
0.5	0.521	1.713	8.092	112.80	8.43	5.50
0.8	0.417	1.307	7.501	104.56	5.25	1.92
1	0.353	1.091	6.734	93.87	4.33	0.71

**Table C.98:** Dissolved O<sub>3</sub> concentration in liquid change at steady state

z (m)	V <sub>sample</sub> (mL)	Abs <sub>Ind</sub> (cm <sup>-1</sup> )	$C_{O_3,L} \times 10^3$ (mmol/L)
0			0
0.2	11	1.190	8.0
0.5	12	1.165	16.2
0.8	11	1.006	23.5
1	13	1.026	31.5

**Table C.99:** TOC and COD change at steady state

z (m)	TOC (mg/L)	COD (mg/L)
0	89.35	294
0.2	83.67	275
0.5	82.45	260
0.8	79.02	244
1	75.62	227

**Experiment:**

Conditions: pH=4,  $Q_G=340$  L/h,  $Q_L=250$  L/h,  $t=20$  min,  $COD_{in}=180$  mg/L,  $C_{d,in,BB41} = 90.54$  mg/L,  $C_{d,in,BR18.1} = 15.76$  mg/L,  $C_{d,in,BY28} = 15.87$  mg/L,  $C_{d,in} = 940$  Pt-Co,  $C_{O_3,G,in} = 0.9 \pm 0.1$  mmol/L gas  $TOC_{in}=62.34$  mg/L, catalyst: PFOA,  $m_{cat} = 400$  g.

**Table C.100:** Dye concentration change at steady state

z (m)	Abs <sub>380nm</sub> (cm <sup>-1</sup> )	Abs <sub>500nm</sub> (cm <sup>-1</sup> )	Abs <sub>617nm</sub> (cm <sup>-1</sup> )	$C_{d,BB41}$ (mg/L)	$C_{d,BY28}$ (mg/L)	$C_{d,BR18.1}$ (mg/L)
0	0.642	2.328	6.547	91.26	15.91	15.03
0.2	0.412	1.322	5.298	73.85	1.95	7.02
0.5	0.289	0.883	4.412	61.50	0.27	3.24
0.8	0.208	0.612	3.685	51.36	0.02	1.09
1	0.181	0.521	3.540	49.34	0.002	0.16

**Table C.101:** Dissolved O<sub>3</sub> concentration in liquid change at steady state

z (m)	V <sub>sample</sub> (mL)	Abs <sub>Ind</sub> (cm <sup>-1</sup> )	$C_{O_3,L} \times 10^3$ (mmol/L)
0			0
0.2	10	0.688	37.2
0.5	11	0.602	52.3
0.8	12	0.508	69.3
1	15	0.518	81.3

**Table C.102:** TOC and COD change at steady state

z (m)	TOC (mg/L)	COD (mg/L)
0	62.34	179
0.2	58.71	168
0.5	55.72	158
0.8	52.89	146
1	49.82	135

**Experiment:**

Conditions: pH=10,  $Q_G=340$  L/h,  $Q_L=250$  L/h,  $t=20$  min,  $COD_{in}=180$  mg/L,  $C_{d,in,BB41} = 90.54$  mg/L,  $C_{d,in,BR18.1} = 15.76$  mg/L,  $C_{d,in,BY28} = 15.87$  mg/L,  $C_{d,in} = 940$  Pt-Co,  $C_{O_3,G,in} = 0.9 \pm 0.1$  mmol/L gas  $TOC_{in}=61.85$  mg/L, catalyst: PFOA,  $m_{cat} = 400$  g.

**Table C.103:** Dye concentration change at steady state

z (m)	Abs <sub>380nm</sub> (cm <sup>-1</sup> )	Abs <sub>500nm</sub> (cm <sup>-1</sup> )	Abs <sub>617nm</sub> (cm <sup>-1</sup> )	$C_{d,BB41}$ (mg/L)	$C_{d,BY28}$ (mg/L)	$C_{d,BR18.1}$ (mg/L)
0	0.653	2.359	6.496	90.56	15.23	15.68
0.2	0.354	1.175	5.128	71.47	5.50	4.64
0.5	0.236	0.734	4.140	57.71	2.32	1.35
0.8	0.180	0.543	3.398	47.36	1.29	0.45
1	0.163	0.485	3.196	44.55	0.95	0.14

**Table C.104:** Dissolved O<sub>3</sub> concentration in liquid change at steady state

z (m)	V <sub>sample</sub> (mL)	Abs <sub>Ind</sub> (cm <sup>-1</sup> )	$C_{O_3,L} \times 10^3$ (mmol/L)
0			0
0.2	10	0.679	33.2
0.5	11	0.599	40.2
0.8	13	0.546	49.1
1	13	0.504	55.2

**Table C.105:** TOC and COD change at steady state

z (m)	TOC (mg/L)	COD (mg/L)
0	61.85	175
0.2	57.69	164
0.5	54.87	153
0.8	51.28	141
1	48.94	129

**Experiment:**

Conditions: pH=4,  $Q_G=340$  L/h,  $Q_L=250$  L/h,  $t=20$  min,  $COD_{in}=300$  mg/L,  $C_{d,in,BB41} = 150.9$  mg/L,  $C_{d,in,BR18.1} = 26.4$  mg/L,  $C_{d,in,BY28} = 26.2$  mg/L,  $C_{d,in} = 1570$  Pt-Co,  $C_{O_3,G,in} = 0.9 \pm 0.1$  mmol/L gas  $TOC_{in}=92.34$  mg/L, catalyst: PFOA,  $m_{cat} = 400$  g.

**Table C.106:** Dye concentration change at steady state

z (m)	Abs <sub>380nm</sub> (cm <sup>-1</sup> )	Abs <sub>500nm</sub> (cm <sup>-1</sup> )	Abs <sub>617nm</sub> (cm <sup>-1</sup> )	$C_{d,BB41}$ (mg/L)	$C_{d,BY28}$ (mg/L)	$C_{d,BR18.1}$ (mg/L)
0	1.090	3.961	10.771	150.15	26.73	26.35
0.2	0.794	2.587	9.577	133.50	4.88	15.02
0.5	0.620	1.926	8.619	120.14	0.54	9.00
0.8	0.509	1.540	7.962	110.98	0.12	5.22
1	0.437	1.300	7.435	103.64	0.02	3.06

**Table C.107:** Dissolved O<sub>3</sub> concentration in liquid change at steady state

z (m)	V <sub>sample</sub> (mL)	Abs <sub>Ind</sub> (cm <sup>-1</sup> )	$C_{O_3,L} \times 10^3$ (mmol/L)
0			0
0.2	10	1.143	23.6
0.5	11	1.118	28.4
0.8	13	1.170	37.4
1	15	1.209	46.2

**Table C.108:** TOC and COD change at steady state

z (m)	TOC (mg/L)	COD (mg/L)
0	92.34	290
0.2	89.12	277
0.5	86.78	264
0.8	83.45	251
1	80.83	238

**Experiment:**

Conditions: pH=10,  $Q_G=340$  L/h,  $Q_L=250$  L/h,  $t=20$  min,  $COD_{in}=300$  mg/L,  $C_{d,in,BB41} = 150.9$  mg/L,  $C_{d,in,BR18.1} = 26.4$  mg/L,  $C_{d,in,BY28} = 26.2$  mg/L,  $C_{d,in} = 1570$  Pt-Co,  $C_{O_3,G,in} = 0.9 \pm 0.1$  mmol/L gas  $TOC_{in}=91.34$  mg/L, catalyst: PFOA,  $m_{cat} = 400$  g.

**Table C.109:** Dye concentration change at steady state

$z$ (m)	Abs <sub>380nm</sub> (cm <sup>-1</sup> )	Abs <sub>500nm</sub> (cm <sup>-1</sup> )	Abs <sub>617nm</sub> (cm <sup>-1</sup> )	$C_{d,BB41}$ (mg/L)	$C_{d,BY28}$ (mg/L)	$C_{d,BR18.1}$ (mg/L)
0	1.077	3.900	10.780	150.28	26.01	25.67
0.2	0.741	2.577	9.122	127.16	15.13	13.58
0.5	0.569	1.899	8.308	115.81	9.66	7.30
0.8	0.452	1.450	7.722	107.63	6.81	3.07
1	0.375	1.173	7.010	97.71	5.08	1.13

**Table C.110:** Dissolved O<sub>3</sub> concentration in liquid change at steady state

$z$ (m)	$V_{sample}$ (mL)	Abs <sub>Ind</sub> (cm <sup>-1</sup> )	$C_{O_3,L} \times 10^3$ (mmol/L)
0			0
0.2	11	1.207	13.3
0.5	12	1.178	21.4
0.8	13	1.160	29.4
1	14	1.112	36.2

**Table C.111:** TOC and COD change at steady state

$z$ (m)	TOC (mg/L)	COD (mg/L)
0	91.34	295
0.2	88.34	281
0.5	85.57	266
0.8	82.03	251
1	78.54	236

**Experiment:**

Conditions: pH=4,  $Q_G=150$  L/h,  $Q_L=150$  L/h,  $t=20$  min,  $COD_{in}=300$  mg/L,  $C_{d,in,BB41} = 150.9$  mg/L,  $C_{d,in,BR18.1} = 26.4$  mg/L,  $C_{d,in,BY28} = 26.2$  mg/L,  $C_{d,in} = 1570$  Pt-Co,  $C_{O_3,G,in} = 0.9 \pm 0.1$  mmol/L gas  $TOC_{in}=92.13$  mg/L, no catalyst.

**Table C.112:** Dye concentration change at steady state

z (m)	Abs <sub>380nm</sub> (cm <sup>-1</sup> )	Abs <sub>500nm</sub> (cm <sup>-1</sup> )	Abs <sub>617nm</sub> (cm <sup>-1</sup> )	$C_{d,BB41}$ (mg/L)	$C_{d,BY28}$ (mg/L)	$C_{d,BR18.1}$ (mg/L)
0	1.084	3.925	10.772	150.16	25.88	26.04
0.2	1.012	3.566	10.647	148.42	19.41	22.89
0.5	0.931	3.196	10.548	147.03	14.22	19.27
0.8	0.853	2.825	10.451	145.68	8.50	15.74
1	0.777	2.511	10.299	143.56	5.71	12.46

**Table C.113:** Dissolved O<sub>3</sub> concentration in liquid change at steady state

z (m)	V <sub>sample</sub> (mL)	Abs <sub>Ind</sub> (cm <sup>-1</sup> )	$C_{O_3,L} \times 10^3$ (mmol/L)
0			0
0.2	12	1.473	15.5
0.5	17	1.904	35.6
0.8	11	1.284	44.4
1	10	1.164	48.9

**Table C.114:** TOC and COD change at steady state

z (m)	TOC (mg/L)	COD (mg/L)
0	92.13	302
0.2	90.98	292
0.5	89.81	284
0.8	88.47	273
1	87.39	264

**Experiment:**

Conditions: pH=4,  $Q_G=200$  L/h,  $Q_L=200$  L/h,  $t=20$  min,  $COD_{in}=300$  mg/L,  $C_{d,in,BB41} = 150.9$  mg/L,  $C_{d,in,BR18.1} = 26.4$  mg/L,  $C_{d,in,BY28} = 26.2$  mg/L,  $C_{d,in} = 1580$  Pt-Co,  $C_{O_3,G,in} = 0.9 \pm 0.1$  mmol/L gas  $TOC_{in}=91.26$  mg/L, no catalyst.

**Table C.115:** Dye concentration change at steady state

$z$ (m)	Abs <sub>380nm</sub> (cm <sup>-1</sup> )	Abs <sub>500nm</sub> (cm <sup>-1</sup> )	Abs <sub>617nm</sub> (cm <sup>-1</sup> )	$C_{d,BB41}$ (mg/L)	$C_{d,BY28}$ (mg/L)	$C_{d,BR18.1}$ (mg/L)
0	1.068	3.869	10.839	151.09	26.08	25.13
0.2	0.962	3.348	10.551	147.07	16.78	20.74
0.5	0.879	2.986	10.299	143.57	12.42	17.34
0.8	0.794	2.593	10.257	142.98	6.89	13.38
1	0.719	2.289	9.993	139.30	4.30	10.40

**Table C.116:** Dissolved O<sub>3</sub> concentration in liquid change at steady state

$z$ (m)	$V_{sample}$ (mL)	Abs <sub>Ind</sub> (cm <sup>-1</sup> )	$C_{O_3,L} \times 10^3$ (mmol/L)
0			0
0.2	11	1.364	13.3
0.5	12	1.389	33.2
0.8	19	2.027	40.4
1	16	1.685	45.5

**Table C.117:** TOC and COD change at steady state

$z$ (m)	TOC (mg/L)	COD (mg/L)
0	91.26	285
0.2	89.15	272
0.5	87.41	261
0.8	85.78	250
1	84.03	238

**Experiment:**

Conditions: pH=4,  $Q_G=250$  L/h,  $Q_L=250$  L/h,  $t=20$  min,  $COD_{in}=300$  mg/L,  $C_{d,in, BB41} = 150.9$  mg/L,  $C_{d,in, BR18.1} = 26.4$  mg/L,  $C_{d,in, BY28} = 26.2$  mg/L,  $C_{d,in} = 1580$  Pt-Co,  $C_{O_3, G, in} = 0.9 \pm 0.1$  mmol/L gas  $TOC_{in}=93.04$  mg/L, no catalyst.

**Table C.118:** Dye concentration change at steady state

z (m)	Abs <sub>380nm</sub> (cm <sup>-1</sup> )	Abs <sub>500nm</sub> (cm <sup>-1</sup> )	Abs <sub>617nm</sub> (cm <sup>-1</sup> )	$C_{d, BB41}$ (mg/L)	$C_{d, BY28}$ (mg/L)	$C_{d, BR18.1}$ (mg/L)
0	1.078	3.906	10.751	149.87	25.930	25.80
0.2	0.932	3.210	10.362	144.43	14.62	19.70
0.5	0.820	2.738	10.079	140.49	9.76	15.01
0.8	0.752	2.423	9.959	138.83	5.14	12.07
1	0.671	2.115	9.651	134.53	3.30	8.94

**Table C.119:** Dissolved O<sub>3</sub> concentration in liquid change at steady state

z (m)	V <sub>sample</sub> (mL)	Abs <sub>Ind</sub> (cm <sup>-1</sup> )	$C_{O_3, L} \times 10^3$ (mmol/L)
0			0
0.2	11	1.350	10.4
0.5	13	1.477	25.4
0.8	12	1.340	36.4
1	11	1.202	41.9

**Table C.120:** TOC and COD change at steady state

z (m)	TOC (mg/L)	COD (mg/L)
0	93.04	293
0.2	90.98	278
0.5	88.86	265
0.8	86.72	252
1	84.51	239

**Experiment:**

Conditions: pH=4,  $Q_G=150$  L/h,  $Q_L=150$  L/h,  $t=20$  min,  $COD_{in}=300$  mg/L,  $C_{d,in,BB41} = 150.9$  mg/L,  $C_{d,in,BR18.1} = 26.4$  mg/L,  $C_{d,in,BY28} = 26.2$  mg/L,  $C_{d,in} = 1580$  Pt-Co,  $C_{O_3,G,in} = 0.9 \pm 0.1$  mmol/L gas  $TOC_{in}=90.14$  mg/L, catalyst: alumina,  $m_{cat} = 300$  g.

**Table C.121:** Dye concentration change at steady state

$z$ (m)	Abs <sub>380nm</sub> (cm <sup>-1</sup> )	Abs <sub>500nm</sub> (cm <sup>-1</sup> )	Abs <sub>617nm</sub> (cm <sup>-1</sup> )	$C_{d,BB41}$ (mg/L)	$C_{d,BY28}$ (mg/L)	$C_{d,BR18.1}$ (mg/L)
0	1.085	3.940	10.836	151.06	26.75	25.94
0.2	0.984	3.429	10.615	147.97	17.02	21.64
0.5	0.883	2.982	10.514	146.56	11.72	17.02
0.8	0.830	2.727	10.417	145.20	7.39	14.74
1	0.772	2.494	10.302	143.61	5.74	12.22

**Table C.122:** Dissolved O<sub>3</sub> concentration in liquid change at steady state

$z$ (m)	$V_{sample}$ (mL)	Abs <sub>Ind</sub> (cm <sup>-1</sup> )	$C_{O_3,L} \times 10^3$ (mmol/L)
0			0
0.2	10	1.276	9.1
0.5	10	1.231	26.4
0.8	12	1.403	33.2
1	10	1.182	40.2

**Table C.123:** TOC and COD change at steady state

$z$ (m)	TOC (mg/L)	COD (mg/L)
0	90.14	308
0.2	88.78	295
0.5	87.19	287
0.8	85.62	279
1	84.16	268

**Experiment:**

Conditions: pH=4,  $Q_G=200$  L/h,  $Q_L=200$  L/h,  $t=20$  min,  $COD_{in}=300$  mg/L,  $C_{d,in,BB41} = 150.9$  mg/L,  $C_{d,in,BR18.1} = 26.4$  mg/L,  $C_{d,in,BY28} = 26.2$  mg/L,  $C_{d,in} = 1580$  Pt-Co,  $C_{O_3,G,in} = 0.9 \pm 0.1$  mmol/L gas  $TOC_{in}=91.28$  mg/L, catalyst: alumina,  $m_{cat} = 300$  g.

**Table C.124:** Dye concentration change at steady state

$z$ (m)	Abs <sub>380nm</sub> (cm <sup>-1</sup> )	Abs <sub>500nm</sub> (cm <sup>-1</sup> )	Abs <sub>617nm</sub> (cm <sup>-1</sup> )	$C_{d,BB41}$ (mg/L)	$C_{d,BY28}$ (mg/L)	$C_{d,BR18.1}$ (mg/L)
0	1.087	3.950	10.777	150.23	26.84	26.16
0.2	0.940	3.245	10.413	145.16	14.92	20.02
0.5	0.859	2.872	10.225	142.53	9.50	16.58
0.8	0.760	2.463	9.997	139.35	5.86	12.36
1	0.713	2.265	9.851	137.32	3.69	10.48

**Table C.125:** Dissolved O<sub>3</sub> concentration in liquid change at steady state

$z$ (m)	$V_{sample}$ (mL)	Abs <sub>Ind</sub> (cm <sup>-1</sup> )	$C_{O_3,L} \times 10^3$ (mmol/L)
0			0
0.2	11	1.361	7.9
0.5	13	1.500	23.7
0.8	11	1.270	28.5
1	11	1.238	35.4

**Table C.126:** TOC and COD change at steady state

$z$ (m)	TOC (mg/L)	COD (mg/L)
0	91.28	301
0.2	89.05	289
0.5	87.29	275
0.8	85.68	261
1	83.56	248

**Experiment:**

Conditions: pH=4,  $Q_G=250$  L/h,  $Q_L=250$  L/h,  $t=20$  min,  $COD_{in}=300$  mg/L,  $C_{d,in,BB41} = 150.9$  mg/L,  $C_{d,in,BR18.1} = 26.4$  mg/L,  $C_{d,in,BY28} = 26.2$  mg/L,  $C_{d,in} = 1580$  Pt-Co,  $C_{O_3,G,in} = 0.9 \pm 0.1$  mmol/L gas  $TOC_{in}=92.36$  mg/L, catalyst: alumina,  $m_{cat} = 300$  g.

**Table C.127:** Dye concentration change at steady state

z (m)	Abs <sub>380nm</sub> (cm <sup>-1</sup> )	Abs <sub>500nm</sub> (cm <sup>-1</sup> )	Abs <sub>617nm</sub> (cm <sup>-1</sup> )	$C_{d,BB41}$ (mg/L)	$C_{d,BY28}$ (mg/L)	$C_{d,BR18.1}$ (mg/L)
0	1.092	3.952	10.834	151.02	25.93	26.28
0.2	0.911	3.118	10.358	144.39	13.38	18.76
0.5	0.792	2.607	9.972	139.01	7.40	13.99
0.8	0.711	2.267	9.789	136.45	4.05	10.55
1	0.656	2.058	9.560	133.26	2.97	8.43

**Table C.128:** Dissolved O<sub>3</sub> concentration in liquid change at steady state

z (m)	V <sub>sample</sub> (mL)	Abs <sub>Ind</sub> (cm <sup>-1</sup> )	$C_{O_3,L} \times 10^3$ (mmol/L)
0			0
0.2	10	1.257	6.0
0.5	10	1.189	20.5
0.8	11	1.253	25.4
1	15	1.572	31.4

**Table C.129:** TOC and COD change at steady state

z (m)	TOC (mg/L)	COD (mg/L)
0	92.36	295
0.2	90.13	280
0.5	87.59	266
0.8	85.02	253
1	82.61	239

**Experiment:**

Conditions: pH=4,  $Q_G=150$  L/h,  $Q_L=150$  L/h,  $t=20$  min,  $COD_{in}=300$  mg/L,  $C_{d,in,BB41} = 150.9$  mg/L,  $C_{d,in,BR18.1} = 26.4$  mg/L,  $C_{d,in,BY28} = 26.2$  mg/L,  $C_{d,in} = 1570$  Pt-Co,  $C_{O_3,G,in} = 0.9 \pm 0.1$  mmol/L gas  $TOC_{in}=90.95$  mg/L, catalyst: PFOA,  $m_{cat} = 300$  g.

**Table C.130:** Dye concentration change at steady state

$z$ (m)	Abs <sub>380nm</sub> (cm <sup>-1</sup> )	Abs <sub>500nm</sub> (cm <sup>-1</sup> )	Abs <sub>617nm</sub> (cm <sup>-1</sup> )	$C_{d,BB41}$ (mg/L)	$C_{d,BY28}$ (mg/L)	$C_{d,BR18.1}$ (mg/L)
0	1.088	3.950	10.854	151.31	26.71	26.05
0.2	0.965	3.373	10.621	148.05	17.78	20.72
0.5	0.892	3.029	10.458	145.78	12.48	17.59
0.8	0.814	2.669	10.391	144.84	7.38	14.02
1	0.761	2.451	10.213	142.36	5.30	11.92

**Table C.131:** Dissolved O<sub>3</sub> concentration in liquid change at steady state

$z$ (m)	$V_{sample}$ (mL)	Abs <sub>Ind</sub> (cm <sup>-1</sup> )	$C_{O_3,L} \times 10^3$ (mmol/L)
0			0
0.2	10	1.269	12.9
0.5	12	1.412	31.4
0.8	13	1.478	40.2
1	16	1.724	44.2

**Table C.132:** TOC and COD change at steady state

$z$ (m)	TOC (mg/L)	COD (mg/L)
0	90.95	319
0.2	89.34	308
0.5	87.52	297
0.8	86.07	285
1	84.46	274

**Experiment:**

Conditions: pH=4,  $Q_G=200$  L/h,  $Q_L=200$  L/h,  $t=20$  min,  $COD_{in}=300$  mg/L,  $C_{d,in,BB41} = 150.9$  mg/L,  $C_{d,in,BR18.1} = 26.4$  mg/L,  $C_{d,in,BY28} = 26.2$  mg/L,  $C_{d,in} = 1570$  Pt-Co,  $C_{O_3,G,in} = 0.9 \pm 0.1$  mmol/L gas  $TOC_{in}=91.23$  mg/L, catalyst: PFOA,  $m_{cat} = 300$  g.

**Table C.133:** Dye concentration change at steady state

z (m)	Abs <sub>380nm</sub> (cm <sup>-1</sup> )	Abs <sub>500nm</sub> (cm <sup>-1</sup> )	Abs <sub>617nm</sub> (cm <sup>-1</sup> )	$C_{d,BB41}$ (mg/L)	$C_{d,BY28}$ (mg/L)	$C_{d,BR18.1}$ (mg/L)
0	1.073	3.871	10.778	150.25	25.12	25.48
0.2	0.935	3.222	10.420	145.25	14.75	19.75
0.5	0.834	2.790	10.106	140.88	9.70	15.67
0.8	0.750	2.414	9.998	139.37	4.98	11.90
1	0.695	2.191	9.709	135.34	2.94	9.93

**Table C.134:** Dissolved O<sub>3</sub> concentration in liquid change at steady state

z (m)	V <sub>sample</sub> (mL)	Abs <sub>Ind</sub> (cm <sup>-1</sup> )	$C_{O_3,L} \times 10^3$ (mmol/L)
0			0
0.2	13	1.560	10.5
0.5	14	1.570	27.8
0.8	12	1.351	33.9
1	17	1.750	39.0

**Table C.135:** TOC and COD change at steady state

z (m)	TOC (mg/L)	COD (mg/L)
0	91.23	305
0.2	89.07	290
0.5	86.62	278
0.8	84.59	262
1	82.71	248

**Experiment:**

Conditions: pH=4,  $Q_G=250$  L/h,  $Q_L=250$  L/h,  $t=20$  min,  $COD_{in}=300$  mg/L,  $C_{d,in,BB41} = 150.9$  mg/L,  $C_{d,in,BR18.1} = 26.4$  mg/L,  $C_{d,in,BY28} = 26.2$  mg/L,  $C_{d,in} = 1570$  Pt-Co,  $C_{O_3,G,in} = 0.9 \pm 0.1$  mmol/L gas  $TOC_{in}=92.46$  mg/L, catalyst: PFOA,  $m_{cat} = 300$  g.

**Table C.136:** Dye concentration change at steady state

z (m)	Abs <sub>380nm</sub> (cm <sup>-1</sup> )	Abs <sub>500nm</sub> (cm <sup>-1</sup> )	Abs <sub>617nm</sub> (cm <sup>-1</sup> )	$C_{d,BB41}$ (mg/L)	$C_{d,BY28}$ (mg/L)	$C_{d,BR18.1}$ (mg/L)
0	1.083	3.936	10.759	149.98	26.73	26.04
0.2	0.894	3.061	10.185	141.97	13.26	18.37
0.5	0.776	2.564	9.957	138.79	8.45	13.23
0.8	0.699	2.219	9.732	135.66	3.70	10.09
1	0.639	1.997	9.399	131.02	2.61	8.02

**Table C.137:** Dissolved O<sub>3</sub> concentration in liquid change at steady state

z (m)	V <sub>sample</sub> (mL)	Abs <sub>Ind</sub> (cm <sup>-1</sup> )	$C_{O_3,L} \times 10^3$ (mmol/L)
0			0
0.2	11	1.334	8.9
0.5	13	1.466	23.4
0.8	12	1.330	29.2
1	12	1.269	37.9

**Table C.138:** TOC and COD change at steady state

z (m)	TOC (mg/L)	COD (mg/L)
0	92.46	317
0.2	89.82	302
0.5	87.17	284
0.8	84.51	266
1	82.06	249

## APPENDIX D

### SEMI-BATCH EXPERIMENTS DATA

**Table D.1:**  $C_d$  at different time. Conditions: Dye: BB 41,  $C_{d,i}=300$  mg/L, stirrer rate=300 rpm,  $Q_G=150$  L/h, pH=4,  $C_{O_3,G,in} = 0.9 \pm 0.1$  mmol/L gas,  $TOC_{in} = 149.12$  mg/L,  $TOC_{out} = 110.38$  mg/L,  $COD_{in}= 295$  mg/L,  $COD_{out}= 201$  mg/L, catalyst: none

Time (min)	Abs. (cm <sup>-1</sup> )	$C_d$ (mg/L)	Dilution Factor (times)
0	18.560	302.6	10
1	17.860	291.2	10
3	13.720	223.7	10
5	9.920	161.7	10
8	6.343	103.4	10
10	4.890	79.7	10
15	2.771	45.2	1
20	1.692	27.6	1
30	1.064	17.3	1
45	0.606	9.9	1
60	0.234	3.8	1
90	0.127	2.1	1

**Table D.2:**  $C_d$  at different time. Conditions: Dye: BB 41,  $C_{d,i}=300$  mg/L, stirrer rate=300 rpm,  $Q_G=150$  L/h, pH=10,  $C_{O_3,G,in} = 0.9 \pm 0.1$  mmol/L gas,  $TOC_{in} = 153.56$  mg/L,  $TOC_{out} = 75.38$  mg/L,  $COD_{in}= 300$  mg/L,  $COD_{out}=133$  mg/L, catalyst: none

Time (min)	Abs. (cm <sup>-1</sup> )	$C_d$ (mg/L)	Dilution Factor (times)
0	18.660	304.2	10
1	17.020	277.5	10
3	11.980	195.3	10
5	8.100	132.0	10
8	4.880	79.6	10
10	3.670	59.8	10
15	1.188	19.4	1
20	0.573	9.3	1
30	0.101	1.6	1
45	0.017	0.3	1
60	0.008	0.1	1
90	0.000	0.0	1

**Table D.3:**  $C_d$  at different time. Conditions: Dye: BB 41,  $C_{d,i}=300$  mg/L, stirrer rate=300 rpm,  $Q_G=150$  L/h, pH=10,  $C_{O_3,G,in} = 0.9 \pm 0.1$  mmol/L gas,  $TOC_{in} = 153$  mg/L,  $TOC_{out} = 68.96$  mg/L,  $COD_{in}= 299$  mg/L,  $COD_{out}= 121$  mg/L, catalyst: PFOA,  $m_{cat} = 5$  g.

Time (min)	Abs. (cm <sup>-1</sup> )	$C_d$ (mg/L)	Dilution Factor (times)
0	18.220	297.0	10
1	13.020	212.2	10
3	10.540	171.8	10
5	4.560	74.3	10
8	3.060	49.9	10
10	1.850	30.2	1
15	1.007	16.4	1
20	0.253	4.1	1
30	0.075	1.2	1
45	0.010	0.2	1
60	0.000	0.0	1
90	0.000	0.0	1

**Table D.4:**  $C_d$  at different time. Conditions: Dye: BB 41,  $C_{d,i}=300$  mg/L, stirrer rate=300 rpm,  $Q_G=150$  L/h, pH=4,  $C_{O_3,G,in} = 0.9 \pm 0.1$  mmol/L gas,  $TOC_{in} = 155.43$  mg/L,  $TOC_{out} = 11.14$  mg/L,  $COD_{in}= 289$  mg/L,  $COD_{out}= 191$  mg/L, catalyst: alumina,  $m_{cat} = 5$  g.

Time (min)	Abs. (cm <sup>-1</sup> )	$C_d$ (mg/L)	Dilution Factor (times)
0	18.140	295.7	10
1	16.420	267.7	10
3	11.460	186.8	10
5	7.960	129.8	10
8	6.020	98.1	10
10	3.700	60.3	10
15	1.813	29.6	1
20	0.652	10.6	1
30	0.398	6.5	1
45	0.198	3.2	1
60	0.072	1.2	1
90	0.028	0.5	1

**Table D.5:**  $C_d$  at different time. Conditions: Dye: BB 41,  $C_{d,i}=300$  mg/L, stirrer rate=300 rpm,  $Q_G=150$  L/h, pH=4  $C_{O_3,G,in} = 0.9 \pm 0.1$  mmol/L gas,  $TOC_{in} = 159.5$  mg/L,  $TOC_{out} = 103.19$  mg/L,  $COD_{in}= 297$  mg/L,  $COD_{out}= 181$  mg/L, catalyst: PFOA,  $m_{cat} = 5$  g.

Time (min)	Abs. (cm <sup>-1</sup> )	$C_d$ (mg/L)	Dilution Factor (times)
0	18.570	302.7	10
1	14.675	239.2	10
3	9.657	157.4	10
5	6.590	107.4	10
8	4.872	79.4	10
10	3.000	48.9	1
15	1.394	22.7	1
20	0.581	9.5	1
30	0.392	6.4	1
45	0.152	2.5	1
60	0.068	1.1	1
90	0.015	0.2	1

**Table D.6:**  $C_d$  at different time. Conditions: Dye: BB 41,  $C_{d,i}=300$  mg/L, stirrer rate=300 rpm,  $Q_G=150$  L/h, pH=10,  $C_{O_3,G,in} = 0.9 \pm 0.1$  mmol/L gas,  $TOC_{in} = 148.71$  mg/L,  $TOC_{out} = 62.01$  mg/L,  $COD_{in}= 290$  mg/L,  $COD_{out}= 107$  mg/L, catalyst: alumina,  $m_{cat} = 5$  g.

Time (min)	Abs. (cm <sup>-1</sup> )	$C_d$ (mg/L)	Dilution Factor (times)
0	18.550	302.4	10
1	13.555	220.9	10
3	5.670	92.4	10
5	2.445	39.8	1
8	1.920	31.3	1
10	0.870	14.2	1
15	0.370	6.0	1
20	0.180	2.9	1
30	0.054	0.9	1
45	0.018	0.2	1
60	0.004	0.1	1
90	0.002	0.0	1

**Table D.7:**  $C_d$  at different time. Conditions: Dye: BR 18.1,  $C_{d,i}=300$  mg/L, stirrer rate=300 rpm,  $Q_G=150$  L/h, pH=4  $C_{O_3,G,in} = 0.9 \pm 0.1$  mmol/L gas,  $TOC_{in} = 174.3$  mg/L,  $TOC_{out} = 150.67$  mg/L,  $COD_{in}= 298$  mg/L,  $COD_{out}= 240$  mg/L, catalyst: none.

Time (min)	Abs. (cm <sup>-1</sup> )	$C_d$ (mg/L)	Dilution Factor (times)
0	26.480	302.9	10
1	21.670	247.9	10
3	17.430	199.4	10
5	13.550	154.9	10
8	10.000	114.4	10
10	8.980	102.7	10
15	5.654	64.7	10
20	2.344	26.8	1
30	1.045	11.9	1
45	0.289	3.3	1
60	0.053	0.6	1
90	0.001	0.0	1

**Table D.8:**  $C_d$  at different time. Conditions: Dye: BR 18.1,  $C_{d,i}=300$  mg/L, stirrer rate=300 rpm,  $Q_G=150$  L/h, pH=10,  $C_{O_3,G,in} = 0.9 \pm 0.1$  mmol/L gas,  $TOC_{in} = 178.26$  mg/L,  $TOC_{out} = 98.75$  mg/L,  $COD_{in}= 310$  mg/L,  $COD_{out}= 163$  mg/L, catalyst: none.

Time (min)	Abs. (cm <sup>-1</sup> )	$C_d$ (mg/L)	Dilution Factor (times)
0	26.660	304.9	10
1	21.550	246.5	10
3	16.450	188.2	10
5	12.240	140.00	10
8	9.100	104.09	10
10	7.670	87.7	10
15	4.765	54.5	10
20	1.734	19.8	1
30	0.765	8.7	1
45	0.234	2.7	1
60	0.032	0.4	1
90	0.000	0.002	1

**Table D.9:**  $C_d$  at different time. Conditions: Dye: BR 18.1,  $C_{d,i}=300$  mg/L, stirrer rate=300 rpm,  $Q_G=150$  L/h, pH=10  $C_{O_3,G,in} = 0.9 \pm 0.1$  mmol/L gas,  $TOC_{in} = 173.98$  mg/L,  $TOC_{out} = 72.92$  mg/L,  $COD_{in}= 289$  mg/L,  $COD_{out}= 119$  mg/L, catalyst: alumina,  $m_{cat} = 5$  g.

Time (min)	Abs. (cm <sup>-1</sup> )	$C_d$ (mg/L)	Dilution Factor (times)
0	25.450	291.1	10
1	15.340	175.5	10
3	12.780	146.2	10
5	10.430	119.3	10
8	8.420	96.3	10
10	4.040	46.2	10
15	2.452	28.0	1
20	0.987	11.3	1
30	0.566	6.5	1
45	0.098	1.1	1
60	0.007	0.1	1
90	0.001	0.0	1

**Table D.10:**  $C_d$  at different time. Conditions: Dye: BR 18.1,  $C_{d,i}=300$  mg/L, stirrer rate=300 rpm,  $Q_G=150$  L/h, pH=4,  $C_{O_3,G,in} = 0.9 \pm 0.1$  mmol/L gas,  $TOC_{in} = 176.23$  mg/L,  $TOC_{out} = 141.9$  mg/L,  $COD_{in}= 306$  mg/L,  $COD_{out}= 233$  mg/L, catalyst: alumina,  $m_{cat} = 5$  g.

Time (min)	Abs. (cm <sup>-1</sup> )	$C_d$ (mg/L)	Dilution Factor (times)
0	25.480	291.4	10
1	22.090	252.7	10
3	18.340	209.8	10
5	12.510	143.1	10
8	11.760	134.5	10
10	8.860	101.3	10
15	6.080	69.5	10
20	3.109	35.6	1
30	1.933	22.1	1
45	0.725	8.3	1
60	0.445	5.1	1
90	0.037	0.4	1

**Table D.11:**  $C_d$  at different time. Conditions: Dye: BR 18.1,  $C_{d,i}=300$  mg/L, stirrer rate=300 rpm,  $Q_G=150$  L/h, pH=4  $C_{O_3,G,in} = 0.9 \pm 0.1$  mmol/L gas,  $TOC_{in} = 170$  mg/L,  $TOC_{out} = 123.27$  mg/L,  $COD_{in}= 291$  mg/L,  $COD_{out}= 186$  mg/L, catalyst: PFOA,  $m_{cat} = 5$  g.

Time (min)	Abs. ( $cm^{-1}$ )	$C_d$ (mg/L)	Dilution Factor (times)
0	26.180	299.4	10
1	21.610	247.2	10
3	17.880	204.5	10
5	15.150	173.3	10
8	8.720	99.7	10
10	6.150	70.3	10
15	3.620	41.4	1
20	2.531	28.9	1
30	1.181	13.5	1
45	0.453	5.2	1
60	0.230	2.6	1
90	0.033	0.4	1

**Table D.12:**  $C_d$  at different time. Conditions: Dye: BR 18.1,  $C_{d,i}=300$  mg/L, stirrer rate=300 rpm,  $Q_G=150$  L/h, pH=10,  $C_{O_3,G,in} = 0.9 \pm 0.1$  mmol/L gas,  $TOC_{in} = 179.03$  mg/L,  $TOC_{out} = 92.74$  mg/L,  $COD_{in}= 294$  mg/L,  $COD_{out}= 135$  mg/L, catalyst: PFOA,  $m_{cat} = 5$  g.

Time (min)	Abs. ( $cm^{-1}$ )	$C_d$ (mg/L)	Dilution Factor (times)
0	26.630	434.1	10
1	17.470	284.8	10
3	12.430	202.6	10
5	9.530	155.3	10
8	7.392	120.5	10
10	5.050	82.3	10
15	3.022	49.3	1
20	1.121	18.3	1
30	1.011	16.5	1
45	0.330	5.4	1
60	0.205	3.3	1
90	0.013	0.2	1

**Table D.13:**  $C_d$  at different time. Conditions: Dye: BY 28,  $C_{d,i}=300$  mg/L, stirrer rate=300 rpm,  $Q_G=150$  L/h, pH=4  $C_{O_3,G,in} = 0.9 \pm 0.1$  mmol/L gas,  $TOC_{in} = 167.12$  mg/L,  $TOC_{out} = 83.16$  mg/L,  $COD_{in}= 296$  mg/L,  $COD_{out}= 131$  mg/L, catalyst: none.

Time (min)	Abs. (cm <sup>-1</sup> )	$C_d$ (mg/L)	Dilution Factor (times)
0	21.266	306.2	10
1	15.870	228.5	10
3	10.960	157.8	10
5	7.250	104.4	10
8	4.900	70.6	1
10	2.940	42.3	1
15	1.310	18.9	1
20	0.742	10.7	1
30	0.150	2.2	1
45	0.066	0.9	1
60	0.023	0.3	1
90	0.001	0.0	1

**Table D.14:**  $C_d$  at different time. Conditions: Dye: BY 28,  $C_{d,i}=300$  mg/L, stirrer rate=300 rpm,  $Q_G=150$  L/h, pH=10,  $C_{O_3,G,in} = 0.9 \pm 0.1$  mmol/L gas,  $TOC_{in} = 162.34$  mg/L,  $TOC_{out} = 127.81$  mg/L,  $COD_{in}= 279$  mg/L,  $COD_{out}= 197$  mg/L, catalyst: none.

Time (min)	Abs. (cm <sup>-1</sup> )	$C_d$ (mg/L)	Dilution Factor (times)
0	21.120	304.1	10
1	19.650	282.9	10
3	17.880	257.5	10
5	13.432	193.4	10
8	10.280	148.0	10
10	8.620	124.1	10
15	6.607	95.1	10
20	4.750	68.4	1
30	3.282	47.3	1
45	2.082	29.9	1
60	1.034	14.9	1
90	0.143	2.1	1

**Table D.15:**  $C_d$  at different time. Conditions: Dye: BY 28,  $C_{d,i}=300$  mg/L, stirrer rate=300 rpm,  $Q_G=150$  L/h, pH=10  $C_{O_3,G,in} = 0.9 \pm 0.1$  mmol/L gas,  $TOC_{in} = 166.90$  mg/L,  $TOC_{out} = 107.69$  mg/L,  $COD_{in} = 301$  mg/L,  $COD_{out} = 178$  mg/L, catalyst: alumina,  $m_{cat} = 5$  g.

Time (min)	Abs. (cm <sup>-1</sup> )	$C_d$ (mg/L)	Dilution Factor (times)
0	20.720	298.4	10
1	16.310	234.9	10
3	14.030	202.0	10
5	10.032	144.5	10
8	6.350	91.4	10
10	4.650	66.9	1
15	3.630	52.3	1
20	2.710	39.0	1
30	1.840	26.5	1
45	0.765	11.0	1
60	0.503	7.2	1
90	0.353	5.1	1

**Table D.16:**  $C_d$  at different time. Conditions: Dye: BY 28,  $C_{d,i}=300$  mg/L, stirrer rate=300 rpm,  $Q_G=150$  L/h, pH=4,  $C_{O_3,G,in} = 0.9 \pm 0.1$  mmol/L gas,  $TOC_{in} = 162.98$  mg/L,  $TOC_{out} = 62.94$  mg/L,  $COD_{in} = 306$  mg/L,  $COD_{out} = 101$  mg/L, catalyst: PFOA,  $m_{cat} = 5$  g.

Time (min)	Abs. (cm <sup>-1</sup> )	$C_d$ (mg/L)	Dilution Factor (times)
0	21.740	313.1	10
1	13.100	188.6	10
3	9.021	129.9	10
5	5.825	83.9	10
8	3.723	53.6	1
10	2.076	29.8	1
15	1.153	16.6	1
20	0.453	6.5	1
30	0.280	4.0	1
45	0.101	1.5	1
60	0.035	0.5	1
90	0.030	0.4	1

**Table D.17:**  $C_d$  at different time. Conditions: Dye: BY 28,  $C_{d,i}=300$  mg/L, stirrer rate=300 rpm,  $Q_G=150$  L/h, pH=4  $C_{O_3,G,in} = 0.9 \pm 0.1$  mmol/L gas,  $TOC_{in} = 164.52$  mg/L,  $TOC_{out} = 72.67$  mg/L,  $COD_{in}= 288$  mg/L,  $COD_{out}= 120$  mg/L, catalyst: alumina,  $m_{cat} = 5$  g.

Time (min)	Abs. (cm <sup>-1</sup> )	$C_d$ (mg/L)	Dilution Factor (times)
0	21.430	308.6	10
1	13.950	200.9	10
3	10.032	144.5	10
5	6.892	99.2	10
8	4.654	67.0	1
10	3.012	43.4	1
15	1.011	14.6	1
20	0.353	5.1	1
30	0.203	2.9	1
45	0.045	0.6	1
60	0.083	1.2	1
90	0.021	0.3	1

**Table D.16:**  $C_d$  at different time. Conditions: Dye: BY 28,  $C_{d,i}=300$  mg/L, stirrer rate=300 rpm,  $Q_G=150$  L/h, pH=10,  $C_{O_3,G,in} = 0.9 \pm 0.1$  mmol/L gas,  $TOC_{in} = 165.40$  mg/L,  $TOC_{out} = 121.63$  mg/L,  $COD_{in}= 295$  mg/L,  $COD_{out}= 206$  mg/L, catalyst: PFOA,  $m_{cat} = 5$  g.

Time (min)	Abs. (cm <sup>-1</sup> )	$C_d$ (mg/L)	Dilution Factor (times)
0	21.550	310.3	10
1	18.530	266.8	10
3	15.520	223.5	10
5	11.930	171.8	10
8	9.620	138.5	10
10	8.260	118.9	10
15	6.561	94.5	10
20	4.452	64.1	1
30	3.042	43.8	1
45	2.475	35.6	1
60	1.200	17.3	1
90	0.150	2.2	1

## APPENDIX E

### ACCURACY OF TOC AND COD RESULTS

In order to be sure if the TOC and COD results are accurate enough, the TOC and COD values of the samples taken from the reactor were measured three times. The standard deviation and the percent error of the values were calculated using equations (E.1) and (E.2) and then the closeness of the data to each other was determined because it is known that the more close the data to each other the more consistent they are.

$$s_N = \sqrt{\frac{1}{N} \sum_{i=1}^N (x_i - \bar{x})^2} \quad (\text{E.1})$$

$N$ : numbers in the set of data

$$\text{Error \%} = \frac{s_N}{\bar{x}} \quad (\text{E.2})$$

The results obtained from some of the experiments were shown below:

#### **Experiment:**

Conditions: pH=4,  $Q_G=170$  L/h,  $Q_L=150$  L/h,  $t=20$  min,  $COD_{in}=60$  mg/L,  $C_{d,in,BB41} = 30.18$  mg/L,  $C_{d,in,BR18.1} = 5.26$  mg/L,  $C_{d,in,BY28} = 5.29$  mg/L,  $C_{d,in} = 315$  Pt-Co,  $C_{O3,G,in} = 0.9 \pm 0.1$  mmol/L gas  $TOC_{in}=20.73$  mg/L, no catalyst.

**Table E.1:** TOC data, standard deviation of TOC data and percent error

z (m)	TOC <sub>1</sub>	TOC <sub>2</sub>	TOC <sub>3</sub>	TOC <sub>mean</sub>	s <sub>N</sub>	% error
0	21.19	20.54	20.46	20.73	0.33	1.58
0.2	19.98	20.34	19.71	20.01	0.26	1.29
0.5	19.02	19.13	19.54	19.23	0.22	1.16
0.8	18.23	18.65	18.89	18.59	0.27	1.47
1	17.63	17.72	17.3	17.55	0.18	1.03

**Table E.2:** COD data, standard deviation of COD data and percent error

z (m)	COD <sub>1</sub>	COD <sub>2</sub>	COD <sub>3</sub>	COD <sub>mean</sub>	SN	% error
0	57	60	57	58	1.41	2.44
0.2	53	53	56	54	1.41	2.62
0.5	53	50	50	51	1.41	2.77
0.8	46	48	47	47	0.82	1.74
1	43	45	44	44	0.82	1.86

**Experiment:**

Conditions: pH=4,  $Q_G=170$  L/h,  $Q_L=150$  L/h,  $t=20$  min,  $COD_{in}=120$  mg/L,  $C_{d,in,BB41} = 60.3$  mg/L,  $C_{d,in,BR18.1} = 10.51$  mg/L,  $C_{d,in,BY28} = 10.58$ mg/L,  $C_{d,in} = 628$  Pt-Co,  $C_{O_3,G,in} = 0.9 \pm 0.1$  mmol/L gas  $TOC_{in}=43.03$  mg/L, no catalyst.

**Table E.3:** TOC data, standard deviation of TOC data and percent error

z (m)	TOC <sub>1</sub>	TOC <sub>2</sub>	TOC <sub>3</sub>	TOC <sub>mean</sub>	SN	% error
0	42.87	43.15	43.07	43.03	0.12	0.27
0.2	42.01	41.92	42.49	42.14	0.25	0.59
0.5	40.13	40.19	40.52	40.28	0.17	0.43
0.8	38.64	38.89	38.75	38.76	0.10	0.26
1	36.97	37.02	37.58	37.19	0.28	0.74

**Table E.4:** COD data, standard deviation of COD data and percent error

z (m)	COD <sub>1</sub>	COD <sub>2</sub>	COD <sub>3</sub>	COD <sub>mean</sub>	SN	% error
0	117	118	119	118	0.82	0.69
0.2	110	114	112	112	1.63	1.46
0.5	105	108	105	106	1.41	1.33
0.8	100	99	104	101	2.16	2.14
1	90	94	95	93	2.16	2.32

**Experiment:**

Conditions: pH=4,  $Q_G=340$  L/h,  $Q_L=250$  L/h,  $t=20$  min,  $COD_{in}=180$  mg/L,  $C_{d,in,BB41} = 90.54$  mg/L,  $C_{d,in,BR18.1} = 15.76$  mg/L,  $C_{d,in,BY28} = 15.87$  mg/L,  $C_{d,in} = 942$  Pt-Co,  $C_{O_3,G,in} = 0.9 \pm 0.1$  mmol/L gas  $TOC_{in}=61.18$  mg/L, no catalyst.

**Table E.5:** TOC data, standard deviation of TOC data and percent error

z (m)	TOC <sub>1</sub>	TOC <sub>2</sub>	TOC <sub>3</sub>	TOC <sub>mean</sub>	S <sub>N</sub>	% error
0	61.18	60.74	61.61	61.18	0.35	0.58
0.2	60.04	60.24	60.32	60.20	0.12	0.19
0.5	58.17	57.93	58.51	58.20	0.24	0.41
0.8	55.04	55.93	56.31	55.76	0.53	0.95
1	53.45	53.87	53.36	53.56	0.22	0.42

**Table E.6:** COD data, standard deviation of COD data and percent error

z (m)	COD <sub>1</sub>	COD <sub>2</sub>	COD <sub>3</sub>	COD <sub>mean</sub>	S <sub>N</sub>	% error
0	189	184	191	188	2.94	1.57
0.2	178	183	182	181	2.16	1.19
0.5	172	175	175	174	1.41	0.81
0.8	161	167	161	163	2.83	1.74
1	155	158	158	157	1.41	0.90

**Experiment:**

Conditions: pH=4,  $Q_G=340$  L/h,  $Q_L=250$  L/h,  $t=20$  min,  $COD_{in}=300$  mg/L,  $C_{d,in,BB41} = 150.9$  mg/L,  $C_{d,in,BR18.1} = 26.4$  mg/L,  $C_{d,in,BY28} = 26.2$  mg/L,  $C_{d,in} = 1570$  Pt-Co,  $C_{O_3,G,in} = 0.9 \pm 0.1$  mmol/L gas  $TOC_{in}=93.76$  mg/L, no catalyst.

**Table E.7:** TOC data, standard deviation of TOC data and percent error

z (m)	TOC <sub>1</sub>	TOC <sub>2</sub>	TOC <sub>3</sub>	TOC <sub>mean</sub>	S <sub>N</sub>	% error
0	93.46	93.92	93.90	93.76	0.21	0.23
0.2	91.98	92.31	92.47	92.25	0.20	0.22
0.5	90.87	91.21	90.53	90.87	0.28	0.31
0.8	88.89	89.18	89.77	89.28	0.37	0.41
1	86.92	87.63	87.43	87.33	0.30	0.34

**Table E.8** COD data, standard deviation of COD data and percent error

z (m)	COD <sub>1</sub>	COD <sub>2</sub>	COD <sub>3</sub>	COD <sub>mean</sub>	S <sub>N</sub>	% error
0	300	310	311	307	4.97	1.62
0.2	298	294	305	299	4.55	1.52
0.5	290	291	286	289	2.16	0.75
0.8	280	276	287	281	4.55	1.62
1	271	273	278	274	2.94	1.07

**Experiment:**

Conditions: pH=10,  $Q_G=340$  L/h,  $Q_L=250$  L/h,  $t=20$  min,  $COD_{in}=180$  mg/L,  $C_{d,in,BB41} = 90.54$  mg/L,  $C_{d,in,BR18.1} = 15.76$  mg/L,  $C_{d,in,BY28} = 15.87$  mg/L,  $C_{d,in} = 945$  Pt-Co,  $C_{O_3,G,in} = 0.9 \pm 0.1$  mmol/L gas  $TOC_{in}=52.50$  mg/L, no catalyst.

**Table E.9:** TOC data, standard deviation of TOC data and percent error

z (m)	TOC <sub>1</sub>	TOC <sub>2</sub>	TOC <sub>3</sub>	TOC <sub>mean</sub>	SN	% error
0	53.01	52.03	52.46	52.50	0.40	0.76
0.2	50.01	51.03	50.96	50.67	0.47	0.92
0.5	48.32	48.45	48.76	48.51	0.18	0.38
0.8	45.23	47.13	47.30	46.55	0.94	2.02
1	44.28	45.38	45.24	44.97	0.49	1.09

**Table E.10** COD data, standard deviation of COD data and percent error

z (m)	COD <sub>1</sub>	COD <sub>2</sub>	COD <sub>3</sub>	COD <sub>mean</sub>	SN	% error
0	188	193	192	191	2.16	1.13
0.2	181	184	175	180	3.74	2.08
0.5	170	176	173	173	2.45	1.42
0.8	160	164	159	161	2.16	1.34
1	155	163	156	158	3.56	2.25

**Experiment:**

Conditions: pH=10,  $Q_G=340$  L/h,  $Q_L=250$  L/h,  $t=20$  min,  $COD_{in}=300$  mg/L,  $C_{d,in,BB41} = 150.9$  mg/L,  $C_{d,in,BR18.1} = 26.4$  mg/L,  $C_{d,in,BY28} = 26.2$  mg/L,  $C_{d,in} = 1570$  Pt-Co,  $C_{O_3,G,in} = 0.9 \pm 0.1$  mmol/L gas  $TOC_{in}=93.23$  mg/L, no catalyst.

**Table E.11:** TOC data, standard deviation of TOC data and percent error

z (m)	TOC <sub>1</sub>	TOC <sub>2</sub>	TOC <sub>3</sub>	TOC <sub>mean</sub>	SN	% error
0	93.02	94.05	92.62	93.23	0.60	0.65
0.2	90.34	90.89	90.52	90.58	0.23	0.25
0.5	87.81	88.27	87.48	87.85	0.32	0.37
0.8	85.23	84.36	85.18	84.92	0.40	0.47
1	84.01	83.12	81.89	83.01	0.87	1.05

**Table E.12:** COD data, standard deviation of COD data and percent error

z (m)	COD <sub>1</sub>	COD <sub>2</sub>	COD <sub>3</sub>	COD <sub>mean</sub>	SN	% error
0	284	284	293	287	4.24	1.48
0.2	278	279	280	279	0.82	0.29
0.5	260	269	269	266	4.24	1.59
0.8	255	256	263	258	3.56	1.38
1	250	252	251	251	0.82	0.33

**Experiment:**

Conditions: pH=4,  $Q_G=340$  L/h,  $Q_L=250$  L/h,  $t=20$  min,  $COD_{in}=180$  mg/L,  $C_{d,in,BB41} = 90.54$  mg/L,  $C_{d,in,BR18.1} = 15.76$  mg/L,  $C_{d,in,BY28} = 15.87$  mg/L,  $C_{d,in} = 940$  Pt-Co,  $C_{O_3,G,in} = 0.9 \pm 0.1$  mmol/L gas  $TOC_{in}=59.83$  mg/L, catalyst: alumina,  $m_{cat} = 300$  g.

**Table E.13:** TOC data, standard deviation of TOC data and percent error

z (m)	TOC <sub>1</sub>	TOC <sub>2</sub>	TOC <sub>3</sub>	TOC <sub>mean</sub>	SN	% error
0	60.23	59.73	59.53	59.83	0.29	0.49
0.2	55.86	56.39	56.44	56.23	0.26	0.47
0.5	53.12	53.87	52.73	53.24	0.47	0.89
0.8	50.03	50.59	50.01	50.21	0.27	0.54
1	47.91	46.98	47.67	47.52	0.39	0.83

**Table E.14:** COD data, standard deviation of COD data and percent error

z (m)	COD <sub>1</sub>	COD <sub>2</sub>	COD <sub>3</sub>	COD <sub>mean</sub>	SN	% error
0	180	179	190	180	4.97	2.71
0.2	167	165	175	167	4.32	2.56
0.5	154	160	160	154	2.83	1.79
0.8	145	147	149	145	1.63	1.11
1	131	139	138	131	3.56	2.62

**Experiment:**

Conditions: pH=10,  $Q_G=340$  L/h,  $Q_L=250$  L/h,  $t=20$  min,  $COD_{in}=180$  mg/L,  $C_{d,in,BB41} = 90.54$  mg/L,  $C_{d,in,BR18.1} = 15.76$  mg/L,  $C_{d,in,BY28} = 15.87$  mg/L,  $C_{d,in} = 940$  Pt-Co,  $C_{O_3,G,in} = 0.9 \pm 0.1$  mmol/L gas  $TOC_{in}=62.10$  mg/L, catalyst: alumina,  $m_{cat} = 300$  g.

**Table E.15:** TOC data, standard deviation of TOC data and percent error

z (m)	TOC <sub>1</sub>	TOC <sub>2</sub>	TOC <sub>3</sub>	TOC <sub>mean</sub>	SN	% error
0	62.09	63.02	61.19	62.1	0.75	1.20
0.2	55.13	56.78	59.78	57.23	1.92	3.36
0.5	53.19	53.55	53.04	53.26	0.21	0.40
0.8	49.23	49.98	49.14	49.45	0.38	0.76
1	45.12	45.99	45.72	45.61	0.36	0.80

**Table E.16:** COD data, standard deviation of COD data and percent error

z (m)	COD <sub>1</sub>	COD <sub>2</sub>	COD <sub>3</sub>	COD <sub>mean</sub>	SN	% error
0	180	176	169	175	4.55	2.60
0.2	160	164	162	162	1.63	1.01
0.5	145	151	148	148	2.45	1.66
0.8	130	136	136	134	2.83	2.11
1	120	121	122	121	0.82	0.67

**Experiment:**

Conditions: pH=4,  $Q_G=340$  L/h,  $Q_L=250$  L/h,  $t=20$  min,  $COD_{in}=300$  mg/L,  $C_{d,in,BB41} = 150.9$  mg/L,  $C_{d,in,BR18.1} = 26.4$  mg/L,  $C_{d,in,BY28} = 26.2$  mg/L,  $C_{d,in} = 1570$  Pt-Co,  $C_{O_3,G,in} = 0.9 \pm 0.1$  mmol/L gas  $TOC_{in}=92.35$  mg/L, catalyst: alumina,  $m_{cat} = 300$  g.

**Table E.17:** TOC data, standard deviation of TOC data and percent error

z (m)	TOC <sub>1</sub>	TOC <sub>2</sub>	TOC <sub>3</sub>	TOC <sub>mean</sub>	SN	% error
0	92.45	93.12	91.48	92.35	0.67	0.73
0.2	88.03	88.91	88.53	88.49	0.36	0.41
0.5	84.56	85.92	85.54	85.34	0.57	0.67
0.8	81.03	81.90	80.76	81.23	0.49	0.60
1	77.92	78.02	77.64	77.86	0.16	0.21

**Table E.18:** COD data, standard deviation of COD data and percent error

z (m)	COD <sub>1</sub>	COD <sub>2</sub>	COD <sub>3</sub>	COD <sub>mean</sub>	SN	% error
0	300	299	304	301	2.16	0.72
0.2	291	295	284	290	4.55	1.57
0.5	270	272	274	272	1.63	0.60
0.8	253	249	257	253	3.27	1.29
1	236	235	243	238	3.56	1.50

**Experiment:**

Conditions: pH=10,  $Q_G=340$  L/h,  $Q_L=250$  L/h,  $t=20$  min,  $COD_{in}=300$  mg/L,  $C_{d,in,BB41} = 150.9$  mg/L,  $C_{d,in,BR18.1} = 26.4$  mg/L,  $C_{d,in,BY28} = 26.2$  mg/L,  $C_{d,in} = 1570$  Pt-Co,  $C_{O_3,G,in} = 0.9 \pm 0.1$  mmol/L gas  $TOC_{in}=93.45$  mg/L, catalyst: alumina,  $m_{cat} = 300$  g.

**Table E.19:** TOC data, standard deviation of TOC data and percent error

z (m)	TOC <sub>1</sub>	TOC <sub>2</sub>	TOC <sub>3</sub>	TOC <sub>mean</sub>	SN	% error
0	93.66	93.99	92.70	93.45	0.55	0.59
0.2	89.01	89.26	89.24	89.17	0.11	0.13
0.5	85.46	85.92	85.63	85.67	0.19	0.22
0.8	81.98	80.13	81.58	81.23	0.79	0.98
1	77.50	77.92	77.23	77.55	0.28	0.37

**Table E.20:** COD data, standard deviation of COD data and percent error

z (m)	COD <sub>1</sub>	COD <sub>2</sub>	COD <sub>3</sub>	COD <sub>mean</sub>	SN	% error
0	278	271	270	273	3.56	1.30
0.2	261	258	252	257	3.74	1.46
0.5	240	241	242	241	0.82	0.34
0.8	220	225	233	226	5.35	2.37
1	210	215	208	211	2.94	1.40

**Experiment:**

Conditions: pH=4,  $Q_G=340$  L/h,  $Q_L=250$  L/h,  $t=20$  min,  $COD_{in}=180$  mg/L,  $C_{d,in,BB41} = 90.54$  mg/L,  $C_{d,in,BR18.1} = 15.76$  mg/L,  $C_{d,in,BY28} = 15.87$  mg/L,  $C_{d,in} = 943$  Pt-Co,  $C_{O_3,G,in} = 0.9 \pm 0.1$  mmol/L gas  $TOC_{in}=60.92$  mg/L, catalyst: PFOA,  $m_{cat} = 300$  g.

**Table E.21:** TOC data, standard deviation of TOC data and percent error

z (m)	TOC <sub>1</sub>	TOC <sub>2</sub>	TOC <sub>3</sub>	TOC <sub>mean</sub>	SN	% error
0	60.23	59.73	62.80	60.92	1.34	2.21
0.2	56.86	56.39	59.91	57.72	1.56	2.70
0.5	53.12	53.87	55.58	54.19	1.03	1.90
0.8	50.03	50.59	51.00	50.54	0.40	0.79
1	47.91	46.98	45.84	46.91	0.85	1.80

**Table E.22:** COD data, standard deviation of COD data and percent error

z (m)	COD <sub>1</sub>	COD <sub>2</sub>	COD <sub>3</sub>	COD <sub>mean</sub>	SN	% error
0	180	179	190	183	4.97	2.71
0.2	167	162	166	165	2.16	1.31
0.5	150	160	152	154	4.32	2.81
0.8	145	146	138	143	3.56	2.49
1	130	137	129	132	3.56	2.70

**Experiment:**

Conditions: pH=10,  $Q_G=340$  L/h,  $Q_L=250$  L/h,  $t=20$  min,  $COD_{in}=180$  mg/L,  $C_{d,in,BB41} = 90.54$  mg/L,  $C_{d,in,BR18.1} = 15.76$  mg/L,  $C_{d,in,BY28} = 15.87$  mg/L,  $C_{d,in} = 944$  Pt-Co,  $C_{O_3,G,in} = 0.9 \pm 0.1$  mmol/L gas  $TOC_{in}=61.04$  mg/L, catalyst: PFOA,  $m_{cat} = 300$  g.

**Table E.23:** TOC data, standard deviation of TOC data and percent error

z (m)	TOC <sub>1</sub>	TOC <sub>2</sub>	TOC <sub>3</sub>	TOC <sub>mean</sub>	SN	% error
0	61.23	60.85	61.04	61.04	0.16	0.25
0.2	56.72	56.01	57.46	56.73	0.59	1.04
0.5	52.16	51.98	51.89	52.01	0.11	0.22
0.8	49.92	48.91	49.85	49.56	0.46	0.93
1	46.91	46.24	47.49	46.88	0.51	1.09

**Table E.24:** COD data, standard deviation of COD data and percent error

z (m)	COD <sub>1</sub>	COD <sub>2</sub>	COD <sub>3</sub>	COD <sub>mean</sub>	SN	% error
0	179	172	177	176	2.94	1.67
0.2	160	165	164	163	2.16	1.33
0.5	153	155	145	151	4.32	2.86
0.8	141	135	141	139	2.83	2.03
1	125	126	130	127	2.16	1.70

**Experiment:**

Conditions: pH=4,  $Q_G=340$  L/h,  $Q_L=250$  L/h,  $t=20$  min,  $COD_{in}=300$  mg/L,  $C_{d,in,BB41} = 150.9$  mg/L,  $C_{d,in,BR18.1} = 26.4$  mg/L,  $C_{d,in,BY28} = 26.2$  mg/L,  $C_{d,in} = 1570$  Pt-Co,  $C_{O_3,G,in} = 0.9 \pm 0.1$  mmol/L gas  $TOC_{in}=91.24$  mg/L, catalyst: PFOA,  $m_{cat} = 300$  g.

**Table E.25:** TOC data, standard deviation of TOC data and percent error

z (m)	TOC <sub>1</sub>	TOC <sub>2</sub>	TOC <sub>3</sub>	TOC <sub>mean</sub>	SN	% error
0	91.43	90.67	91.62	91.24	0.41	0.45
0.2	87.76	88.02	87.35	87.71	0.28	0.31
0.5	83.98	83.67	85.01	84.22	0.57	0.68
0.8	81.16	80.91	80.27	80.78	0.37	0.46
1	77.83	76.92	77.03	77.26	0.41	0.52

**Table E.26:** COD data, standard deviation of COD data and percent error

z (m)	COD <sub>1</sub>	COD <sub>2</sub>	COD <sub>3</sub>	COD <sub>mean</sub>	SN	% error
0	292	300	281	291	7.79	2.68
0.2	270	278	274	274	3.27	1.19
0.5	261	269	253	261	6.53	2.50
0.8	241	246	248	245	2.94	1.20
1	233	231	226	230	2.94	1.28

**Experiment:**

Conditions: pH=10,  $Q_G=340$  L/h,  $Q_L=250$  L/h,  $t=20$  min,  $COD_{in}=300$  mg/L,  $C_{d,in,BB41} = 150.9$  mg/L,  $C_{d,in,BR18.1} = 26.4$  mg/L,  $C_{d,in,BY28} = 26.2$  mg/L,  $C_{d,in} = 1570$  Pt-Co,  $C_{O_3,G,in} = 0.9 \pm 0.1$  mmol/L gas  $TOC_{in}=92.86$  mg/L, catalyst: PFOA,  $m_{cat} = 300$  g.

**Table E.27:** TOC data, standard deviation of TOC data and percent error

z (m)	TOC <sub>1</sub>	TOC <sub>2</sub>	TOC <sub>3</sub>	TOC <sub>mean</sub>	SN	% error
0	92.31	93.04	93.23	92.86	0.40	0.43
0.2	88.92	87.76	88.43	88.37	0.48	0.54
0.5	85.83	85.12	85.97	85.64	0.37	0.43
0.8	82.02	81.83	82.54	82.13	0.30	0.37
1	77.18	76.71	77.26	77.05	0.24	0.31

**Table E.28:** COD data, standard deviation of COD data and percent error

z (m)	COD <sub>1</sub>	COD <sub>2</sub>	COD <sub>3</sub>	COD <sub>mean</sub>	SN	% error
0	296	302	317	305	8.83	2.90
0.2	280	283	295	286	6.48	2.27
0.5	272	266	269	269	2.45	0.91
0.8	251	258	247	252	4.55	1.80
1	231	242	235	236	4.55	1.93

**Experiment:**

Conditions: pH=12,  $Q_G=340$  L/h,  $Q_L=250$  L/h,  $t=20$  min,  $COD_{in}=300$  mg/L,  $C_{d,in,BB41} = 150.9$  mg/L,  $C_{d,in,BR18.1} = 26.4$  mg/L,  $C_{d,in,BY28} = 26.2$  mg/L,  $C_{d,in} = 1580$  Pt-Co,  $C_{O3,G,in} = 0.9 \pm 0.1$  mmol/L gas  $TOC_{in}=92.36$  mg/L, no catalyst.

**Table E.29:** TOC data, standard deviation of TOC data and percent error

z (m)	TOC <sub>1</sub>	TOC <sub>2</sub>	TOC <sub>3</sub>	TOC <sub>mean</sub>	SN	% error
0	91.87	92.34	92.87	92.36	0.41	0.44
0.2	88.21	87.94	88.72	88.29	0.32	0.37
0.5	85.67	85.88	84.83	85.46	0.45	0.53
0.8	82.21	82.56	82.25	82.34	0.16	0.19
1	80.03	79.45	79.98	79.82	0.26	0.33

**Table E.30:** COD data, standard deviation of COD data and percent error

z (m)	COD <sub>1</sub>	COD <sub>2</sub>	COD <sub>3</sub>	COD <sub>mean</sub>	SN	% error
0	298	292	301	297	3.74	1.26
0.2	285	286	290	287	2.16	0.75
0.5	270	273	279	274	3.74	1.37
0.8	260	268	270	266	4.32	1.62
1	251	253	261	255	4.32	1.69

**Experiment:**

Conditions: pH=12,  $Q_G=340$  L/h,  $Q_L=250$  L/h,  $t=20$  min,  $COD_{in}=300$  mg/L,  $C_{d,in,BB41} = 150.9$  mg/L,  $C_{d,in,BR18.1} = 26.4$  mg/L,  $C_{d,in,BY28} = 26.2$  mg/L,  $C_{d,in} = 1570$  Pt-Co,  $C_{O3,G,in} = 0.9 \pm 0.1$  mmol/L gas  $TOC_{in}=91.24$  mg/L, catalyst: alumina,  $m_{cat} = 300$  g.

**Table E.31:** TOC data, standard deviation of TOC data and percent error

z (m)	TOC <sub>1</sub>	TOC <sub>2</sub>	TOC <sub>3</sub>	TOC <sub>mean</sub>	SN	% error
0	90.87	90.94	91.91	91.24	0.47	0.52
0.2	86.73	85.02	86.37	86.04	0.74	0.86
0.5	79.01	78.91	81.84	79.92	1.36	1.70
0.8	73.89	75.56	74.11	74.52	0.74	0.99
1	69.24	68.62	69.11	68.99	0.27	0.39

**Table E.32:** COD data, standard deviation of COD data and percent error

z (m)	COD <sub>1</sub>	COD <sub>2</sub>	COD <sub>3</sub>	COD <sub>mean</sub>	SN	% error
0	297	306	318	307	8.60	2.80
0.2	280	279	284	281	2.16	0.77
0.5	261	269	259	263	4.32	1.64
0.8	238	235	244	239	3.74	1.57
1	210	216	225	217	6.16	2.84

**Experiment:**

Conditions: pH=12,  $Q_G=340$  L/h,  $Q_L=250$  L/h,  $t=20$  min,  $COD_{in}=300$  mg/L,  $C_{d,in,BB41} = 150.9$  mg/L,  $C_{d,in,BR18.1} = 26.4$  mg/L,  $C_{d,in,BY28} = 26.2$  mg/L,  $C_{d,in} = 1570$  Pt-Co,  $C_{O_3,G,in} = 0.9 \pm 0.1$  mmol/L gas  $TOC_{in}=90.91$  mg/L, catalyst: PFOA,  $m_{cat} = 300$  g.

**Table E.33:** TOC data, standard deviation of TOC data and percent error

z (m)	TOC <sub>1</sub>	TOC <sub>2</sub>	TOC <sub>3</sub>	TOC <sub>mean</sub>	SN	% error
0	90.12	91.24	91.37	90.91	0.56	0.62
0.2	86.71	85.19	87.27	86.39	0.88	1.02
0.5	82.35	81.17	82.06	81.86	0.50	0.61
0.8	77.65	69.56	83.85	77.02	5.85	7.60
1	71.92	72.85	72.10	72.29	0.40	0.56

**Table E.34:** COD data, standard deviation of COD data and percent error

z (m)	COD <sub>1</sub>	COD <sub>2</sub>	COD <sub>3</sub>	COD <sub>mean</sub>	SN	% error
0	300	309	303	304	3.74	1.23
0.2	280	283	292	285	5.10	1.79
0.5	267	261	270	266	3.74	1.41
0.8	250	241	247	246	3.74	1.52
1	226	220	235	227	6.16	2.72

According to the standard deviation and percent error results of some of the chosen experiments, it was found out that the experimental error was not higher from 3 % and the set of data were close enough to each other to be consistent. The experiments chosen were both sole and catalytic ozonation experiments in order to be sure that the catalyst were effective and the reduction in TOC and COD values were due to the catalyst and not because of experimental error.

## APPENDIX F

### REPEATIBILITY OF THE EXPERIMENTS

The results obtained from the experiments conducted were investigated if they are producible or not by repeating the experiments at the same conditions with and without catalyst particles. Tables F.1 and F.2 showed the results of repeated experiments conducted on different days in terms of overall color (in terms of Pt-Co unit), TOC and COD removals and ozone consumptions.

**Table F.1:** The color, COD and TOC removals with ozone consumption for reproducibility of WW ozonation experiments,  $COD_{in} = 180$  mg/L ( $C_{d,in} = 850$  Pt-Co),  $Q_G = 170$  L/h,  $Q_L = 150$  L/h, pH = free (4),  $C_{O_3,in} = 0.9 \pm 0.1$  mmol/L gas, catalyst: none.

Experiment Date	TOC Removal (%)	COD Removal (%)	Color Removal (%)	$Cons_{O_3}$ (mmol/L liq.)
15.02.2009	9.39	19.90	83.61	0.864
27.07.2009	10.01	19.34	82.48	0.855
11.10.2010	9.73	18.87	83.03	0.859

**Table F.2:** The color, COD and TOC removals with ozone consumption for reproducibility of WW ozonation experiments,  $COD_{in} = 300$  mg/L ( $C_{d,in} = 1580$  Pt-Co),  $Q_G = 340$  L/h,  $Q_L = 250$  L/h, pH = 10,  $C_{O_3,in} = 0.9 \pm 0.1$  mmol/L gas, catalyst: none.

Experiment Date	TOC Removal (%)	COD Removal (%)	Color Removal (%)	$Cons_{O_3}$ (mmol/L liq.)
05.06.2010	10.97	12.54	70.05	2.038
22.08.2010	10.81	13.09	69.88	2.021
28.11.2010	11.03	12.32	69.43	2.027

Some of the catalytic ozonation experiments were also repeated for the reliability of the experimental results. In the case of catalytic ozonation experiments, the effect of

catalysts used more than one time becomes important and thus, the stability of the catalysts was investigated. Depending on the catalyst characterization results, catalyst particles were decided to be used three times at most because of the differences occurred on the surfaces of the particles. Table F.3 showed the results of the experiments conducted at same operating conditions using the catalyst particles more than one time. PFOA was chosen as the catalyst; since it was prepared by the impregnation of PFO acid onto alumina and thus, PFOA particles tend to decompose more easily than alumina particles. Color, TOC and COD removals were observed to be below 5% indicating that the efficiency of the reused catalyst did not decrease very much during the experimental runs. However, the catalyst particles were not used more than three times in order to protect the reliability.

**Table F.3:** The color, COD and TOC removals with ozone consumption for reproducibility of WW ozonation experiments,  $COD_{in} = 300$  mg/L ( $C_{d,in} = 1580$  Pt-Co),  $Q_G = 170$  L/h,  $Q_L = 150$  L/h, pH = 4,  $C_{O_3,in} = 0.9 \pm 0.1$  mmol/L gas,  $m_{cat} = 150$  g.

Experiment Date	Catalyst	TOC Removal (%)	COD Removal (%)	Color Removal (%)	$Cons_{O_3}$ (mmol/L liq.)
05.04.2009	PFOA (fresh)	7.29	15.81	41.41	0.921
07.04.2009	PFOA (used once)	7.21	14.53	41.34	0.934
08.04.2009	PFOA (used twice)	6.97	14.06	40.12	0.918
10.04.2009	PFOA (used three times)	6.61	12.98	38.26	0.897